DOCTOR OF PHILOSOPHY

Marine phytoplankton in a high CO2 world

Crawfurd, Katharine

Award date:
2010

DOCTOR OF PHILOSOPHY

Marine phytoplankton in a high CO2 world

Katharine Crawfurd

2010

University of Dundee

MARINE PHYTOPLANKTON IN A HIGH CO_2 WORLD

KATHARINE CRAWFURD

A THESIS SUBMITTED IN PARTIAL FULFILLMENT FOR THE DEGREE OF

DOCTOR OF PHILOSOPHY

UNIVERSITY OF DUNDEE
COLLEGE OF LIFE SCIENCES

IN COLLABORATION WITH
PLYMOUTH MARINE LABORATORY

MARCH 2010

AUTHORS DECLARATION

I am the sole author of this thesis and have consulted all of the references cited either in full or abstract form. The work reported was all carried out by myself, with the exception of that performed by other members of the consortia in the Bergen mesocosm project and aboard the STS Lord Nelson, as acknowledged within the text.

None of the work discussed in this thesis has previously been submitted for a higher degree. This programme of advanced study was financed with the aid of a studentship from the Natural Environment research Council.

ACKNOWLEDGEMENTS

I would like to express my sincere thanks to Dr. Ian Joint for his constant support and supervision of this project and to Prof. John Raven for his inspirational guidance. The success of the long term experiment would not have been possible without the aid of Emily Baxter. I would like to thank Glen Wheeler, Jack Gilbert, Mike Allen and Martin Mühling for their assistance in the art of molecular biology; Glen Tarran and Susan Kimmance for flow cytometry and fluorometry tuition. Many thanks to Declan Schroeder and George Sorensen-Pound for DGGE assistance, Paul Somerfield and Bob Clarke for help with statistical analyses. The work in Bergen and aboard the STS Lord Nelson was only possible with a dedicated team, my thanks to all those involved and also to the University of Plymouth electron microscopy unit. Thanks to Karen Weynberg and Nicole Bale for their encouragement and Helen Findlay for CO_2 equilibration assistance. Finally I must thank Jez and Isabel for their unfailing patience, support and nourishment during this project.

LIST OF CONTENTS

LIST OF FIGURES

LIST OF TABLES

LIST OF ABBREVIATIONS

α	the affinity of photosynthesis for light
ACQ	Aquatronica
ADP	adenosine diphosphate
ANOVA	analysis of variance
ANOSIM	analysis of similarities
ATP	adenosine triphosphate
AFC	analytical flow cytometry
C	centigrade
CA	carbonic anhydase
CEH	Centre of Ecology and Hydrology
CCM	carbon concentrating mechanisms
CCMP	Provasoli Guillard national centre for culturing marine phytoplankton
cDNA	complementary DNA
$CO_{2(aq)}$	dissolved carbon dioxide
Ct	threshold cycle
d	day
Δ	change in
df	degrees of freedom
DNA	deoxyribonucleic acid
dNTP	deoxynucleotide triphosphate
DIC	dissolved inorganic carbon
Δ[DIC*]	change in carbon drawdown due to phtotsynthesis
DIN	dissolved inorganic nitrate
DOC	dissolved organic carbon
dsDNA	double stranded DNA
dpm	disintegrations per minute
eCA	extracellular carbonic anhydrase
EDTA	ethylenediaminetetraacetic acid
EF1α	elongation factor 1a
E_k	light saturation coefficient
EMS	expectations of mean squares
F	Fisher's F statistic
fCO_2	free CO_2

FSC	flow cytomery forward scatter
F/2	medium based on natural autoclaved seawater
F/50	more dilute version of F/2
Fv/Fm	quantum yield of PSII
GC	guanine cytosine
gDNA	genomic DNA
GOI	gene of interest
GPA	gene with high glutamic acid, proline and alanine
GPA-F1	forward primer for 1st round PCR using GPA gene
GPA-F2	forward primer for 2nd round PCR using GPA gene
GPA-R1	reverse primer for both rounds of PCR using GPA gene
HAB	harmful algal bloom
Hr	hour
ISAMS	integrated science assessment model
$k_{0.5}$	half saturation constant
kBq	kilobecquerel
l	litre
L	log
m	metre
M	molar
µ	specific growth rate
µatm	microatmophere
µl	microlitre
µm	micrometre
µM	micromole
mg	milligram
ml	millilitre
mol	moles
MTF	multiple turnover flash
MTRI	multiple turnover repetition interval
MTRP	multiple turnover repetition period
mW	milliwat
N	number
$NADP^+$	oxidised nicotinamide adenine dinucleotide phosphate
NADPH	reduced nicotinamide adenine dinucleotide phosphate

ng	nanogram
nm	nanometre
NOCS	National Oceanographic Centre Southampton
Ω	saturation state of calcite
P^B_{max}	maximum biomass normalised, light saturated carbon fixation rate
pCO_2	partial pressure of carbon dioxide
PCR	polymerase chain reaction
perm	permutations
p (perm)	probability based on permutation based analysis
PERMANOVA	permutation based analysis of variance
pers. comm.	personal communication
Pg	Petagram
pH	potentiometric hydrogen ion concentration
pK_a	logarithmic measure of the acid dissociation constant
PIC	particulate inorganic carbon
pmol	picomoles
POC	particulate organic carbon
PON	particulate organic nitrate
PRIMER	Plymouth Routines in Multivariate Ecological Research
PSI	photosystem 1
PSII	photosystem 2
ppm	parts per million
qRT-PCR	quantitative reverse transcription polymerase chain reaction
R	correlation coefficient
RCF	relative centrifugal force
REST	Relative Expression Software Tool
Red fl	red fluorescence
RNA	ribonucleic acid
rRNA	ribosomal RNA
rpm	revolutions per minute
RuBisCO	ribulose-1,5-bisphosphate carboxylase/oxygenase
RuBP	ribulose bisphosphate
s	second
σ_{PSII}	the relative functional absorption cross section of PSII

SDS	sodium dodecyl sulphate
SEM	Scanning Electron Microscopy
SET	lysis buffer
sp.	Species
SS	Sums of squares
SRES	Special report on Emissions Scenarios
SSC	flow cytometry side scatter
STF	single turnover flash
STRI	single turnover repetition interval
STS	sail training ship
SYBR Green	fluorescent dye for staining nucleic acid
t	time
τ	selectivity of RuBisCO for CO_2:O_2
Taq	DNA polymerase from *Thermus aquaticus*
TAE	buffer containing a mixture of Tris base, acetic acid and EDTA
tris	Tris (hydroxymethyl) aminomethane
Φ_{max}	maximum yield for carbon fixation
UEA	University of East Anglia
UV	Ultra Violet
V_{max}	maximum rate of carboxylation
3GP	glyceraldehyde 3-phosphate

ABSTRACT

Marine phytoplankton is responsible for ~50% of global primary productivity, it supports the oceanic food web and affects biogeochemical cycles. I participated in a large mesocosm experiment that observed altered community structure and carbon drawdown in response to increased CO_2. There was a 27% reduction in community primary production at the peak of an *Emiliania huxleyi*-dominated bloom in mesocosms initially at 760 ppm CO_2 compared to present day pCO_2. There were changes in community structure but not dominance; *Synechococcus* and large pico-eukaryote abundances were reduced by ~60%, *E. huxleyi* was reduced by ~50%. A number of *E. huxleyi* strains persisted throughout the experiment in both treatments and no malformation or significant change in lith size occurred at increased CO_2. In a second field experiment in the oligotrophic ocean off the Canary Islands, 760 ppm pCO_2 did not change community structure or cell division rates of *Synechococcus, Prochlorococcus* or pico-eukaryotes. In laboratory experiments, I maintained the diatom, *Thalassiosira pseudonana* CCMP1335 at 760 ppm and present day pCO_2 for ~100 generations in gas equilibrated continuous cultures – one of the longest experiments that has been attempted to investigate the effect of increased CO_2 on marine phytoplankton. No clear evidence of adaptation or acclimation to increased CO_2 was found, neither were there consistent changes in transcription of RuBisCO or carbonic anhydrase genes. Non-calcified *E. huxleyi* CCMP1516 and calcified CCMP371 grown in gas equilibrated semi-continuous cultures for several weeks showed no change in cell division rate at 760 ppm CO_2. An understanding of the processes underlying changes in communities is required for modelling responses to increasing CO_2, molecular tools may prove useful for this task. The strong community response in the mesocosms shows that rising atmospheric CO_2 can greatly affect phytoplankton productivity and biogeochemical cycling.

Chapter 1.

GENERAL INTRODUCTION

This thesis is concerned with the effects of increasing carbon dioxide (CO_2) on the marine phytoplankton. The phytoplankton is the vast number of single celled marine primary producers inhabiting the surface layer of the oceans. Phytoplankton use energy of sunlight to convert carbon dioxide, water and nutrients into biomass and oxygen through photosynthesis. They are the producers which sustain the entire marine food web and influence the Earth's biogeochemical cycles. In recent centuries man has become dependent upon burning fossil fuels for energy. This has released large quantities of carbon dioxide into the atmosphere. By the end of the century this is expected to amount to a two to three fold increase in CO_2 compared to preindustrial levels (IPCC 2007). A considerable proportion of this has dissolved in the ocean where it forms a weak acid and causes re-equilibration of the carbonate system. As a result the pH of the oceans is reducing; ie. they are becoming less alkaline. These two effects, increased CO_2 and reduced pH are likely to affect the phytoplankton. In turn this will affect the food web and biogeochemical cycles; thus elucidating the response of phytoplankton to increasing CO_2 is of great importance. The experimental work carried out for this thesis examined the effects of increased CO_2 on several key species of the phytoplankton and two natural assemblages.

In this introduction I will briefly describe ocean acidification, the marine carbonate system, and physical, biological and carbonate pumps. I will then describe the marine phytoplankton, their role as primary producers and the theoretical effects of increased CO_2 on different types of phytoplankton, before reviewing the current state of

knowledge about these effects. The effects of increased CO_2 may be manifested as changes in growth rate, photosynthetic rate, carbon to nitrogen ratio, calcification, cell size or a combination of these factors. These variables were examined in the experimental work and therefore the introduction will concentrate on these subjects.

1.1 CARBON DIOXIDE AND THE OCEANS

In this section I will outline the concept of ocean acidification, examine the past, present and future predicted CO_2 emissions and briefly describe the ocean carbonate system.

1.1.1 Ocean acidification

Ocean acidification is a term used to describe the decrease in pH of the oceans caused by the absorption of increasing amounts of CO_2 from the atmosphere. Many organisms, particularly those which produce shells or skeletons of calcium carbonate, may be sensitive to these changes. The evidence suggests that the burning of fossil fuels has led to a large increase in atmospheric CO_2 and that a portion of this has been absorbed by the oceans. Seawater contains effective chemical buffers which reduce the magnitude of pH change. A decrease in pH of slightly less than 0.1 units, from around 8.2 to 8.1 has been seen since pre-industrial times (Orr et al. 2005). This seems fairly modest but due to the log scale of pH this relates to a 30% increase in H^+. Ocean acidification models predict a further fall in pH of 0.14 to 0.35 units by the year 2100 due to continued carbon emissions (IPCC 2007).

1.1.2 Carbon emissions

Prior to the industrial revolution the global carbon system had been in steady state for at least two thousand years. Measurements of air bubbles trapped within ice-cores show that atmospheric CO_2 concentrations were approximately 280 ppm throughout this

period (Raven and Falkowski 1999). Since the beginning of the industrial revolution large reserves of oil and coal have been burnt as fuel, amounting to approximately 400 Pg of carbon (Pg C)(1 Pg = 10^{15} g = a thousand million tonnes) (Raven and Falkowski 1999; Le Quéré et al. 2009). In 2008 CO_2 emissions from combustion, cement production and gas flaring were estimated to be 8.7 ± 0.5 Pg of carbon per annum (Le Quéré et al. 2009). Atmospheric CO_2 has increased from 280 parts per million (ppm) in the pre-industrial era to 385 ppm today (Le Quéré et al. 2009).

The oceans contain approximately 50 times more inorganic carbon than the atmosphere (Raven and Falkowski 1999). The estimated total oceanic uptake of anthropogenic carbon emissions since 1750 is 140 ± 25 Pg C (Khatiwala et al. 2009). Thus the oceans have stored approximately 35% of man-made carbon emissions. In 2008 it was estimated that the oceans absorbed approximately 2.3 (± 0.4) Pg C, 26% of the total carbon emitted. The terrestrial biosphere took up 4.7 (± 1.2) Pg C leaving approximately 4 Pg C in the atmosphere (Le Quéré et al. 2009) (**Fig. 1.1**). The terrestrial uptake was higher in 2008 than in the previous three years due to the El Nino/Southern Oscillation being in a positive state with the tropics being cooler and wetter. The oceanic sink was reduced due to greater upwelling of carbon rich waters. However a trend for a reduction in oceanic and terrestrial uptake has been seen, leaving a greater fraction of the annual CO_2 released in the atmosphere (Le Quéré et al. 2009).

1.1.3 Climate models

Climate models are mathematical representations of the climate system, they are based on established physical laws and a wealth of observational data (IPCC 2007). Since the first IPCC report in 1990 the models used have evolved, becoming increasingly complex and robust, with frequent evaluation against observed changes in climate.

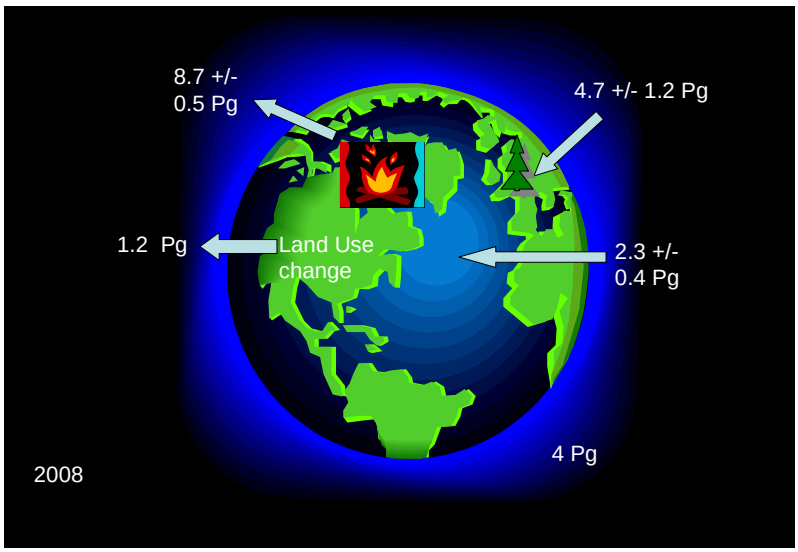

Fig. 1.1 Carbon fluxes between the atmosphere and terrestrial and ocean biospheres in 2008. Values are concentrations of carbon in petagrammes (1 Pg = 10^{15} g = a thousand million tonnes), data taken from (Le Quéré et al. 2009).

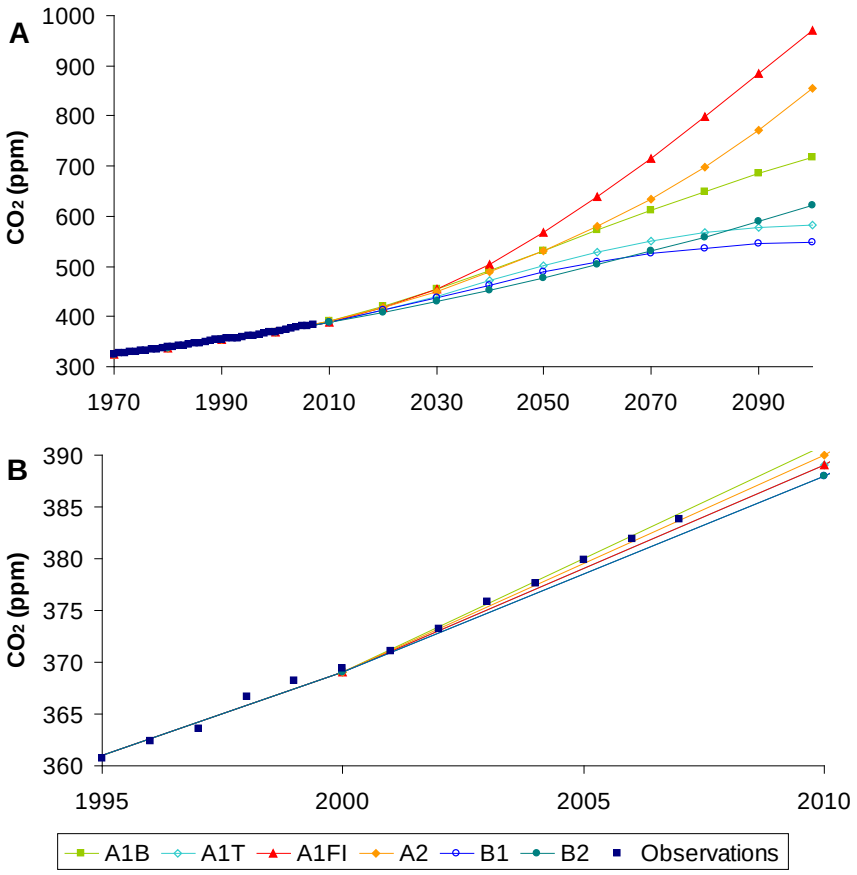

Fig. 1.2 A. 1970 to 2100 model projections for future atmospheric CO_2 concentrations from ISAMS model using six SRES scenarios for future carbon emissions and mitigation strategies (Table of abbreviations p. xviii). Superimposed are observed atmospheric CO_2 concentrations from Mauna Loa (■). B. detail from Fig. 1.2A, observed and projected CO_2 emissions 1995-2010 (IPCC 2007).

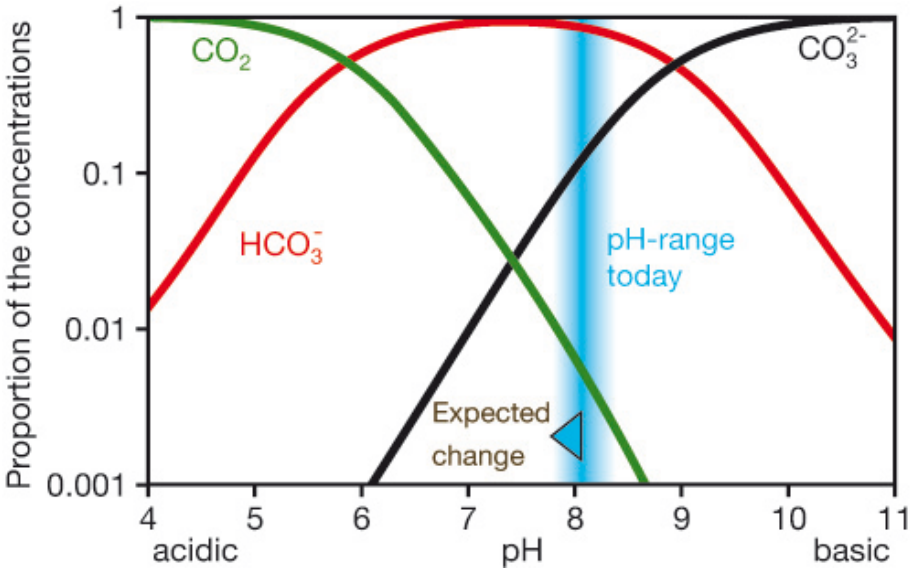

Fig. 1.3. The inter-relationship of different carbonate system species and pH. Current pH of around 8.1 shown in blue which is expected to reduce to approximately 7.8 by 2100 (Raven et al. 2005).

The models contain 'driving forces' which have been identified from 'scenarios'. The scenarios are storylines for future human social and economic development. Amongst the driving forces coming from these are population growth, technological advances and land use. These are used alongside atmospheric, terrestrial, oceanic, cryospheric and aerosol physical processes to predict future trends in a wide range of biogeochemical and physical variables. The IPCC fourth assessment (IPCC 2007) used a multi-model approach with six models to generate projections of future carbon dioxide emissions and climate variables for six scenarios. There are uncertainties within the models due to the many variables and unknown future technological advances which result in a broad spread of predictions. The projected 2100 atmospheric CO_2 levels range from ~500 to 1,000 ppm (**Fig. 1.2**). At present the observed CO_2 increase has been found to closely track the A1FI scenario trajectory (Le Quéré et al. 2009). This is based on rapid economic growth and intensive fossil fuel use resulting in CO_2 concentrations of over 900 ppm by the end of the century (IPCC 2007). However, there is little divergence

between the scenarios at present and future strategies will greatly influence the CO_2 level reached at the end of this century.

1.1.4 The ocean carbonate system

There are four components of the carbonate system that are inter-related (**Fig. 1.3**). Measurement of any two of these components allows the others to be calculated. They are: total dissolved inorganic carbon; the partial pressure of CO_2 (pCO_2); total alkalinity and pH. This section will outline the relationships between these variables, each of which may exert influences over phytoplankton physiology.

Dissolved inorganic carbon (DIC) is present in seawater as free carbon dioxide, $CO_{2(aq)}$, bicarbonate ions (HCO_3^-) and carbonate ions (CO_3^{2-}). $CO_{2(aq)}$ is in equilibrium with a small concentration of carbonic acid (H_2CO_3) (Hurd et al. 2009) . The relationships between the species are shown in **equation 1.1** and the hydroxylation reaction consuming OH^- ions in **equation 1.2** (Zeebe and Wolf-Gladrow 2001).

$$CO_{2\,(aq)} + H_2O \leftrightarrow H_2CO_3 \leftrightarrow HCO_3^- + H^+ \leftrightarrow CO_3^{2-} + 2H^+ \quad [1.1]$$

$$CO_{2\,(aq)} + OH^- \leftrightarrow HCO_3^- \quad [1.2]$$

The total alkalinity of seawater (TA) is primarily determined by the quantity of H^+ and OH^- from the carbonate system although other acid/base interactions are also influential, particularly the borate/boric acid equilibrium (**equation 1.3**).

$$TA = [HCO_3^-] + 2[CO_3^{2-}] + [B(OH)_4^-] + [OH^-] - H^+ + \text{minor components}] \quad [1.3]$$

The relative quantities of CO_2, HCO_3^- and CO_3^{2-} are linked to seawater pH. In natural seawater the current pH is estimated to be on average 8.07; 91% of DIC is present as HCO_3^- ions, 1% as $H_2CO_3/CO_{2\,(aq)}$ and 8% as CO_3^{2-} (**Fig. 1.3**) (Hurd et al. 2009). The projected increase in CO_2 will push the equilibrium to the left and is expected to reduce pH to 7.65. Carbonate ions will decrease by 56%, $H_2CO_3/CO_{2(aq)}$ will increase by 300% and HCO_3^- by 9% (Hurd et al. 2009). The phytoplankton exerts an influence over the carbonate system by taking up CO_2 for photosynthesis. This increases pH and CO_3^{2-} and decreases HCO_3^-. This effect is most obvious in laboratory cultures or natural blooms, a daily and seasonal signal is also noticeable. Calcifying phytoplankton affects the dissolved inorganic carbon and the TA of seawater. CO_3^{2-} ions are removed from seawater by precipitation of calcium carbonate ($CaCO_3$) causing HCO_3^- ions to dissociate to restore the CO_3^{2-} lost. The H^+ ion released by the dissociation generates H_2CO_3 by combining with a second HCO_3^- ion (Frankignoulle et al. 1994). The deposition of 1 mol of calcium carbonate releases 0.6 mol CO_2 into seawater, reducing TA by 2 equivalents (**equation 1.4**) (Gattuso et al. 1995).

$$Ca^{2+} + 2HCO_3^- \rightarrow CaCO_3 + CO_2 + H_2O \qquad [1.4]$$

CO_2 is released during calcification and if the rate of calcification is greater than that of photosynthesis it is possible that calcifying phytoplankton may act as a source rather than a sink of CO_2. The ratio of inorganic carbon fixed by calcification, to inorganic carbon fixed by photosynthesis may be described as the PIC:POC ratio. There are three main crystalline forms of calcium carbonate: aragonite, and low or high magnesium calcite. Aragonite is approximately 50% more soluble than the low magnesium calcite precipitated by the majority of the phytoplankton. The saturation state for calcium carbonate (Ω) is based on the concentrations of Ca^{2+} and CO_3^{2-} in seawater (**equation**

1.5). Increasing CO_2 reduces pH and the carbonate saturation state (Ω) (Schulz et al. 2009). Below the saturation horizon, the depth at which Ω < 1, the mineral will start to dissolve. $[Ca^{2+}]sw$ and $[CO_3^{2-}]sw$ are the concentrations of calcium and carbonate ions in the seawater and K^*_{sp} is the stoichiometric solubility constant of calcium carbonate (Schulz et al. 2009).

$$\Omega=([Ca^{2+}]sw\ [CO_3^{2-}]sw)/K^*_{sp} \quad [1.5]$$

1.2 THE PHYSICAL, BIOLOGICAL AND CARBONATE PUMPS

Inorganic carbon is present in the atmosphere as carbon dioxide. Any CO_2 in the atmosphere, in excess of equilibrium with CO_2 in the surface ocean, is taken up by the oceans by two major processes. Firstly, it dissolves in cold water at high latitudes and sinks into deeper water by temperature-driven currents. The gases absorbed remain in this deep water for hundreds of years until it surfaces in the tropics and the gases are released. This is known as the 'physical carbonate pump' or 'solubility pump'. Secondly phytoplankton takes up dissolved carbon dioxide from the surface oceans and converts it to biomass (particulate organic carbon, POC) by photosynthesis. The phytoplankton either dies or is consumed and this carbon may sink into the deep ocean and ultimately be incorporated into marine sediments. This is termed the 'biological pump'; it relies on the removal of carbon from the surface layer to the deep ocean by sinking of particles, 'carbon export'.

In addition to the removal of POC, inorganic carbon may be fixed as calcite or aragonite (particulate inorganic carbon, PIC) by marine organisms and sunk to the deep ocean; this is known as the 'carbonate pump' (Westbroek et al. 1993). PIC production involves the parallel production of CO_2. 30-40 Pg of carbon per year are fixed as POC by marine algae but only 0.1% of this is removed from the water column by

sedimentation. 1-1.3 Pg of calcium carbonate are formed by marine organisms of which 15% is incorporated into the sediment (Westbroek et al. 1993). The majority of carbon export occurs through phytoplankton 'blooms'. In temperate regions these occur mainly during spring, when increasing light and temperature together with nutrients brought up by deep mixing in the winter, allow rapid growth of phytoplankton. These blooms cover vast areas of the ocean, that can be over a hundred thousand square kilometers (Sorensen et al., 2009). When the nutrient supply is exhausted, or viruses end the bloom, it 'crashes'. This results in a mass of dying cells, bacteria, exuded material and the faeces of grazers. These may aggregate into larger, heavier clumps known as 'marine snow' and sink removing fixed carbon from the surface to the deep ocean (Passow et al. 1994).

1.3 MARINE PHYTOPLANKTON

Marine phytoplankton is responsible for almost one half of global primary production, amounting to ~50 Pg C yr^{-1}, (Field et al. 1998). Phytoplankton is a generic term for all autotrophic planktonic algae. This includes prokaryotic and eukaryotic single cells and colonial drifting species. Major groups of phytoplankton are diatoms, coccolithophores, dinoflagellates and cyanobacteria (**Fig. 1.4**).

Cyanobacteria are the most abundant of the phytoplankton groups, numerically, accounting for the majority of the phytoplankton (Falkowski et al. 2004). They are the most ancient group of phytoplankton, simple single celled prokaryotic organisms from which all others evolved. They dominate low nutrient environments such as the mid ocean gyres and may be responsible for ~50% of carbon fixation in marine environments (Fu et al. 2007) (**Fig. 1.4D**). *Synechococcus* and *Prochlorococcus* are widely distributed cyanobacteria genera.

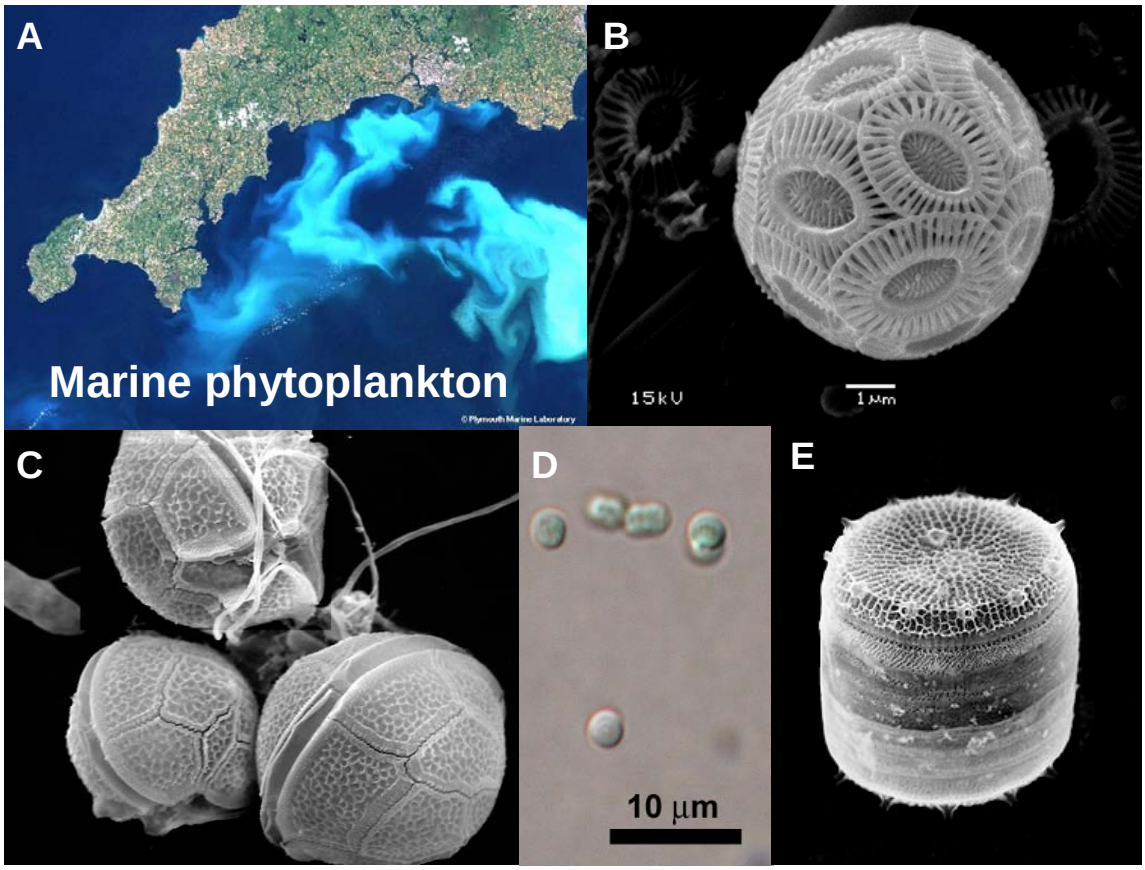

Fig. 1.4 A. Coccolithophore bloom off the coast of Plymouth, these may cover vast areas and are visible from space. B. *Emiliania huxleyi*, a coccolithophore C. *Gonyaulax*, a dinoflagellate (http://www.aad.gov.au/); D. *Synechococcus*, a cyanobacterium (http://www.butbn.cas.cz); E *Thalassiosira pseudonana*, centric diatom, image by Nils Kröger (http://gtresearchnews.gatech.edu/)

Dinoflagellates are a diverse group of autotrophs and heterotrophs common in both marine and freshwater ecosystems. Certain species produce toxins, when these grow intensely 'harmful algal blooms' (HAB) are formed (Sellner et al. 2003). These may kill marine organisms, produce aerosols (Pierce et al. 2005) and be bioaccumulated by shellfish rendering them harmful to humans (Sellner et al. 2003)(**Fig. 1.4C**).

Coccolithophores form exquisite spheres of calcium carbonate plates, termed liths. There are estimated to be about 150 extant species (Westbroek et al. 1993), of which the most prevalent in the modern ocean is *Emiliania huxleyi* (**Fig. 1.4B**). It has a worldwide distribution, often accounting for 20-50% of any oceanic coccolithophore

community. The dense spring blooms in both coastal and oceanic waters may annually cover 1.4 x 10^6 km^2 (Westbroek et al. 1993) (**Fig. 1.4A**).

Diatoms form silica shells, known as tests or frustules. They are of major importance in biogeochemical cycling being the most productive of the eukaryotic phytoplankton (Granum et al. 2009). They are responsible for approximately 40% of marine primary production or 20% of total global primary production (Falkowski and Raven 1997) (**Fig. 1.4E**). They are also common in freshwater ecosystems.

In this study I have chosen the coccolithophore, *Emiliania huxleyi* (**Fig. 1.4B**) and the diatom, *Thalassiosira pseudonana* (**Fig. 1.4E**) as representatives of two major phytoplankton groups for laboratory experiments. Two natural assemblage studies were performed, one with a mixed community from the fjords of Norway including all four key phytoplankton groups outlined in this section. The second, a *Synechococcus* and *Prochlorococcus* dominated tropical assemblage.

1.4 PRIMARY PRODUCTION

Primary production is the generation of energy rich organic compounds from inorganic molecules. In the ocean autotrophic phytoplankton fix CO_2 initially into simple sugars, a process which ultimately supports all marine life. These sugars, plus other nutrients, form the building blocks for growth of the phytoplankton. The phytoplankton is then consumed by higher trophic levels which are able to use the carbon, nitrogen, phosphorus and energy for their own growth and metabolic processes. Carbon fixation is achieved by the process of photosynthesis which requires light, water, CO_2 and nutrients. Photosynthesis consists of two stages. In the first stage, light-dependent reactions use energy from light to convert ADP to ATP and to reduce $NADP^+$ to

NADPH. During the second stage, carbon fixation is fuelled by the products from the light reactions in the light-independent reactions. The two stages of photosynthesis will be briefly described in the following sections.

1.4.1 Light

Light provides the energy for carbon fixation. It is electromagnetic radiation of different wavelengths, longer wavelengths are greatly absorbed by water but short ones, blue light, may penetrate clear waters to a depth of several hundred meters. Blue light has a wavelength of around 400-500 nm and red light 600-700 nm. The energy exists as discrete packets (photons) which must be harvested by the phytoplankton, this is achieved by their photosynthetic pigments. Chlorophyll-a and b absorb red and blue light and the accessory pigments, including carotenoids and phycobilins absorb light of the intermediate wavelengths. The pigment molecules are organized into antenna systems for efficient light harvesting. In eukaryotes, these are found in membrane bound compartments known as thylakoids within a larger compartment, the chloroplast (Falkowski and Raven 1997).

1.4.2 The light dependent reactions of photosystems I and II

When a photon of light is absorbed it may be used to raise a pigment molecule from its ground state to an excited state and this energy may be transferred to another pigment molecule in the form of an energized electron. Pigment molecules transfer this energy from one to another and finally to the reaction centres of photosystems I (PSI) and II (PSII). In PSII, an electron is passed to the primary acceptor, phaeophytin *a*, and is replaced ultimately by an electron extracted from a water molecule. The overall reaction involves the movement of an electron from water in the intrathylakoid space to phaeophytin *a* on the stroma side of the thylakoid, with production of 0.25 oxygen and a

proton in the intrathylakoid space and a reduced phaeophytin *a* on the stroma side of the thylakoid.

The electron from reduced phaeophytin *a* then passes down an electron transport and proton transport chain to the oxidizing end of PSI, with part of the energy released being used to pump two protons for each electron from the stroma to the intrathylakoid space. In PSI an electron (ultimately from PSII) is passed to a primary electron acceptor, chlorophyll-a, and ultimately to CO_2. The overall reaction involves movement of an electron from the electron transport chain to 0.25 CO_2 producing 0.25 CH_2O, with uptake of one proton from the stroma. Overall three protons are transferred from the stroma to the intrathylakoid space per electron moved from water to CO_2, and the backflow of these protons to the stroma through the ATP synthetase is used to phosphorylate ADP to ATP for use to the CO_2 assimilation pathway.

1.4.3 The light independent reactions, Calvin-Benson cycle

The light independent reactions are known as the Calvin-Benson cycle. The energy, stored as ATP and reducing power, NADPH are used to fix 3 CO_2 molecules into a three carbon sugar, glyceraldehyde 3-phosphate. Initially the CO_2 is combined with ribulose bisphosphate in a reaction catalysed by ribulose 1,5 bisphosphate carboxylase oxygenase (RuBisCO) to form two 3-phosphoglycerate, each of which gains an additional phosphate group from the ATP and is then reduced to glyceraldehyde 3-phosphate (G3P). For every 3 CO_2 molecules entering the Calvin cycle one G3P is released. The remaining 15 C atoms are used to generate the co-substrate, three ribulose 1,5-bisphosphate, for the assimilation of another three CO_2 and thus continue the cycle.

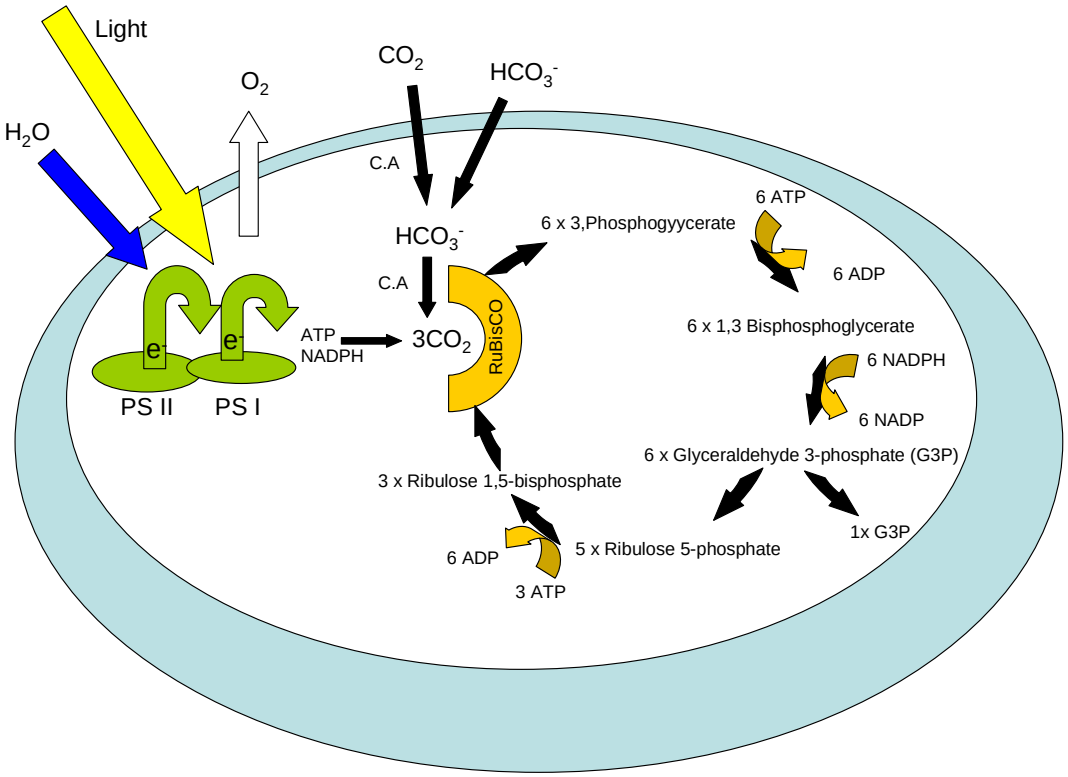

Fig. 1.5 Simplified schematic diagram of algal photosynthesis including carbon uptake, the light dependent reactions of PS I and II (■) and the light-independent reactions of the Calvin-Benson cycle (■). The blue area represents the cell and white area the chloroplast. C.A. is carbonic anhydrase, which may be found in various locations within the cell to catalyse the interconversion of HCO_3^- and CO_2.

1.4.4 RuBisCO, photorespiration and CCMs

Ribulose-1,5-bisphosphate carboxylase/oxygenase (RuBisCO) catalyses the rate determining reaction of the Calvin-Benson cycle. The efficiency of this enzyme will therefore regulate the rate of photosynthetic carbon fixation.

RuBisCO is a slow enzyme with maximum turnover rates of ~12 mol substrate transformed enzyme^{-1} s^{-1} (**Table 1.1**) (Raven et al. 2000). In addition it has the capacity to act as both a carboxylase and an oxygenase. The carboxylase reaction, as seen in the Calvin-Benson cycle (**Fig. 1.5**) results in the fixation of CO_2 to G3P. The competing, oxygenase reaction, also known as photorespiration, produces phosphoglycolate that

cannot enter the Calvin-Benson cycle (Parker et al. 2004). This sequesters P, and can act as a metabolic inhibitor, if allowed to accumulate. Excretion as glycolate deprives the cell of the carbon and the energy used to produce glycolate. The phosphoglycolate is metabolized in the photorespiratory pathway, this produces a succession of organic compounds including glycolate, glycine and serine. Ultimately G3P is generated which enters the Calvin-Benson cycle, but this involves energy input and one in every four carbons is used to produce CO_2 (Parker et al. 2004). The use of CCMs requires energy, however this cost may be partially, or completely offset by the energy saved from reduced processing of the products of photorespiration (Raven et al. 2000).

For the most catalytically efficient RuBisCOs the concentration of CO_2 required to half saturate the rate of photosynthesis, $k_{0.5}$ (CO_2), is ~10 µM (Tortell 2000); as the current concentration of CO_2 in seawater at 15°C is ~14.2 µM (Beardall and Raven 2004), RuBisCO is under-saturated for CO_2 at present day concentrations. As a consequence of its slow catalytic rate large quantities of RuBisCO are necessary to maintain adequate carbon fixation rates (Tcherkez et al. 2006). Although highly conserved, RuBisCO shows phylogenetic variability and four main types, I, II, III and IV have been identified; type I is further sub-divided into forms 1A, 1B, 1C and 1D (Raven 2009). The RuBisCOs of the marine cyanobacteria are type 1A or 1B, the dinoflagellates type II, diatoms and coccolithophores type 1D. These types differ in their kinetic properties in particular the specificity of the RuBisCO for CO_2 and O_2 (**Table 1.1**). Highly specific RuBisCOs are able to discriminate between CO_2 and O_2 more effectively thus increasing the rates of carboxylation: oxygenation. Specificity for CO_2 over O_2 (τ) is calculated from the substrate saturated rates of catalysis for carboxylation (V_{max} CO_2) and oxygenation (V_{max} O_2), in mol substrate transformed enzyme^{-1} s^{-1}; and the

corresponding half saturation constants $k_{0.5}(CO_2)$ and $k_{0.5}$ (O_2), in mol m^{-3}; according to **equation 1.6** (Beardall and Raven 2004).

$$\tau = \frac{V_{\max}(CO_2) \times k_{0.5}(O_2)}{V_{\max}(O_2) \times k_{0.5}(CO_2)}$$

[1.6]

Table 1.1 Types, specificity factors (τ) and maximum carboxylation rates of RuBisCO of the major phytoplankton taxa. Data taken from Raven (2000).

Taxa	Rubisco type	τ	Max carboxylation rate K_{cat}^{c} (s^{-1})	CCMs
α cyanobacteria	1A	35-56	11.4-12	Yes
β cyanobacteria	1B	35-90		Yes
Dinoflagellates	II	~37		Yes
Diatoms	1D	106-114	0.78-5.7	Yes
Coccolithophores	1D			Yes

Theoretically phytoplankton with highly specific RuBisCOs should have a competitive advantage over those with less specific forms, and selective pressure would favour them. However cyanobacteria which have the lowest specificity are the most numerous phytoplankton in the oceans (Falkowski et al. 2004). The reason for the lack of selection for highly specific RuBisCO may be the inverse relationship between specificity and maximum carboxylation rate. Highly specific RuBisCOs such as those of the diatoms ($\tau \sim 108$) have low maximum carboxylation rates; conversely, the cyanobacteria ($\tau \sim 46.6$) have much higher rates of carboxylation. This trade off may be due to a tighter bond being formed between the CO_2 and RuBP, in transition state during carboxlyation, which causes a reduction in the maximum rate of catalytic turnover of more specific RuBisCOs (Tcherkez et al. 2006). In order to achieve adequate rates of carboxylation, with little selectivity for CO_2 over O_2, the CO_2:O_2 concentrations in the vicinity of RuBisCO must be higher in cyanobacteria than in diatoms. This requires

CO_2 concentrating mechanisms (CCM). Not all phytoplankton possess CCMs however they are widespread, even amongst species with high selectivity for CO_2 (Beardall and Raven 2004). Species with high specificity RuBisCOs may require less CCM activity to saturate their RuBisCO (Raven et al. 2000). CCMs take a variety of forms, biophysical active uptake of CO_2 or HCO_3^- and biochemical C_4 and CAM metabolism which are fully reviewed by Giordano et al. (2005).

The goal of the CCMs is to accumulate CO_2 at the RuBisCO active site. In order to accomplish this RuBisCO is usually concentrated in membrane bound compartments which can contain the concentrated DIC. Most algae actively take up both CO_2 and HCO_3^- (Giordano et al. 2005). In biophysical CCMs, there is a requirement for membranes with low permeability to the carbonate species being transported across them (Giordano et al. 2005). A series of inter-conversions of CO_2 and HCO_3^- accompanied by active transport or diffusion across membranes concentrates and contains the DIC. Uncatalysed inter-conversion between CO_2 and HCO_3 is slow and the reaction is usually catalysed by carbonic anhydrase (CA), according to **equation 1.7**. Carbonic anhydrases are a diverse and widely distributed family of enzymes with a range of functions, metal requirements and locations. Most taxa across the whole spectrum of life have several or many CAs, where many CAs are present in an organism they are usually in different intracellular locations. CA synthesis and CCM activity in eukaryotes is controlled by the concentration of CO_2 in those species examined (Giordano et al. 2005).

$$CO_2 + H_2O \leftrightarrow H_2CO_3 \leftrightarrow H^+ + HCO_3^- \quad [1.7]$$

Carbon concentrating mechanisms are capable to raising the internal:external CO_2 concentration by up to 100 fold if external CO_2 concentrations are low (Badger 2003)

(Burns and Beardall 1987). At present day pCO_2 phytoplankton concentrate CO_2 to ~2 to 3 fold that of the external concentration (Raven 1991). The ratio of intracellular: extracellular CO_2 is known as the carbon concentrating factor (CCF) and has been found to decrease with increasing τ (Tortell 2000). Thus those cells with low specificity, eg. cyanobacteria, compensate by increasing the concentration of CO_2 at the RuBisCO active site. In most phytoplankton the affinity of intact cells for CO_2 is much greater than that of the RuBisCO, with $k_{0.5}$ (CO_2) of cells: RuBisCO of at least 2:30 (Badger et al. 1998). The effect of this is that in phytoplankton with a CCM the rate of photosynthesis at air-equilibrium CO_2 concentrations is >90% that of the rate at CO_2 saturation (Beardall and Raven 2004).

The ability of phytoplankton with different RuBisCO types and CCMs to thrive is testament to the success of the strategies. However, in an atmosphere with rapidly increasing CO_2 concentrations the strategies may be differentially advantageous to the phytoplankton employing them. The following sections will first describe the hypothetical effects of increased CO_2 on the different groups of phytoplankton and then review the current observed effects.

1.5 THEORETICAL EFFECTS OF INCREASED CO_2 ON PHYTOPLANKTON

At increased CO_2 those species relying on diffusive CO_2 entry or those able to suppress CCMs are most likely to benefit (Raven and Johnston 1991). Most phytoplankton actively take up both CO_2 and HCO_3^- (Giordano et al. 2005) therefore species benefitting from reduced CCM activity may be of any functional type. A further benefit may be incurred by species with low specificity RuBisCO with higher carboxylation rates, if CCM activity can be reduced. This is because a reduction in CCM activity may save energy, the high CO_2:O_2 concentrations will ensure high rates of

carboxylation:photorespiration and the carboxylation rate of this RuBisCO is higher than that of the highly specific RuBisCOs. Those species with high specificity RuBisCO and slower maximum carboxylation rates will not benefit because the added specificity will not be necessary and the trade off of slower carboxylation will be detrimental. From these theoretical considerations species, such as diatoms with highly specific RuBisCO, will not benefit as much as any other phytoplankton, as long as these groups can suppress their CCM activity. Species with highly specific RuBisCO and low carboxylation rates require greater investment in RuBisCO to maintain an adequate rate of CO_2 fixation per unit biomass (Raven et al. 2000; Tcherkez et al. 2006). This would not be reduced at increased CO_2, so the additional N costs would still be incurred.

The benefit from a reduction in CCM activity is seen in terms of a saving of resources, such as light and nitrogen (Raven and Johnston 1991). The number of photons required per net C assimilated would be reduced if the costs of CCM activity was reduced (Raven and Johnston 1991). Even with no CCM reduced photorespiration should increase efficiency of C fixed per photon absorbed (Raven et al. 2000; Beardall and Raven 2004). This may be particularly beneficial under low light conditions where energy supply is reduced but growth may be maintained at increased CO_2 due to reduced costs of CCM (Beardall and Raven 2004). In low light environments some algae lack CCMs as they have not been selected for by evolution, due to their high energetic cost, they rely on diffusive CO_2 entry. Increased CO_2 leakage may occur in these species but this is not as energetically wasteful as it is for species actively acquiring DIC (Raven 2003). For species relying on diffusive entry of CO_2 an increase in pCO_2 would increase the rate of carbon uptake and could allow RuBisCO to be saturated for CO_2, without the need of a costly CCM. These species could also benefit from reduced resource allocation to the pathways involved in processing the products of

the oxygenase reactions of RuBisCO. In this case the savings would be in terms of nitrogen, saved by reduced enzyme production (Raven and Johnston 1991). The occurrence of CCMs does not necessarily depend on CO_2 availability.

Emiliania huxleyi is one species which may benefit from increased CO_2 as cells have a low affinity for CO_2 and do not show saturation of photosynthesis below concentrations of ~25 µM dissolved CO_2 (current concentration is ~14µM) (Raven and Johnston 1991). *E. huxleyi* is not typical of coccolithophores in this respect as other species have much higher affinities for CO_2 (Raven and Johnston 1991). It has been suggested that some strains may not possess a CCM (Badger et al. 1998) whilst other studies show a low-affinity CCM (Rost et al. 2002). Coccolithophores may use the CO_2 released during calcification to supply RuBisCO (Buitenhuis et al. 1999), however recent evidence suggests that photosynthesis and calcification are not linked in this way (Leonardos et al. 2009).

1.6 Regulation, Acclimation and adaptation

Phytoplankton are able to adjust their photosynthetic apparatus to maximize their evolutionary success, or fitness in response to changes in the environment (Raven 2003). They may do this by "regulation": changes in catalytic efficiency with no net synthesis or break-down of macromolecules. "Acclimation": the synthesis or break-down of macromolecules, or "adaptation": genetic, heritable changes (Raven 2003). The time scale for implementing these responses clearly varies. Regulation occurs over periods of seconds to ten of minutes, acclimation over hours to days, and adaptation may require thousands of million of years (Raven 2003). The response of phytoplankton to increased CO_2 may occur on all of these scales. Short term changes in maximum photosynthetic rates may be the result of RuBisCO activation and

deactivation, regulatory changes. Acclimation may be seen as a change in RuBisCO content of cells or CCM machinery, and adaptation is responsible for the range of kinetic properties of the different RuBisCOs (Raven 2003). In very short term experiments designed to examine the kinetic properties of carbon acquisition, cells are only able to "regulate" their cellular machinery and not acclimate to the conditions (Raven 2003). The duration of most studies to date, has permitted only acclimation and not adaptation (Hurd 2009), however see Collins and Bell (2004).

1.7 THE EFFECTS OF INCREASED CO_2 ON A RANGE OF PHYTOPLANKTON ATTRIBUTES

This section will summarise the recent literature on the effects of increased CO_2 on the phytoplankton. There are a number of key ways in which increased CO_2 may affect the phytoplankton. If they are carbon limited then photosynthetic parameters and possibly growth may be increased. If they are sensitive to pH changes then calcification may be affected. The evidence is varied and for each of the following areas there is evidence supporting and disputing an effect of increased CO_2. This section covers: specific growth rate (μ) (cell division rate); stoichiometry (carbon: nitrogen ratios); calcification; photosynthesis and primary production; enzyme activities; species composition and succession.

1.7.1 Specific growth rate (μ)

There is a fairly large body of evidence suggesting that growth rates are CO_2 dependent and are reduced at below 10 μM CO_2 (Riebesell et al. 1993; Chen and Durbin 1994; Buitenhuis et al. 1999; Burkhardt et al. 1999a). These levels are rarely encountered in the modern ocean except in intense blooms, however, lower pCO_2 has predominated during the last few million years, especially at the glacial maxima.

At CO_2 concentrations anticipated at the end of this century some species, particularly diatoms have shown increased cell division rates. During an experimental mesocosm bloom a 40% (± 25%) increase in µ of *Skeletonema costatum* was seen at 750 compared to 250 and 400 µ atm (Kim et al. 2006). At 1000 ppm CO_2 a 24% increase in µ of the diatom *Chaetoceros muelleri* was seen (Beardall and Raven 2004). In three separate incubations of summer assemblage diatoms from the Ross Sea, Tortell et al. (2008) observed increased growth rates at 800 compared with 380 ppm CO_2 (Tortell et al. 2008a). However this was not an invariable response, as other natural diatom dominated communities eg. a *Thalassiosira spp.* dominated community from the Californian upwelling region did not show increased µ with the same treatment (Tortell et al. 1997). Of six incubations of coastal Pacific seawater, dominated by large diatoms, five remained unaffected by pCO_2 as low as 100 ppm (Tortell et al. 2000). Two diatoms, *Thalassiosira pseudonana* and *T. weissflogii* showed no increase in µ with increased CO_2 (Pruder and Bolton 1979) (Shi et al. 2009).

The coccolithophore, *E. huxleyi* has been found to show increased, decreased and unaffected cell division rates in response to increased CO_2. It is probable that these differences are strain specific (Langer et al. 2009; Ridgwell et al. 2009). Leonardos and Geider (2005) report significantly increased cell densities of the non-calcified strain PML92A at 2000 ppm compared with 360 ppm CO_2. However, only under particular conditions of, high light intensities (500 µmol photons m^{-2} s^{-1}) and nitrate limitation in continuous cultures. *E. huxleyi* has been found to be unaffected by increases in pCO_2 of up to 1,050 ppm (Buitenhuis et al. 1999; Clark and Flynn 2000; Zondervan et al. 2002; Leonardos and Geider 2005; Riebesell et al. 2007; Feng et al. 2008; Shi et al. 2009). Engel et al. (2005) report lower growth rates of a calcifying strain of *E. huxleyi* at 710 ppm compared to 190 ppm CO_2 in mesocosm enclosures, which normalised to DIC

drawdown, resulted in a 24% decrease in POC. Iglesias-Rodriguez et al. (2008) similarly report significantly reduced growth rates in calcifying *E. huxleyi* at 750 ppm CO_2 compared with 280, 300, 490 ppm but an overall increase in POC. Shi et al. (2009) found a slight increase in growth rate of *E. huxleyi* strain PLY M219 at 750 ppm CO_2 when acid/base manipulation was used but not with CO_2 bubbling.

No effects of increased pCO_2 on growth rates were seen in the cyanobacteria, *Synechococcus* and *Prochlorococcus* in either laboratory (Fu et al. 2007) or mesocsom conditions (Engel et al. 2005). At higher temperatures a synergistic effect of CO_2 was seen to slightly increase the growth rate of *Synechococcus* above that of temperature alone (Fu et al. 2007). An increase in growth rate of up to three fold was seen in *Trichodesmium*, a bloom forming, colonial, nitrogen fixing cyanobacterium at 900 compared to 400 and 250 ppm CO_2. A longer exponential phase was also seen and greater eventual biomass. Nitrogen fixation increased three to four fold in the high CO_2 cultures compared to ambient and low pCO_2 treatments (Levitan et al. 2007). At 1000 ppm CO_2 a 35% increase in growth rate was seen in the chlorophyte *Dunaliella tertiolecta* (Beardall and Raven 2004). In the freshwater microalgae *Chlamydomonas reinhardtii*, *Chlorella pyrenoidosa* and *Scenedesmus obliquus* Yang and Gao (2003) discovered that growth rates increased at relevant levels up to 30, 100 and 60 µM CO_2 respectively. Clarke and Flynn (2000) saw 14-15% increases in µ of the raphidophyte, *Heterosigma akshiwo* and the chlorophyte *Stichococcus bacillaris* when the CO_2 concentration was doubled (20-22% when CO_2 was trebled) but pH was maintained.

1.7.2 Stoichiometry and DIC uptake

According to the Redfield ratio, phytoplankton use the major nutrients, nitrate, phosphate and carbon in an atomic ratio of C:N:P = 106:16:1 (Redfield 1934) cited in (Geider and La Roche 2002). Although the Redfield ratio is a useful concept and may be broadly true in terms of average phytoplankton composition there are many exceptions to the rule. The C:N:P ratios of phytoplankton are dynamic, show diel variation and alter in response to environmental changes. Changes in stoichiometry are seen as one of the few ways that phytoplankton can alter the carbon drawdown, assuming that nutrients are the limiting factor (Doney et al. 2009). Increased CO_2 has been found to increase carbon drawdown, this carbon may be retained or exuded from cells. The C:N ratio is related to the carbohydrate: protein content of the cell. As RuBisCO accounts for much of the N content of phytoplankton, changes in RuBisCO could alter the C:N ratio. Evidence that changes in pCO_2 may alter the phytoplankton stoichiometry has been found in a number of experimental studies. This takes several forms, firstly at increased CO_2 measured C:N or C:P may be higher. This has been found in filtered culture samples (Feng et al. 2008) and in the material which sank to the bottom during a mesocosm experiment (Engel et al. 2005). Secondly, DIC uptake may be higher than the C:N ratio of the filtered material and DIC content of the dissolved organic matter (DOM) can account for (Riebesell et al. 2007). Thirdly, DIC uptake may be higher than predicted by the Redfield ratio and nitrate availability data (Sambrotto et al. 1993; Körtzinger et al. 2001) or a measured nitrate uptake ratio (Engel et al. 2005). When carbon drawdown per unit N is increased at higher pCO_2 this has been termed ‘carbon overconsumption’ (Toggweiler 1993).

When nitrate or phosphate are limiting during the latter stages of a bloom it appears that carbon can still be assimilated altering the C:N ratio (Engel et al. 2004a). The additional

carbon may not be incorporated into cells but exuded as dissolved organic carbon (DOC). It has been estimated that as much as 40% of the organic matter synthesised during a bloom may be lost as exudate, this flocculates and sinks contributing to the biological pump (Antia et al. 1963; Engel et al. 2002). However it may be difficult to distinguish this from viral lysis. In a mesocosm bloom of *E. huxleyi* increased DIC drawdown which could not be accounted for by the difference in growth rate nor the increase in DOC in the surface layer, was seen at increased CO_2 (Engel et al. 2002). Flocs collected from below the surface of the bloom showed increased C:N and C:P, thus suggesting that the missing DIC was incorporated in carbon rich exported material (Engel et al. 2005). Similar increases in DIC drawdown were seen in a diatom and *E. huxleyi* dominated mesocosm, with net community carbon consumption 27% higher at 700 ppm, and 39% higher at 1,050 ppm than at 350 ppm (Riebesell 2007). The C:N ratio was found to be significantly increased from 6 to 7.1 to 8 at 350, 700 and 1,050 ppm CO_2 respectively. In a diatom dominated mesocosm total net production was found to be 72% higher than the theoretical value calculated from the Redfield ratio and dissolved inorganic nitrogen (DIN) decrease (Engel et al. 2002). During the exponential phase C:N were tightly coupled but as the bloom peaked the levels of POC continued to rise and PON did not. The eventual molar [POC]:[PON] increased from 5.7 to 12.4.

Sambrotto et al. (1993) found deviations from the expected carbon production in natural populations from eutrophic regions in the North Atlantic and continental shelf regions of the Bering Sea and Gerlache strait. Based on nitrate availability net organic carbon production was calculated from the Redfield ratio however the measured net organic carbon production was, on average, more than 50% higher.

A transect of the northeast Atlantic Ocean thoroughly examined the carbon and nitrogen pools and fluxes associated with the seasonal cycle (Körtzinger et al. 2001). An increase from 5 to 7.2 in particulate C:N was observed associated with decreasing nitrogen later in the season. The calculated C:N ratio of exported production increased from around 5 in the spring to between 10 and 16 in the post-bloom summer period. This suggests a massive over consumption of carbon by natural communities associated with nutrient limitation with evidence both from measured POC and calculated carbon drawdown. However in natural seawater it is impossible to distinguish phytoplankton from detritus (Flynn et al. 2009).

In laboratory cultures of *E. huxleyi* varied responses have been seen. An increase in C:N from 6.8 at 280 ppm to 8.3 at 750 ppm CO_2 was found in *E. huxleyi* COWP06 (Iglesias-Rodriguez et al. 2008b). Several other studies revealed interactive effects of CO_2 with light and temperature. In a non-calcifying strain of *E. huxleyi*, PML92A, in nutrient limited continuous cultures at high light (500 µmol photons m^{-2} s^{-1}) C:N and C:P increased, with pCO_2 of 2000 compared to 360 ppm (Leonardos and Geider 2005). An increase in POC of 46% due to both increased cell density and cellular organic carbon content was seen (Leonardos and Geider 2005). The extent, of the increase depended on light intensity and the ratio of N:P, no increase in C:N or C:P was seen under low light (80 µmol photons m^{-2} s^{-1}) or nutrient replete conditions (Leonardos and Geider 2005). Similar results were found in a calcifying strain, *E. huxleyi* CCMP 371; C:P was significantly increased at 750 ppm CO_2 compared to 375 ppm with high light (400 µmol photons m^{-2} s^{-1}) in high and low temperature treatments (Feng et al. 2008). Buitenhuis et al. (1999) found C:N ratios in experimental manipulations of *E. huxleyi* to be independent of pH, and of concentrations of any of the carbonate ion species at twice natural concentrations, and at reduced levels.

In cyanobacteria a 20% increase in C:P and N:P was seen at increased CO_2 in *Synechococcus* at 20 and 24°C, with temperature having a smaller effect than CO_2 (Fu et al. 2007). C:N ratios in *Trichodesmium* of 7 at 900 ppm CO_2 were significantly higher than at 400 or 250 ppm CO_2 with an average C:N of 6.5 (Levitan et al. 2007).

In phosphate limited cultures *Skeletonema costatum* showed decreased C:N ratios at the higher pCO_2 concentrations of, 20.6 µmol CO_2 l^{-1} (pH 8) compared to 4.5 µmol CO_2 l^{-1} (pH 8.6) (Gervais and Riebesell 2001). These cultures were manipulated by HCl and $NaHCO_3$ addition and the lower pCO_2 level was consistent with a bloom situation rather than steady state oceanic pCO_2. It has also been found that most significant alterations of stoichiometry in six diatom species and one dinoflagellate species, occurred at CO_2 levels lower than those commonly found in the modern ocean (Burkhardt et al. 1999b). Tortell et al. (2000) saw no changes in C:N of natural diatom dominated phytoplankton communities incubated at 350 and 800 ppm CO_2. There was a significant decrease in C:N at 100 ppm CO_2 which was mirrored by a decrease in the carbohydrate to protein ratio.

It is probable that the differences between results in this section are due to the different measurements described. There is a large dataset describing increased C:N and C:P uptake when nutrients are limiting, in both laboratory cultures and natural communities. Nutrient limitation in nature is common in steady state and blooming assemblages. The excess carbon may be taken up and then possibly exuded. Increased CO_2 may have synergistic effects when for example light (Leonardos and Geider 2005) or temperature (Fu et al. 2007) are altered or may only have effects under certain nutrient regimes (Leonardos and Geider 2005).

1.7.3 Calcification

Increasing CO_2 leads to a decrease in both CO_3^{2-} concentration and the degree of oversaturation of calcite and aragonite in surface waters but an increase in HCO_3^- (Wolf-Gladrow et al. 1999). This may have consequences for calcifying marine organisms however the degree of severity will largely depend on the form of mineral precipitated and the carbon source used. Coccolithophores produce calcite and have been found to use HCO_3^- for calcification (Buitenhuis et al., 1999), thus theoretically they may be unaffected or even benefit from increased HCO_3^- (Iglesias-Rodriguez et al. 2008b). The saturation state for calcium carbonate ($\Omega_{calcite}$) is a measure of its tendency to form or dissolve in a solution. Decreasing carbonate ions in seawater increases the likelihood that calcite will dissolve. The ratio of particulate inorganic carbon (PIC) deposited by calcification, to particulate organic carbon (POC) from photosynthesis is commonly used as a measure of the response to increased CO_2. This will determine the direction of flux of CO_2 in or out of a cell. If PIC:POC is greater than 1 calcifying organisms may act as a source of CO_2, because the ratio of CO_2 released by calcification may exceed that fixed by photosynthesis (Crawford and Purdie 1997).

In 2000 a paper by Riebesell et al. was published in *Nature* with dramatic pictures of malformed coccoliths of *E. huxleyi* and *Gephyrocapsa oceanica* which had been incubated at 780-850 ppm CO_2. Since then a wealth of literature, examining the responses of the coccolithophores to increased CO_2, has been published with widely disparate results. Inter- and intra-species differences have been found, from which generalized responses cannot be drawn (Langer et al. 2006; Ridgwell et al. 2009). Initial experiments consistently showed a reduction in calcification at increased pCO_2. *E. huxleyi* has been the most commonly used species in these experiments, but a number of different strains have been used. In an experimental mesocosm in 2005, Engel et al.

found significant reductions in sizes of both coccospheres and individual coccoliths of *E. huxleyi* at increasing pCO_2 of 190, 410 and 710 ppm. No malformations were seen in the 600 cells examined. A systematic decrease was seen in the PIC:POC ratio with increasing CO_2. Similarly Feng et al. (2008) reported reduced PIC in cultures of a tropical calcifying strain of *E. huxleyi* CCMP 371 when grown under increased pCO_2 at high light at 20^{o}C; PIC was 50% reduced. No obvious malformations were seen in the coccoliths. Zondervan et al. (2001) saw a 25% decrease in calcification and 20% increase in cellular POC with increased CO_2 in *E. huxleyi* strain PML B92/11 (Zondervan et al. 2001). A similar response was seen in the closely related *Gephyrocapsa oceanica* (Schneider 2004) with light regime affecting the degree of response in both species. Calcification was more greatly reduced at high light with increased pCO_2 (Zondervan et al. 2002).

Contrary to the previous evidence, Iglesias-Rodriguez et al. reported a significant increase in calcification and primary production in two strains of *E. huxleyi* COWP06 and 61/12/4 MBA at 750 ppm CO_2. This is consistent with their observations of 40% increases in coccolithophore mass over the past 220 years from deep ocean sediments. PIC, POC, cell volume, lith size and number of detached coccoliths were all increased significantly at 750 ppm compared with 280, 300 and 490 ppm CO_2 but growth rate was reduced. The water chemistry revealed a large reduction in $\Omega_{calcite}$ at increased CO_2 but this was still well above 1, the level at which dissolution would occur. Less than 10% of the available DIC was taken up and the biological effect on pH was less than 0.04 units. Shi et al (2009) also report increases in both POC and PIC in *E. huxleyi* strain PLY M219 at 750 ppm CO_2 in acidified cultures. Langer et al. (2006) observed no significant differences in calcification in *Coccolithus pelagicus* between current at 760 ppm pCO_2. *Calcidiscus leptoporus* showed a calcification optimum curve, with PIC

being reduced at both higher and lower pCO_2 with little change in POC. Even with increased calcification there is no evidence that coccolithophore calcification will act as a net source of CO_2 in the future (Iglesias-Rodriguez et al. 2008b).

1.7.4 Photosynthetic parameters /Primary production

The hypothesis behind many of the studies described here is that an increase in CO_2 may increase primary production and growth. There is some evidence for this with just an increase in pCO_2, and further evidence that pCO_2 may have a synergistic effect with temperature and light. There have been some well thought out experiments examining multiple effects, with increased temperature and pCO_2 referred to as "greenhouse treatments" (Fu et al. 2007; Feng et al. 2008).

Hein and Sand-Jensen (1997) report small but significant increases in ^{14}C uptake in natural populations in the North Atlantic incubated at 36 µM (855 ppm) compared to 10 µM CO_2 (present day). These results were similar in both surface and chlorophyll maximum populations with increases of 15% and 19% respectively. There was no further increase in primary production at 91 µM and there were much greater reductions at 3 µM. CO_2 was altered by manipulating pH with HCl and NaOH. In a series of incubation experiments Tortell and colleagues investigated the responses of natural communities to increased pCO_2. Increases in primary productivity of 10-20% were seen in Southern Ocean diatoms, predominantly *Chaetoceros*, at 800 ppm compared with 380 ppm CO_2 (Tortell et al. 2008a). An assemblage from the equatorial Pacific was incubated at 150 and 750 ppm CO_2. Despite a large shift in species dominance from *Phaeocystis* to diatoms at increased pCO_2 no change in primary productivity or total biomass was seen (Tortell et al. 2002).

E. huxleyi CCMP 371, a tropical calcifying strain, was found to respond to both increased CO_2 alone and when coupled with a temperature increase. The maximum Chl-a normalised light-saturated carbon fixation rate (P^B_{max}) and the affinity of photosynthesis for light (α) values increased with increased CO_2 alone. Light harvesting and PSII efficiency were increased in greenhouse treatments. P^B_{max} was increased by 95% in the low light treatment at increased CO_2 without an increase in temperature. It was further increased in the greenhouse treatment to two and a half times that of the ambient value. α values were almost doubled by increased CO_2 alone at low light and were 4 fold higher than ambient in the greenhouse treatment, POC was not affected (Feng et al. 2008). Nielsen (1995) (Nielsen 1995) found photosynthetic efficiency and maximum quantum yield increased by more than a factor of 2 between 2.4 (ambient) and 12.4 mM DIC in high and low calcite cells of the same strain of *E. huxleyi*.

Four fold increases in P^B_{max} and E_k were seen for *Synechococcus* in greenhouse treatments. A significant increase in the quantum yield of PSII (Fv/Fm) and a small but non significant increase in the maximum yield for carbon fixation (Φ_{max}) were also found (Fu et al. 2007). The results suggest that there is increased light harvesting efficiency and PSII efficiency at high CO_2 and temperature. At lower temperature pCO_2 had no effect on P^B_{max} , therefore the effect may only become apparent if CO_2 or DIC becomes rate limiting at higher temperatures, due to increased enzyme activity (Fu et al. 2007). Despite three to four fold increases in growth rate of *Trichodesmium*, no significant differences were seen in photochemical activity of PSII or in gross oxygen evolution. Levitan et al. (2007) conclude that increased growth rates at 900 ppm were not caused by increased photosynthesis but rather by energy saved by some other process, potentially suppression of CCMs (Levitan et al. 2007).

There appears to be mixed evidence for increased primary productivity in response to increased CO_2. There also appears to be evidence that despite increased growth in some species this is not related to increased primary production.

1.7.5 Enzyme activities and regulation

Enzymes catalyse the many chemical reactions involved in photosynthesis. If increased CO_2 affects photosynthesis it will almost certainly affect the enzymes involved in the photosynthetic pathways. RuBisCO and carbonic anhydrase (CA) are key enzymes in carbon acquisition and fixation. At low pCO_2, cellular concentrations of these enzymes, and transcription of the genes coding for them, are expected to increase. This has been seen in natural diatom dominated communities grown at 100 ppm CO_2 Tortell et al. (2000). The upregulation of RuBisCO and carbonic anhydrase resulted in ^{14}C fixation rates which were significantly higher than communities grown at 350 or 800 ppm CO_2 (Tortell et al. 2000). Over a range of pCO_2: 36, 180, 360 and 1800 ppm large and consistent decreases in both intracellular and extracellular carbonic anhydrase activity was found in *Thalassiosira weissflogii* (similar intracellular carbonic anhydrase results were seen in *Phaeodactylum tricornutum* (Burkhardt et al. 2001)). In higher plants it is well established that an increase in CO_2 often causes a reduction in photosynthetic genes and their associated proteins (Moore et al. 1999; Long et al. 2004). Reductions in RuBisCO protein of up to 40% appear to be regulated by transcription of the small subunit (*rbcs*) (Moore et al. 1999). Changes in carbonic anhydrase and RuBisCO activase expression have also been recorded, the magnitude and direction of all these responses is species specific (Moore et al. 1999). However in *Thalassiosira pseudonana* no differences in *rbcL* gene transciption or RBCL protein were found between cultures incubated at 380 and 100ppm CO_2 (Roberts et al. 2007; Granum et al. 2009). Some phytoplankton have the ability to produce extracellular carbonic anhydrase

(eCA) which converts bicarbonate in the seawater at the cell surface to CO_2 which can then diffuse, or be actively transported into the cell. CA activity is dependent on a higher than equilibrium concentration of the substrate, thus the CO_2 must be removed for further catalysis of HCO_3^- to CO_2. Increased CO_2 should reduce eCA activity, however in incubations of natural diatom dominated communities from the Ross Sea, with pCO_2 ranging from 100-800 ppm little effect of CO_2 on eCA expression was seen (Tortell et al. 2008a) . Extracellular carbonic anhydrase is therefore constitutively expressed by many Antarctic phytoplankton. There was also no change in HCO_3^- uptake, which remained at ~60-90% of total carbon uptake, suggesting that these diatoms use HCO_3^- even when CO_2 is abundant (Tortell et al. 2008a).

1.7.6 Community structure

There is some evidence for changes in the phytoplankton community with increased CO_2. Phytoplankton occupy subtly different niches in the oceans. Within certain species many strains have been found with different optimal requirements of an environmental variable such as light (Rocap et al. 2003). At increased pCO_2, shifts in strains or species more capable of taking advantage of increases in available CO_2 may occur. This may affect biogeochemical cycles and also food web dynamics.

Tortell and colleagues have performed several high CO_2 incubation experiments with natural phytoplankton assemblages from different oceanic regions. In the equatorial Pacific an increase from 150 ppm to 750 ppm CO_2 caused a shift in dominance from the prymnesiophyte, *Phaeocystis* to diatoms (Tortell et al. 2002). In the Southern Ocean they performed two incubations. In the first no change in diatom species composition was seen over an eight day period, *Phaeocystis* was present but not abundant and did not rise to dominance (Tortell et al. 2008a). In the second a change in dominance from thin, pennate to large *Chaetoceros* diatoms was seen with increased CO_2 (Tortell et al.

2008b). Tortell et al. (2008) also carried out underway surveys of the Ross sea and determined that there was no correlation between pCO_2 and species composition in the natural phytoplankton assemblage. pCO_2 levels ranged from 126 ppm to ~380 ppm, undersaturated relative to the atmosphere at all stations.

Three separate incubation experiments set out, specifically, to examine community shifts, in response to increased pCO_2, in spring and summer assemblages from the Norwegian fjords. Very little difference in species composition was observed under present and future CO_2 regimes. *E. huxleyi* was significantly reduced at high CO_2, but the diatom community was not significantly changed (Schneider 2004). Similarly no significant differences in species composition or succession were seen in mesocosm enclosures maintained at 350, 700 and 1,050 ppm CO_2 (Riebesell 2007). An initial bloom of diatoms was followed by an *Emiliania huxleyi* bloom and prasinophytes, dinoflagellates and cyanobacteria rose to dominance successively (Riebesell 2007).

It appears that in general diatoms may be more able to take advantage of increases in CO_2, but this will always depend on the availability of silicate.

1.8 General Conclusions

Recent reviews of the literature have attempted to reconcile the disparity of results described in this section (Ridgwell et al. 2009) and (Schulz et al. 2009). Various theories have been proposed; differences in experimental design and specifically CO_2 manipulation (Iglesias-Rodriguez et al. 2008b); differences in strains within species or their adaptation to decades of laboratory culturing (Ridgwell et al. 2009). Ridgwell et al. (2009) further propose that a calcification optimum may exist for strains of *E. huxleyi*. The choice of strain may therefore result in an up-regulation or down-

regulation of calcification at the same pCO_2 in different strains. Guidelines for future research have been set out to improve coherence of results (Riebesell et al., 2010). The cumulative effects of increased CO_2 in conjunction with other factors, particularly light, may lead to more efficient carbon uptake (Beardall and Raven 2004).

1.9 THESIS AIMS

In this thesis I will describe the experiments I performed to examine the effects of increased CO_2 on the marine phytoplankton. Chapter 3 contains laboratory experiments with *T. pseudonana* and *E. huxleyi*, Chapter 4, a mesocosm in Bergen in the Norwegian fjords and Chapter 5 a short cruise in the oligotrophic Northeastern Atlantic, South of the Canary Islands.

The specific questions addressed by the experiments included in this thesis were:

i. Does specific growth rate increase if more carbon dioxide is available?
ii. Does the C:N ratio increase with more CO_2 available?
iii. Does the expression of RuBisCO or carbonic anhydrase change at increased CO_2?
iv. Do phytoplankton adapt to increased pCO_2?
v. Does primary production increase with increased pCO_2?
vi. Is calcification reduced at lower pH?
vii. Is the community structure altered by increased pCO_2?
viii. Do the RuBisCO selectivity and CCMs have any bearing on the dominance of different groups of phytoplankton?

Laboratory experiments were performed to answer questions related to cellular physiological responses to increased CO_2 (questions: i-iv). Initial batch culture

laboratory experiments examined specific growth rates (μ) of the diatom *Thalassiosira pseudonana* and the coccolithophore *Emiliania huxleyi*, supplied with air with enhanced pCO_2. However the growth of the phytoplankton quickly used CO_2 and the pH increased. To determine μ under steady state increased pCO_2, low cell density semi-continuous cultures were used. These maintained pH by bubbling and daily dilution of cultures with fresh gas-equilibrated media. The experimental design was further developed to maintain pH and pCO_2 in actively growing continuous cultures in order to answer question iv concerning adaptation of phytoplankton to increased pCO_2 conditions. pH was maintained by automatic dilution with fresh, gas-equilibrated media when the pH increased. The diatom, *T. pseudonana* was grown in continuous culture for 3 months under either present day or future conditions of pCO_2, and physiological attributes were monitored. To determine whether heritable, genetic adaptations had occurred, innocula of these cultures were made into both present day and future pCO_2 conditions. If adaptation had occurred over this time period the ability to cells adapted to high pCO_2 conditions to then grow in present day conditions may have altered (Collins 2010).

The mesocosm experiment in Bergen was designed to examine whether community structure altered in response to increased pCO_2. Specific growth rates of the major phytoplankton groups were determined, total C:N, primary production and chlorophyll were measured to answer questions ii and v. Due to the dominance of the coccolithophore *Emiliania huxleyi* in the mesocosms I was able to examine whether calcification was affected (question vi).

The deck incubation experiment in the N.E Atlantic examined community structure and specific growth rates of phytoplankton in a low nutrient environment, the assemblage

was dominated by cyanobacteria and pico-eukaryotes. Both the mesocosm and deck incubation allowed me to address question vii, the hypothesis that phytoplankton with less selective RuBisCO, more reliant on CCMs may benefit more from increased pCO_2.

The results of my research will be discussed in relation to the questions above in the general discussion section, Chapter 6.

Chapter 2.

METHODS

2.1 CULTURE STRAINS

Axenic cultures of the diatom *Thalassiosira pseudonana* CCMP1335 (Coscinodiscophyceae) (Hustedt) Hasle et Heimdal and the cocolithophore *Emiliania huxleyi* CCMP371 (Prymnesiophyceae) (Lohm.) Hay et Mohler, were obtained from the Provasoli-Guillard National Center for Culture of Marine Phytoplankton (CCMP), Maine, U.S.A. *E. huxleyi* strain CCMP1516 was obtained from the Marine Biological Culture Collection, UK.

2.2 CULTURE GROWTH CONDITIONS

T. pseudonana and *E. huxleyi* CCMP1516 were grown in F/2 media (section 2.2.1a) at a constant temperature of 14°C with a light:dark cycle of 16:8 hours, dark from midnight till 08:00. Stock cultures were maintained by sub-culturing into fresh media approximately every 14 days. *E. huxleyi* CCMP371 was grown in F/50 media (section 2.2.1b) at 22°C with a 16:8 hour light:dark cycle. Cells were sub-cultured every 7 days. Light was provided by white fluorescent tubes, giving a photon flux of at 100 µmol m^{-2} sec^{-1} at the surface of the culture vessel.

2.2.1 Media, F/2 (+Si) and F/50

F/2 is a culture medium based on seawater which is supplemented with nutrients (Guillard and Ryther 1962). Seawater was collected from the L4 site 14 miles off the coast of Plymouth, UK. This was filtered through a Sterivex-GP Sterile Vented Filter Unit, 0.22 µm (Millipore) and stored in the dark at room temperature. Filtered seawater

was autoclaved at 121 °C for 90 minutes, in <6 litre quantities. Before inoculation, the seawater was allowed to cool and reabsorb gases from filtered air in a sterile flow hood for 24 hours. Once cooled sterilised nutrients were added in a laminar flow hood. The following nutrient additions were made to each litre of autoclaved seawater: 1ml of a stock solution of 75 g l^{-1} $NaNO_3$ dissolved in deionized water, yielding a final concentration of 8.82 x 10^{-4} M, 1ml of 5 g l^{-1} NaH_2PO_4 H_2O, in de-ionized water, final concentration, 3.62 x 10^{-5} M, 1 ml of F/2 trace metal solution and 500µl of vitamin solution were added aseptically. For diatoms F/2 + Si was made by adding 1 ml of 30 g l^{-1} Na_2SiO_3 $9H_2O$ dissolved in de-ionized water, final concentration 1.06 x 10^{-4} M. F/50 was prepared as F/2 but with 40 µl of sterile nutrients and trace metals and with 20µl of sterile vitamins.

2.2.2 Axenic cultures

Cells were checked for bacterial contamination on a regular basis by staining with Sybr Green and observation with a Nikon diaphot microscope with dark field filter. If cultures showed signs of contamination, the bacteria were killed by antibiotic treatment. 0.5-2ml of dense cells were washed and treated with 1mg ml^{-1} Ampicillin followed by a cocktail of antibiotics that targeted gram negative bacteria: 0.1 mg ml^{-1} Kanamycin, 4.8 mg ml^{-1} Tetracycline, 1.2 mg ml^{-1} Chloramphenicol. Flow cytometry was used to assess the health of the cells with chlorophyll per cell and tight clustering of the population in the same location as an untreated control taken as a sign of good health. The full procedure followed is outlined below.

Cells were transferred to fresh media (F/2 + Si) and allowed to grow for several days. They were washed by centrifugation at 1000 rpm for 1 minute and supernatant removed. 10 ml fresh media was added and cells were spun down again for 1 minute at 1000rpm.

Cells were re-suspended in 10 ml fresh media. Cells were spun down for 1 minute at 1000 rpm and supernatant removed. Ampicillin was dissolved in 20 ml distilled water and filter sterilised before dilution with sterile F/2. The following dilutions were used: 1, 0.5, 0.25, 0.1 and 0.05 mg ml^{-1} in 10 ml F/2. The washed cells were incubated in the media for 48 hours in the light at 14°C.

Cell health was assessed by flow cytometry. Cells appeared healthy in all Ampicillin concentrations so cells were taken from the 1mg ml^{-1} treatment. Using aseptic techniques and sterile centrifuge tubes, these cells were spun down for 1 minute at 1000 rpm. 10 ml fresh media was added and cells were spun down again for 1 minute at 1000 rpm. Cells were re-suspended in 10 ml F/2 with a range of concentrations of Kanamycin, Tetracycline and Chloramphenicol (μg ml^{-1}) (**Table 2.1**). Kanamycin and tetracycline were dissolved in 20 ml distilled water and chloramphenicol in 20 ml 100% ethanol, filter sterilised and then added to sterile F/2 and made up to 1 litre. Cells were left in bright light for 48 hours at 14°C. Flow cytometry showed the 100μg ml^{-1} Kanamycin treatment to have the highest red fluorescence per cell so these cultures were assumed to be healthy and were retained as stock cultures. Cells were washed by centrifugation and re-suspended in fresh F/2.

Table 2.1 Concentrations of gram negative antibiotics used in combination for treatment of infected *T. pseudonana* cultures.

Kanamycin	1000	500	250	100	50	25
Tetracycline	48	24	12	4.8	2.4	1.2
Chloramphenicol	12	6	3	1.2	0.6	0.3

2.3 EXPERIMENTAL PROCEDURES

2.3.1 Acclimation

All cells were acclimated to experimental conditions for >3 days prior to the start of each experiment.

2.3.2 Bubbling of cultures

For all laboratory experiments and the deck incubation (Chapter 5) a pre-mixed cylinder of air with a certified concentration of 760 ppm CO_2 was used (BOC, Special products, Guildford, UK). Gas was passed through a 0.3 µm Whatman HEPA-VENT™ 0.3 µm filter and supplied to the cultures at a rate of around 40 ml per minute with sintered glass diffusers (Dixon glass, Beckenham, UK). This created small bubbles which maximised gas absorption. For the control cultures ambient air of pCO_2 was supplied using a small air pump equipped with a Whatman HEPA-VENT™ 0.3 µm filter.

2.3.3 Reservoirs of pre-equilibrated media

Media (section 2.2.1) was bubbled with 0.3 µm filtered air for several days. The pH was monitored and once it reached 8.2 aeration stopped. Half the media was then bubbled with the 760 ppm CO_2 in air gas mix until the pH reached 7.8. The equilibrated media was stored in 5 litre vessels aerated with the appropriate gas mix at 14°C.

2.3.4 Buffers

Buffers supply positive and negative ions, hence reducing pH change on the addition of H^+, so maintaining pH around the pK_a. Tris (hydroxymethyl) aminomethane (tris) was dissolved in F/2 media at various concentrations. The solution was titrated with 1M HCl until the required pH was reached and solutions made up to the final volume with

F/2. The media was autoclaved and allowed to cool and re-absorb gases in a sterile flow-hood for >24 hr.

2.3.5 Semi-continuous cultures

To control pH without the use of acid/base or buffers low cell density cultures were diluted daily with fresh pre-equilibrated media. Reservoirs of pre-equilibrated media were prepared as in section 2.3.2. For initial experiments, half the culture volume was removed and an equal volume of fresh media added. For more refined experiments, cells were counted either on the Coulter Multisizer II Coulter counter (Beckman Coulter, High Wycombe, UK) or FACScan benchtop flow cytometer (Becton Dickinson, Oxford, UK) equipped with 15 mW lasers exciting at 488 nm and standard filter setups. The volume of culture required to maintain the cell concentration at 10^5 cells ml^{-1} was calculated. The necessary volume of culture was then replaced with fresh media.

2.3.6 Continuous cultures

To maintain cultures for longer time periods, in a more stable pH environment an automated continuous culture system was set up. This also reduced the time consuming task of twice daily cell counting. The system used an Aquatronica, aquarium control system (Aquatronica, Cavriago, Italy) in control pH. Six cultures were maintained, three at increased CO_2 and three at ambient CO_2 levels (**Fig. 2.1**). A control unit (ACQ001) was attached to pH probes (ACQ 310-pH), within the cultures and peristaltic pumps (ACQ450). When the pH rose above a designated value, the pumps were activated and fresh pre-equilibrated media (section 2.3.3) was supplied to the vessels. 6 x 2 litre glass vessels with 4 ported lids were used in which to grow the continuous cultures. The cultures were gently aerated at a rate of approximately 40 ml min^{-1}. Gas

(section 2.3.2) passed through a 0.3 µm filter and was delivered to the bottom of the vessel with a sintered glass diffuser to maximise aeration.

Prior to the experiment the 350ml level of the vessels was marked. Waste tubes were then suspended at this level and attached to polyethylene containers of 20 litre capacity. The gas entering the experimental vessel forced culture up the waste tube when the volume exceeded 350ml. The culture and gas passed up the waste tube and into the waste vessel. The gas was allowed to escape via a second port in the waste vessel equipped with a 0.3 µm filter. Each vessel contained a magnetic bead and the six cultures were placed side by side on magnetic stirrer plates. The experimental system was kept at 14°C with a light:dark cycle of 16:8 hours. Prior to the experiment a light probe was inserted into the centre of each empty vessel, vessels were aligned such that the light was 60 µmol $m^{-2}sec^{-1}$ at this position, in each vessel. Media and waste reservoirs were replaced every two to three days as required. These procedures were carried out in situ using a Bunsen burner to flame the glass ends of the connector tubes and provide a sterile environment. Aseptic sampling procedures were used to take samples from continuous cultures by transporting the whole system to a sterile flow hood.

2.3.7 Evaluation experiments

Following growth for 3 months in the continuous culture experimental system (section 2.3.5), an evaluation of the effects of high CO_2 treatment was performed. Two separate experiments were performed, one with larger volumes to produce biomass for analysis and some with more smaller volumes for greater statistical power.

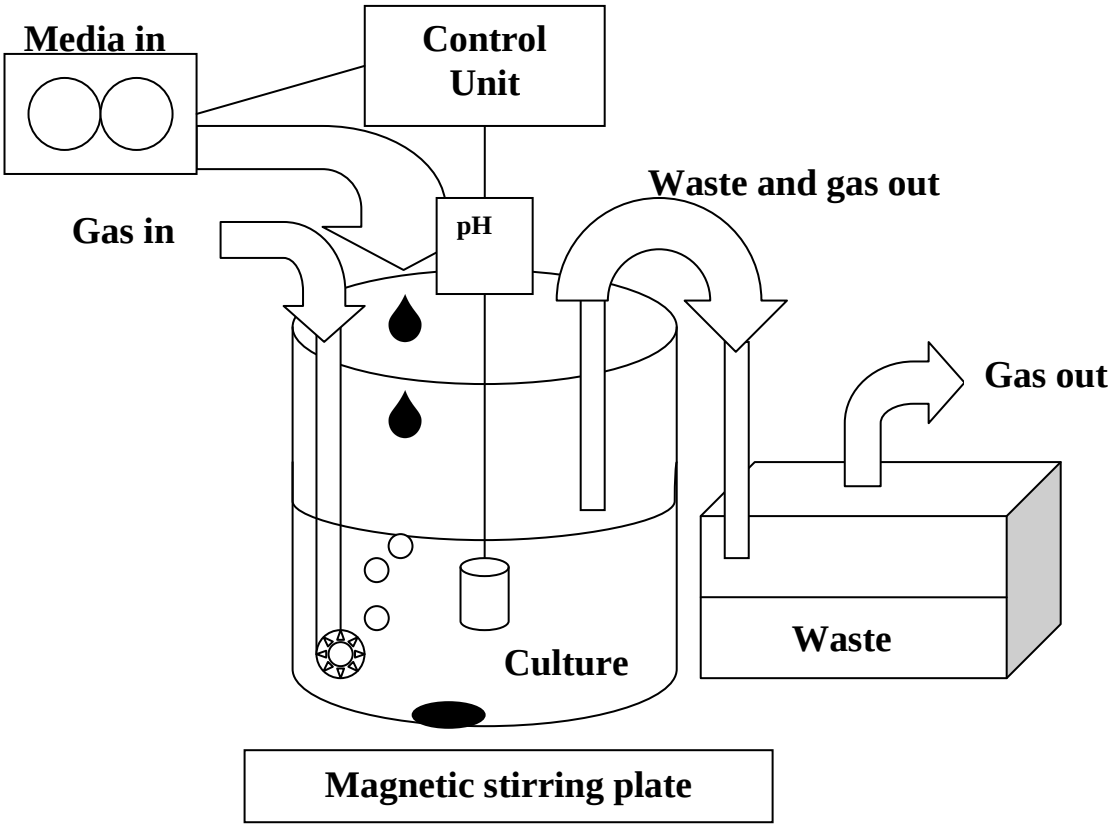

Fig. 2.1 Design of a single continuous culture vessel. Six of these were maintained attached to a single control unit.

2.3.7 .a 900ml bottle experiment

An inoculum of 1x 10^5 cells was made into each of twelve vessels containing 900ml of pre-equilibrated media (section 2.3.3). Cultures were maintained under the same light and temperature conditions as during the long-term growth period and were aerated with either air or high CO_2 air mix. Cell numbers were measured daily by Coulter counter and pH was assessed using a pH meter. Cells reached stationary phase very rapidly, therefore two dilutions were made to refresh the nutrients and stimulate continued growth. On the final day cells were harvested for C:N analysis, flow cytometry and gene expression. All cultures were growing exponentially at this time.

2.3.7 b 1.5ml plate experiment

From each of the six continuous cultures, six replicate 1.5ml cultures were grown in polystyrene 24 well micro-titre plates (NUNC, Fisher scientific, UK). Each well was filled with pre-equilibrated media (section 2.3.3) and an inoculum of 1 x 10^5 cells was added, the total volume being 1.5 ml. The plates, without lids, were placed in glass chambers flushed with the correct gas mix. The chambers were incubated at the same conditions as the continuous cultures (section 2.3.5). The plates were read in a Bio-Tek ELx800 plate reader (Bio-Tek, Potton, UK) at 590 nm using Bio-Tek KC Junior software.

2.4 MEASUREMENTS

2.4.1. Coulter Counter

Cell counts were necessary for calculating cell division rates. These were interesting in themselves and also many other variables altered with specific growth rate. The Coulter Multisizer™ II Coulter Counter® (Beckman Coulter, High Wycombe, UK) estimates cell number by drawing them in suspension through a small aperture in the instrument. An electric current flows between two electrodes on either side of the aperture. As a particles passes through the orifice, they displace their own volume of conducting fluid. This is converted to a voltage pulse, from which, both the number of cells and their volume can be determined. The Coulter Counter is not capable of counting picoplankton or discriminating different species of overlapping sizes. It is less accurate than the flow cytometer because particles of debris, bacteria and air bubbles cannot be distinguished from cells.

The Coulter counter was used to measure live cells. For accurate counts the concentration was 2,000-15,000 cells ml^{-1}. At higher concentrations, there is inaccuracy

due to coincidence, when a higher proportion of cells pass through the aperture together. Samples usually required a 1/20 dilution with a total volume of 20 ml made up with fresh media or filtered seawater. 3 x 500 µl samples were analysed and a mean of these was taken. For *T. pseudonana* analyses cells of between 2.799 and 8.370 µm were recorded. The specific growth rate per day (µ) was calculated using **equation 2.1**. where *N* is the number of cells and t is time in days.

$$\mu = \mathrm{LN}(N_t/N_0)/t \qquad [2.1]$$

2.4.2 Analytical flow cytometry (AFC)

Flow cytometry was used to count and analyse the laboratory cultures. The side scatter and fluorescence per cell were examined to determine whether treatment affected the size or fluorescence of the cells. In Bergen, flow cytometry was used to separate different groups of phytoplankton according to their scatter and fluorescence properties. The cruise samples were analysed by flow cytometry and indicated three groups of small cells which appeared to be cyanobacteria. These different aspects of flow cytometry will be discussed in the following sections.

A Becton Dickinson FACScan benchtop flow cytometer (Becton Dickinson, Oxford, UK) fitted with 15 mW air cooled lasers exciting at 488 nm and standard filter setups was used. The flow cytometer aligns cells in solution and they are passed in a narrow stream through the laser beam. The maximum number of particles that can be analysed is approximately 1,000 sec^{-1}. The flow rate for analysis was approximately 200µl min^{-1}. Particles were analysed for two properties, light scatter and fluorescence. The light scattered by each particle is related to the particles' refractive index, size and shape. Particles containing fluorescent compounds (in this case chlorophyll) will emit light

(fluoresce) at a longer wavelength than that of the light absorbed. For example, blue light, with a wavelength of 488 nm, is absorbed by chlorophyll and red light, with a wavelength of 690 nm, is emitted. The scatter and light pulses are detected by photodiodes or photomultipliers and converted to digital signals (Marie et al. 2005). CELLQuest v 3.0 software (Becton Dickinson) was used to analyse the data. Cytograms, which are dot-plots with data points for each individual cell (**Fig. 2.2**) allow groups of cells to be selected according to their fluorescence and scatter signals and the geometric means for each variable is calculated.

Laboratory samples and those taken from the mesocosms were counted live. In the laboratory samples were maintained under experimental conditions of light and temperature until analysed. Samples from the Tall Ships cruise incubation were fixed with 1% formaldehyde. They were returned to the UK on dry ice, stored at -80°C and analysed within one month. Where dilution was necessary, samples were diluted with filtered seawater. Three samples were always analysed for each measurement and the mean was calculated. The flow rate was calibrated using fluorescent microspheres of a known concentration, Beckman coulter flow set fluorospheres.

2.4.2.a Side scatter and forward scatter

Forward scatter detectors are located at 180^{o} and side scatter at 90^{o} to the light source. Both are related to cell size but side scatter is more influenced by the cell surface and internal cellular structure (Marie et al. 2005). In diatoms and coccolithophores light scatter would be related to external rather than internal structure due to the presence of the silica or calcium carbonate shells. Geometric means were calculated for scatter and auto-fluorescence readings because it is more robust than the arithmetic mean, being less affected by outliers.

2.4.2.b Auto-fluorescence

The fluorescence emitted by individual cells at particular light wavelengths can be monitored by the flow cytometer. This gives information related to the concentration of different pigments within the cells. This information can be used to separate different groups of phytoplankton (section 2.4.2.3), to judge whether cells are healthy and to examine possible changes in their pigment content. Whilst the fluorescence emitted by individual cells is a useful tool for determining the relative health of cells care must be taken in interpretation of this data (Kruskopf and Flynn 2006).

2.4.2.c Separating different groups of phytoplankton

It is possible to identify populations of cells that have similar properties on the basis of light scatter and/or fluorescence properties. For example *E. huxleyi* cells can be distinguished from other nanophytoplankton by their high side scatter signals compared to other cells with similar levels of red fluorescence. In Bergen flow cytometry was performed by Andy Whiteley, CEH, Oxford and Isabel Mary, NOCS. Fixed samples from the deck incubation on STS Lord Nelson were analysed in Plymouth. Three separate groups were distinguished with fluorescence and side scatter properties which were suggestive of *Synechococcus* and *Prochlorococcus* populations. *Synechococcus* contains high concentrations of the pigment phycoerythrin, which fluoresces at a wavelength of 570 nm (orange light). This was used to distinguish between the two groups of cyanobacteria. Orange fluorescence was plotted against side scatter; these data points were identified, counted and marked (**Fig. 2.2**). A plot of red fluorescence against side scatter was then created in which both *Synechococcus* and *Prochlorococcus* co-occurred. The marked cells were removed leaving the *Prochlorococcus* cells to be counted. Two groups of *Synechococcus* were distinguished by the different intensity of red fluorescence. These were referred to as ‘bright’ and ‘dim’ *Synechococcus*.

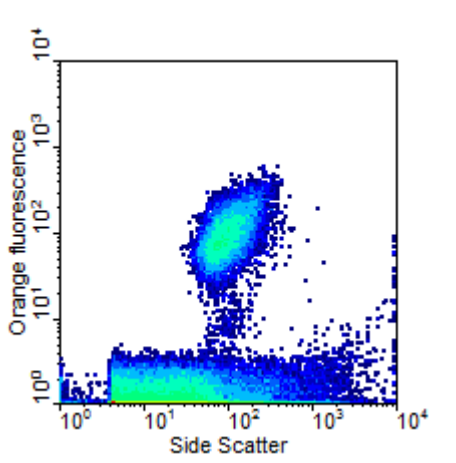

Fig. 2.2 Flow cytometry plot with a population of *Synechococcus* cells easily distinguishable by their orange fluorescence and side scatter properties.

2.4.3 Satlantic FIRe Fluorescence Induction and Relaxation system

Fluorometry provides information concerning the flow of electrons through PSII which is indicative of the overall rate of photosynthesis. In culture experiments, Fv/Fm, the ratio of variable to maximum fluorescence and $\sigma_{PSII,}$ the efficiency of light utilisation for photosynthesis in open PSII reaction centres were measured using a SATLANTIC FIRe, Fluorescence Induction and Relaxation, system (Satlantic, Halifax, CA). Fv/Fm is the quantum efficiency of photochemistry in Photosystem II (PSII) and σ_{PSII} the relative functional absorption cross section of PSII.

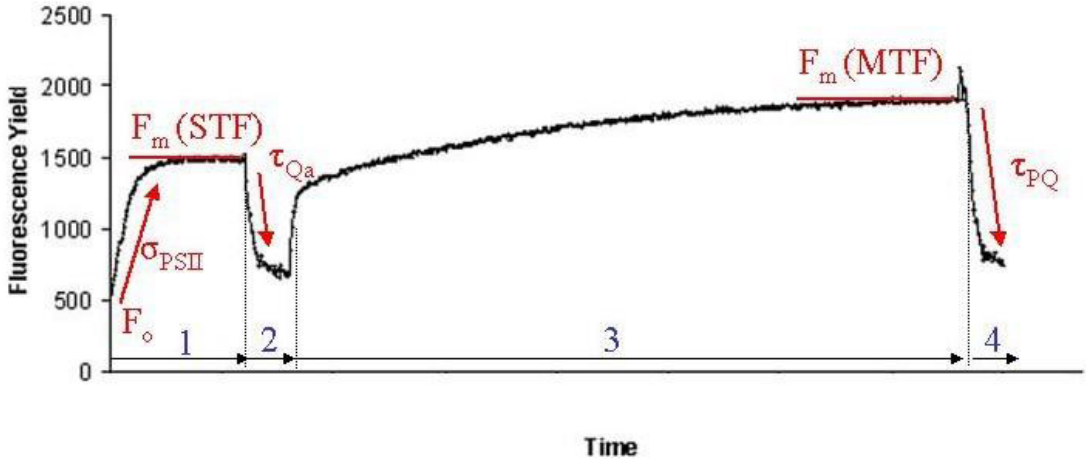

Fig. 2.3 An example of the FIRe measurement protocol (Satlantic)

Samples were held in the dark for a period of 30 minutes to allow all PSII reaction centres to open (F_o). 3ml samples in a quartz cuvette were loaded in the dark and were diluted with fresh F/2 media if necessary. A blank was run using 0.2 µm filtered sample. The samples were subjected to an initial short strong pulse of high luminosity blue light (450 nm with 30 nm bandwidth) lasting 100µs, the single turnover flash (STF). This cumulatively saturates PSII and provides an estimate of maximum (F_m) fluorescence. The fluorescence signal is isolated by red (678 nm, with 20 nm bandwidth fluorescence) interference filters and detected by a sensitive avalanche photodiode module. The signal is amplified and digitised by a 12 bit analog-to digital converter. From these signals the dark-adapted, minimal, level of fluorescence (F_o) is measured when the light is turned on and maximum fluorescence (F_m) measured following the STF. The quantum efficiency of photochemistry (Fv/Fm) is calculated from $(F_o\text{-}F_m)/F_m$. The relative functional absorption cross section of PSII (σ_{PSII}) is also obtained from the STF, as the slope of the initial increase in fluorescent yield (**Fig 2.3**). The Gain setting was varied according to the intensity of the fluorescent signal in each sample, related to biomass. A sample delay of 500 miliseconds was used to allow the F_o value to recover, this is the time interval between consecutive acquisitions. Thirty sample acquisitions were made from which mean values were calculated. The STF lasted for 100 µs. Fluorescence was then allowed to relax using a sequence of 60 weak modulated pulses with an initial interval of 60 µs (STRI). This ensured that fluorescence reached a low plateau before the beginning of the multiple turnover flash. The relaxation kinetics of fluorescence yields reflects the rates of electron transport on the acceptor side of PSII and between PSI and PSII. The multiple turnover flash (MTF) lasted for 600 millliseconds, this is much longer than the 20 second flash recommended in the manual but is optimised to saturate the fluorescent yield for *E. huxleyi*, there were 60 pulses (MTRP) with an interval of 100µsec (MTRI) (Satlantic).

2.4.4 C:N

Alterations in the C:N ratio are an important mechanism, by which phytoplankton could increase carbon drawdown in a high CO_2 world. Carbon to nitrogen content and ratios of phytoplankton cultures and environmental samples were analysed using a Thermoquest Flash EA1112, elemental analyser. All samples were filtered through ashed 25mm GF/C glass fibre filters (Whatman) which had been heated at 500°C for 12 hr in a muffle furnace to remove all traces of carbon and nitrogen. In culture experiments, sample volume was adjusted to yield approximately 7µg of nitrogen per sample. *T. pseudonana* at 14^{o}C contains approx 1.2 pg N cell^{-1} (Berges et al. 2002). Cells were counted prior to filtration and the exact volume required was filtered, in duplicate, onto ashed GF/C filters. The filters were stored at 60°C until analysed. Sample preparation involved carefully folding the filters, which were packaged in small squares of pre-ashed tin foil cups. The samples were loaded into the instrument carousel which automatically fed them into the elemental analyser. The instrument was calibrated using acetanilide. This contains 10.36% N, 71.09% C. To calibrate the instrument, ten standards were prepared containing between 0 and 2 mg acetanilide: 65 µg, 150 µg , 278 µg , 405 µg , 575 µg , 712 µg , 958 µg , 1005 µg, 1747 µg and 1748 µg. Six of the standards were used for the initial calibration of the analyser, and four were analysed during the run as an internal standard to check accuracy. I analysed the culture samples but the Bergen mesocosm samples were analysed by Bob Head at Plymouth Marine Laboratory.

2.4.5 Total Chlorophyll

During the Bergen experiment, chlorophyll was analysed fluorometrically with a Turner designs fluorometer using the method of (Holm-Hansen et al. 1965). Samples (100 ml) were filtered through 25 mm GF/F glass fibre filters (Whatman), and extracted at 4°C in

90% acetone for >4 hours before analysis in the fluorometer. The data were used to give an indication of phytoplankton growth during the experiment. Since these were only relative fluorescence values, a calibration was performed following the spectrophotometric method described in Strickland and Parsons (1968). Several samples of 250-500ml were taken from the mesocosms in the mid-exponential growth phase and filtered through 47mm diameter GF/F filters. Chlorophyll extraction was performed as outlined above with 5ml acetone. The extinction of the extraction was measured in a spectrophotometer at wavelengths of 665 and 750nm. At 665 nm, maximum chlorophyll and phaeopigment absorption occurs. At 750 nm chlorophyll absorption will be negligible so this acts as a blank for the reagent. Two drops of 1M HCl were then added to convert all chlorophyll molecules to phaeopigments by removing the magnesium ion from the tetrapyrrole ring of the chlorophyll molecule. Samples were re-analysed at 665 and 750 nm. The difference between the absorbance readings before and after acid at 665 nm was corrected for any change in the absorbance of the reagent due to acid at 750 nm. The concentration of chlorophyll was then determined by the following equation:

$$\text{Chlorophyll (mg m}^{-3}) = \quad 26.7(a-b)\, v/\, V\, p \qquad [2.2]$$

Where a= 665 (before acid) – 750 (after acid); b = 665 (after acid)-750 (after acid); V is the volume filtered (l); v is the volume of extract (ml); p is the pathlength of the cuvette (cm). The analysis provides an absolute concentration of chlorophyll in mg m^{-3}. Samples from the same acetone extraction were analysed using the Turner designs fluorometer to produce a calibration calculation that was used to convert relative fluorescence units of the fluorometer to quantitative chlorophyll values (mg m^{-3}).

2.4.6 Scanning electron microscopy (SEM)

In the Bergen experiment, daily samples were taken for SEM analysis of the phytoplankton population to determine whether any change in size or malformation of coccoliths occurred at increased CO_2. Each day, samples were taken from each of the six bags and the fjord at 10:00 local time prokaryotic sampling. Four litre water samples were passed through 110 mm GF/C glass fibre filters (Whatman) as a pre-treatment for metagenomic analysis. Since the filters were not required for metagenomics, they were stored for subsequent SEM by snap freezing in liquid nitrogen, kept at -80^{o}C and returned to the UK on dry ice. To ascertain that this had not damaged the cells 2ml samples of fresh *Emiliania huxleyi* strain 371 culture were filtered onto Nuclepore 0.2µm filters. Six filters were allowed to air dry, three were placed in liquid nitrogen for 2 minutes and then air dried again. These filters were examined by the method described for the Bergen samples. Close observation revealed superficial cracking of the surface of the liths but this was present in both frozen and non-frozen samples and was probably an artifact of the gold sputtering process. There were no obvious differences between frozen and non-frozen samples and I concluded that it was appropriate to examine with the SEM, the samples from the Bergen experiment that had been frozen in liquid nitrogen and stored for several months.

SEM preparation involved cutting 2 cm^2 pieces of the filter, which were placed in 10 ml sterile F/2 media for 5 min to resuspend the phytoplankton from the surface of the filter. The solution was then gently vacuum-filtered through a 20 µm Nuclepore filter using a syringe. This removed glass fibres but allowed eukaryotic cells to pass through. 2 ml aliquots of the phytoplankton suspension were gently filtered onto 0.2 µm Nuclepore filters, air dried for at least 12 hours and stored in a desiccating cabinet until analysis.

Critical point drying was assessed as an alternative method. A trial batch of samples was critical point dried by dehydration in a series of ethanol dilutions: 30%; 50%; 70%; 90%; 100% and 100% again. Samples were dried in 100% ethanol in a Samdri 780. However, the results of critical point drying were no better than the air dried samples, probably due to the robust nature of the calcium carbonate coccospheres, so all further samples were air dried. After drying, small pieces of filter were mounted on stubs and sputter coated with gold in an EMITech K550. The samples were viewed with a JEOL 5600 scanning electron microscope at the University of Plymouth electron microscope unit.

Detailed analysis of the coccolith structures was performed using image analysis techniques and the Image-Pro®PLUS software package. The parameters measured were: lith width, length and area; central element length, width and area; spoke number, width and length and the width between spokes. As many measurements as possible were made for each image, but this varied between samples, due to the overlapping of liths.

2.4.7 pH

pH was measured using a Mettler Toledo MP220 pH meter Calibrated with pH 4, 7 and 10 standards. pH measurements in seawater are not very accurate when calibrated with standard buffers but give an indication of pH for experimental purposes. The differences between the dilute buffers prepared in distilled water and the relatively concentrated seawater cause a departure from the pH scale. Critical measurements were calculated from measured and extrapolated total alkalinity (TA) and fCO_2 measurements by Dorothee Bakker using CO2SYS. This is a program which calculates the remaining variables of the carbonate system for a given temperature and pressure when two variables are entered (Pierrot et al. 2006). The calcite saturation state was

also calculated from these data using CO2SYS. For laboratory experiments pH was used to determine whether media had equilibrated with the certified gas mixtures. The cultures were supplied with a known, accurate concentration of CO_2.

2.4.8 Salinity and Temperature

In Bergen salinity and temperature were measured with a YSI conductivity, salinity and temperature meter supplied by the University of Bergen.

2.4.9 Measuring primary production and photosynthetic ability

Primary productivity of the phytoplankton community in the Bergen mesocosm was measured by Dr. Ian Joint using the ^{14}C technique (Joint and Pomroy 1983). This method measures the assimilation of radioactive bicarbonate and its incorporation into organic matter (POC) by phytoplankton. Samples were taken pre-dawn to ensure that deeper water samples were not light-shocked. Aliquots were placed in 60ml polycarbonate bottles and 370 kBq ^{14}C- sodium bicarbonate ($NaH^{14}CO_3$) was added to each sample. Samples were incubated in triplicate in the fjord adjacent to the mesocosms, at 5 depths between the surface and 5 metres for a 24 h period. At the end of the incubation period, samples were filtered through 0.2µm Nuclepore filters, exposed to fuming HCl to remove unfixed ^{14}C, and dried in a dessicator. The ^{14}C content of each sample (disintegrations per minute – dpm) was measured in a scintillation counter. Primary production was calculated as:

$$P = R_L \times [CO_2] \times 1.05/ (R \times t) \qquad [2.3]$$

P = Production; R = dpm added, R_L = dpm of light bottle samples, $[CO_2]$ = concentration of total CO_2 in sea water (analysed for each sample by Dorothea Bakker,

UEA); t = incubation time. The factor 1.05 was used to account for the discrimination by the carbon fixation process (principally RuBisCO) against ^{14}C isotopes.

2.4.10 pCO_2 and total alkalinity

The filtrate (100 ml) from the chlorophyll samples was fixed with 50µl mercuric chloride for subsequent determination of total alkalinity. Total alkalinity and pCO_2 were measured by Dorothee Bakker (UEA).

2.4.11 Nutrients

Dr. Ian Joint analysed the nutrients at Bergen. Dissolved nutrient concentrations were determined within 4 hours of sampling using colorimetric methods. Nitrate and nitrite were analysed using modifications of the methods of Brewer and Riley (1965), and phosphate by the method of Kirkwood (1989).

2.4.12 Pigments

Samples for pigment analysis were obtained by vacuum filtering one litre volumes of seawater through 25 mm GF/F filters. Filters were immediately transferred to liquid nitrogen and stored at -80°C. They were returned to the UK on dry ice. High performance liquid chromatography (HPLC) pigment analysis (Jeffrey et al. 1997) was performed by Carole Llewellyn, PML

2.4.13 Phytoplankton identification

100 ml water samples were fixed with 0.5 ml Lugol iodine solution. Samples for one mesocosm for each treatment were analysed at PML by Claire Widdicombe.

Sub-samples of 25 ml were settled for >24 hours and analysed by settlement microscopy at x 400 magnification for flagellates and x 200 for all other groups. Cell

volumes were calculated using simple geometric shapes and cellular carbon calculated using the equations of Menden-Deuer and Lessard (2000).

2.4.14 Gene expression as determined by quantitative RT PCR

2.4.14 a. Introduction

The effect of high CO_2 on phytoplankton cultures was investigated by a number of methods, including qRT-PCR, which was used to quantify transcription of several key genes in photosynthesis and carbon acquisition through changes in mRNA. The assay examined whether the genes of interest were up or down-regulated at increased CO_2 compared to present day concentrations. The genes investigated were four copies of carbonic anhydrase (CA1-4) and the RuBisCO small subunit (*rbcs*). A relative assay design was employed using two housekeeping genes as endogenous controls. Shifts in gene expression may not necessarily equate to changes in the activity or concentration of intracellular enzymes, since post-transcriptional and translational controls may affect activity. However, transcription is a useful indicator of response to the treatment at the molecular level. Analyses were performed on samples from the continuous cultures exposed to increased CO_2 for approximately 3 months and from the subsequent evaluation experiment.

2.4.14 b. Quantitative RT- PCR

Real-time polymerase chain reaction (PCR) is also known as quantitative reverse transcription PCR or qRT-PCR. The following paragraph briefly summarises the procedure, which will then be explained in more detail in each section. Cells were harvested and RNA extracted with as little change and degradation as possible. The messenger ribonucleic acid (mRNA) was isolated from the total RNA and treated with DNAse. RNA was quantified and a reverse transcription step carried out to produce

complementary DNA (cDNA) from the mRNA. The cDNA was used as the template for the real time PCR. Several procedures were necessary to validate and optimize the assay. The polymerase chain reaction was followed in real time with the aid of a fluorescent probe, in this case SYBR® Green I Dye. This dye binds to double stranded DNA and the intensity of the fluorescent signal increases as the cDNA is amplified by the polymerase chain reaction. Typically 40 cycles of amplification are used with primers specific to genes of interest (GOI) and housekeeping genes. When the fluorescent intensity was plotted against the reaction cycle an exponential curve was produced. The amplification cycle at which the signal reaches a predetermined threshold level is know as Ct and is the value that is used to determine relative changes in abundance of the cDNA and thus the mRNA. The Cts for the genes of interest were examined in relation to that of the housekeeping genes.

Housekeeping genes are endogenous reference genes which should not fluctuate under the experimental conditions. Commonly used housekeeping genes are actin, glyceraldehyde-3-phosphate dehydrogenase, ribosomal genes and the elongation factor 1-α (EF1-α) (Nicot et al. 2005). The cycle at which the fluorescent signal reaches the designated threshold (Ct) relates to the initial amount of cDNA of the gene being examined. A greater initial amount will reach the threshold level sooner giving a lower Ct value. The Ct of the gene of interest is expressed as a relative value using the housekeeping genes to normalise the Ct value (ΔCt). The normalised Ct values, ΔCt, of the high CO_2 and present day treatments may then be compared with each other, the difference is known as ΔΔCt. The methods of qRT-PCR data analysis are frequently refined and it has been recommended that the efficiency of each reaction is taken into account. The efficiency can be calculated fairly simply from standard curves for each gene of interest and the results can be weighted accordingly. Data was analysed using

the REST software package. A fuller discussion of the experimental design of qRT-PCR analyses will be covered in the final discussion.

2.4.14 c. Assay design

The assay was designed as a relative quantification experiment using actin and elongation factor 1-α (EF1α) as endogenous controls or housekeeping genes against which to measure the expression of genes of interest.

2.4.14 d. Primer design

Primers were designed from GenBank (http://www.ncbi.nlm.nih.gov/) sequences using Primer 3 software. They were all approximately 20 bases long and amplified products of 200-300 bases. Melting points and GC content were examined and designed to be as similar as possible for forward and reverse primer pairs. Primers were designed for *T. pseudonana* RuBisCO small sub unit located in the chloroplast (*rbcs*), and for the nuclear encoded genes, actin, EF1α and several carbonic anhydrases (**Table 2.2**). The primers designed for CA1 consistently gave a product in the no DNA template control; therefore alternative primers were produced using the sequences published in McGinn and Morel (2007).

2.4.14 e. Genes of interest

The genes of interest in these experiments were RuBisCO, the key enzyme in the Calvin-Benson cycle and the carbonic anhydrases involved in carbon acquisition.

RuBisCO is made up of two subunits, the small unit, *rbcs*, is coded for in the chloroplast of *T. pseudonana*. In terrestrial C3 plants the *rbcs* was found to be down-regulated at increased CO_2 which is why I chose to use this gene.

Table 2.2 Primer sequences for qRT-PCR. Forward (F) and reverse (R) primer pairs were designed to amplify regions of 200-300 bases for real-time PCR analysis. The gene identity in parenthesis refers to its identity in McGinn and Morel (2007).

Gene	Protein ID		Sequence 5'-3'	T_m (^oC)	GC (%)
EF1α		F	-GTA TCG GCA CTG TCC CTG TT-	59.4	55
		R	-ATC TCC TCG CCG AAT ATC CT-	59.4	55
Actin		F	-ACG TGA CCT CAC GGA CTA CC-	61.4	60
		R	-CAG TAA GGT TGG GCT GGA AA-	57.3	50
rbcs		F	-TAA AGG CTG GGC TAT GAA CG-	57.3	50
		R	-AAC CTG GCT CAT TAG CTG GA-	57.3	50
CA1	34125	F	-ACG GTG ACG GTC CCC ACG GTA ACATC-	69.5	61.5
(TWCAtp2)		R	-ACC CAC AGC AGA GGC GAT ATC CTG A-	66.3	56
CA2	34094	F	-ATG CGT CTG CAG AAG AAG AG-	59.4	55
(TWCAtp3)		R	-TGC TCT CCC AAT GCA TTA AA-	53.2	40
CA3	233	F	-CAG TGA TGG TGC AGC TGT TG-	59.4	55
(TWCAtp1)		R	-CGC CAA GCG TAG TGA AAC TC-	59.4	55
CA4	814	F	-GAA CAG CGT CAA CAA CAA CC-	57.3	55
(TWCAtp4)		R	-AAC TTC TCC TCA TCC AAG TTG C-	57.3	50

The Carbonic anhydrases (CA) are a family of metalloenzymes present in both plant and animal cells which catalyse the interconversion of bicarbonate (HCO_3^-) and CO_2.

In phytoplankton this enzyme may occur at the cell surface to increase the external concentration of CO_2 and aid diffusive entry into the cell, external carbonic anhydrase. It also occurs internally to prevent leakage of CO_2 from the cell. At the active site of RuBisCO, CA is present to convert HCO_3^- to CO_2, the necessary substrate for RuBisCO. The expression of these CAs has been found to be CO_2 dependent in *T. pseudonana* and other phytoplankton (McGinn and Morel 2007). A BLAST search of the genomic sequence of *T. pseudonana* (http://genome.jgi-psf.org/Thaps3/Thaps3.home.html) with the δ-CA identified in *Thalassiosira weissflogii*, TWCA1 identified four putative homologs. The delta class of carbonic anhydrases are zinc containing enzymes and are found in a wide range of phytoplankton (McGinn and Morel 2007).

2.4.14 f. Housekeeping genes

Housekeeping genes are expected to remain unaffected by the experimental conditions, They are typically constitutive genes that are transcribed at relatively constant levels

and which code for proteins involved in cell maintenance. They act as an internal reference for comparison of the effects of the treatment on the expression of the GOIs. Actin performs several roles in cell structure and maintenance, the elongation factor 1-α (EF1α) facilitates protein synthesis. Both genes are commonly used as endogenous controls (Nicot et al. 2005). However, actin has been shown to alter in *T. pseudonana* in response to nitrate addition (Granum et al. 2009). The use of several housekeeping genes is recommended so that the stability of gene expression may be compared and makes the assay more robust (Thellin et al. 1999).

2.4.14 g. Harvesting cells

I found that 3 x 10^6 cells were needed for a good yield of RNA. Cells were harvested 2 hours after the end of the dark period of the light/dark culture conditions, at 10:00 and samples were processed as quickly as possible to reduce any effect of circadian change in expression of RuBisCO. Strong diel cycles in RuBisCO expression have been reported for *T. pseudonana* (Granum et al. 2009). Two 45 ml samples of culture were centrifuged for 4 min at 15,000 g at 4^{o}C in Falcon tubes in an Eppendorf 5810R centrifuge. The supernatant was removed and the remaining 1-2 ml placed in an Eppendorf tube and centrifuged for 1 min at 16,000 g in a benchtop Eppendorf 5415D centrifuge. This was the minimum time necessary to produce a good pellet. Supernatant was removed and the pellet re-suspended in 100-200 µl RNAlater to preserve RNA. RNAlater is a commercially produced RNA stabilisation reagent which conserves mRNA and allows it to be stored prior to analysis. If RNA was not to be extracted immediately samples were stored at -20^{o}C.

2.4.14 h. RNA extraction

Total RNA extraction was performed using an RNeasy mini kit (QIAGEN, Hilden,

Germany) as described by the manufacturer. The lysis buffer (RLT) contained guanidinium thiocyanate and β mercaptoethanol which are highly denaturing and inactivate RNAses. This method readily lysed the *E. huxleyi* cells giving good RNA yields. For smaller samples, cell debris was removed by centrifugation but larger pellets were passed through Qiagen plant shredder columns to remove excess material; if not removed, this was found to block the nucleic acid binding columns in subsequent steps. The supernatant was mixed with a half volume of 100% ethanol to promote selective binding of RNA to the membrane, and passed through a nucleic acid binding column. DNA and RNA bound to a membrane filter and were then washed several times with ethanol containing buffers. As genomic DNA contamination of the sample would give an overestimation of mRNA, the DNA was hydrolysed on the column using a Qiagen RNAse free DNAse set. The pure total RNA was then eluted from the column with RNAse free water. The sample was checked for DNA contamination by PCR and gel electrophoresis, since taq will amplify DNA but not RNA without a reverse transcription step.

T. pseudonana proved more difficult to lyse presumably due to the hard silica frustules. Neither vortexing with RLT buffer nor glass beads yielded good RNA. However, grinding cells in a pestle and mortar with liquid nitrogen was very successful. This was achieved by resuspending pelleted cells in the residual media, and dropping into a chilled pestle of liquid nitrogen and grinding. Once ground, RLT buffer was added and RNA extracted in the usual way.

2.4.14 i. RNA Quantification

An initial examination of the quantity and purity of the RNA was made using spectrophotometry. Nucleic acids absorb UV radiation with an absorption peak at

260nm wavelength and proteins with a peak at 280nm. The ratio of absorbance at 260:280 can be used as a measure of purity or protein contamination. 100% nucleic acid purity gives a reading of 2.00, 70% = 1.94 and 30% = 1.73. A more sophisticated examination of RNA quality was made using Agilent's RNA LabChip and 2100 Bioanalyser. This is a microfluidic capillary electrophoresis system. Only 1µl of sample is needed which is run on a miniature gel within a capillary. Components are separated by electrophoresis according to their size and detected by fluorescence. The results may be viewed as either bands on a gel or as an electropherogram trace (**Fig. 2.4**). The Agilent Bioanalyser is recommended as a reliable, reproducible means of assessing RNA quality (Bustin and Nolan, 2004).

2.4.14 j. Reverse transcription

Real time PCR requires a double stranded DNA template so it is necessary to reverse transcribe the single stranded RNA to produce complementary DNA (cDNA). The use of oligo $d(T)_{16}$ primers which bind to the poly-A tail of mRNA strands results in transcription of only the mRNA from the total RNA. The reaction mixture contains dNTPs, RNAse inhibitor, multiscribe reverse transcriptase and magnesium chloride. The mixture is heated to 25°C for 10 minutes and then to 48°C for 30 minutes, the reverse transcriptase is then inactivated by 5 minutes at 95°C. The cDNA can then be run on an agarose gel with primers to check the reverse transcription was successful.

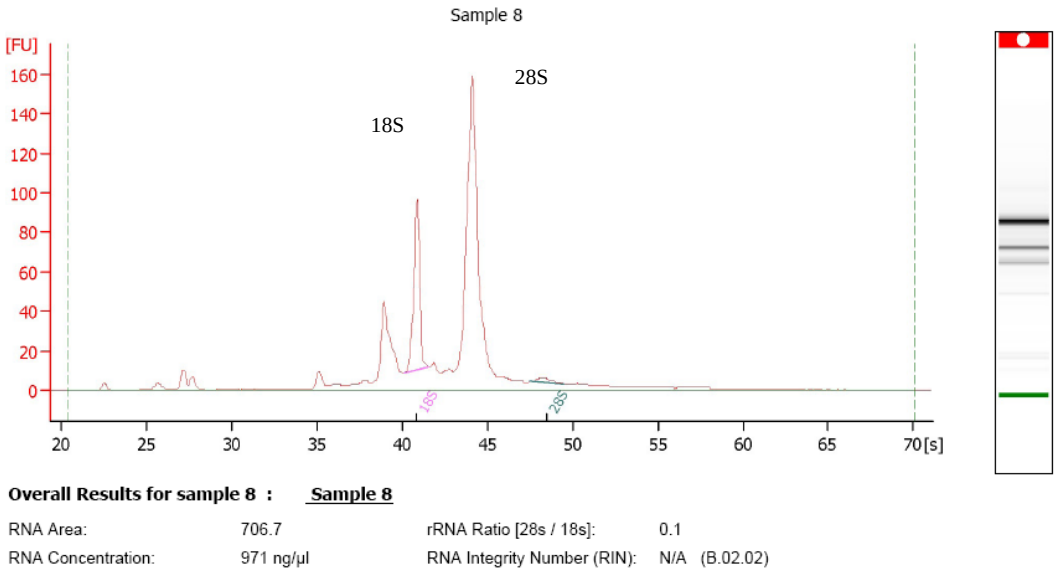

Fig. 2.4 Agilent trace for a *T. pseudonana* RNA sample. The RNA is of good quality, there is minimal low molecular weight noise and the RNA is not degraded which would be seen as a lower peak of the 28S than that of the 18S ribosomal RNA and noise between the 18S and 28S peaks.

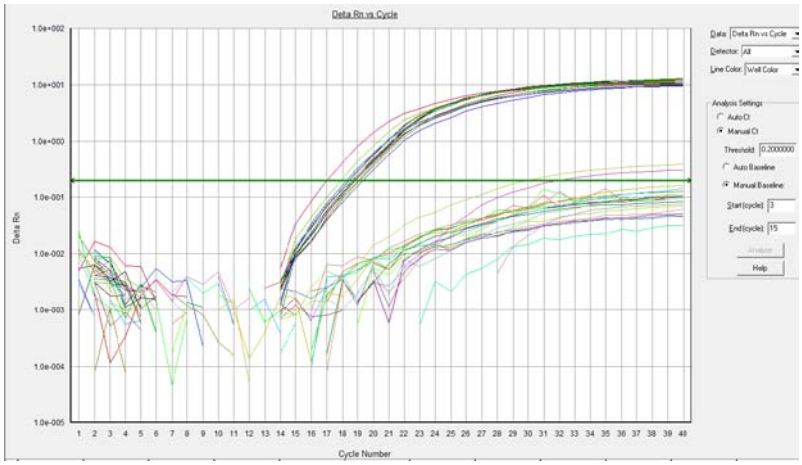

Fig. 2.5 The amplification of *T.pseudonana rbcs* followed in real time as an increase in fluorescence caused by the Sybr Green stain bound to the cDNA.

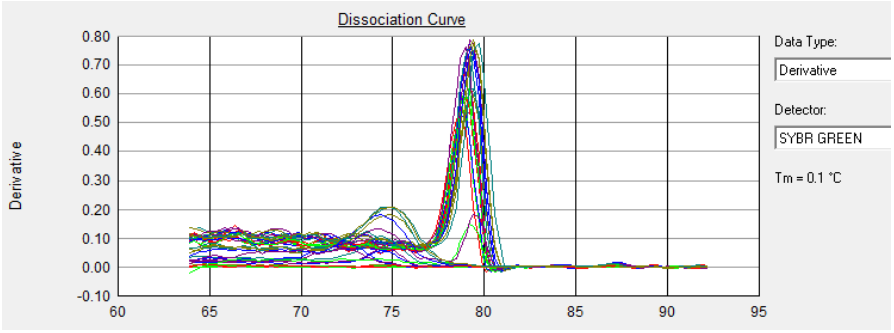

Fig. 2.6 Dissociation (melt curve) for *E.huxleyi rbcs.*

2.4.14 k. Gene quantification

Gene quantification was performed with an ABI PRISM 7000, sequence detection system (Applied Biosystems, Foster city, USA). Reaction mixes were made up such that each contained the appropriate primers to amplify a section of a gene of interest - an amplicon. 25µl of Power SYBR® Green PCR Master Mix was used for each reaction with a total volume of 50µl. The master mix contained: deoxynucleoside triphosphates (dNTPs), from which the amplicons were constructed; AmpliTaq Gold® DNA Polymerase, to catalyse binding of the dNTPs; buffer and magnesium chloride to provide optimum amplification conditions; SYBR® Green I Dye, which binds to double stranded DNA; and a passive reference dye. 10 ng of cDNA in a 5µl volume was added to each reaction; this was calculated from the RNA quantification, the cDNA was not quantified. Variable concentrations of forward and reverse primers, as calculated from a primer optimization cycle, were used, with the remaining volume made up with molecular grade water.

The thermal cycling conditions were as follows: 10 min at 95°C, to activate the DNA Polymerase, followed by 40 cycles of 15 s at 95°C and 1 min at 60°C, to denature the DNA and for annealing and extension. Data collection was performed during each extension phase. Duplicate positive controls (gDNA), negative controls (molecular grade water), and RT-negative controls (total RNA sample) were included in each run. Duplicate reactions were run for each RNA extraction and the amplification observed in real time as the increase in fluorescence (**Fig. 2.5**) A dissociation analysis was performed following the amplification to confirm that primers were specific and a single product was amplified (**Fig. 2.6**). This is particularly important when Sybr Green is used as it will amplify any double stranded DNA so genomic or other DNA

contaminants will distort the results. For all primer pairs single products were amplified. In some cases minimal primer dimer formation occurred.

2.4.14 l. Primer optimization

Primer concentrations were optimized to ensure efficient, accurate quantification of the mRNA. Excess primers may form primer dimers, when two primer molecules anneal to each other. Primer dimers may be amplified and interfere with accurate quantification. Three concentrations of forward and reverse primer were used (50, 300 and 900 nM) in all possible combinations, making a total of nine reaction mixes. These were carried out in duplicate and for each combination, duplicate no-template controls were performed. The real time PCR results gave good amplification of all the combinations with minimal amplification in the no template controls. The most appropriate primer pairs had low Ct values and undetectable amplification in their no template controls.

2.4.14 m. Standard curves

To check the precision and sensitivity of the qRT-PCR, standard curves were produced for each primer pair using four, ten-fold dilutions of cDNA template: 50, 5, 0.5, and 0.05 ng. For a perfect result these should all lie along one line with an R^2 value of 1. My results gave R^2 values above 0.99 for all the *T. pseudonana* genes.

2.4.14 n. Validation of housekeeping genes

To determine whether the housekeeping genes are robust internal controls it is necessary to ensure that they do not alter over a range of template concentrations. From the standard curves, the difference between the GOI and housekeeping gene for each template concentration is calculated (ΔCt). This is then plotted against the log of the

input template (ng) (**Fig. 2.7**). The slope of the trendline for these data points should be <0.1 to be valid. Most of these values were not below 0.1, however the use of two housekeeping genes would improve the analysis (**Table 2.3**).

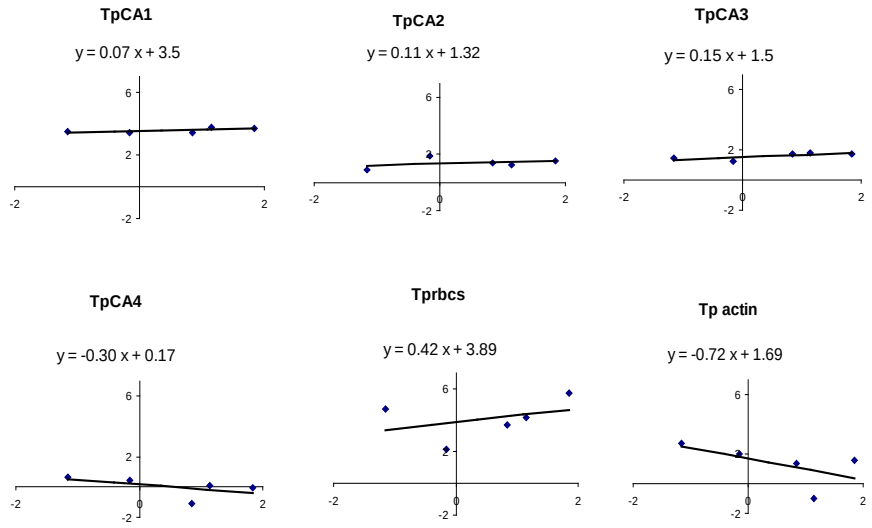

Fig. 2.7 Plots of ΔCt (y-axis) against log template input (x-axis). ΔCt is the difference between the EF1α and GOI Ct. Over the range of template concentrations this should remain stable, with a slope <0.1.

Table 2.3 Validation of housekeeping genes. Slope of the trendline for data points of ΔCt against log input template.

	actin	EF1α
CA1	-0.35	0.07
CA2	-0.07	0.11
CA3	-0.29	0.15
CA4	-0.37	-0.3
rbcs	0.21	0.42
actin	-	-0.72

2.4.14 o. Data analysis

Data were analysed using the Relative Expression Software Tool, REST 2008 (www.gene-quantification.info) software package. This package has several features which make the analysis robust. Firstly it allows several housekeeping genes to be used to calculate the expression ratio. The geometric mean of the expression of the housekeeping genes is used to correct the raw values for the genes of interest. Secondly

the efficiencies of individual reactions are taken into account. Thirdly a randomisation test which can accept these parameters is incorporated into the package to allow statistical analysis of the data (REST software manual, 2008). The efficiencies of the individual reactions are also taken into account. These are calculated from the standard curves using **equation 2.4**.

$$E=10^{[-1/slope]} \qquad [2.4]$$

The relative expression ratio of the target genes to housekeeping genes in the high CO_2 and ambient treatments were calculated from **equation 2.5**.

$$\text{Ratio} = (E_{\text{target}})^{\Delta Ct}{}_{\text{target}}\,(\text{control} - \text{sample}) / (E_{\text{ref}})^{\Delta Ct}{}_{\text{ref}}\,(\text{control} - \text{sample}) \qquad [2.5]$$

Ct is the point where the fluorescent signal crosses the threshold value. ΔCt is the difference between the crossing points for the high CO_2 and ambient samples. In the equation above the ambient treatment was designated the control and high CO_2 treatment as the sample. *Target* refers to the gene of interest and *Ref* to a housekeeping gene.

2.4.14 p. Statistical analysis

A hypothesis test was carried out by the REST program to determine whether there was a significant difference between the samples (high pCO_2) and controls (present-day pCO_2). Due to the difficulty of incorporating ratios and multiple sources of error this is based on randomisation techniques and it is able to take into account the reaction efficiencies and normalisation to housekeeping genes. 50,000 random re-allocations of samples and controls were performed and the number of times the relative expression of the randomly assigned group is greater than the sample data was counted. This was

then plotted as box and whisker plots and tabulated (REST software manual, 2008). Where the data fall above or below 1, an up or down-regulation of the gene is suggested. The box shows the inter-quartile range, with whiskers for the upper and lower 25% of observations, a dotted line shows the median. The plot visually presents the data in a way that the range and skew can be easily observed. The tabulated results give the input and output data, the hypothesis test and probability of up or down-regulation.

2.4.15 DGGE

2.4.15a. Introduction

Denaturing gradient gel electrophoresis (DGGE) is a molecular technique used in microbial ecology to qualitatively separate genotypes in natural samples. It was used to determine the presence or absence of *Emiliania huxleyi* genotypes within the Bergen mesocosms. The aim was to identify any changes in *E. huxleyi* clades in the community at increased CO_2. PCR was used to amplify regions of DNA which are specific to a particular genotype, the amplified fragments can then be separated by DGGE and visualized. Primers to distinguish among genetically distinct morphotypes based on genetic variations were kindly given to me by Dr. Schroeder, Marine Biological Association, UK.

2.4.15b. Sampling

Samples were analysed from three time points, pre-bloom, mid-exponential and bloom peak from each of the six mesocosms. Sampling was carried out at 10:00 local time, water was stored at 4°C until it was filtered which occurred within several hours. 5 litres of water from each mesocosm were filtered through a Sterivex-GP Sterile Vented Filter Unit, 0.22 µm (Millipore). Filters were snap frozen in liquid nitrogen, stored at -80°C, returned to the UK on dry ice and maintained at -80°C until they were processed.

2.4.15c. DNA extraction

1.6 ml of SET lysis buffer (40 mM EDTA, 50mM Tris HCl, pH9, 0.75 M sucrose, autoclaved) was injected directly into the Sterivex cartridge using a 2.5 ml syringe with 25 gauge 5/8" needle. 180 µl of fresh lysozyme was added and the cartridge re-sealed. It was incubated for 30 min at 37°C with rotation in a hybaid oven. 200 µl of 10% sodium dodecyl sulphate (SDS) and 55 µl of 20 mg ml^{-1} proteinase-k were added to denature the proteins. This removes nucleases from the sample to protect the nucleic acids from degradation. The sample was incubated for 2 hr at 55°C in the rotating hybaid oven. The lysate was withdrawn with a syringe and 1 ml SET buffer was used to rinse out the final lysate which was also collected. The lysate was added to 2ml phenol:chloroform:isoamyl alcohol (25:24:1) and shaken gently until mixed. This mixture separates into an organic and an aqueous phase after centrifugation for 5 min at 1,500 x g. A further addition of an equal volume of phenol:chloroform:isoamyl alcohol (25:24:1) was made and this was centrifuged again for 5 min at 1,500 x g. An equal volume of chloroform:isoamyl alcohol (24:1) was added, shaken gently and centrifuged for 5 min at 1,500 x g. DNA collects in the upper aqueous phase, which was decanted and a half volume of 7.5M NH_4 acetate and 2.5 volume of pure ethanol were added to dehydrate the DNA so that it would precipitate. This was mixed and incubated at 20°C for >1 hour, often overnight.

The sample was centrifuged in an Eppendorf 5810R at 15,000 x g for 30 min at 4°C. The ethanol was decanted and 2 ml of ice cold 80% ethanol added. The sample was centrifuged again at 15, 000 x g for 20 min at 4°C. Ethanol was decanted and a further wash with ice cold 80% ethanol was performed, The sample was centrifuged for 20 min at 4°C, the ethanol decanted and the tube was inverted and left to dry for 15 min. The DNA pellet was re-suspended in 200µl molecular grade water. The dissolution of the pellet was aided by tapping the tube walls and it was gently dissolved for 1 hour before

freezing. DNA was stored at -20°C. The DNA was quantified in the spectrophotometer and the volume containing 100 ng DNA was calculated. This was used as the template for the first round of the nested PCR.

2.4.15d. PCR

A nested PCR design was employed. This was a two-stage PCR with two sets of primers (**Table 2.4**). The first round, using primers GPA-F1and GPA-R1, amplified a section of the variable region of the GPA gene. The second round, using primers GPA-F2 and GPA-R1, then amplified a specific section of this product. This reduced contamination by products unintentionally amplified in the first round. The reaction mixes for the two rounds are shown in **Table 2.5** and the PCR conditions in **Table 2.6**. The templates for round 2 are the products of the round 1 reactions. The products from each round were visualized by electrophoresis on a 1.2% gel.

Table 2.4 Primers used to assess *E. huxleyi* genotypic diversity.

Primer	Sequence
GPA-F1	5-GAG GAG GAG AAG CCG AGC CT-3
GPA-F2	5-CAG GCG CTC TTC GGG CTG GG-3
GPA-R1	5-CTT GAA TCC TCT GTG CTG AGC GAG-3

Table 2.5 Reaction mixes for the nested PCR. GPAF1 primer used in the first round and GPAF2 in the second.

	1st Round		2nd Round	
	Final concentration	volume (µl)	Final concentration	Volume (µl)
GPAF1 (or 2)	0.4 pmol μl^{-1}	1	1 pmol μl^{-1}	1
GPAR1	0.4 pmol μl^{-1}	1	1 pmol μl^{-1}	1
Buffer	1x	5	1x	5
$MgCl_2$	2-3 mM	2.5	2-3 mM	2.5
Taq	1 U	0.25	1 U	0.25
dNTPs	0.25 mM	2.5	0.25 mM	2.5
Template	100 ng	1-5		10.25
water		Remainder		2.5
Total		25		25

Table 2.6 PCR conditions for the nested PCR

Repetition	Step	Temperature(°C)	Time (Min)
1x	Denaturing	95	5
30x	Denaturing	95	1
	Annealing	63.5(1st Round) 62 (2nd Round)	1
	Extension	72	1
1x	Denaturing	95	0.5
	Annealing	63.5(1st Round) 62 (2nd Round)	5
	Extension	72	5

2.4.15e. Denaturing gradient gel electrophoresis (DGGE)

This procedure was kindly performed for me by George Sorensen-Pound for Dr. Schroeder's group at the Marine Biological Association, UK. The procedure and primers were developed by Dr. Schroeder (Schroeder et al. 2003). The PCR products from the 2nd round of the nested PCR were treated with mung bean nuclease (Promega) according to the manufacturer's recommendations in order to degrade single-stranded DNA ends. 8µl PCR product, 1µl of 10x buffer and 1µl of mung enzyme (2units μl^{-1}) were incubated at 30°C for 30 min, no heat activation was required.

PCR products amplified may be of the same size and thus could not be separated by conventional electrophoresis. Using DGGE it was possible to separate fragments of the same size with different sequences, using their melting properties. An 8% polyacrylamide gel containing a 30-50% gradient of the DNA denaturant was prepared, where 100% consisted of 7M urea and 40% de-ionized formamide. 10µl of mung bean treated PCR product and10µl of 2x DGGE loading buffer (70% [vol/vol] glycerol, 0.05% [vol/vol] bromophenol blue, and 0.05% [vol/vol] xylene cyanol) were loaded into separate wells. Electrophoresis was carried out in 1x TAE buffer at a constant temperature of 60ºC for 3.5 h in a D-code electrophoresis system (Bio-Rad). As the fragments passed through the gel, the denaturing gradient gradually increased and the

DNA fragments melted at different denaturant concentrations, depending on their sequence. The denaturant caused the strands to separate and their mobility through the gel was decreased by the protruding single strands. The strands were prevented from dissociating totally by a 40-nucleotide 'GC-clamp', a GC rich region attached to the 5' end of one of the PCR primers. The gel was stained in a 0.1x Sybr Gold (Molecular probes) solution for 20 min. This dye bound to the DNA which was then visualised and appeared as distinct bands within the gel.

2.4.15.f DGGE data Analysis

Twenty two distinct bands were identified. In order to analyse this, a binary matrix of presence or absence was compiled for each band by visual analysis. It is possible to digitize gel photographs and use band-finding algorithms. However, it has been suggested that visual inspection is the most sensitive method of identifying bands (Ferrari and Hollibaugh 1999). The binary data was transformed into a distance matrix using the Jaccard co-efficient of PRIMER software (section 2.5). Multivariate analyses were then performed using the CLUSTER and SIMPROF tools in PRIMER 6 (section 2.5). These represent the similarities between samples as dendrograms and spatial plots and analyse the results (section 2.5). The Jaccard co-efficient does not consider the double-absence of bands in calculating pairwise similarities and therefore avoids spuriously high similarity values between samples with many double-absent bands (Schafer 2001).

2.5 DATA ANALYSIS

PRIMER 6 (Plymouth Routines In Multivariate Ecological Research) is a statistical package with a wide range of univariate, graphical and multivariate routines for analysing ecological data. It allows analysis of matrices of physical values, chemical

concentrations and biological data to be analysed in parallel aimed at 'explaining community structure by physico-chemical conditions' (Clarke and Gorley 2001). It has been suggested that the assumptions of a normal distribution of data with common variance are often unrealistic in biological experiments (Anderson 2001 and refs therein). The 'non-metric' ordination and permutation based techniques make few assumptions about the form of the data and take straightforward, robust approaches. All data sets are reduced to a triangular matrix representing the (dis)similarity of each pair of samples in terms of the biological variables specified. Permutation tests are used to examine the data. These calculate the probability of a value greater than or equal to the test statistic, F, being obtained by re-calculating the data after randomly re-ordering the data. Clustering and ordination techniques are then used to represent the relationships between the samples (Clarke and Gorley 2001). Primer V. 6 univariate analyses were used to test for differences between high CO_2 and ambient treatments in some laboratory experiments. Where a number of measurements were taken from the same day of an experiment, and to analyse the Bergen data multivariate PERMANOVA analyses were used. The techniques used are explained below.

2.5.1 Transformation of data

In order to normalise data and to reduce the dominance of the more abundant groups eg. species in the flow cytometry analyses, data was standardised to the totals. This resulted in each cell abundance measurement becoming a fraction of the total number of cells of that type, summed across the period being analysed. The data sets then satisfied the assumptions of normality and constant variance across groups required for an ANOVA.

2.5.2 Matrix generation

Matrices representing the (dis)similarity between each pair of samples were generated using Euclidean distance which is the natural distance between any two points in space. For the DGGE analysis, the Jacaard co-efficient was used.

2.5.3 Permutation

Permutation randomly re-allocates the labels identifying the samples and runs a test similar to an ANOVA, called an ANOSIM, to examine whether there are differences. If there are no differences then this should make no difference to the outcome. The whole set of possible permutations is not necessarily run, but a specified number of random permutations are examined. To test data at a significance level of 0.05, 1000 permutations of the data are recommended. With only 3 replicates for each treatment, in most of my experiments, the total possible number of permutations is only 10. This reduces the power of the test as the smallest p value possible is 0.1. The ANOSIM is a robust test which makes few assumptions about the data but is less sensitive than some other tests. With few replicates a more sensitive test, a PERMANOVA using Monte Carlo methods may be performed (Anderson and Robinson 2001). This makes more assumptions about the data and imagines that they are drawn from a larger data set. This increases the range of possible probability values to below 0.1.

2.5.4 Univariate tests, ANOSIM

The ANOSIM test in PRIMER V. 6 is analogous to a traditional univariate ANOVA. This tests whether, the null hypothesis, that there is no difference between treatments is true. One statistic used to test for this difference is Fisher's *F* statistic. If *F* is close to 1 then the null hypothesis must be accepted but larger values suggest that it may be false.

The p value gives a measure of the probability that the observed means could have occurred if the null hypothesis is in fact true (Anderson 2001).

To explain the output of an ANOSIM an example is presented in **Table 2.7** and will be explained. The global test gives an overall R and p value from which H_0 may be accepted or rejected. The linear correlation coefficient R, varies between 1 and -1, if R=1 or -1 then a perfect linear correlation exists between the two variables. If R is close to zero but is significant then there is a slight but significant difference in the data. Large numbers of replicates may create significant values from small differences and few replicates can reduce the significance of very different treatments. As R is largely not a function of the number of replicates but an absolute measure of differences whereas p is always influenced by the number of replicates, R is more important than p. If the global test shows no differences then there is no licence to look at pairwise tests (Anderson 2008). In this example only 45 permutations were possible, due to the lack of replicates, so the power of the test was very low. Of these 45 permutations 7 gave R values greater than or equal to the observed R value. This led to the calculation of a significance level of 15.6% that the observed value actually reflects a significant difference between treatments. A significance level of p=0.001 is the same as p=0.1%. If there is a significant difference, further tests between pairs of treatments may be performed to examine where differences lie. Pairwise tests vary between 0 and 1. 0 means that there are no differences and 1 means that variation between groups is larger than within groups.

Table 2.7 Results table from an ANOSIM test.

Global Test
Sample statistic (Global R): 0.615
Significance level of sample statistic: 15.6%
Number of permutations: 45 (All possible permutations)
Number of permuted statistics greater than or equal to Global R: 7

2.5.5 Multivariate tests, PERMANOVA

Where the response of many variables is tested simultaneously a multi-factorial ANOVA approach is necessary. The PERMANOVA, permutational ANOVA, performs a partitioning of the total sums of squares and calculates a distance-based pseudo-*F* statistic for each term based on the expectations of mean squares (EMS). The pseudo-*F* is directly analogous to the F value calculated by a multi-factorial ANOVA. P values are calculated using appropriate permutation procedures from the raw data or residuals using a full or reduced model (Clarke and Gorley 2001). An example of a PERMANOVA results table is shown in **Table 2.8**. In the first column the 'source', is the source of variation. The degrees of freedom (df) are shown in the second column, in this case there were two treatments and measurements of μ for 20 days. The residuals are the deviations of the observations from the sample mean. PERMANOVA is usually run as a permutation of residuals under a reduced model. This refers to a reduced model being one where terms not of interest have been removed. The permutation of the residuals are the errors obtained after removing the terms that are not of interest. The sums of squares (SS) is the sum of squared deviations of observations from the overall mean. There are three different sums of squares:

SS_T= the sum of squared distances from each sample to an overall mean value of all the variables

SS_{RES}= the sum of squared distances of data for one variable from the mean value for that variable

SS_A= the sums of squared distances from the means of each variable to the overall mean of all variables

Pseudo-F is calculated from the sums of squares using **equation 2.6**, where (a-1) = the degrees of freedom associated with the factor and (N-a) the residual degrees of freedom.

$$\text{Pseudo-F} = \frac{SS_A/(a-1)}{SS_{RES}/(N-a)} \qquad [2.6]$$

The p(perm) is then calculated as the proportion of calculated F values that are greater or equal to the observed F value (**equation 2.7**).

$$P=\frac{(\text{No. calculated F values} \geq F) + 1}{(\text{Total no. F values calculated}) + 1} \quad [2.7]$$

The 'unique perms', are the number of unique values of the test statistic that were obtained under permutation. Type III sums of squares is used because it is the most conservative method of calculating the sums of squares and is suitable for unbalanced as well as balanced designs (Anderson 2008).

Table 2.8 Results of permutation-based Analysis of Variance tests (PERMANOVA) for differences in μ between air and high CO_2 treatments. Quantified using Euclidean distance and Type III sums of squares based on 999 permutations of residuals under a reduced model

Source	df	SS	MS	Pseudo-F	P (perm)	permutations
treatment	1	0.91	0.91	6.03	0.017	995
day	19	6.69	0.35	23.33	0.001	998
Treatment x day	19	1.35	0.71	4.69	0.001	998
Residual	80	1.21	0.15			
Total	119	9.34				

2.5.6 Multivariate techniques

Hierarchical clustering, CLUSTER, and multi-dimensional scaling, MDS, start from a matrix of similarity coefficients computed between every pair of samples. A similarity matrix was computed for the DGGE data using the Jacaard coefficient. In a CLUSTER analysis the samples are linked in hierarchical groups based on their similarity, to produce a dendrogram. The MDS analysis produces a two or three dimensional 'map' from which the distance between the samples may be seen. SIMPROF runs a series of similarity profile permutation tests to identify the data primarily causing the differences between the clusters and to determine the degree of probability that groups are different.

Chapter 3.

INVESTIGATION OF THE EFFECT OF INCREASED CO_2 ON LABORATORY CULTURES OF TWO PHYTOPLANKTON SPECIES

3.1 INTRODUCTION

The aim of this project was to examine the long term effects of steady state, elevated CO_2 on marine phytoplankton. This objective addresses two areas of research which have been relatively unexplored despite the large number of studies of phytoplankton at increased CO_2 performed during the last decade. Firstly, there have been very few investigations which have lasted for longer than a month. It has been found that terrestrial C_3 plants initially respond to increased CO_2 with increased photosynthetic production and growth, however, in the long term, this effect diminishes (Long et al. 2004). No such long term studies have been performed with marine phytoplankton. Secondly, many of the previous studies have not controlled pH during the experiment and the uptake of CO_2 by the phytoplankton has reduced the CO_2 availability. These studies mimic a bloom situation in a high CO_2 world rather than effects of increased CO_2 under steady state conditions. The following introductory section will explain the different approaches that were taken to maintain cultures under comparable conditions of present day and increased CO_2 and the reasons for the choice of species examined.

3.1.1 Carbonate system control

Four methods have been used to adjust and maintain pH and pCO_2 in this and previous studies: acid and base manipulation; chemical buffering; CO_2 gas injection and dilution with gas-equilibrated media. All four have direct or indirect side-effects on the phytoplankton.

The definition of pH is that it is the logarithm of hydrogen ion availability, simple addition of acid (increasing hydrogen ions) is an easy way to adjust the pH of seawater. However, acid addition alters total alkalinity (TA) whilst DIC remains unchanged. I chose not to use this method because altering TA introduces a further variable which may have unknown consequences eg. effects on nutrient availability (Wurts 1992). A second approach is to chemically buffer the system. Buffers supply positive and negative ions, reducing pH change on the addition of H^+. Buffers can affect the growth rate of phytoplankton (Blanchemain et al. 1994) and TA may be altered by the addition of buffers but in some initial experiments, I used buffers because they are an established way to control culture pH. A third approach involves the addition of CO_2; this is closest to the natural changes that will occur. Addition of CO_2 decreases seawater pH and CO_3^{2-} but DIC, CO_2 and HCO_3^- are all increased. Alkalinity remains unchanged because there is an equal decrease in OH^-, CO_3^{2-}, and increase in H^+ and HCO_3^-. However, the CO_2 must be bubbled into the cultures as diffusion from the overlying atmosphere is not capable of maintaining pCO_2 whilst cells are actively growing. Bubbling may have adverse effects on phytoplankton growth. Shi et al. (2009) found that *Emiliania huxleyi* and low density cultures of *T. weissflogii* were particularly sensitive to bubbling. Gas injection with pure CO_2 or high pCO_2 in air may have small scale intense effects near inlets. I used 760 ppm CO_2 mixed with air to avoid this problem however this was not capable of maintaining pH in the fast growing *T. pseudonana* cultures. The fourth approach, which was used in the final experiments of this project, was to dilute cultures from reservoirs of gas-equilibrated media (section 2.3.3). In low cell density cultures of *T. pseudonana*, this method was capable of maintaining pH. Cultures were also bubbled with 760 ppm CO_2 in air so mechanical damage was not negated.

3.1.2 Phytoplankton species

Two species of phytoplankton were used in my laboratory experiments: a diatom, *Thalassiosira pseudonana*, and a coccolithophore *Emiliania huxleyi*. These were chosen because they are important in biogeochemical cycling, their physiology is well understood, much of their genetic sequences have been published (Armbrust et al. 2004) and there is evidence that they may be sensitive to the effects of increased CO_2 (Riebesell et al. 2000; Riebesell et al. 2007; Iglesias-Rodriguez et al. 2008). The measurements taken during the laboratory experiments aimed to discover if increased CO_2 was beneficial to phytoplankton. The rationale for this is that there may be a reduced need for carbon concentrating mechanisms which could reduce the machinery and enzymes required to maintain efficient carboxylation at the RuBisCO active site, saving energy. Additional energy savings could be gained by the reduced cost of actively transporting CO_2 compared to HCO_3^- with a greater availability of CO_2 (Burkhardt et al. 2001) and a reduction in the amount of RuBisCO required at increased CO_2. Evidence of increased carbon fixation or energy saved could be manifested as increased cell division, cellular POC or PON, cell size, chlorophyll per cell or photosynthetic activity. Evidence of reduced enzyme synthesis was examined by molecular analysis as a down-regulation of the transcription of mRNA coding for RuBisCO and carbonic anhydrase. *T. pseudonana* has been found to actively take up HCO_3^- and probably also CO_2 using an inducible CCM (Thompson et al. 1994; Fielding et al. 1998; Laws et al. 1998). Thus increased CO_2 may reduce the necessity for carbonic anhydrase involved in the CCMs. *E. huxleyi* is a calcifying species and may be sensitive to reduced pH. The photosynthetic rate of *E. huxleyi* in short term incubation experiments has been found to be undersaturated with respect to carbon at normal DIC concentrations of 2 mmol l^{-1} (Paasche 2002). Therefore *E. huxleyi* may either benefit or be adversely affected by increased CO_2.

My initial experiments examined the effects of increased CO_2 on the growth of *T. pseudonana* CCMP 1335 and *E. huxleyi* CCMP1516 in batch culture. These showed an increase in specific growth rate of *T. pseudonana* at increased CO_2 but a large increase in the pH occurred as cells grew and took up the CO_2 from the media. Much of the following experimental work was concerned with controlling this rise in pH. A number of experiments using Tris (hydroxymethyl) aminomethane (tris) to buffer changes in pH, were performed with both *T. pseudonana* and *E. huxleyi*. Despite a well controlled experiment to determine the optimal concentration of tris to maintain pH without adversely affecting cell health, cells grew less well with tris buffer, than unbuffered controls. Cell physiology may have been altered by the use of buffer and the conditions were less realistic than that of the subsequent continuous cultures. Therefore I have decided not to include this work. To further investigate the increase in specific growth rate seen in batch culture, semi-continuous culture experiments were performed. These involved the daily dilution of cultures with media that had been equilibrated with either air or 760 ppm CO_2 in air. Specific growth rates were thoroughly examined in *T. pseudonana* and *E. huxleyi* strains 1516 and 371, by this method. Ultimately, long-term continuous cultures of *T. pseudonana* were grown at present day or 760 ppm CO_2 in air for 3 months. The effect of this treatment on their ability to grow subsequently at present day or increased pCO_2 was tested. Growth, C:N, Fv/Fm, red fluorescence $cell^{-1}$, cell size and the transcription of genes regulating carbon acquisition and fixation were all examined in the final long-term experiment.

3.2 BATCH CULTURE OF *THALASSIOSIRA PSEUDONANA* AT PRESENT DAY AND HIGH CO_2

In this experiment batch cultures were bubbled with a mix of 760 ppm CO_2 in air to reduce pH. *T. pseudonana* reproduces by asexual division; it is a fast growing species and may divide more than once a day, in optimal conditions. In this experiment *T. pseudonana* grew significantly faster (F=18.97, p=0.01, **Table 3.1**) and the maximum cell density reached was higher, 4.93 (± 6.84) x 10^6 cells ml^{-1}, at increased CO_2, than in cultures grown at present day CO_2 concentrations – from now on referred to as present day controls, 3.67 (± 0.95) x 10^6 cells ml^{-1} (**Fig. 3.1**). The difference in maximum cell density was not significant (F=3.42, p=0.14, **Table 3.1**). Continuous aeration of the culture with air enhanced with 760 ppm CO_2 was able to reduce pH by around 0.2 units, compared with cultures bubbled with air. Despite this the pH of the increased CO_2 cultures rose from around pH 8 to almost 9 by day 4 (**Fig. 3.2)**. The carbonate chemistry therefore reflected a bloom situation rather than a steady state effect.

3.3 *THALASSIOSIRA PSEUDONANA* CCMP1335 AND *EMILIANIA HUXLEYI* CCMP 1516 AT INCREASED CO_2; USING LOW CELL DENSITY SEMI-CONTINUOUS CULTURE TO MAINTAIN PH

Surprisingly, contrary to previous research (Pruder and Bolton 1979), my preliminary experiments showed enhancement of cell division rates of *T. pseudonana* at 760 ppm CO_2 compared to present day controls. This occurred in the experiment described in the previous section and also in a culture buffered with tris to maintain pH. In the following experiment pH was controlled by daily dilution of low cell density cultures with media which had been pre-equilibrated by bubbling with either air or air enhanced with CO_2 to 760 ppm. From a preliminary experiment lasting two weeks, a cell density of 1 x 10^5 cells ml^{-1} was determined, as a density at which the target pH could be maintained by this technique. Cultures were bubbled throughout the experiment. The

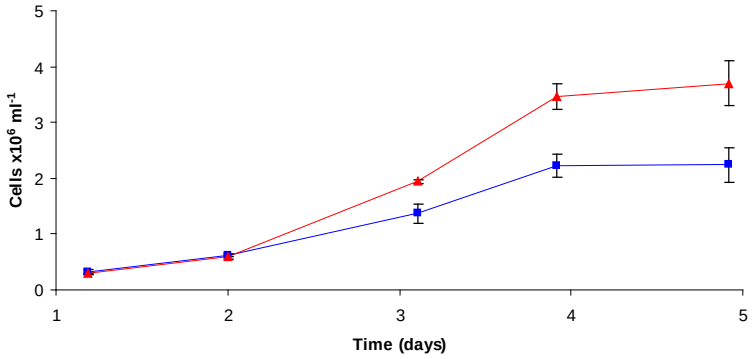

Fig. 3.1 Mean cell number (10^6 ml^{-1}) determined in triplicate, nutrient replete, batch cultures of *Thalassiosira pseudonana* aerated with air (—■—) or air enriched with CO_2 at 760 ppm (– ▲–). Error bars are standard deviations of the three cultures.

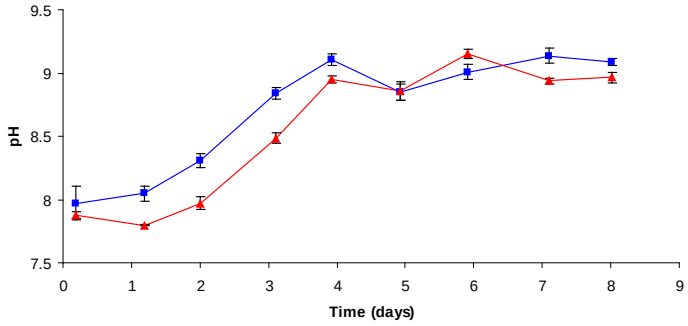

Fig. 3.2 Mean pH of triplicate, nutrient replete, batch cultures of *Thalassiosira pseudonana* aerated with air (—■—) or air enriched with CO_2 at 760 ppm (– ▲–). Error bars are standard deviations of three cultures.

Table 3.1 Single factor Analysis of variance results for mean μ, during exponential phase (days 1-4) and maximum cell densities of *T. pseudonana* cultures, grown in air or high CO_2 conditions.

Source of Variation	*SS*	*df*	*MS*	*F*	*P-value*	*F crit*
μ						
Between Groups	0.05	1	0.05	18.97	0.01	7.71
Within Groups	0.01	4	0.00			
Total	0.06	5				
Max cell density						
Between Groups	2.36×10^{12}	1	2.36×10^{12}	3.42	0.14	7.71
Within Groups	2.76×10^{12}	4	6.89×10^{11}			
Total	5.11×10^{12}	5				

pH was very well controlled by daily dilution with pre-equilibrated media (**Fig. 3.4**) and daily measurements of cell division were made for the duration of the experiment. A significant difference in the pH between the two treatments was maintained throughout the experiment for both species (p=0.001) (**Table 3.3**). The pH of the present day controls did not rise above 8.4, mean pH 8.08 ± 0.01 (**Fig. 3.4**), mean pH of the high CO_2 cultures was pH 7.88 ± 0.05. For the *E. huxleyi* cultures, mean pH of the high CO_2 cultures was 7.89 ± 0.01, and of the present day controls pH 8.1 ± 0.02 (**Fig. 3.4**). Cell density did not differ significantly between the treatments, *T. pseudonana* (Pseudo-F=0.41, p=0.52), *E.huxleyi* (Pseudo-F=0.15, p=0.65) (**Table 3.3**) so all cells would have been exposed to the same light per cell. These analyses suggest that the experiment was well controlled and suitable for the purpose of the investigation.

Cells were counted and diluted every 24h and daily variations in specific growth rate were calculated. My previous experiments had suggested that there may be an increase in μ associated with increased CO_2 in *T. pseudonana* but those experimental conditions were never very well controlled. μ was calculated from the cell densities on consecutive days, for the two species. The maximum and minimum growth rates for *T. pseudonana* were 1.45 and 0.38 (d^{-1}) in the high CO_2 cultures, 1.33 and 0.32 (d^{-1}) in the present day cultures. The mean μ (d^{-1}) of the three high CO_2 cultures was 0.97 (± 0.25) and 0.92 (± 0.28) in the present day cultures (**Fig 3.3**). Differences between treatments were examined by PERMANOVA (**Table 3.2**). This gave a significant difference between treatments, days and treatment x day. Examination of the data suggests that although there is a significant difference between the treatments, ie. they could not be drawn from the same population, there is no consistent increase in μ in the high CO_2 cultures. *E. huxleyi* cultures did not differ significantly in growth rate between treatments nor grow significantly differently on different days (**Table 3.2**).

Table 3.2 PERMANOVA results for differences in μ between air and high CO_2 treatments in *T. pseudonana* and *E. huxleyi*. Differences between treatments, days and the interaction of the two were analysed.

T. pseudonana Specific growth rate

Source	df	SS	MS	Pseudo-F	P (perm)	permutations
treatment	1	0.91	0.91	6.03	0.017	995
day	19	6.69	0.35	23.33	0.001	998
Treatment x day	19	1.35	0.71	4.69	0.001	998
Residual	80	1.21	0.15			
Total	119	9.34				

E. huxleyi Specific growth rates

Source	df	SS	MS	Pseudo-F	P (perm)	permutations
treatment	1	0.00005	0.00005	0.002	0.97	995
day	5	0.35	0.07	2.47	0.06	999
Treatment x day	5	0.06	0.01	0.44	0.82	999
Residual	24	0.68	0.03			
Total	35	1.09				

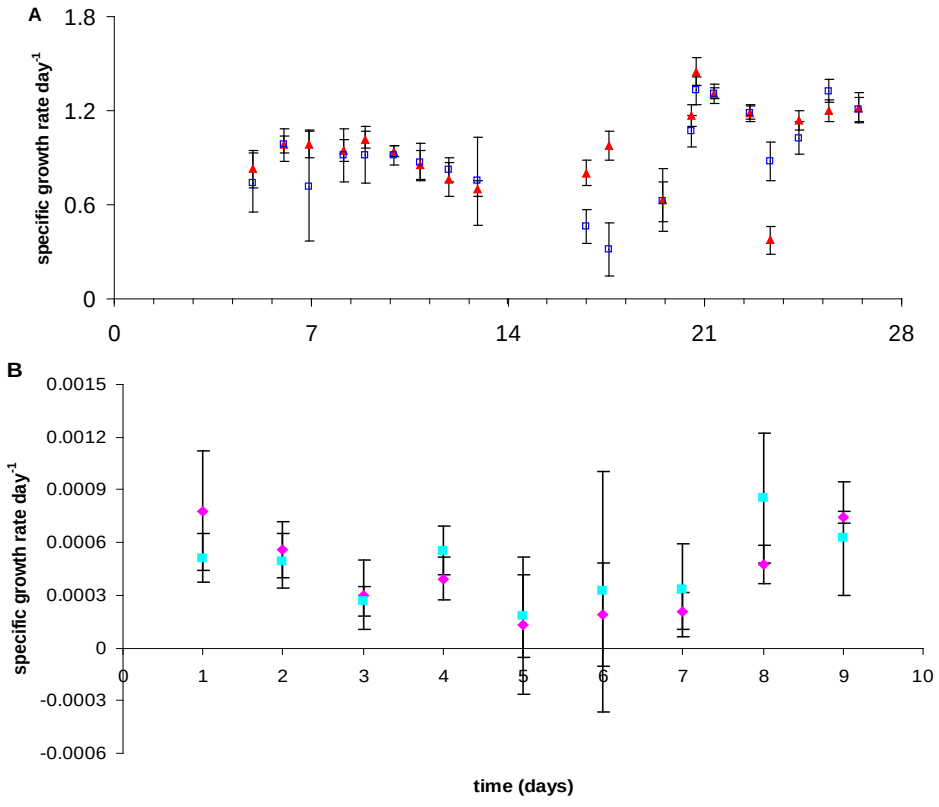

Fig. 3.3 Specific growth rates per day of (A) *T. pseudonana*; (B) *E. huxleyi* in semi-continuous culture at present day (□,■) or 760 ppm CO_2 (▲,♦). Measurements taken in triplicate on Coulter Multisizer II Coulter counter. Error bars show standard deviations of triplicate cultures and three readings for each data point.

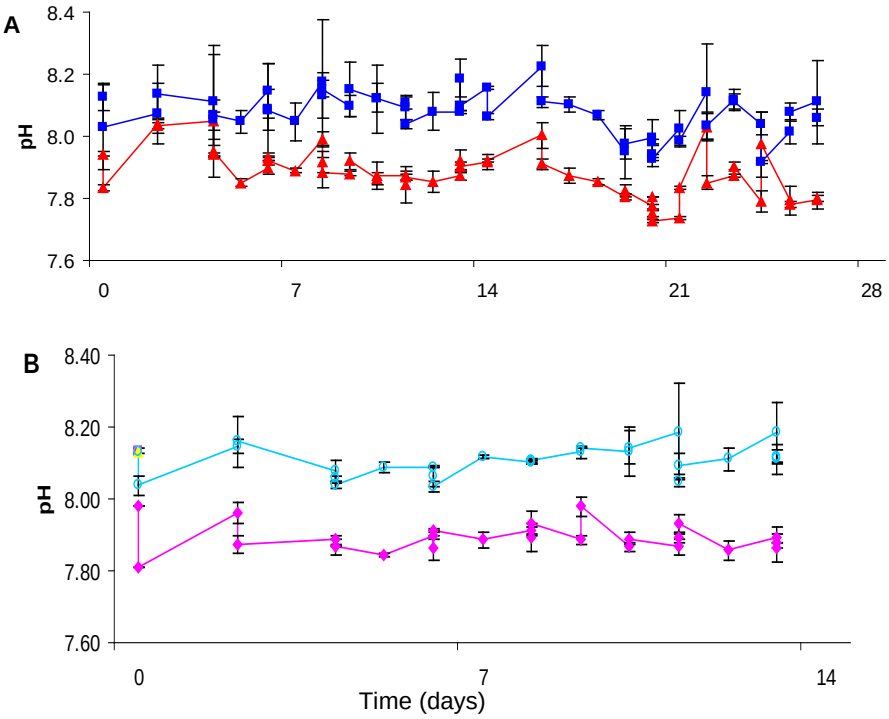

Fig. 3.4 pH of: A *T. pseudonana* air bubbled culture (-■-), high pCO_2 culture (-▲-); B: *E. huxleyi* air bubbled culture (-○-), high pCO_2 cultures(-♦-). Error bars are standard deviations of triplicate cultures.

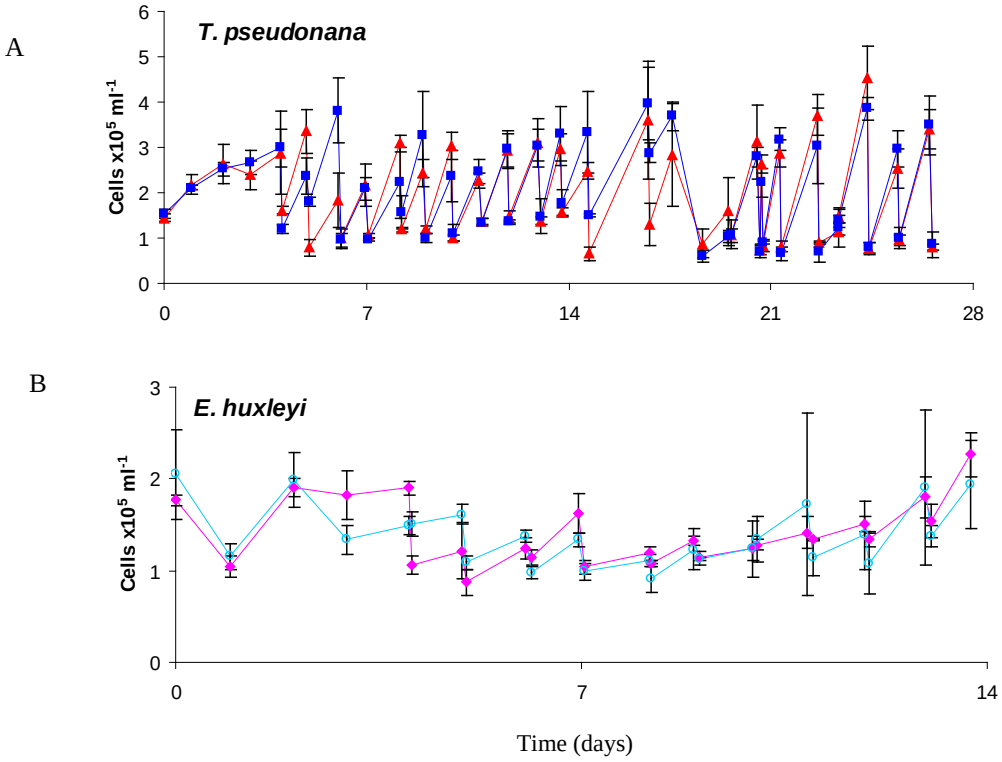

Fig. 3.5 Mean cell numbers of A: *T. pseudonana* air bubbled cultures (-■-), high pCO_2 cultures (-▲-); B: *E. huxleyi* air bubbled culture (-○-), high pCO_2 cultures(-♦-). Error bars show standard deviations of triplicate cultures

Table 3.3 ANOSIM of the difference in pH and cell number, between the two treatments for *T. pseudonana* and *E. huxleyi*. There were no significant differences, therefore the experimental conditions were well controlled.

Thalassiosira pseudonana pH

Source	df	SS	MS	Pseudo-F	P (perm)	permutations
treatment	1	2.53	2.53	614.62	0.001	998
day	26	1.05	0.05	9.86	0.001	998
Treatment x day	26	0.21	0.008	1.97	0.006	999
Residual	246	1.01	0.004			
Total	299	5.10				

Emiliania huxleyi pH

Source	df	SS	MS	Pseudo-F	P (perm)	permutations
treatment	1	1.59	1.59	987.92	0.001	996
day	13	0.11	0.008	5.41	0.001	997
Treatment x day	13	0.04	0.003	1.89	0.053	999
Residual	122	0.20	0.002			
Total	149	2.08				

Thalassiosira pseudonana Cells ml^{-1}

Source	df	SS	MS	Pseudo-F	P (perm)	permutations
treatment	1	4.64×10^{9}	4.64×10^{9}	0.41	0.52	995
day	26	4.12×10^{11}	1.58×10^{10}	1.38	0.12	999
Treatment x day	26	1.02×10^{11}	3.94×10^{9}	0.34	1	997
Residual	246	2.82×10^{12}	1.14×10^{10}			
Total	299	3.34×10^{12}				

Emiliania huxleyi Cells ml^{-1}

Source	df	SS	MS	Pseudo-F	P (perm)	permutations
treatment	1	1.37×10^{8}	1.37×10^{8}	0.15	0.69	996
day	13	1.08×10^{11}	8.33×10^{9}	8.81	0.001	998
Treatment x day	13	9.36×10^{9}	7.20×10^{8}	0.76	0.69	999
Residual	122	1.15×10^{11}	9.45×10^{8}			
Total	149	2.33×10^{11}				

3.4 Effects of increased CO_2 on calcifying *Emiliania huxleyi* CCMP 371 using semi-continuous culture to maintain pH.

A calcifying, warm water strain of *E. huxleyi* was grown at 24°C and liths were detected by light microscope. The light conditions during this experiment were 25 µmol photons m^{-2} s^{-1}. A semi-continuous culture experiment was set up as in the previous sections, with four replicates. Cells were diluted daily to 1×10^{5} ml^{-1}. Specific growth rates and maximum cell densities were measured. After 9 days cells were allowed to reach stationary phase without dilution, this was to provide samples for a metabolomics assay,

which proved inconclusive. It also allowed the maximum cell density attained to be examined and resulted in a decrease in pH, presumably due to calcification adding CO_2 to the culture. Samples were analysed in a Satlantic FIRe Fluorescence Induction and Relaxation system (Satlantic, Halifax, CA, section 2.4.3) to determine whether there were any differences in the efficiency of the light reactions of photosynthesis.

The pH was well maintained and cells grew rapidly, specific growth rates were just less than one per day in exponential phase (**Fig. 3.6**). There was no significant difference in growth rate between treatments (F=0.05, p=0.81, **Table 3.4**). Fv/Fm, the quantum efficiency of photosystem II was consistently higher in present day cultures than in high CO_2 cultures and was significant at the 10% level (F=3.25, p=0.08, **Table 3.4**) There was no difference between the relative functional absorption cross section of PSII (σ_{PSII}) (F=0.014, p=0.91, **Table 3.4**).

Table 3.4 Single factor ANOVAs to examine differences in specific growth rate, Fv/Fm and sigma in *Emiliania huxleyi* strain 371 at 760 ppm and present day CO_2.

Source of Variation	*SS*	*df*	*MS*	*F*	*P-value*	*F crit*
μ						
Between Groups	0.004	1	0.004	0.05	0.82	3.99
Within Groups	4.65	62	0.075			
Total	4.66	63				
Fv/Fm						
Between Groups	0.0002	1	0.0002	3.25	0.08	4.05
Within Groups	0.003	46	5.91×10^{5}			
Total	0.003	47				
Sigma						
Between Groups	67	1	67	0.014	0.91	4.05
Within Groups	218667	46	4753			
Total	218735	47				

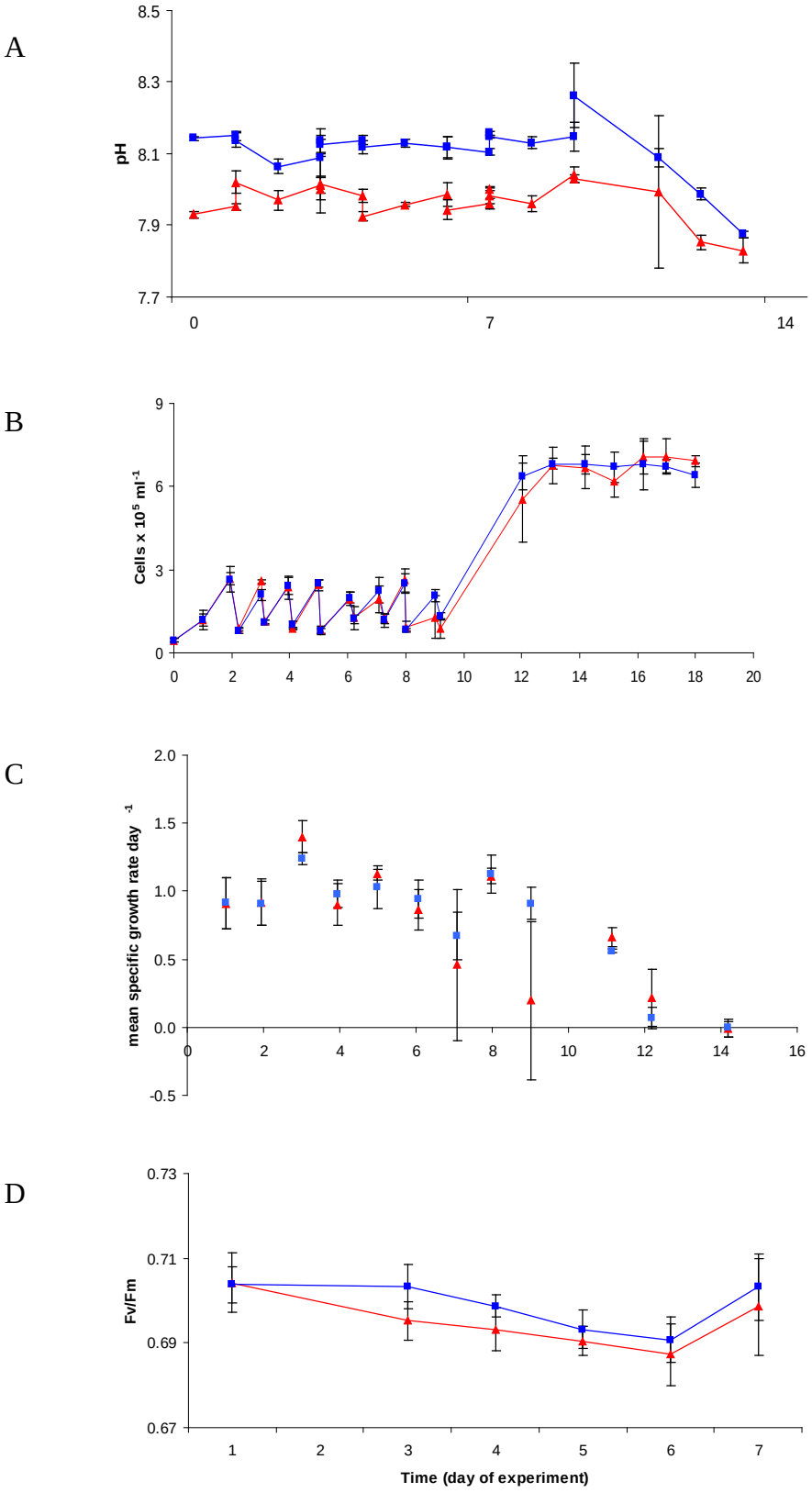

Fig. 3.6 A. pH, B. Cells ml^{-1}, C. Specific growth rate [μ (d^{-1})] and D. Fv/Fm of *E. huxleyi* 371. Means of four air bubbled cultures (-■-) and high CO_2 cultures (-▲-). Error bars show standard deviations of cultures. Cells were diluted daily to 1x 10^5 cells ml^{-1}.

3.5 LONG TERM CONTINUOUS CULTURE OF *THALASSIOSIRA PSEUDONANA* MAINTAINED AT INCREASED CO_2 FOR THREE MONTHS, APPROXIMATELY 100 GENERATIONS.

The aim of this experiment, and indeed the whole project, was to examine whether marine phytoplankton would adapt to increased CO_2. Adaptation, in this context, refers to genetic changes caused by a change in the environment. *T. pseudonana*, with its short generation time was therefore an ideal choice for this experiment. It is possible that genetic adaptation to increased CO_2 may occur within the time frame of a few hundred generations (Collins and Bell 2004). During the 3 month period for which this continuous culture was maintained I estimate that approximately 100 generations of *T. pseudonana* would have been exposed to increased CO_2. Not only may the genetic line adapt to the conditions, phytoplankton may acclimate to changes in the environment by altering their cellular constitution. For example, cells may alter the concentration of enzymes required for photosynthesis to optimize partitioning of cellular resources to the environmental conditions. There were two parts to this experiment. The initial 3 month growth period where cells were maintained at increased CO_2 or in air, in continuous culture with pH maintained, ie. steady state. In the second part, the effect of this treatment on the cells was determined by examining their growth at either high CO_2 or in air after ~100 generations in continuous culture. Two approaches were taken, one with fewer replicates but larger volumes for RNA and other analyses and a second approach, with a greater number of smaller volume replicates for statistical robustness (**Fig. 3.7**).

3.5.1 pH control

Continuous cultures were maintained by pumping media into the culture vessel at a rate sufficient to maintain a constant, low cell number. The pH was maintained by equilibrating the diluents with the appropriate gas mix. Since low cell densities were

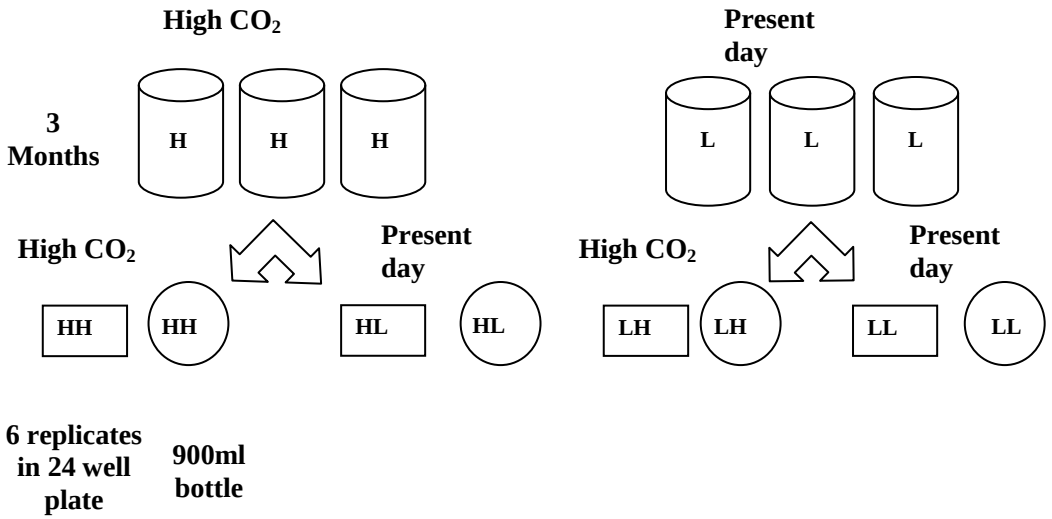

Fig. 3.7 Illustration of the two approaches and four treatments in the evaluation experiments to follow up the effects of growth at high CO_2 for three months.

used, there were no significant changes to pH as the cultures grew. The approach is fully explained in section 2.3.6. Culture pH was measured daily, and the results are displayed in **Fig. 3.8**. The experimental design was successful in maintaining a significant difference (slightly greater than 0.2 pH units) between the mean pH of the two treatments throughout the experiment. Mean pH of the present day cultures was 8.22 ± 0.11; and the high CO_2 culture was 8.01 ± 0.11. During the experiment, there were fluctuations in pH. Periodic large deviations were caused by rapid phytoplankton growth and a blockage or exhaustion of the fresh media supply. However, these were detected within a day, rapidly solved and pH returned to the appropriate level.

The media in which the phytoplankton grew (F/2 + Si) was based on filtered autoclaved natural seawater. Filtering removes larger particles from the water and autoclaving kills any remaining bacteria; however it also removes the gases from the water. Freshly autoclaved seawater has a pH of around 9. Autoclaved media was initially bubbled with filtered air to reduce the pH to 8.2 and then with the high CO_2 gas mix until pH 7.8 was

reached. This procedure took several days and occasionally the system used the media at such a rate that the input had not fully equilibrated and pH was not as low as required. As the priority was to keep the system running this media was used, on occasion, and the control system altered to a slightly higher pH for a short period of time.

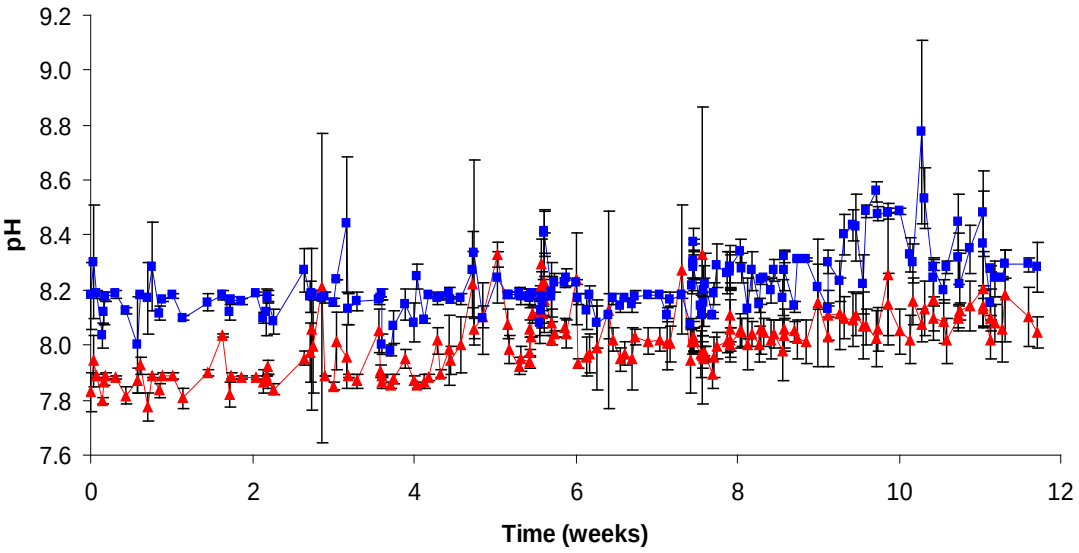

Fig. 3.8 Mean pH of triplicate cultures of *T. pseudonana* grown in continuous culture aerated with either high CO_2 (-▲-) or air (-■-). Error bars indicate standard deviation of the three cultures.

3.5.2 Measurements of cell physiology

A number of measurements of cell physiology were taken from the cells in the continuous cultures after 3 months of growth. The results are summarised in **Table 3.13** and will be described in more detail in this section. There were no cell division measurements for cells during this period.

3.5.3 Carbon and nitrogen content of the cultures

At the end of the three month experiment, when any acclimation might have been expected to have occurred, samples were taken for carbon and nitrogen (C:N) analysis (section 2.4.4). Triplicate filters for each of the triplicate cultures were analysed to give

mean C:N values. The mean C:N of high CO_2 samples was 6.94 ± 0.21 and air samples was 7.47 ± 0.47. There was a significant difference between the two treatments with the cells grown in air having a higher C:N ratio than those at increased CO_2 (F=9.18, p=0.008, **Table 3.5**). There was much higher variability in the air grown samples and the mean was increased by the samples taken from the third of the three cultures (**Fig 3.9**).

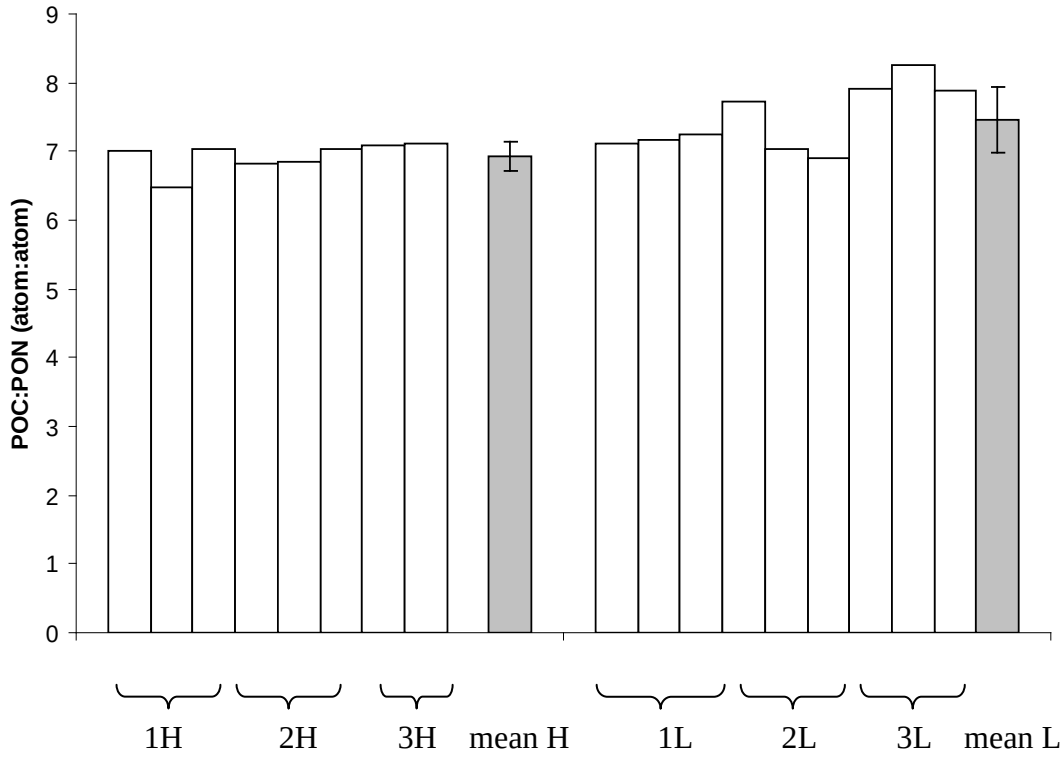

Fig. 3.9 C:N analyses of individual filters from either high CO_2 (H) or air (L) continuous cultures of *T. pseudonana* (white bars) and means of triplicate C:N analyses from triplicate continuous cultures of *T. pseudonana* maintained at high CO_2 (H) or air (L) for three months (grey bars). Error bars indicate standard deviations of the nine samples for each treatment.

Table 3.5 Analysis of variance of POC:PON (atom:atom) for cells grown in continuous culture for 3 months at either present day or high CO_2.

POC:PON						
Source of Variation	*SS*	*df*	*MS*	*F*	*P-value*	*F crit*
Between Groups	1.23	1	1.23	9.18	0.008	4.49
Within Groups	2.15	16	0.13			
Total	3.38	17				

3.5.4 Photophysiology

The quantum efficiency of photochemistry in Photosystem II (PSII) (Fv/Fm) and the relative functional absorption cross section of PSII (σ_{PSII}) were measured using a SATLANTIC FIRe (Fluorescence Induction and Relaxation) system. Fv/Fm is the ratio of variable to maximum fluorescence and σ_{PSII} describes the efficiency of light utilisation for photosynthesis in PSII. Fv/Fm was 0.62 ± 0.01 in the present day cultures and 0.60 ± 0.02 in the high CO_2 cultures, σ_{PSII} was 742 ± 52 in the present day cultures and 772 ± 65 in the high CO_2 cultures and were not significantly different. Fv/Fm is often used to describe the health of cells, values were close to the theoretical maximum and appropriate for nutrient replete diatoms (McMinn and Hegseth 2004).

3.5.5 Fluorescence and light scatter by flow cytometry

At the end of the experiment, mean values for side and forward scatter were identical for the two treatments. Side scatter was 41 (± 1 in the present day cultures, ± 3 in the high CO_2), forward scatter 42 (±1 in the present day treatments and ±2 in the high CO_2) (measurements in arbitrary unts related to laser detection). Red fluorescence per cell was significantly higher (F=5.23, p=0.04) and more variable for the high CO_2 grown cells 250 ± 23 compared to 235 ± 4 in the present day cultures (**Table 3.6**). Red fluorescence per cell correlated with side scatter and forward scatter, suggesting that smaller cells had less red fluorescence. Although the mean was significantly higher, one of the high CO_2 cultures did not show any increase in red fluorescence cell^{-1} (**Fig. 3.10**).

Table 3.6 Analysis of variance of red fluorescence cell^{-1} for cells grown in continuous culture for 3 months at either present day or high CO_2.

Red fluorescence cell^{-1}						
Source of Variation	*SS*	*df*	*MS*	*F*	*P-value*	*F crit*
Between Groups	1124	1	1124	5.23	0.04	4.49
Within Groups	3437	16	214			
Total	4561	17				

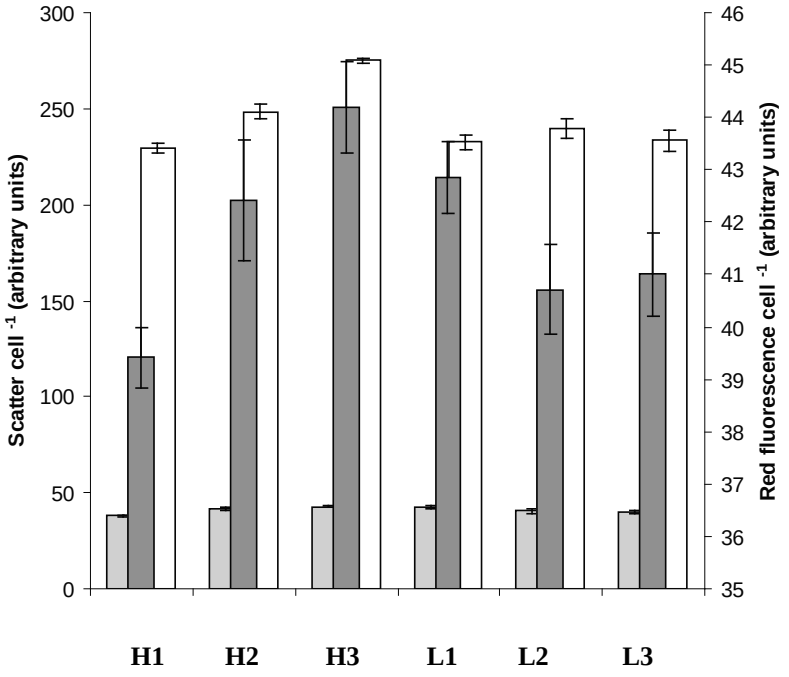

Fig. 3.10 Flow cytometry results for triplicate continuous cultures of *T. pseudonana* maintained at high CO_2 (H) or air (L) for three months. Side scatter per cell (▫); forward scatter per cell (▪); red fluorescence per cell (□). Units are arbitrary measurements of laser beam deflection and detection of fluorescence.

3.5.6 Gene expression as determined by quantitative PCR

It was hypothesised that *rbcs* and carbonic anhydrase transcription would be down-regulated at increased CO_2 due to a reduced need for carbon concentrating mechanisms and RuBisCO carboxylation. However, no significant difference was found in *rbcs* transcription in the continuous cultures grown at increased CO_2 or present day CO_2 for 3 months. Up-regulation was seen in one carbonic anhydrase gene. For this analysis, cells were harvested rapidly by centrifugation, RNA was chemically stabilised and isolated from the cells, quantified and reverse transcribed to produce copy DNA. Similar quantities of cDNA from high CO_2 and present day treatment samples were analysed by qRT-PCR to determine the relative gene transcription. A comprehensive description of the procedures is included in the methods chapter. Rigorous optimization of the procedures was performed and the protocol was tested using samples taken from

a tris buffered experiment and found to perform well. The elongation factor EF1α gene and actin, two commonly used housekeeping genes, were used as internal references. They showed good correlation and the final analysis using REST software (2.4.14 o-p) normalised results taking both genes into account. The results of the qRT-PCR analysis showed an up-regulation of CA4 at increased CO_2 compared to present day of a mean factor of 1.8 (S.E. range 1.2 - 2.4), the probability that this was significant was p=0.008. No significant differences in transcription of the other genes were found (**Fig. 3.11, Table 3.7**).

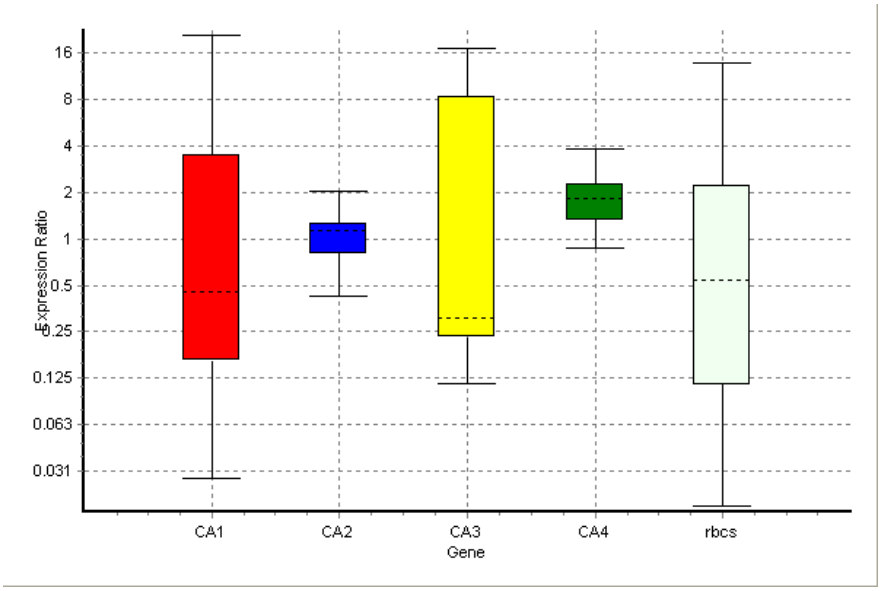

Gene	Type	Reaction Efficiency	Expression	Std. Error	95% C.I.	P(H1)	Result
EF1a	REF	1.10	0.99				
CA1	TRG	1.07	0.64	0.06 - 5.9	0.03 - 18.28	0.60	
CA2	TRG	0.86	1.05	0.66 - 1.51	0.49 - 1.97	0.84	
CA3	TRG	1.03	0.89	0.17 - 13.40	0.11 - 16.96	0.86	
CA4	TRG	1.28	1.79	1.24 - 2.43	0.95 - 3.8	0.008	UP
rbcs	TRG	0.92	0.52	0.08 - 3.62	0.03 - 12.19	0.42	
actin	REF	1.37	1.01				

Fig. 3.11 and Table 3.7 REST analysis of the differences between mean expression of four carbonic anhydrases and *rbcs* in high CO_2 continuous cultures compared to present day controls using EF1α and actin as housekeeping genes. The box represents the inter quartile range with the whiskers showing the upper and lower 25% of observations. The dotted line, within the box, indicates the median value. CA4 was significantly up-regulated (p=0.005). P(H1) is the calculated probability of there being no difference between treatments.

3.6 EVIDENCE FOR ACCLIMATION OF *THALASSIOSIRA PSEUDONANA* TO HIGH CO_2 AFTER APPROXIMATELY 100 GENERATIONS.

The following experiments were conducted to examine whether continuous cultures grown for three months, under either high CO_2 or air conditions had acclimated or adaptated to the conditions. If cells grown at increased CO_2 for 100 generations were then able to grow better at high CO_2 than cells which had not had this treatment, it would suggest that they had adapted. If cells grown at high CO_2 were then less able to grow at ambient CO_2 then they may have down-regulated their carbon acquisition or fixation mechanisms, by acclimation. Two analyses were performed, one in larger volumes for analyses and a second with more, smaller volume replicates for improved statistical analysis (**Fig. 3.7**).

3.6.1. Large volume (900ml) experiment

Twelve batch cultures were set up containing 900ml of pre-equilibrated F/2 + Si media. Inocula of 1x 10^5 cells, from the continuous cultures grown under high or present day CO_2, were made into each vessel. Cultures were maintained under the same light and temperature conditions as during the long-term growth period and were aerated with either air or high CO_2 air mix (methods section 2.3.7a). Cell number and pH were measured daily. Cells reached stationary phase very rapidly, therefore two dilutions were made to refresh the nutrients and stimulate continued growth. On the final day cells were harvested for C:N analysis, flow cytometry and gene expression. All cultures were growing exponentially at this time.

3.6.1a pH

Despite aeration of cultures in this phase of the experiment, pH was not maintained and rose rapidly as the cell density increased (**Fig. 3.12**). A permutation based analysis of

variance, PERMANOVA (section 2.5) confirmed a significant difference in pH was maintained between the high CO_2 and present day treatments, despite the increase in pH (Pseudo-F=5.99, p=0.002, **Table 3.8**).

Table 3.8 Results from permutation-based Analysis of Variance tests for differences in *T. pseudonana* pH between the four treatments and between different days of the experiment.

Source	df	SS	MS	Pseudo-F	P (perm)	permutations
treatment	3	0.80	0.27	5.99	0.002	998
day	6	6.66	1.11	24.95	0.001	998
Treatment x day	18	0.96	0.05	1.19	0.285	997
Residual	56	2.49	0.04			
Total	83	10.90				

3.6.1b Specific growth rates

Cell samples were counted daily by Coulter Multisizer II Coulter Counter (section 2.4.1, **Fig. 3.13**). There was an initial short lag phase followed by exponential growth in all cultures by day 3. Unexpectedly, growth then slowed in all cultures. On day 6, cells were diluted with fresh media to replenish nutrients and cultures immediately started to grow exponentially again. The following day they were again diluted and again grew exponentially. Three separate exponential growth phases were compared: the initial period, days 3 to 4 and subsequent phases following dilution, days 6 to 7 and 7 to 8. Mean specific growth rates (μ d^{-1}) for the three periods of exponential growth were 0.88 ± 0.29 in the LL treatment, 0.64 ± 0.13 in the LH treatment, 0.91 ± 0.33 in the HL treatment and 1.02 ± 0.19 in the HH treatment. Results of a permutation-based analysis of variance (PERMANOVA, section 2.5) for each exponential phase showed no differences between treatments and also no significant differences between the three time points or interaction between time point and treatment (**Table 3.9**).

Table 3.9 Results of permutation-based Analysis of Variance tests for differences in *T. pseudonana* specific growth rate of the four treatments on three different days.

Source	df	SS	MS	Pseudo-F	P (perm)	permutations
treatment	3	0.19	0.06	0.73	0.55	9952
day	2	0.55	0.27	3.23	0.06	9954
Treatment x day	6	0.98	0.16	1.91	0.13	9952
Residual	24	2.04	0.09			
Total						

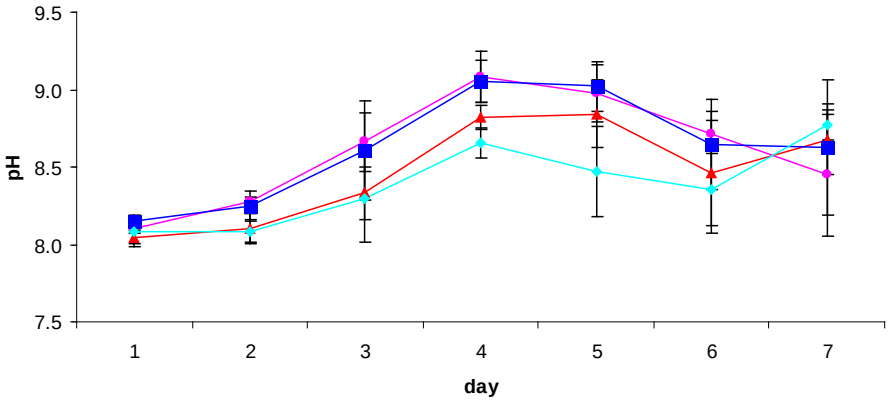

Fig. 3.12 Mean pH of triplicate batch cultures of *T. pseudonana* grown under four different treatments: HH (-▲-); HL(-●-); LH (-♦-) LL(-■-). Error bars are standard deviations of the three cultures. Each replicate was inoculated with cells from a separate continuous culture.

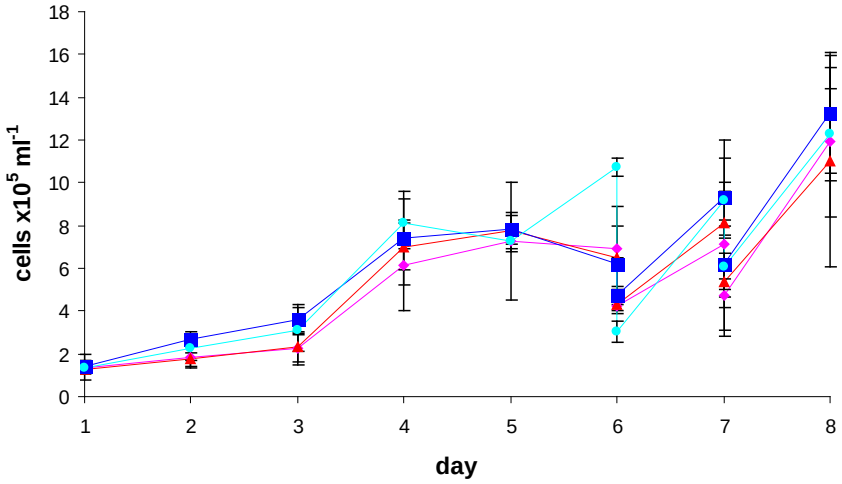

Fig. 3.13 Mean cell numbers of triplicate batch cultures of *T. pseudonana* under four different treatments. HH (-▲-); HL(-●-); LH (-♦-) and LL (-■-). Error bars are standard deviations of the three cultures. Each replicate arose from an inoculum from a separate continuous culture

3.6.1c Carbon and nitrogen content

POC and PON were analysed as described in section 2.4.4. Means and standard deviations of POC:PON (atom:atom) in the HL culture were 7.36 ± 0.6, in the HH culture were 7.16 ± 0.54, in the LH culture were 6.93 ± 0.32 and in the LL culture were 7.19 ± 0.31. No significant differences were seen between the means of the four conditions. Global test ANOSIM (R=0.03, p=19.5%). (**Table 3.10**).

Table 3.10 Results from a permutation based analysis of variance (section 2.5) examining the differences between all treatments. The very low R statistic shows the high degree of confidence that there is no difference between treatments.

Global Test
Sample statistic (Global R): 0.032
Significance level of sample statistic: 19.5%
Number of permutations: 999 (Random sample from a large number)
Number of permuted statistics greater than or equal to Global R: 194

3.6.1d Photophysiology

The quantum efficiency of photochemistry in PSII (Fv/Fm) and the relative functional absorption cross section of PSII (σ_{PSII}) were measured using a SATLANTIC FIRe Fluorometer system. There were no significant differences between the treatments for either parameter (**Table 3.11**). Mean Fv/Fm values were 0.59 ± 0.010 in LL, 0.60 ± 0.02 in LH, 0.58 ± 0.03 in HL and 0.59 ± 0.02 in HH. Mean σ values were 877 ± 19 in LL, 829 ± 37 in LH, 908 ± 98 in HL and 856 ± 40 in HH.

Table 3.11 PERMANOVA analysis of Fv/Fm and σ in all 4 treatments of the evaluation experiment. p (perm) is the probability that the results are significantly different between treatments.

Source	df	SS	MS	Pseudo-F	P(perm)	Unique perms
Fv/Fm						
Treatment	3	9.2×10^{4}	3×10^{-4}	0.58	0.72	801
Res	8	4.3×10^{3}	5.3×10^{-4}			
Total	11	5.1×10^{-3}				
σ						
Treatment	3	10112	3370	1.05	0.48	940
Res	8	25759	3219			
Total	11	35871				

3.6.1e Flow cytometry

Three samples from each of the three replicate cultures for each treatment were analysed using a PERMANOVA. There were no significant differences between treatment means of forward scatter, side scatter or red fluorescence per cell (**Table 3.12, Fig. 3.14**).

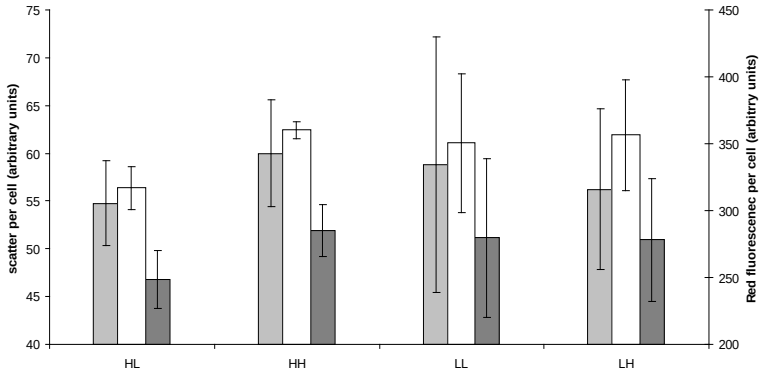

Fig 3.14 Flow cytometry of triplicate HH, HL, LH and LL. Error bars are standard deviations of the three cultures. Side scatter per cell (▪); forward scatter per cell (■); red fluorescence per cell (□). Units are arbitrary measurements of laser beam deflection and detection of fluorescence.

Table 3.12 PERMANOVA analysis of means and standard deviations of flow cytometry measurements for triplicate cultures for each treatment (section 2.5).

Source	df	SS	MS	Pseudo-F	P(perm)	Unique perms
Red fl cell^{-1} geomean						
Treatment	3	3537	1179	1	0.45	972
Residual	8	994	1180			
Total	11	12980				
SSC geomean						
Treatment	3	51	17	0.23	0.86	978
Residual	8	601	75			
Total	11	653				
Red fl cell^{-1} standard deviation						
Treatment	3	859	286	1.16	0.38	996
Residual	8	1981	247			
Total	11	2840				
SSC standard deviation						
Treatment	3	407	135	0.72	0.79	967
Residual	8	1519	189			
Total	11	1927				
FSC standard deviation						
Treatment	3	30	10	2.46	0.15	971
Residual	8	33	4			
Total	11	64				

3.6.1f Gene expression

Very mixed results were obtained in the analysis of the abundance of mRNA transcripts of the *rbcs* and carbonic anhydrase genes (**Fig. 3.15, Fig. 3.16**). In the 900ml acclimation experiment consistent up- or down-regulation was not seen. The carbonic anhydrases and *rbcs* did not show the same response to a treatment. Conflicting results were seen in treatments which should have been similar, eg. H>L but LL>HH. The results did not support the hypothesis and some were difficult to explain. There was a significant down-regulation of *rbcs* at LL compared to HH and to HL suggesting that cells acclimated to increased CO_2 had higher RuBisCO transcription than those in present day conditions. This was the opposite of the hypothesised response, of reduced transcription at increased CO_2. Cells grown at increased CO_2 for 3 months then returned to present day conditions had greater transcription of *rbcs* than cells which were always in present day conditions suggesting an acclimatory response.

The carbonic anhydrases showed mixed results. CA1 was down-regulated in the HL treatment compared to HH. Here the cells experienced lower pCO_2 and yet more CA1 was transcribed. CA2 was down-regulated in HH compared to LH suggesting that cells acclimated to present day CO_2, then grown at increased CO_2, transcribed less CA2 than those maintained at increased CO_2. This might be due to a reduced requirement for this CA. CA3 was not significantly affected by any treatment. CA4 was the most variable gene. It was significantly down-regulated in present day conditions compared to high CO_2 in the continuous cultures. However when those cells were transferred to batch cultures with the same CO_2 treatment, CA4 was down-regulated in the high CO_2 cultures compared to the present day. When present day acclimated cells were then grown at increased CO_2, CA4 was up-regulated compared to cells maintained at increased CO_2. When high CO_2 acclimated cells were grown in present day CO_2, CA4

was up-regulated compared to those maintained at increased CO_2; this is consistent with the fact that carbonic anhydrase is up-regulated at lower pCO_2 .

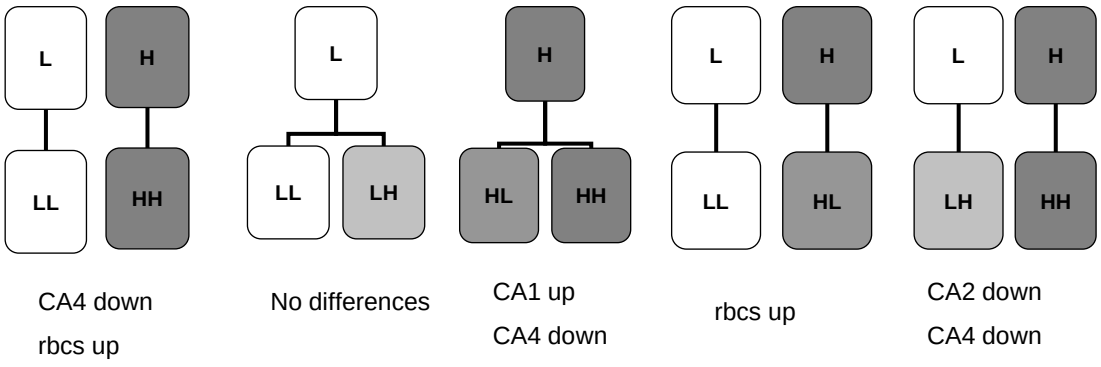

Fig. 3.15 Schematic representation of differences in gene expression between treatments.

Table 3.13 Means and standard deviations from three continuous cultures for each treatment (Present day and High CO_2) and the 900 ml evaluation experiment (LL, LH, HL and HH, see Fig 3.7). Cell specific growth rate μ (d^{-1}), flow cytometry readings for red fluorescence (Red fl), side scatter (SSC) and forward scatter (FSC) per cell, Fv/Fm, σ, C:N. *rbcl* and CA1-4 are gene expression results, paired analyses of treatments were performed with REST software (section 2.4.14 0-p) to determine the treatment with higher transcription of the gene.

	Present day	High CO_2	LL	LH	HL	HH
μ (d^{-1})			0.88 ± 0.29	0.64 ± 0.13	0.91 ± 0.33	1.02 ± 0.19
Red fl $cell^{-1}$	235 ± 4	251 ± 23	350 ± 52	356 ± 41	317 ± 16	360 ± 6
SSC $Cell^{-1}$	41 ± 1	41 ± 3	59 ± 13	56 ±8	55 ± 4	60 ± 6
FSC $Cell^{-1}$	42 ± 1	42 ± 2	51 ± 8	51 ± 6	47 ± 3	52 ± 3
Fv/Fm	0.62 ± 0.01	0.60 ± 0.02	0.59 ± 0.01	0.60 ± 0.02	0.58 ± 0.03	0.59 ± 0.02
σ	742 ± 52	772 ± 65	877 ± 19	829 ± 37	908 ± 98	856 ± 40
C:N	6.40 ± 0.40	5.96 ± 0.12	6.17 ± 0.23	5.95 ± 0.25	6.31 ± 0.52	6.14 ± 0.15
rbcl					HL>LL	HH>LL
CA1						HH>HL
CA2				LH>HH		
CA3						
CA4		H>L	LL>HH	LH>HH	HL>HH	

Table 3.14 Results of REST analysis of differences in gene expression between treatments. P(H1) shows the computed probability that there is no difference between treatments. The final column shows the direction of this difference. Analyses were always performed such that this relates to high CO_2 treatments being up or down-regulated compared to present day controls.

Gene	Reaction Efficiency	Expression	Std. Error	95% C.I.	P(H1)	Result
LH-HH						
EF1a	1.10	0.78				
CA1	1.07	1.39	0.08 - 37.39	0.02 - 94.5	0.77	
CA2	0.86	0.79	0.63 - 0.98	0.51 - 1.13	0.04	DOWN
CA3	1.03	0.51	0.02 - 4.03	0.01 - 11.98	0.50	
CA4	1.28	0.47	0.32 - 0.65	0.23 - 0.95	0.003	DOWN
rbcs	0.92	2.09	0.76 - 7.0	0.51 - 14.27	0.178	
actin	1.63	1.29				
LL-LH						
EF1a	1.10	0.82				
CA1	1.072	0.8	0.025 - 109.8	0 - 183.6	0.87	
CA2	0.86	0.64	0.18 - 1.8	0.14 - 2.5	0.37	
CA3	1.03	0.40	0.004 - 50.4	0.001 - 67.9	0.56	
CA4	1.28	0.6	0.14 - 1.6	0.09 - 2.04	0.36	
rbcs	0.92	1.95	0.5 - 4.7	0.37 - 6.06	0.15	
actin	1.64	1.22				
HL-HH						
EF1a	1.10	0.73				
CA1	1.07	4.46	1.4 - 11.9	0.75 - 25.1	0.01	UP
CA2	0.86	0.85	0.36 - 1.5	0.26 - 2.2	0.69	
CA3	1.03	0.63	0.06 - 3.6	0.03 - 6.9	0.54	
CA4	1.28	0.42	0.29 - 0.6	0.21 - 0.87	0.002	DOWN
rbcs	0.92	1.62	0.72 - 3.95	0.47 - 8.88	0.23	
actin	1.64	1.37				
LL-HL						
EF1a	1.10	0.87				
CA1	1.06	0.24	0.004 - 3.28	0.002 - 5.26	0.43	
CA2	0.85	0.59	0.13 - 1.71	0.07- 5.10	0.33	
CA3	1.02	0.32	0.004 - 12.04	0.002 - 23.16	0.36	
CA4	1.28	0.66	0.18 - 1.65	0.09 - 2.22	0.41	
rbcs	0.92	5.65	1.41 - 34.75	0.78 - 48.62	0.02	UP
actin	1.63	1.13				
LL-HH						
EF1a	1.10	0.63				
CA1	1.06	1.11	0.02 - 17.08	0.005 - 28.30	0.93	
CA2	0.85	0.50	0.15 - 1.45	0.12 - 1.65	0.18	
CA3	1.02	0.20	0.004 - 2.58	0.003 - 4.22	0.32	
CA4	1.28	0.27	0.07 - 0.65	0.05 - 0.74	0.002	DOWN
rbcs	0.92	4.08	2.50 - 6.86	1.85 - 10.17	0.00	UP
actin	1.63	1.56				

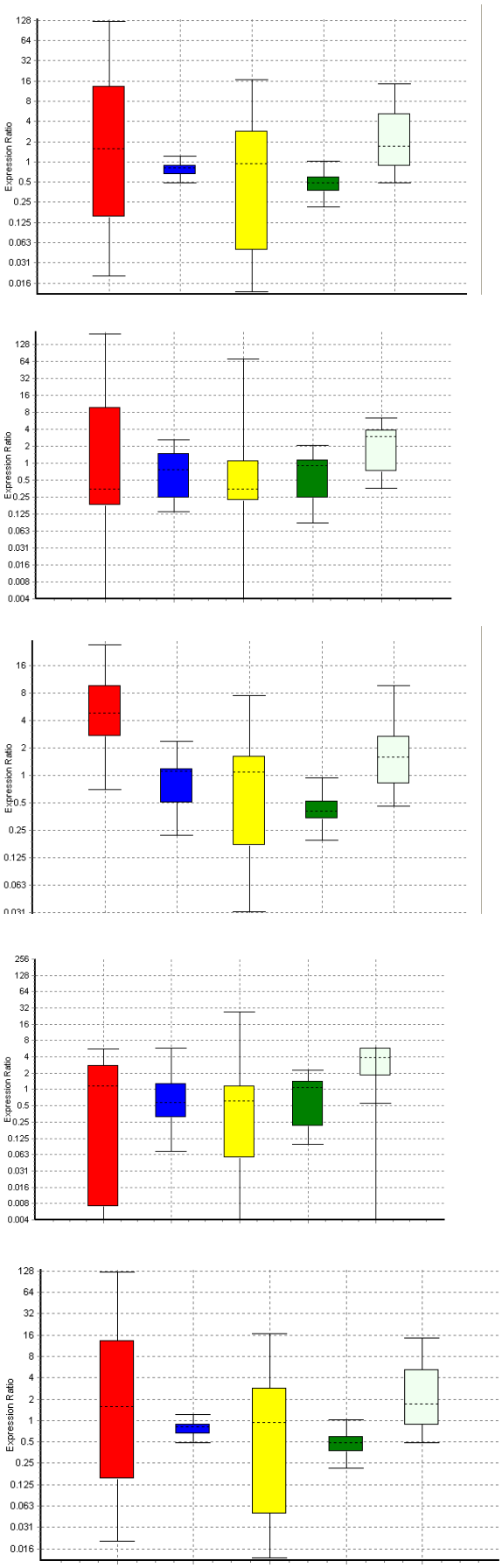

Fig. 3.16 REST analyses of qRT-PCR data for the 900 ml acclimation experiment. From the top: LH-HH, LL-LH, HL-HH, LL-HL and LL-HH. Genes from left to right, red: CA1, blue: CA2, yellow: CA3, green: CA4, and pale green: *rbcs*. The box represents the inter quartile range with the whiskers showing the upper and lower 25% of observations. The dotted line, within the box, indicates the median value.

3.6.2 High replication experiment to evaluate the effects of growth of Thalassiosira pseudonana at 760 ppm CO_2

To add statistical weight to my evaluation, I grew a larger number of small cultures in micro-titre plates (volume only 1.5 ml), and assessed growth as increase in optical density. There were eighteen replicates for each treatment, six from each of three continuous cultures, and six blanks in each of four 24 well plates. Cultures were grown in plates, without lids, in chambers flushed with the appropriate gas mix. The optical density of the cultures was read daily at 590 nm (**Fig. 3.17**).

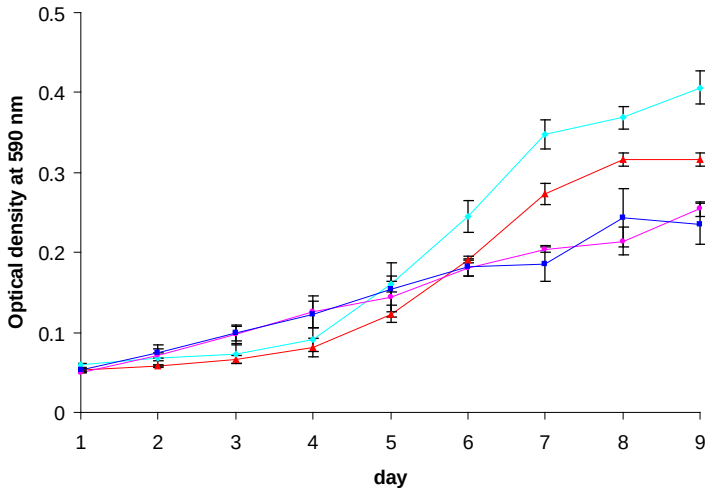

Fig. 3.17 Mean optical densities of the six replicate cultures of *T. pseudonana* under four different treatments. HH (-▲-); HL(-●-); LH(-♦-) and LL (-■-). Error bars are standard deviations of the 18 replicates for each treatment, combining six replicates from each of the three continuous cultures.

There was a linear increase in optical density for cultures growing in air which started to increase almost immediately whilst those in high CO_2 showed exponential growth following a short lag period. The relative growth constant (k), equivalent to μ, is defined as ($\log_e N_t$ / $\log_e N_0$) /t), where N = optical density and t = time, was calculated for the four treatments (**Table 3.15**). Maximum growth constants for the HL and LL treatments of 0.34 (± 0.06) and 0.35 (± 0.16) respectively were measured on day 2 and

gradually decreased over the course of the experiment. The HH and LH treatments showed lag phases, and maximum growth constants of 0.44 (± 0.1) and 0.57 (± 0.12) were measured on days 6 and 5 for the HH and LH cultures respectively. There was no significant difference in k between treatments when these were averaged across days 1-8, (R=-0.01, p=65.3%). Final optical densities were significantly different amongst treatments (R=0.179, p=0.1%). HH and HL; HH and LL; LH and HL and LH and LL treatments differed significantly at the 0.1% significance level (**Table 3.15**).

Table 3.15. ANOSIM for relative growth constants (k) and maximum optical density (OD) for the four treatments; HH, LH, HL and LL.

Global Test k

Sample statistic (Global R): -0.01
Significance level of sample statistic: 65.3%
Number of permutations: 999 (Random sample from a large number)
Number of permuted statistics greater than or equal to Global R: 652

Global Test Max optical density

Sample statistic (Global R): 0.179
Significance level of sample statistic: 0.1%
Number of permutations: 999 (Random sample from a large number)
Number of permuted statistics greater than or equal to Global R: 0

Pairwise Tests

Groups	R Statistic	Significance Level %	Possible Permutations	Actual Permutations	Number >=R Observed
HH, LH	0.027	13	Very large	999	129
HH, HL	0.194	0.1	Very large	999	0
HH, LL	0.232	0.1	Very large	999	0
LH, HL	0.293	0.1	Very large	999	0
LH, LL	0.343	0.1	Very large	999	0
HL, LL	0.00	28.1	Very large	999	280

3.7 DISCUSSION

Several conclusions may be drawn from this series of experiments. Firstly, increased CO_2 had no significant effect on growth rates of either the calcifying strain of *E. huxleyi* CCMP371, or the non-calcified *E. huxleyi* CCMP1516. This is similar to the conclusions drawn by (Riebesell et al. 2007; Buitenhuis et al. 1999; Feng et al. 2008; Clark and Flynn, 2000; Zondervan et al. 2002; Leonardos and Geider. 2005; Shi et al, 2009). Increased CO_2 increased the cell division rate of *T. pseudonana* in batch culture

and with buffers. However when cells were maintained in exponential phase with pH controlled and nutrients refreshed daily, no effect on growth rate was seen. This suggests that when high cell densities decrease the available CO_2, some benefit may be gained by bubbling with a higher pCO_2 gas. This could be applicable in a bloom situation, and a significant proportion of carbon export is associated with blooms (Westbroek et al. 1993). In a well controlled experiment I found that cell division in *T. pseudonana* was unaffected by increased CO_2 at 760ppm, this was also found by Pruder and Bolton (1979). Similar results have been reported for other diatom species (Tortell et al. 1997; Tortell 2000; Kim et al. 2006; Shi et al. 2009).

The other physiological variables measured showed some response to increased CO_2. A significantly lower C:N and significantly higher red fluorescence $cell^{-1}$ was found in the cultures grown at increased CO_2, cell size remained unchanged. As chlorophyll is high in N, there is a strong correlation between chlorophyll and N content in plants so these results suggest increased chlorophyll at high CO_2. The term 'carbon overconsumption' has been applied to the uptake of carbon in excess of the expected amount calculated from the nitrate uptake and Redfield ratio. There is little evidence that C:N is affected but rather the excess carbon is exuded (Engel et al. 2004a; Engel et al. 2005; Riebesell et al. 2007). The increased C:N in the present day treatment is not consistent with this response but measurements are not comparable because exudates are too small to be collected on the filters. Although a significant difference was seen between my present day and high CO_2 treatments, the 3 present day cultures were quite variable and POC:PON really only appeared to be much higher in one culture (**Fig. 3.9**).

Red fluorescence $cell^{-1}$ was significantly higher in the high CO_2 than in present day continuous cultures ($F=5.23$, $p=0.04$), however the results were variable. There is

evidence that increased CO_2 can lead to increased pigment content per cell in phytoplankton (Collins and Bell 2004; Fu et al. 2007). As changes in pigment content are usually associated with photo-acclimation rather than changes in DIC (Raven 2003), the mechanism behind this is unclear. I also saw increases in red fluorescence in the 900ml evaluation experiment, with HH higher than HL but this were not significant and again very variable results were found (**Fig. 3.18**). There is no growth rate data for the continuous cultures so it is possible that the cells in the cultures were growing at different rates. From my preliminary experiments I found that red fluorescence cell^{-1} varied with growth rate. Although not significant, the scatter of the cells with lower red fluorescence was also lower, suggesting that these cells were smaller. Red fluorescence cell^{-1} was higher in the batch cultures inoculated from the long-term continuous culture than at the end of the long-term experiment (**Fig 3.18**). It is probable that cells in the batch cultures were dividing faster than in the continuous cultures where they were continually diluted and appeared less healthy. In future experiments it is essential that a method for taking regular measurements of cell division is established.

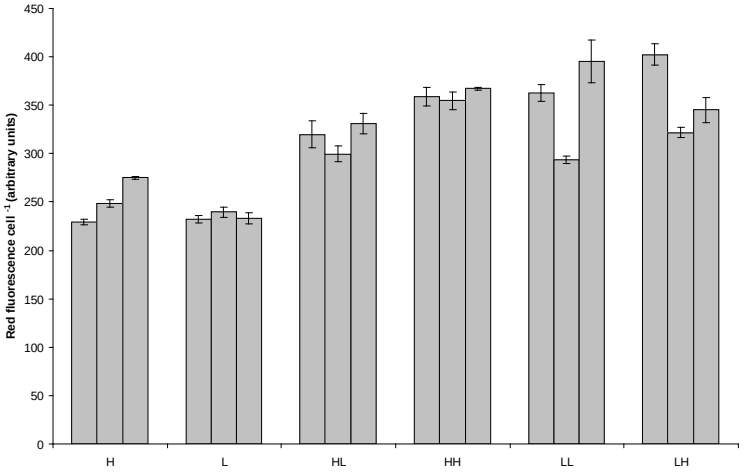

Fig. 3.18 Red fluorescence cell^{-1} in continuous cultures and subsequent acclimation experiment.

No significant differences between treatments were seen for side scatter, forward scatter, Fv/Fm or σ in either the continuous cultures or the acclimation experiment.

A significant difference in the specific growth constants of the HL, HH, LL and LH treatments were seen in the 1.5 ml evaluation experiments. Cells grown at high CO_2 (LH and HH) had higher k values (k is equivalent to μ but based on changes in optical density) and maximum cell densities than those grown under present day pCO_2 (LL and HL), regardless of the previous long term treatment (**Table 3.15**). In the 900 ml evaluation experiment no significant differences in growth rate were seen.

The results of the qRT-PCR analysis were difficult to interpret. Samples were taken from well controlled, comparable cultures in exponential phase. The final results were calculated by normalisation to the two reference genes, actin and EF1α. The inclusion of EF1α as a second reference gene, in this study, was shown to be a wise decision. Granum et al. (2009) found that actin expression did not show consistent transcription in *T. pseudonana*, although this was in response to nitrate addition. My results showed an up-regulation of CA4 in the high CO_2 continuous cultures compared to the present day and no significant differences in transcription of *rbcs* or the other CA genes. The lack of effect on gene transcription is in accordance with the lack of significant effects on growth in the cultures. A lack of sensitivity of *rbcL* (the RuBisCO large subunit) transcription and protein formation to reduced pCO_2 in *T. pseudonana* was also found by Roberts et al. (2007) and Granum et al. (2009). The small, but significant, up-regulation of CA4 by a factor of 1.8 was unexpected as CO_2 was more available. However, carbonic anhydrases catalyse CO_2 and bicarbonate inter-conversion at different locations within the cell, for example at the RuBisCO active site and within cellular compartments to prevent leakage from the cell. The location and function of

the CAs examined has not been established so there may be a biological explanation for this up-regulation. For example, increased HCO_3^- in the vicinity of RuBisCO could cause an increase in CA in order to increase CO_2 supply to the enzyme. CA4 was down-regulated in HH compared to the three other treatments: LL, LH and HL. This result is rather contradictory to that for the continuous cultures and makes a logical explanation difficult. CA2 was up-regulated in HL compared to HH, and CA1 was down-regulated in LH compared to HH. *rbcs* was down-regulated in LL compared to HL and HH. McGinn and Morel (2007) found that CA4 and CA2 (their CA3) were much less expressed than CA1 (their CA2) and CA3 (their CA1) (gene nomenclature will refer to my assignation in the following discussion). High levels of transcription were found in CA4 and CA2, which increased when cells were allowed to grow and reach stationary phase, with a pH of 8.9 suggesting limited pCO_2 (McGinn and Morel 2007). CA2 was modestly increased by reduced pCO_2 and expressed at much lower levels than CA1 and CA3, while CA4 was not affected. My results are very different, in that I found CA4 to be the most responsive gene, CA3 showed no differences between treatments. However, the results of McGinn and Morel (2007) show no large effects on any of the carbonic anhydrases at between pH 7.5 and 8.8, a slight decrease over this range was found. At pH 8.8-9.1 a large increase in transcript abundance of the carbonic anhydrases was found. The RuBisCO large subunit (*rbcL*) was monitored and a decrease in transcription was found in the range of pH 7.5-8.8, which then increased with the increase in CA transcription between pH 8.8 and 9.1. They have not proved that these code for CAs but their regulation by zinc, cobalt and pCO_2 strongly suggests that they do code for functional CAs. Homologs of this gene exist in a wide range of phytoplankton, including prymnesiophytes, dinoflagellates and chlorophytes.

The qRT-PCR analyses appeared to have performed well, however the results were difficult to explain. It would have been useful to run some samples grown at very low

pCO_2 to test the sensitivity of the assay. As transcription dos not necessarily equate to protein production, assays of the proteins would have also been wise. I performed a carbonic anhydrase enzyme assay in a preliminary experiment but this did not appear to be very sensitive. One pitfall of the REST analysis was that it did not allow inter-plate calibration. As the samples were analysed on a series of plates differences between the fluorescence detection in the plates may have resulted in some differences between samples, causing erroneous results.

If an evolutionary change had occurred, it was hypothesised that cells grown at increased CO_2 would fare better than those grown in present day conditions when both were grown at increased CO_2, HH vs LH. CA2 and CA4 were down-regulated in the HH treatment compared to LH treatments. This is consistent with the evolutionary hypothesis, in that less carbonic anhydrase may be necessary in a world with more abundant CO_2, and thus an energetic saving may be made. The specific growth rate, μ, of the HH cells was significantly higher than the LH cells in the 900 ml evaluation experiment. But in 1.5 ml cultures, k and the maximum cell density were higher for the LH cells. There is obviously conflicting data here, but hypothetically, decreased carbonic anhydrase expression linked to a higher cell division rate would suggest that cells grown at high CO_2 may have evolved to be better suited to a high CO_2 world, although this is highly unlikely in 100 generations. A down-regulation of CA due to reduced necessity at higher CO_2 could result in an energy saving translated into increased cell division. This is speculative and there is little substantial evidence to make these assumptions. It is also possible that cultures in the LH treatment showed a shock response to the increased CO_2 whilst the HH cultures had experienced a long period of adjustment to the conditions. My results are not compatible with a short term fertilisation effect which would predict an increase in growth or decrease in *rbcs* and

CA transcription in the LH treatments compared to LL. In the micro-titre plate LH did grow significantly faster and to a higher maximum cell density than LL but the opposite was seen in the 900ml experiment.

Another hypothesis was that acclimation rather than adaptation may have occurred. If cells grown at increased CO_2 acclimated to the conditions they could be disadvantaged when returned to present day CO_2. This hypothesis was tested in the HL vs LL and HL vs HH treatments. An up-regulation of *rbcs* in HL compared to LL, and an up-regulation of CA4 compared to HH was seen. This is consistent with the hypothesis that cells would fare less well in present day conditions if they had previously been acclimated to increased CO_2. Growth rates and other physiological parameters were not significantly different.

These results suggest that *T. pseudonana* CCMP1335 did not adapt to increased CO_2, however when maintained at increased CO_2 for 3 months the concentration of chlorophyll per cell was significantly higher than in present day controls. Cell division rates of *E. huxleyi* CCMP1516 and CCMP371 were not affected by increased CO_2 . *T. pseudonana* showed increased growth rates in batch but not continuous cultures maintained at increased CO_2. These results will be further discussed in Chapter 6.

Chapter 4.

EXAMINATION OF THE EFFECTS OF INCREASED CO_2 ON A NATURAL PHYTOPLANKTON ASSEMBLAGE FROM A NORWEGIAN FJORD

4.1 INTRODUCTION

The ocean system is very complex. A myriad of trophic, symbiotic and commensal relationships exist between the many organismal levels from viruses to large predators. Laboratory experiments are useful in determining responses of key species or groups but do not assess the response of the system as a whole. A more realistic experimental system is one which captures a portion of the natural community and retains it in its natural environment whilst manipulating the variables under investigation. This should be of a scale large enough to encompass many trophic levels but small enough that replicates may be run and the system remain manageable. Such a system exists and has been termed a mesocosm due to being a middle sized 'meso', world 'cosm'. With the cost and effort involved in running such experiments it is important to extract as much information as possible. A consortium of scientists analyzing many variables is the most efficient method.

In order to examine the effects of increased CO_2 on natural assemblages of phytoplankton we carried out a mesocosm experiment at the Bergen large scale facility in the Raunefjorden in western Norway. This was conducted during May 2006 and an international consortium was involved. In this chapter I will firstly describe the mesocosm facility, explain the experimental design and list the measurements taken by the consortium. I will then examine the growth of the phytoplankton and the effect that this had on the seawater chemistry. This section will also include the differences that

were seen between the high CO_2 and present day treatments. In order to explain these differences a number of analyses were performed which will be described. The final discussion will put these results in the context of previous research.

4.2 BACKGROUND TO FACILITY

4.2.1 The Raunefjorden and its phytoplankton community

The experiment was carried out at the Marine Biological Field Station of the University of Bergen, Norway, (Raunefjorden, 60.3°N, 5.2°E). The Raunefjorden is a tidal fjord attached to the North Sea but with shallow sills between the small islands which reduce the exchange of water with the ocean (**Fig. 4.1**). The area is influenced by the Baltic Current which forms the Norwegian Coastal Current running North up the coast. The salinity is variable due to freshwater outflow from the Baltic and runoff from the Norwegian coast. We observed salinities of 31-32 practical salinity units (psu); for comparison, seawater in the north Atlantic is usually around 35.5 psu. Water temperature in the fjord varied between 8-10°C during our experiment. Being at 60.3°N there were 15 hours of daylight at the beginning of the experiment and 17h by the end. The first week was warm and sunny which increased the temperature in the mesocosms and surrounding fjord to nearly 11°C. pCO_2 at the beginning of May was only 260 ppm presumably due to previous phytoplankton growth.

The natural changes in the phytoplankton community during the year in the Raunefjorden are well defined (Larsen et al. 2004) and can be summarized as follows. High nutrient concentrations after winter mixing stimulate an increase in the numbers of autotrophic pico-eukaryotes and *Synechococcus* early in the year. This is followed by a diatom bloom between February and April, stimulated by increased light. This is succeeded by a bloom of *Emiliania huxleyi* (Fernandez et al. 1996) or *Phaeocystis*

pouchetii and may co-occur with a second diatom bloom, which is usually stimulated by upwelling of nutrients due to wind stress ((Larsen et al. 2004) and references therein). Later in the year diatoms are less likely to bloom as the silicate levels are not high enough to support their growth. *Synechococcus* and picoeukaryotes often dominate periods when nutrients are scarce as they are favoured by their greater surface area to volume quotient (Larsen et al. 2004).

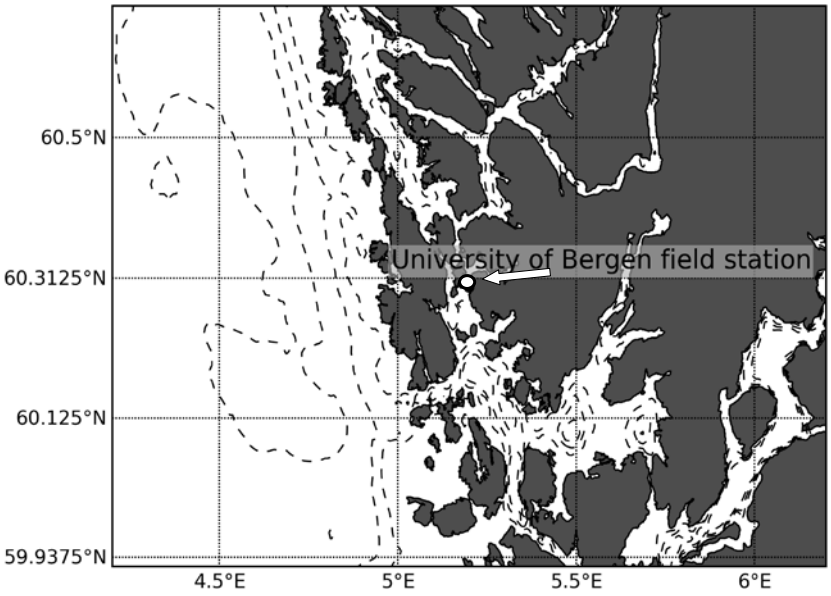

Fig. 4.1 The geographical location of the mesocosm facility within the Raunefjorden, a system of tidal inlets of the North Sea. Bathymetric lines indicate 100, 200 and 300m depths.

4.2.2 Bergen mesocosm system

The facility was constructed in the 1980s and has since been used many times, resulting in a time series and thorough background data set. A search of the literature revealed results published for seventeen experiments carried out at the facility. These were generally dominated by either *Emiliania huxleyi* or diatoms or a combination of the two (**Table 4.1**). To some extent, the dominant phytoplankton type can be determined by the investigators by manipulating the ratio of nutrients added. This was shown experimentally by Egge and Aksnes (1992). However if the natural silicate level is high diatoms tend to bloom.

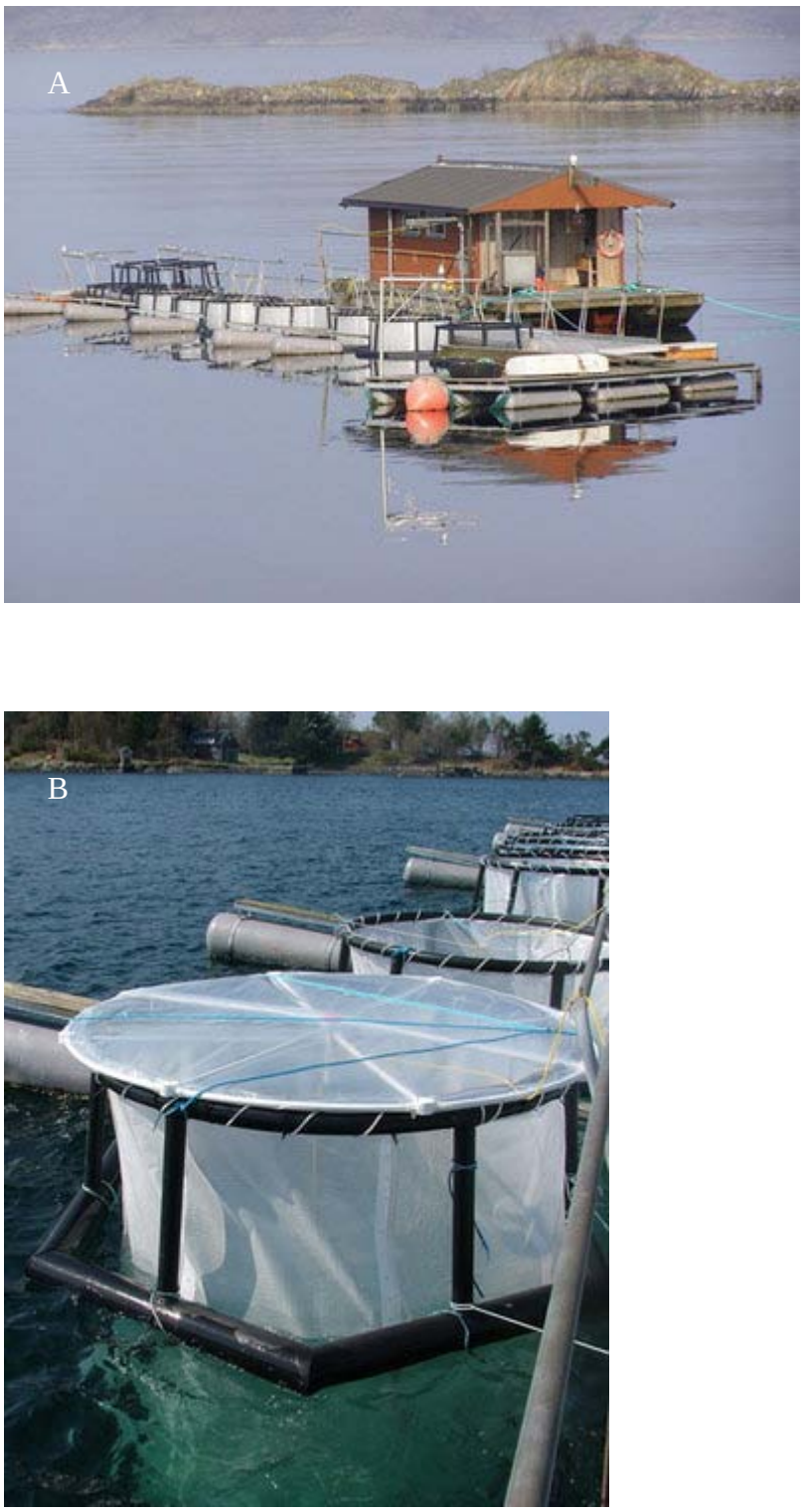

Fig. 4.2 A The mesocosm facility, six mesocosms can be seen on the near side of the raft. B. A mesocosm bag supported within a frame. The 12,000 litre capacity bags enclosed a water column 5m deep. The lid maintained a headspace at the correct pCO_2 whilst allowing light to penetrate.

Table 4.1 Summary of previous experiments carried out at the Bergen large-scale facility. References: 1(Castberg et al. 2001); 2 (Jacquet et al. 2002); 3(Martinez et al. 2007); 4(Benthien et al. 2007); 5(Engel et al. 2005); 7(Nejstgaard et al. 1997); 8 (Riebesell 2007); 9(Engel et al. 2004a); 10 (Søndergaard et al. 2000) 11 (Egge and Aksnes 1992)

Year	Month	Ref	Dominant Phytoplankton	Nutrients N:P:Si	Other manipulations
1983	July x 2	11	Diatoms	None	
1986	April x 4	11	Diatoms/*Phaeocystis*	N:P	
1987	June	11	*E.huxleyi*	N:P	
1987	Sept	11	*E.huxleyi*	N:P	
1988	April-July	11	Diatoms/*Phaeocystis*	5.5:1.5:6	
1988	April-July	11	*E.huxleyi*	5.5:1.5	
1988	September		Diatoms	N:P:Si	
1994	May-July	7	Diatoms with silicate Diatoms/ *E.huxleyi*	16:1:0	Silicate added to some mesocosms, grazing
1997	July	10	Diatoms/prymnesiophytes	0.6:0.04:1	
1999	May-June	1	*E.huxleyi*	16:1:0	
2000	June	2, 3	*E.huxleyi*	15:1:0	
2001	May-June	4, 5	*E.huxleyi*	30:1:0	CO_2: 180, 380, 700 ppm
2005	May-June	8			
2006	May			15:1:0	CO_2 at 380, 760 ppm

4.2.3 Experimental design

The experiment was carried out between 1st May and 23rd May 2006. The experimental system was based on a purpose built raft that was moored 200m from the shore (**Fig. 4.2 A**). Attached to the raft were floating frames designed to support the large mesocosm bags (**Fig. 4.2 B**). The impermeable bags of 12,000 litres capacity were made of reinforced polyethylene by Spartel, Plymouth. Each bag was covered with a lid to maintain a headspace at the target pCO_2 and to prevent rainwater from entering. Lids were made of UV-transparent polyethylene lids, which had high light penetration at all wavelengths absorbed by phytoplankton. Although the lids were not totally gas-tight, the headspace was maintained close to the target pCO_2. The mesocosms had a diameter of approximately 2m and depth of 5m. At the beginning of the experiment, the bags were filled with unfiltered water that was pumped directly from the fjord at a depth of 2m using a submersible pump supplied by the University of Bergen. Six mesocosms were filled over a period of 2 hours by adding water for 5 minutes in turn to each bag.

The aim was to achieve as constant an initial inoculum as was practicable, given the very large volumes of water (almost 70 tonnes) that we were working with. Aeration systems were composed of spargers within the bags at 4.5m below the surface. Three mesocosms were supplied with ambient air via large capacity air pumps and three with ambient air with elevated pCO_2 at 760 ppm. High pCO_2 was achieved using flow meters which were adjusted to give a target 760 ppm CO_2. The actual pCO_2 in the air mixture was measured inline with a LI-COR 6262 CO_2/H_2O analyser. In order to equilibrate the water to the appropriate level, it was necessary to have an immediate measurement of pH, reflecting the target pCO_2. This was achieved with a pH meter and standard electrode, it is not the most accurate method of determining pH and throughout the experiment, high precision pCO_2 and alkalinity measurements were made by Dorothee Bakker (UEA), from which pH was calculated. I was responsible for the initial pH measurements which sufficed for the gas equilibration of the mesocosms. After four days, pH 7.7 was reached in the elevated CO_2 bags and aeration ceased. This was equivalent to pCO_2 concentrations of 744 ppm (± 46) in the high CO_2 bags and 300 ppm (± 6) in the air bubbled bags. During the experiment, the water was not bubbled but target atmospheres of 760 ppm pCO_2 were maintained in the head-space of the high CO_2-treatment mesocosms. Mixing was provided during the experiment from a small submersible pump in each bag which was placed at 4.5m depth, with the outlet pipe just below the water surface. The pumps circulated about 10% of the total volume each day and maintained a homogeneous water column.

The development of a bloom was initiated by adding sodium nitrate and sodium dihydrogen phosphate to give final concentrations of 15 μmol l^{-1} and 1 μmol l^{-1} respectively. Mesocosms were sampled at the same time each day, between 10:00 and 11:00 local time. A suite of measurements were taken and samples stored for future

analysis. A full list of the scientists involved and data collected is given in **Table 4.2**. An effect of phytoplankton growth on water chemistry was to raise the pH in all the mesocosms. At the bloom peak, ten days after the addition of nutrients, the pH in the high CO_2 mesocosms had returned to the pre-equilibration level of 8.1; 333 ppm (± 36) in the high CO_2 mesocosms and 163 (± 7) ppm in the air mesocosms. The priority of this experiment was to examine the bacterial community at increased CO_2 so, on 15th May, it was necessary to re-bubble the mesocosms for the second half of the experiment. One mesocosm from each treatment was left un-bubbled to follow how the system would have responded if the second CO_2 addition was not made.

Table 4.2 Variables measured and scientists involved in the 2006 Bergen mesocosm experiment.

Variable	Institute	Scientists
Total chlorophyll	PML	Kate Crawfurd
Light		
Temperature		
Salinity		
Primary production	PML	Ian Joint
Nutrient analysis		
Bacterial metagenomic library	PML	Jack Gilbert
		John Woolven- Allen
Phytoplankton analysis	PML	Claire Widdicombe
CO_2 equilibration	PML	Phil Nightingale, Malcolm Liddicoat
Pigments (HPLC)	PML	Carole Llewellyn
C:N:H analysis	PML	Bob Head
pCO_2 and Total alkalinity	UEA	Dorothee Bakker
Flow cytometry (phytoplankton counts)	NOCS	Isabel Mary
	CEH	Andy Whiteley
Bacterial gene expression		
Bioinformatics	CEH	Tim Booth
Biogenic gases	UEA	Francis Hopkins
Bacterial use of trace gases	Warwick	Rich Boden
Nitrogen uptake by bacteria	Stirling	Rachel Jones
RuBisCO and NifH expression		Nick Meakin
Bacterial polysaccharide degradation	Liverpool	Mike Cox
Bacterial community composition (CARD-FISH)	Leibniz Institute of Ecology of Freshwater and Inland Fisheries, Germany (Berlin)	Cathleen Koppe
Sediment bacterial community	Cardiff	Louise O'Sullivan

4.3 RESULTS

Our mesocosms followed a similar pattern to several previous experiments carried out in May; initial dominance of nutrient poor water by autotrophic pico-eukaryotes and

Synechococcus followed by an increase in the numbers of flagellates and coccolithophores after nutrient addition. An initial lag phase was observed but growth was then rapid and maximum biomass was achieved after seven days. A mixed assemblage of phytoplankton dominated the mesocosms throughout the period with increasing numbers of larger species of flagellates. The dominant organism was a coccolithophore identified as *Emiliania huxleyi*. At the beginning of the experiment, diatoms were identified by light microscopy at 170 diatoms ml^{-1} in mesocosm 1 and 2120 ml^{-1} in mesocosm 6; but by 11th May, had decreased in number to <1 cell ml^{-1}. The most abundant diatom species were *Pseudonitzschia* sp. and *Leptocylindrus minimus*. During the experiment, pCO_2 decreased, pH increased and nutrients decreased until they were at very low concentrations. This section will first examine the community growth as a whole and the carbon taken up by photosynthesis during this period of growth. The growth of individual groups of phytoplankton will then be examined with a section focusing on the coccolithophores. The effects of the high CO_2 treatment on their calcification and strain dynamics was analysed and will be discussed.

4.3.1 Phytoplankton growth and carbon drawdown

One hypothesis being tested by this experiment was whether increased CO_2 would affect the quantity of carbon drawn down by the phytoplankton. This is fundamental to predicting carbon fluxes in a high CO_2 world. Current theory would suggest that there should be no increase in carbon drawdown as phytoplankton are nutrient limited and will adhere to the Redfield ratio, taking the same quantity of carbon irrespective of pCO_2. However, the results from a similar CO_2 perturbation mesocosm in Bergen reported increased carbon drawdown in response to increased CO_2 (Riebesell 2007). Carbon drawdown may be estimated in a number of ways, directly and indirectly. The most direct method is to incubate samples with radio-labelled bicarbonate (^{14}C) and

examine the uptake. Indirect methods include comparison of the phytoplankton biomass, cell numbers, pigments, particulate organic carbon, oxygen evolution and carbon drawdown may be calculated from the nutrient uptake or the change in dissolved inorganic carbon. We examined all these variables except oxygen evolution (**Table 4.3**), overall different methods yielded similar results and significant differences were seen between the high CO_2 and present day treatments.

Table 4.3 Measurements of community production. All values are means of available data with standard deviations, where applicable, in parentheses.

Variable	Method	Investigator		High CO_2	Present day
Chlorophyll ($\mu g\ l^{-1}$)	Acetone extraction	Kate Crawfurd	Maximum	2.36 (± 0.24)	3.25 (± 0.57)
Chl-a ($\mu g\ l^{-1}$)	HPLC	PML	Maximum	6.87 (± 3.3)	10.41 (± 1.1)
Productivity (mg C m^{-2} d^{-1})	^{14}C	Ian Joint	Maximum	700 (±15)	954 (±61)
POC ($\mu g\ C\ l^{-1}$)	C:N:H	PML	Maximum	919 (± 110)	1176 (no replicates)
Chl-a $cell^{-1}$	HPLC	PML	Cellular	$1x10^5$ ($\pm <1x10^{10}$)	$0.6x10^5$ ($\pm <1x10^{10}$)

A statistical analysis was performed in PRIMER 6 (section 2.5) using the chlorophyll acetone extraction measurements, primary productivity (^{14}C method), POC and PON measurements from 6^{th}-14^{th} May, prior to re-bubbling. Where values were missing an EM algorithm was used to calculate missing data. This was possible due to the tight correlations between the variables (**Fig. 4.3**). The data was then standardized to totals, ie. each measurement for each day was expressed as a percentage of the cumulative total for that measurement over the 8 days. A distance matrix was created using Euclidean distances. An MDS plot of the data (**Fig. 4.4**) shows that he pattern is similar for both treatments, but the present day data points (blu■,□,♦) extend further along the x axis. This suggests that the different measurements agree well and the magnitude of the production measurements is greater in the present day treatment mesocosms. A maximum of p=0.1 can be obtained when analysing differences between

three replicates for two treatments. An ANOSIM (section 2.5) gave an R value of 0.889 with the maximum probability of a difference (p=0.1). A PERMANOVA (section 2.5) using Monte Carlo methods (Anderson and Robinson 2001) which is a test which makes more assumptions about the data, but allows greater power with limited replicates, gave a much more significant probability of a difference between the treatments (pseudo-F = 15.064, p=0.106, Monte Carlo p=0.012, **Table 4.4**).

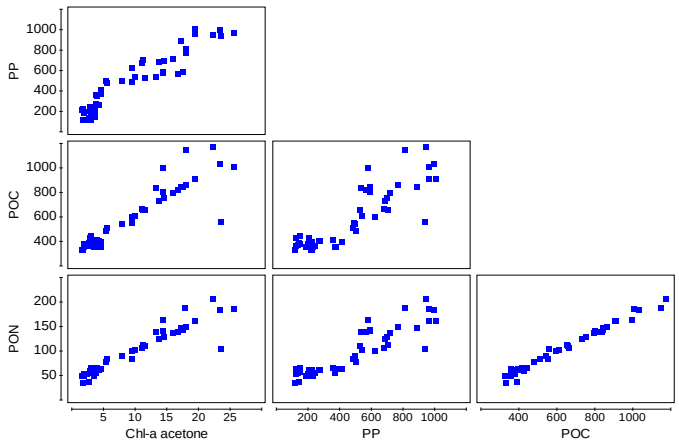

Fig. 4.3 Correlations between the methods used to examine primary production in the mesocosms. Chlorophyll by acetone extraction, primary productivity by the ^{14}C method (PP), particulate organic carbon (POC) and particulate organic nitrogen (PON). The figures include estimated data, where data was not available.

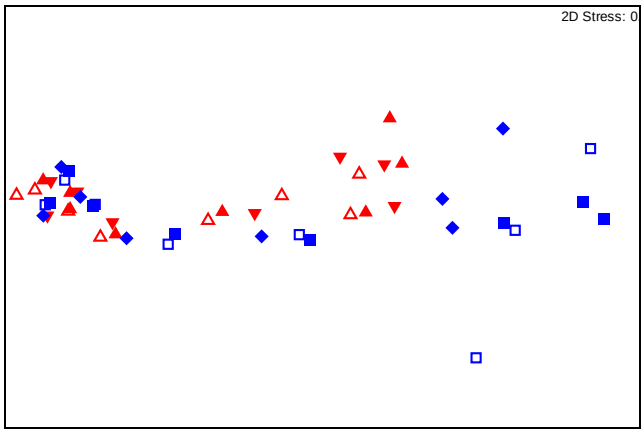

Fig. 4.4 Multidimensional scaling plot of measurements of production. High CO_2 mesocosms, 1: ▲2: ▼3: Δ ambient mesocosms 4: ■ 5: ♦ 6: □. The spread of present day data further to the right (x axis) indicates that the magnitude of the measurements is greater. A difference on the y axis would indicate differences between the different measurements but these are quite similar.

Table 4.4 A: ANOSIM performed in PRIMER 6 (methods section 2.5) on transformed data for POC, PON, primary productivity (PP) and chlorophyll The high R value and maximum possible probability of a difference, with only 10 possible permutations suggests that treatments are different. B: PERMANOVA test using Monte Carlo methods (methods 2.5).

A. *ANOSIM Global test*
Productivity, totals days 1-8 using POC, PON, chlorophyll and PP

Sample statistic (Global R): 0.889
Significance level of sample statistic: 10%
Number of permutations: 10 (All possible permutations)
Number of permuted statistics greater than or equal to Global R: 1

B. *PERMANOVA*
Productivity, totals day 1-8 using POC, PON, chlorophyll and *PP*

Source	df	SS	MS	Pseudo-F	P(perm)	Unique perms	P(MC)
CO_2	1	1.5	1.5	15.06	0.106	10	0.012
Res	4	0.4	0.1				
Total	5	1.9					

4.3.1 a Chlorophyll

Chlorophyll was determined by two methods. I was responsible for analysis of acetone extracts by fluorometry (section 2.4.5) in Bergen. Samples were also taken for high performance liquid chromatography (HPLC) analysis on return to the UK after the experiment (section 2.4.12). The acetone extractions gave us an immediate estimate of the increasing chlorophyll in the mesocosms which was useful for monitoring the progression of the bloom. A complete data set of daily samples for each mesocosm was analysed. HPLC analysis gave more detailed information of all pigments present and more precise quantification but the data set was less complete, since samples were not analysed from every time point. Both the acetone extraction and HPLC data are shown (**Fig. 4.5**).

After addition of nutrients, chlorophyll increased in all mesocosms reaching maximum values on 13th May. The acetone analysis gave an estimate of 2.36 µg l^{-1}(± 0.24) and 3.25 µg l^{-1} (± 0.57) in high CO_2 and present day mesocosms respectively. The HPLC results gave maximum values of 6.87 (± 3.3) and 10.41 (± 1.1) µg l^{-1}. The results are

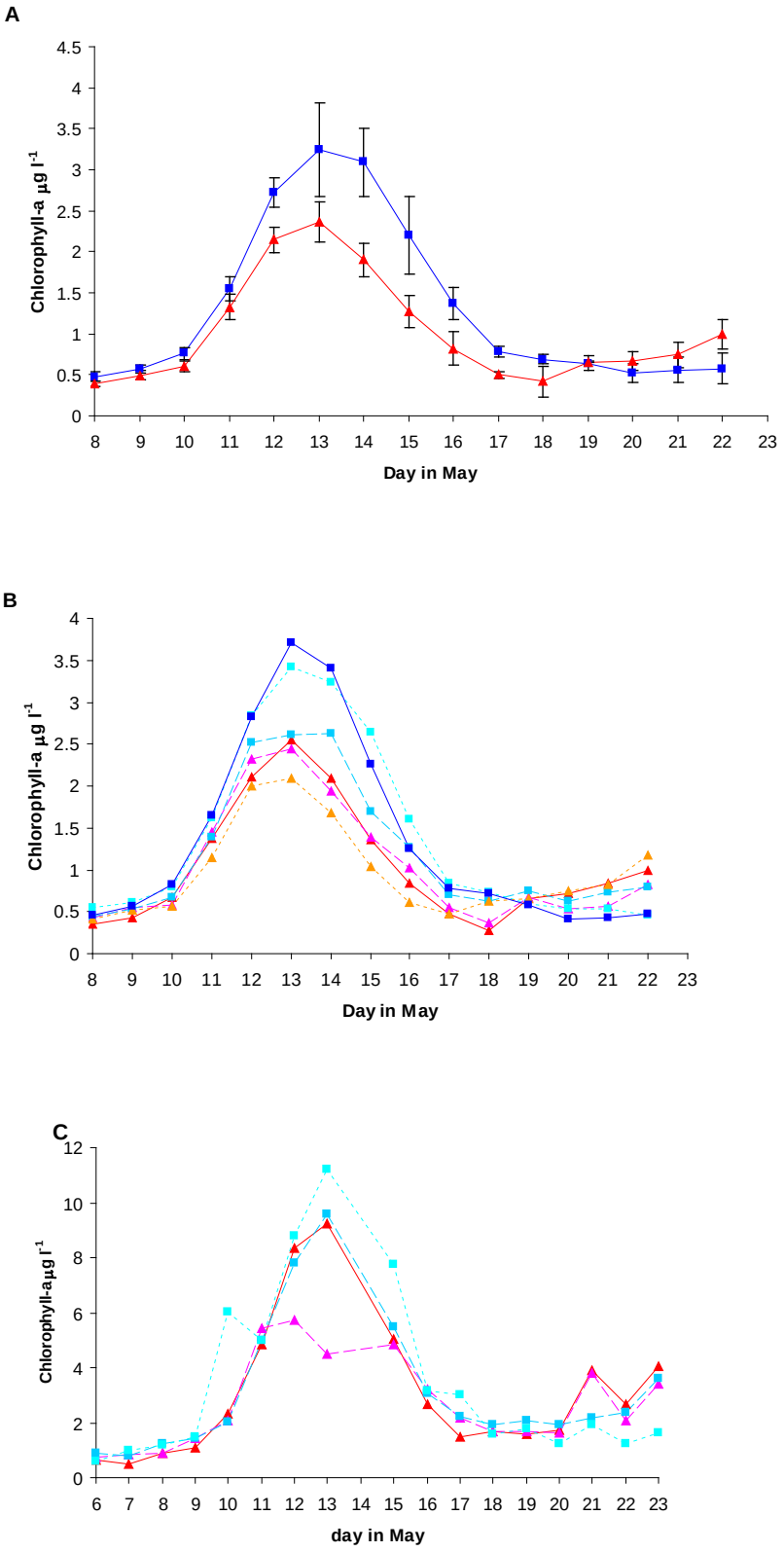

Fig. 4.5 Chlorophyll (µg l^{-1}) from 6th-23rd May. Determined by acetone extraction (A and B) and HPLC (C). A: analyses of triplicate mesocosms with error bars showing one standard deviation. B: all six mesocosms separately, C: mesocosms 1, 2, 5 and 6. Key: mesocosm 1:(-▲-) , 2 :(---▲---), 3: (····▲····), 4: (-■-), 5: (---■---) and 6: (···■····).

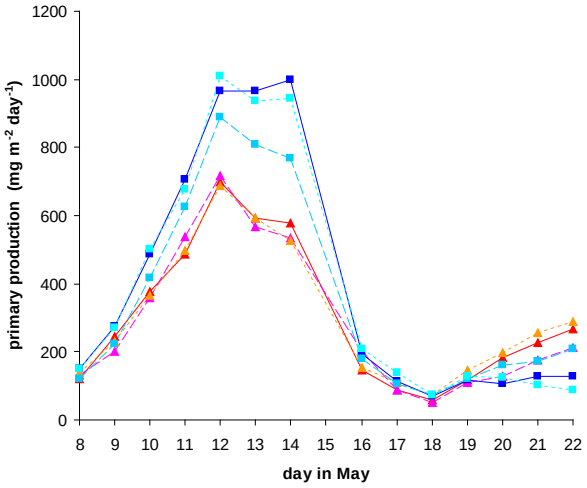

Fig. 4.6 Depth integrated primary production to 3m of samples from each of the six mesocosm enclosures measured by ^{14}C incubation, high CO_2 (1:-▲-, 2: -▲- , 3: -▲-) and present-day air mesocosms (4:-■-, 5: -■-, 6: -■-).

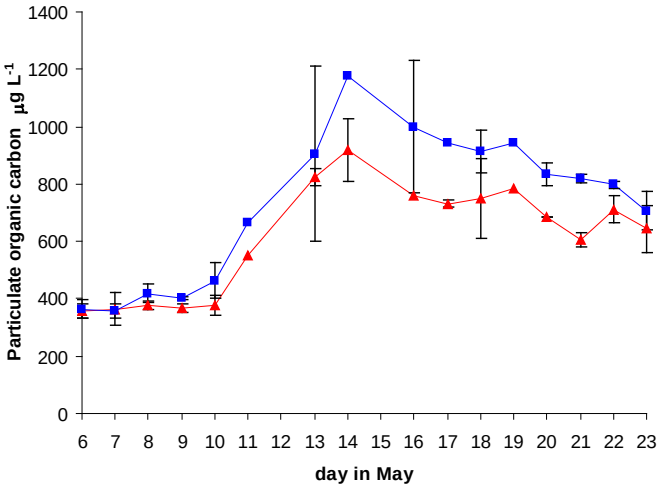

Fig. 4.7 POC (µg l^{-1}) during the experiment, data point are means of available data for high CO_2 (-▲-)and present day mesocosms (-■-). Error bars show standard deviations of the mesocosms of the same treatment.

similar in the extent of the difference between the treatments with the acetone extraction suggesting a 27% decrease in chlorophyll at high CO_2 and HPLC a 34% decrease. Both data sets show that the high CO_2 mesocosm 1 and ambient mesocosm 5 have very similar maximum chlorophyll values (**Fig. 4.5**). The two other ambient mesocosms, 4 and 6, have higher maximum chlorophyll than mesocosm 5. Mesocosm 3 has lower

maximum chlorophyll than 1 and 2. The HPLC data show a large difference in maximum chlorophyll between mesocosms 1 and 2 which is not seen in the acetone extraction data. Overall the two data sets show dissimilarities. Mean maximum chlorophyll was higher in the ambient mesocosms, which is consistent with the biomass and primary production data.

4.3.1b ^{14}C to directly measure primary production

Primary production was measured by the ^{14}C method (section 2.4.9). Maximum rates of 700 (± 15) and 954 (± 61) mg C m^{-2} d^{-1} were measured in the high CO_2 and present day mesocosms respectively on 12th May. There was a large effect of the high CO_2 treatment, with 27% less primary production in the high CO_2 treatment than in the mesocosms with present day pCO_2 (**Fig. 4.6**).

4.3.1c Particulate Organic carbon (POC)

Particulate organic carbon is a measure of the inorganic carbon fixed by the phytoplankton. However, samples were collected on GFF filters and dissolved organic carbon and exudates are smaller than the 1.6 µm pore-size of the filters, so was not measured. Particulate organic carbon was measured in the UK from filters taken during the experiment (section 2.4.4). Data were not available for all days but a fair covering of the three mesocosms on each day gives a good indication of the response of the two treatments (**Fig. 4.7**). Mean total POC production reached maximum values of 919 (± 110) and 1176 (no replicates) µg C l^{-1} in high CO_2 and present day mesocosms respectively. This amounts to 22% less POC at increased CO_2: however the data set is small and lacks replication. The re-bubbling of two mesocosms from each treatment on 15th May reduced the ability to examine POC and PON production in the post bloom period. The data after this event became dissimilar in the mesocosms under the same treatment.

4.3.1d C:N ratio

Mean POC:PON (atom:atom) ratios were calculated from all available data, analyses were made for all 6 mesocosms. Measurements were taken on the same day but did not include every day (**Table 4.5**). The C:N ratio was highest before the phytoplankton started to grow and remained at a value of ~7 from the start of exponential growth until after the bloom crashed. During the exponential growth period (10^{th} and 14^{th} May) mean C:N in the high CO_2 mesocosms was 7.11 (± 0.42) and in present day mesocosms 6.9 ± (0.41) these were not significantly different (F=0.97, p=0.34). Due to re-bubbling it was not possible to compare the C:N ratio after the bloom peak, which is when higher C:N ratios have been reported in past mesocosms (Engel et al. 2005) (Riebesell 2007).

Table 4.5 Single factor ANOVA to examine differences in C:N between the treatments.

ANOVA *C:N*

Source of Variation	*SS*	*df*	*MS*	*F*	*P-value*	*F crit*
Between Groups	0.16	1	0.16	0.97	0.34	4.60
Within Groups	2.39	14	0.17			

4.3.1e Calculated carbon drawdown, Δ[DIC] and calcification by the alkalinity anomaly method*

In several previous CO_2 manipulated mesocosm experiments, carbon drawdown has been calculated from the decrease in dissolved inorganic carbon present (ΔDIC) (Engel et al. 2005; Riebesell 2007). Δ[DIC*] represents the decrease in DIC caused by primary production and is calculated from the total decrease in DIC [ΔDIC] less the decrease caused by calcification $1/2[\Delta TA + \Delta NO_3^-]$ according to **equation 4.1**. Calcification is calculated as half the change in total alkalinity (1/2ΔTA) because the precipitation of 1 mol of calcium carbonate reduces the alkalinity by two molar equivalents (Chisholm and Gattuso 1991).

$$\Delta[DIC^*]=[\Delta DIC]- 1/2[\Delta TA + \Delta NO_3^-] \quad \textbf{[4.1]}$$

The difference between the carbon drawdown attributed to primary production, Δ[DIC*], and the POC build-up has been described as carbon loss caused by exudation of polysaccharides (Engel et al. 2004b; Delille et al. 2005; Engel et al. 2005; Riebesell et al. 2007). This is calculated from **equation 4.2**.

$$\text{Carbon loss} = \Delta[DIC^*] - \Delta POC \quad \textbf{[4.2]}$$

The carbon drawdown attributed to primary production, Δ[DIC*], can then be compared in terms of cell number. A C:N term may be calculated from nitrate drawdown, **equation 4.3**.

$$C{:}N = \Delta[DIC^*]/\Delta[NO_3^-] \ (\mu mol\ kg^{-1}) \quad \textbf{[4. 3]}$$

The results of this analysis showed that most of the terms calculated were higher at ambient CO_2 levels than in the increased CO_2 mesocosms (**Table 4.6**). This included higher, total carbon drawdown, carbon drawdown due to calcification, and carbon drawdown due to photosynthesis. A decrease in the carbon loss term, Δ[DIC*]- ΔPOC was seen at ambient CO_2 suggesting that at increased CO_2 more dissolved organic carbon (DOC) may be exuded than at ambient CO_2. However this apparent difference may be due to the more efficient use of the carbon taken up by the ambient cells. It appears that both calcification and primary production were enhanced and the total carbon drawdown was higher in the ambient mesocosms than the high CO_2 mesocosms. Examining the carbon drawdown in this manner, there was a reduction in the pCO_2 (ΔpCO_2) of 60% in the high CO_2 mesocosms compared to present day, with mean ΔpCO_2 of 360 (± 46) ppm in the high CO_2 mesocosms and 143 (±13) ppm in the present day mesocosms. The greater drop in pCO_2 at increased CO_2 levels was caused by the lower buffer capacity of sea water under these conditions (Riebesell et al. 2007) . The

change in total dissolved inorganic carbon (Δ[DIC]) was lower in the high CO_2 mesocosms with mean values of 99 (±10) and 113 (± 6) µmol kg^{-1} in high and present day mesocosms respectively. This term includes both carbon fixed as calcite and as organic carbon. Total alkalinity may be used to calculate the drawdown due to calcification, which was higher in the present day than high CO_2 mesocosms with mean values of 19.3 (± 3) and 10 (± 7) respectively (**Table 4.6**). The high CO_2 mesocosms were very variable. An ANOVA performed on the data gave a 7% significance value for the probability that calcification per cell was significantly reduced in the high CO_2 treatment (F=6.33, p=0.07, **Table 4.7**). When the calcification term is subtracted from the total carbon drawdown term, a value is obtained for carbon fixed by photosynthesis, Δ[DIC*]. This was not significantly different between the treatments either in total or on a per cell basis (F=3.9, p=0.12, **Table 4.7**). It is strange that the total Δ[DIC*] values between treatments were not significantly different. Carbon lost by exudation may be calculated from the amount of carbon fixed by photosynthesis, Δ[DIC*], minus the actual measured POC. This gave values of 52.41 ± 11.2 and 36.96 ± 13 in the high CO_2 and ambient mesocosms respectively. The reason for the large standard deviations may be that the maximum POC values were taken from either 13th or 14th May, whichever day data was available for that mesocosm (1, 2, 6 on 14th May and 3, 4, 5 on 13th May). Another possible cause for the high variation is that the value is a ratio of two differences, with accumulated variation. The nitrate taken up was used to calculate a C:N ratio of carbon to nitrogen drawdown, there was no significant difference between treatments in this term. From these results it appears that any difference in carbon drawdown between treatments was caused by calcification. There was neither significant increase in the carbon lost in the high CO_2 treatments nor increase in the C:N ratio.

Table 4.6 Calculated carbon drawdown for high CO_2 and present day treatments [ΔDIC], [ΔTA], Δ[DIC*], ΔPOC are calculated for data taken between 7th May when nutrients were added and 13th or 14th May depending on which day POC data was available for each mesocosm.

	high CO_2	Present day
Δ[DIC] (µmol kg^{-1})	99.31 ± 9.57	113.04 ±5.65
ΔTA (µmol kg^{-1})	7.87 ± 8.29	26.31 ±3.21
Δ[DIC*] (µmol kg^{-1})	95.38 ±7.16	99.88 ±4.78
$\Delta[DIC]_{cal}$	9.96 ± 4.01	19.30 ± 2.76
Δ cells l^{-1}	$1.09x10^{6}$ ± 6.9	$2.16x10^{6}$ ±7.1
$\Delta[DIC]_{cal}$ $cell^{-1}$	$3.02x10^{-6}$ ± $2.0x10^{-6}$	$6.36x10^{-6}$ ± $1.2x10^{-6}$
Δ[DIC*] $cell^{-1}$	$3x10^{-6}$ ± $2x10^{-9}$	$6x10^{-6}$ ± $1x10^{-10}$
ΔPOC (µmol kg^{-1})	42.97 ± 4.15	62.92 ± 9.24
Δ[DIC*]- ΔPOC (µmol kg^{-1})	52.41 ± 11.2	36.96 ± 13
Δ $[NO_3^-]$ (µmol kg^{-1})	12.06 ± 0.27	12.28 ± 2.32
Δ[DIC*]:Δ$[NO_3]$ (µmol kg^{-1})	7.92 ± 0.70	8.29 ± 1.28
ΔpCO_2 (ppm)	359.80 ± 46.20	142.97 ± 13.23

Table 4.7 ANOVAs to examine differences between calcification and primary production using values calculated from carbon drawdown.

	Source of Variation	*SS*	*df*	*MS*	*F*	*P-value*	*F crit*
Calcification $0.5(\Delta TA+ \Delta NO_3^-)$	Between Groups	131	1	131	11.03	0.04	7.71
	Within Groups	47	4	12			
	Total						
Calcification $cell^{-1}$ $0.5(\Delta TA+ \Delta NO_3^-)$ $cell^{-1}$	Between Groups	$1x10^{11}$	1	$1x10^{11}$	6.33	0.07	7.71
	Within Groups	$1x10^{11}$	4	$3x10^{12}$			
	Total	$2x10^{11}$	5				
Primary production $cell^{-1}$ ([ΔDIC]-[ΔTA]) $cell^{-1}$	Between Groups	$5x10^{9}$	1	$5x10^{9}$	3.9	0.12	7.71
	Within Groups	$5x10^{9}$	4	$1x10^{9}$			
	Total	$1x10^{8}$	5				
Carbon loss ΔDIC-ΔPOC	Between Groups	357	1	357	2.43	0.19	7.71
	Within Groups	590	4	147			
	Total	948	5				

4.3.2 Flow cytometry

Phytoplankton counts were performed with a FACScan flow cytometer (Becton Dickinson). Fresh, unfixed samples were analysed and phytoplankton groups were distinguished by their auto-fluorescence and light scattering properties (section 2.4.2). Groups of *Synechococcus*, coccolithophores, cryptophytes, nanoflagellates and pico-eukaryotes were identified by their fluorescent and scattering properties. The pico-eukaryotes formed two distinct clusters of larger and smaller cells which were termed, large and small pico-eukaryotes.

A multivariate analysis was performed using PRIMER 6 (section 2.5) to analyse the community structure of the two treatments. Daily cell numbers, as estimated by flow cytometry, were transformed into percentages of the total number for each species over the period of 6^{th}-14^{th} May (before re-bubbling). A distance matrix was calculated using Euclidean distance and a 2 dimensional plot created representing the data in terms of magnitude or cell numbers (x axis) and differences between phytoplankton groups (y axis). This revealed a large increase in the magnitude of growth of the community in the present day mesocosms compared to the high CO_2. The structure of the community also differed between the treatments (**Fig. 4.9**). The significance of the difference in cell numbers between the treatments was analysed by ANOSIM (PRIMER 6, methods 2.5, **Table 4.8**). This gave the most significant level of significance possible for the low number of replicates (R=1, significance level= 10%). A PERMANOVA test was also performed, using Monte Carlo methods (Anderson and Robinson 2001). The results showed that whilst that maximum possible significance level is 10%, there is a much smaller probability that the a treatments are similar (pseudo F=9.24, p=0.99, Monte Carlo p= 0.008, **Table 4.8**).

To determine the effects of increased CO_2 on the community structure a series of plots were created which represent abundances of the different groups in the 6 mesocosms (**Fig. 4.10**). The actual abundances are displayed in **Table 4.9**. Differences between both the treatments and mesocosms within treatments can be seen in **Fig. 4.10**. The most obvious differences in the community structure were the greatly reduced numbers of *Synechococcus* and large picoeukaryotes in the high CO_2 mesocosms. Small picoeukaryotes, nanoflagellates and cryptophytes were fairly similar in abundance in the two treatments. Coccolithophores were reduced by a factor of 2 in two of the high CO_2 mesocosms but in mesocosm 2 the abundances were similar to the present day mesocosms. Mesocosm 5 is slightly different in composition from mesocosms 4 and 6. The untransformed data are displayed in **Fig. 4.8**.

Table 4.8 A: ANOSIM of transformed cell counts for all phytoplankton groups analysed by flow cytometry. The high R value and maximum probability of a difference, with only 10 possible permutations suggests that treatments are different. B: PERMANOVA test (section 2.5) using Monte Carlo methods gives a very low probability P(MC) that the treatments were similar.

A. *Global Test ANOSIM for all phytoplankton groups by flow cytometry*

Sample statistic (Global R): 1
Significance level of sample statistic: 10%
Number of permutations: 10 (All possible permutations)
Number of permuted statistics greater than or equal to Global R: 1

B. *PERMANOVA table of results for all phytoplankton groups by flow cytometry*

Source	df	SS	MS	Pseudo-F	P(perm)	Unique perms	P(MC)
CO_2	1	520.32	520.32	9.2402	0.099	10	0.008
Res	4	225.24	56.31				
Total	5	745.56					

The initial population in each mesocosm was dominated by small pico-eukaryotes. Large pico-eukaryotes, *Synechococcus* and nano-flagellates were all present at around 3-7% of the total phytoplankton abundance. Coccolithophores were present in all mesocosms at mean abundances of 237 (± 60) ml^{-1} in the high CO_2 mesocosms and 243 (± 27) ml^{-1} in the three air mesocosms. The cell numbers as estimated by the FACScan are displayed in **Table 4.9**.

Synechococcus

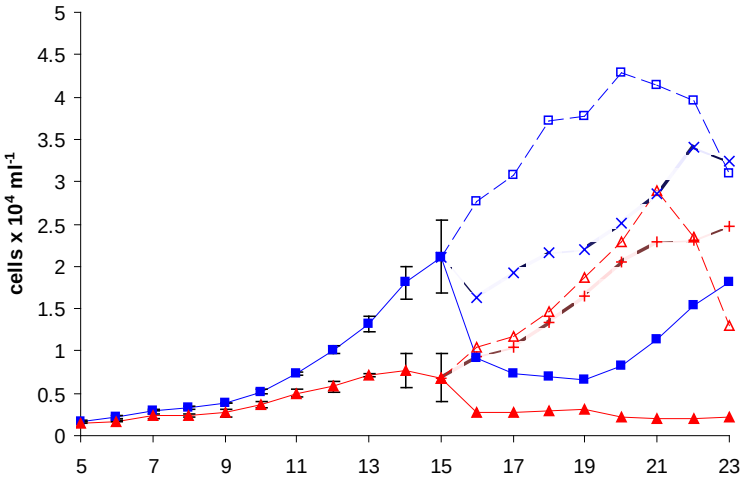

Small pico eukarotes

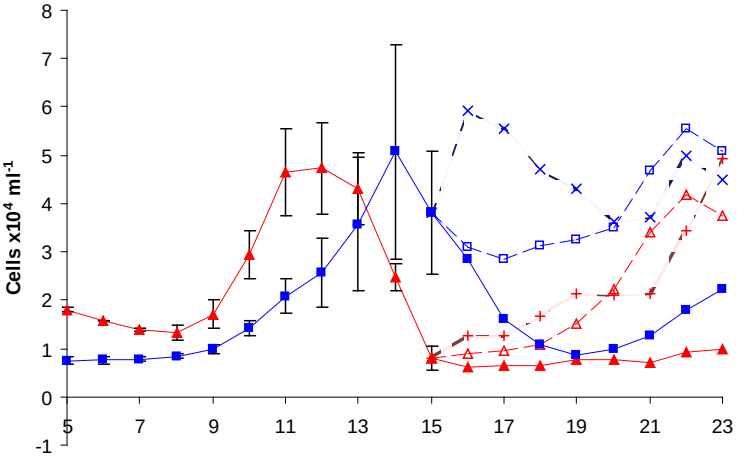

Large pico eukarotes

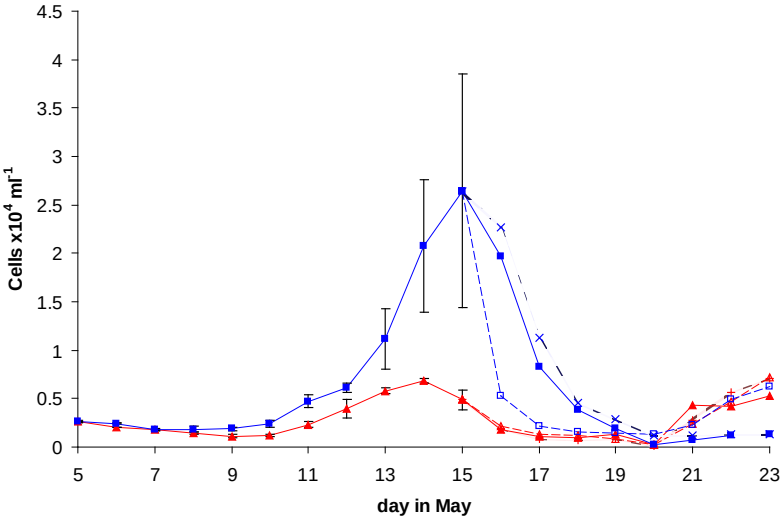

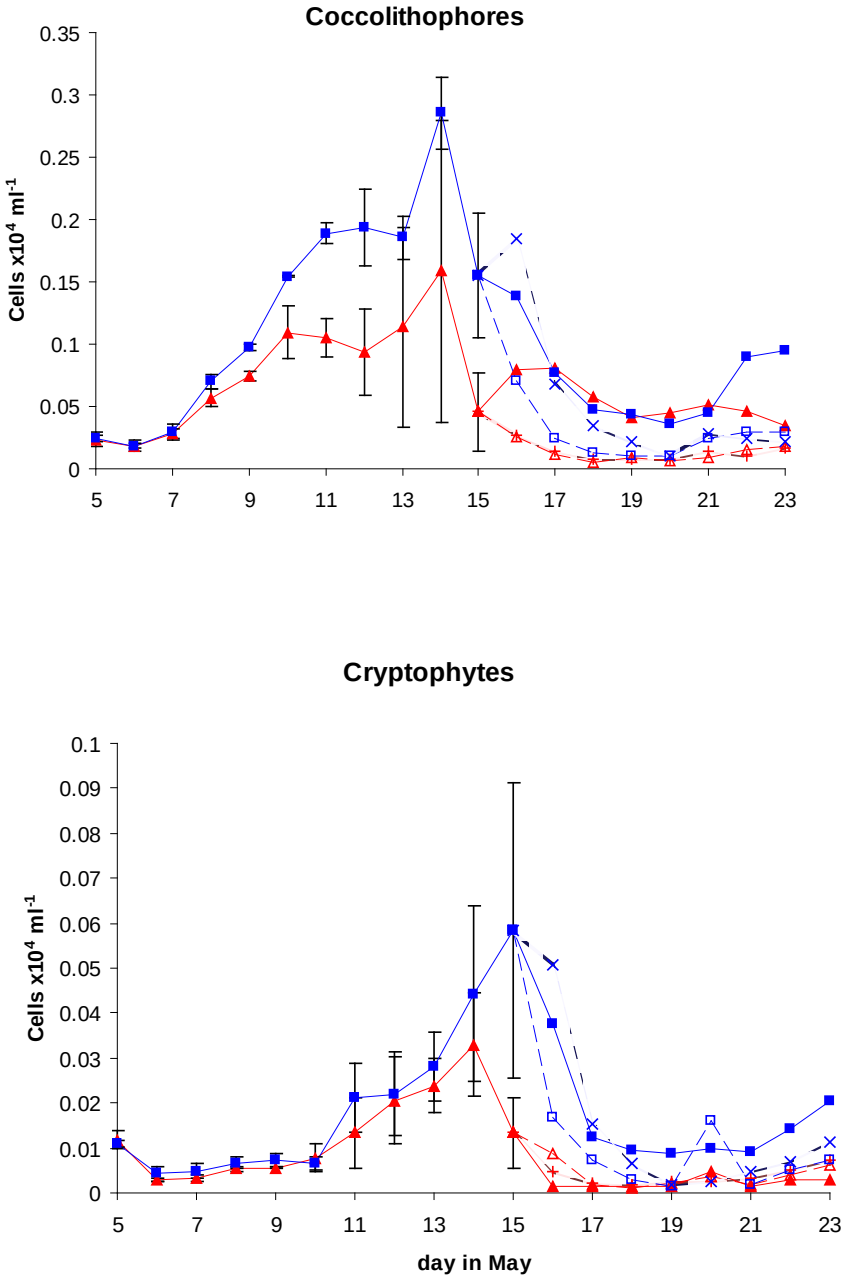

Fig. 4.8 Individual phytoplankton groups identified and enumerated by flow cytometer over the course of the experiment. Data points (5th-15th May), are means of triplicate mesocosms for each treatment with error bars of one standard deviation, high CO_2 (-▲-), present day (-■-). Data points (15th-23rd May) are for individual mesocsoms based on triplicate FACScan analyses. Mesocosms 1 (····+····), 2 (---Δ---), 5 (---□---) and 6 (···x····) were re-bubbled on 15th May. Mesocosms 3 (-▲-) and 4 (-■-) were not re-bubbled.

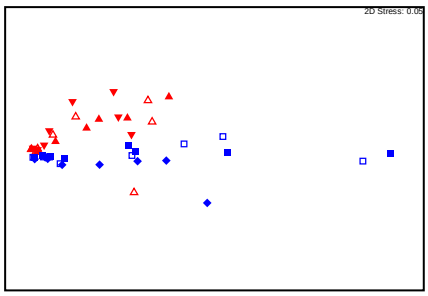

Fig. 4.9 Scaling plot representing cell numbers of phytoplankton groups as estimated by flow cytometry. High CO_2 mesocosms, 1: ▲2: ▼3: Δ ambient mesocosms 4: ■ 5: ♦ 6: □.

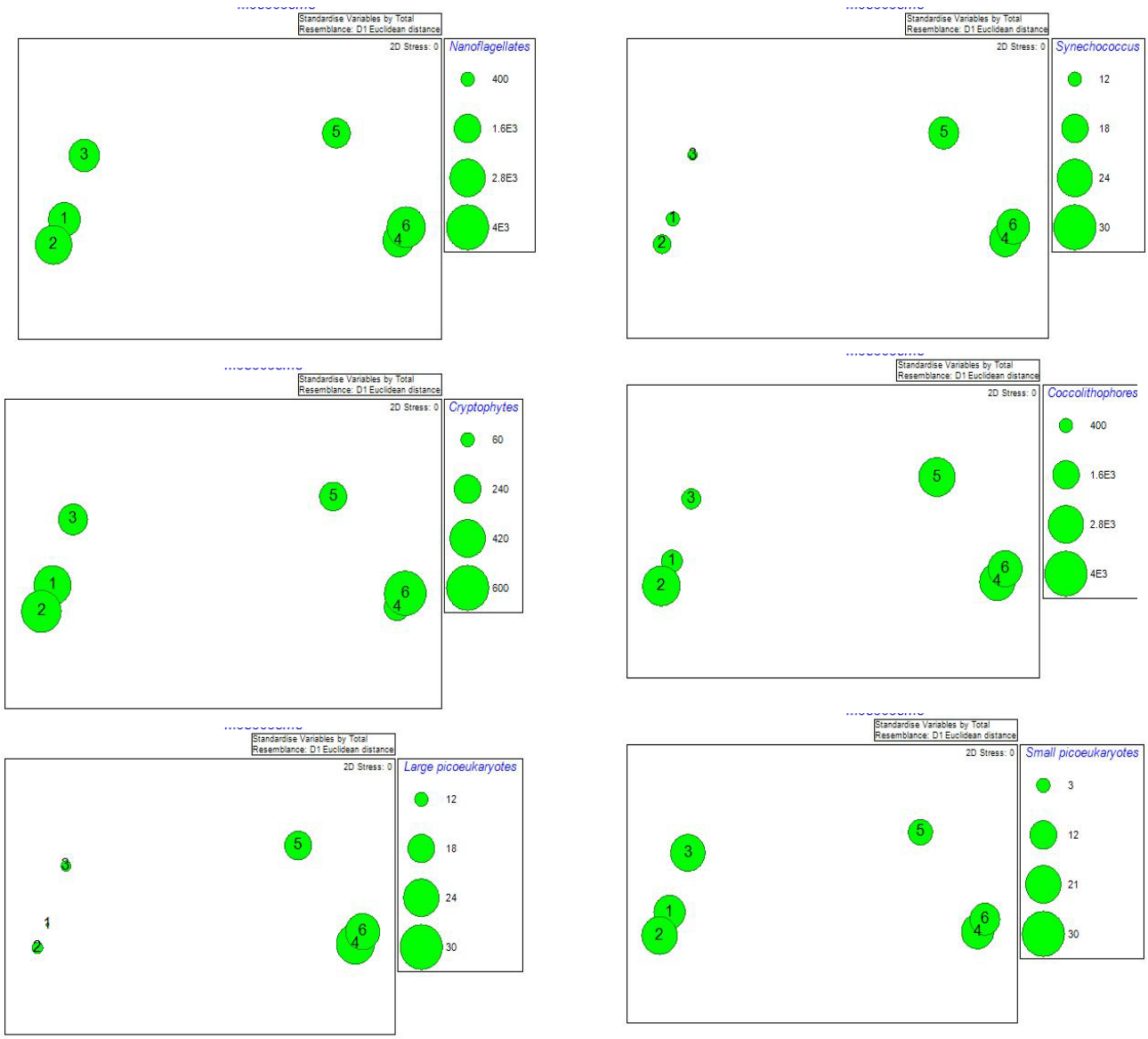

Fig. 4.10 Plots representing relative abundances of different phytoplankton groups (note plots are on different scales). Present day mesocosms, 4-6 (right hand side of each plot); high CO_2 mesocosms 1-3 (left hand side).

Small pico-eukaryotes remained numerically dominant throughout the experiment reaching maximum cell densities of 4.7×10^4 ($\pm 0.9 \times 10^4$) and 5.1×10^4 ($\pm 2.2 \times 10^4$) cells ml^{-1} in the high CO_2 and air mesocosms on days 12 and 14 respectively. *Synechococcus* gradually increased in number throughout the experiment, apparently unaffected by the second bubbling event, reaching maximum densities of 2.6×10^4 ($\pm 0.4 \times 10^4$) and 2.7×10^4 ($\pm 1.7 \times 10^4$) cells ml^{-1} in the high CO_2 and air mesocosms on days 21 and 22 respectively. On 12^{th}-15^{th} May all other phytoplankton groups reached their maximum cell densities. Nanoflagellates peaked first, followed by coccolithophores, large pico-eukaryotes and cryptophytes. Nanoflagellates reached maximum cell densities of 0.33×10^4 ($\pm 0.04 \times 10^4$) and 0.41×10^4 ($\pm 0.03 \times 10^4$) cells ml^{-1} in the high CO_2 and air mesocosms on days 12 and 13 respectively. Coccolithophores were not as numerous as the nano-flagellates with maximum densities of 0.16×10^4 ($\pm 0.12 \times 10^4$) and 0.29×10^4 ($\pm 0.03 \times 10^4$) cells ml^{-1} in the high CO_2 and air mesocosms respectively on day 14. Large pico-eukaryotes were particularly abundant in the present day mesocosms reaching mean maximum cell densities of 0.69×10^4 ($\pm 0.02 \times 10^4$) and 2.65×10^4 ($\pm 1.2 \times 10^4$) cells ml^{-1} in the high CO_2 and air mesocosms on days 14 and 15 respectively. Cryptophytes were scarce but showed a distinct peak in cell number on days 14 and 15 with maximum cell densities of 0.03×10^4 ($\pm 0.01 \times 10^4$) and 0.06×10^4 ($\pm 0.03 \times 10^4$) cells ml^{-1} in the high CO_2 and air mesocosms respectively.

There were very large differences between the present day and high CO_2 mesocosms. The FACScan analysis showed decreased mean numbers of cells of all the phytoplankton types analysed in the high CO_2 mesocosms compared to present day. For the small pico-eukaryotes and *Synechococcus* this was a small difference but for the large pico-eukaryotes cell density was nearly four fold greater in the present day

mesocosms. Coccolithophores were adversely affected by increased CO_2, mean cell density at the bloom peak was ~50% that of the present day mesocosms.

On 15th May, two mesocosms from each treatment were re-bubbled and one was not. Responses to re-bubbling varied, small pico-eukaryotes and *Synechococcus* thrived. Large pico-eukaryotes nano-flagellates and cryptophytes showed little response and coccolithophores gave a mixed response, in mesocosm 3 (un-bubbled) they appeared to grow better than in the re-bubbled treatments (**Fig. 4.8**). The response in the present day mesocosms is less conclusive but still suggests that the physical effects of bubbling might have affected coccolithophore growth. The natural progression of the bloom may be observed by examining the un-bubbled mesocosms. It is obvious from these that phytoplankton numbers had peaked and the bloom was not cut short by re-bubbling.

Table 4.9. Mean and maximum cell numbers and standard deviations for each phytoplankton type as estimated by flow cytometry. Data were calculated from means of three samples from each of the three mesocosms of each treatment. The day on which each group attained maximum density is shown for each treatment. *Synechococcus* cells reached maximum density on 20th and 21st May after re-bubbling but the maximum cell number before re-bubbling is reported.

	Treatment	Max Cells x 10^4 ml^{-1}	Day of peak abundance
Synechococcus	High CO_2	0.77 ± 0.2	14
	Present day	2.11 ± 0.41	15
Small picoeukaryotes	High CO_2	4.7 ± 0.9	12
	Present day	5.1 ± 2.2	14
Large picoeukaryotes	High CO_2	0.69 ± 0.02	14
	Present day	2.65 ± 1.2	15
Nanoflagellates	High CO_2	0.33 ± 0.04	12
	Present day	0.41 ± 0.03	13
Coccolithophores	High CO_2	0.16 ± 0.12	14
	Present day	0.29 ± 0.03	14
Cryptophytes	High CO_2	0.03 ± 0.01	14
	Present day	0.06 ± 0.03	15

4.3.3 Microscopy analysis

To confirm the flow cytometry results and to identify the phytoplankton to species, microscopic analysis was performed on fixed samples by Claire Widdicombe at PML (section 2.4.13). This also allowed identification of the heterotrophic dinoflagellates and ciliates which will have influenced phytoplankton cell numbers by grazing. Samples from the high CO_2 mesocosm 1 and present day mesocosm 6 from selected days were analysed. Biomass (µg C l^{-1}) was calculated from cell number and estimated volume using the equations of Menden-Deuer and Lessard (2000). The results are displayed in **Fig. 4.11**.

Twelve species of diatom were identified, 9 each of autotrophic and heterotrophic dinoflagellate and 11 of ciliated protozoa. Copepod nauplii, rotifers or other mesozooplankton were not found; however, with the small volume of the Lugol's samples (50-100ml) it is unlikely that any of these zooplankton would have been sufficiently abundant to be included in the samples. Flagellates were identified to class level with prymnesiophytes, undetermined flagellates >10µm, cryptophytes and euglenophytes abundant in both treatments. The prymnesiophytes, which include *E. huxleyi*, were not dominant, in terms of biomass but contributed approximately 10% of total biomass throughout the experiment. Diatoms were initially present in low numbers (~ 4% of the initial biomass) but were out-competed and by 11th May their numbers were near zero. Ciliates and heterotrophic dinoflagellates, which are potential grazers on the phytoplankton, were present in both mesocosms. Ciliates made up approximately 80% of the initial identified biomass in the present day mesocosm, 6, and 30% in mesocosm 1, but their contribution to the total biomass decreased as the phytoplankton began to grow. Heterotrophic dinoflagellates were less abundant than ciliates, contributing approximately 5% of the initial biomass in mesocosm 1, and less

in mesocosm 6. They did not become more dominant during the experiment. Autotrophic dinoflagellates became more prolific at the bloom peak and following this as the numbers of other phytoplankton decreased.

4.3.4 Coccolithophores

Particular attention has been paid to coccolithophores in ocean acidification research due to the sensitivity of calcification to pH. As described in section 1.1.4, an increase in CO_2 will reduce pH and also the calcite saturation state, increasing the tendency for calcite to dissolve. Prior to our mesocosm experiment a notable study (Riebesell et al. 2000b) suggested that *E. huxleyi* cells may be so sensitive to pH change that the liths become malformed. Conversely it has been found that *E. huxleyi* cells have a low affinity for CO_2 and do not show saturation of photosynthesis below concentrations of ~25 µM dissolved CO_2 (current concentration is ~14µM) (Raven and Johnston 1991). Therefore *E. huxleyi* may benefit more than other phytoplankton from increased pCO_2. These two mutually exclusive hypotheses were tested in this experiment. This section will firstly examine the growth of coccolithophores in the mesocosms and secondly determine whether any malformation or reduction in calcification occurred at increased CO_2.

4.3.4a Growth of E. huxleyi

It was expected that coccolithophores would not grow as well in the high CO_2 treatment due to the problems associated with calcification at reduced pH. On average this proved to be the case; however the results were variable and maximum cell numbers in mesocosm 3 were as high as those in the present day treatments (**Fig. 4.12**). Specific growth rates (µ) calculated as a mean of days 6 to 14 for the three mesocosms for each treatment were 0.25 (± 0.01) and 0.34 (± <0.001) per day in high CO_2 and present day treatments respectively, these were not significantly different ($F=2.89$, $p=0.17$). The

maximum cell densities with means of 1654 (± 936) and 2856 (± 236) in high CO_2 and present day respectively were not significantly different (F=3.15, p=0.15, **Table 4.10**).

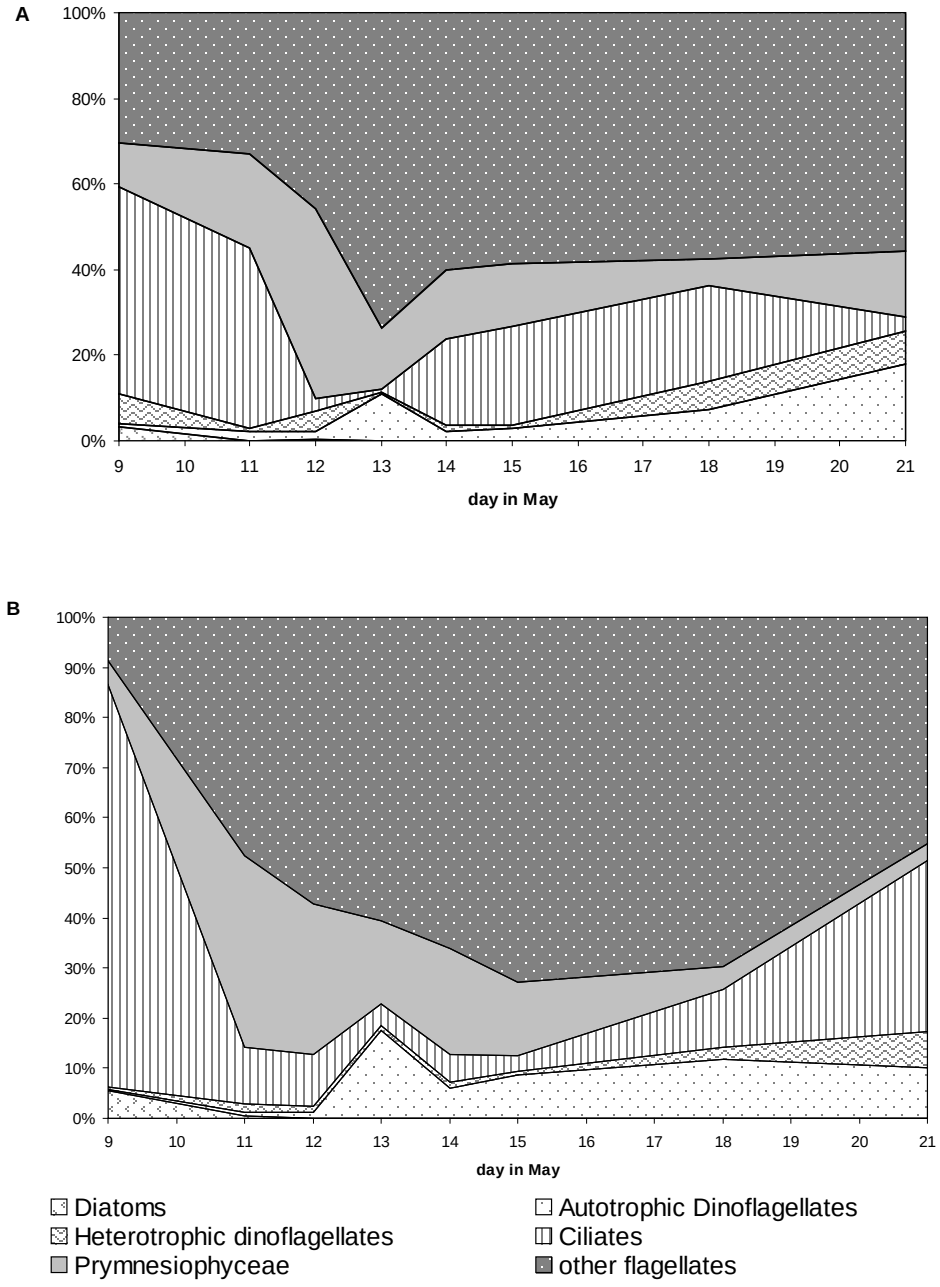

Fig. 4.11 Percentage of total biomass (µg C l^{-1}) of phytoplankton groups identified by light microscopy. A: high CO_2 mesocosm, 1, B: present day mesocosm, 6. Biomass as µg C l^{-1} was calculated from cell number and estimated volume using the equations of Menden-Deuer and Lessard (2000). Percentage of total biomass is shown.

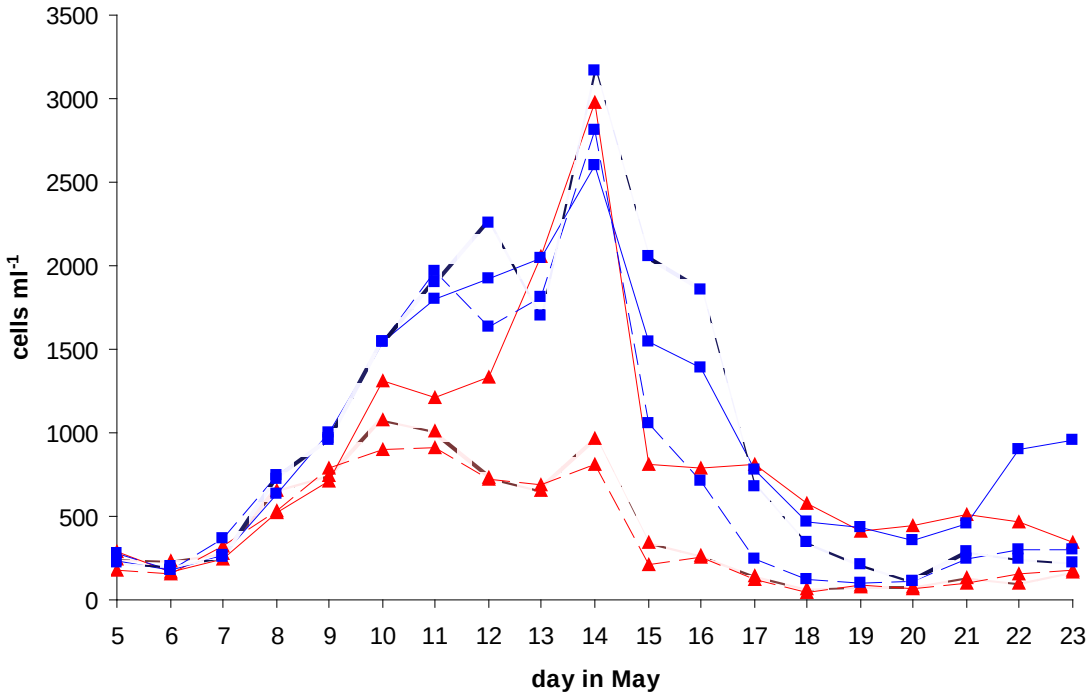

Fig. 4.12 Coccolithophore abundance in the high CO_2 mesocosms: 1 (····▲····), 2 (---▲---), 3 (-▲-) and present day mesocosms: 4 (-■-), 5 (---■---) and 6 (···■···) as estimated by flow cytometry.

Table 4.10 ANOVA of mean specific growth rates per day µ, and maximum cell density (Max) for the exponential period, days 6-14, in high CO_2 and present day treatments.

Source of Variation	*SS*	*df*	*MS*	*F*	*P-value*	*F crit*
Between Groups µ	0.013	1	0.013	2.89	0.17	7.71
Within Groups µ	0.018	4	0.005			
Total	0.031	5				
Between Groups Max	2430355	1	2430355	3.15	0.15	7.71
Within Groups Max	3090100	4	772525			
Total	5520454	5				

4.3.4b Coccolith morphology

I examined cells from the mesocosms using scanning electron microscopy (SEM). This firstly allowed identification of the dominant coccolithophore species as *Emiliania huxleyi* and then cells were examined for malformation and changes in size. A large number of images were assessed for malformation and a small number analysed more rigorously for changes in size of liths.

4.3.4c Malformation

Samples were gold coated and imaged by scanning electron microscope. Scanning electron microscope images of at least 100 cells from each treatment were examined from six preparations made for each treatment. No obvious malformation of cells was observed (**Fig. 4.14** and **4.15**). However this was clearly a very subjective analysis and image analysis was used to attempt to quantify any difference between treatments.

4.3.4d Analysis of coccoliths

In order to explain the analysis, I will first define the names of the individual elements of the coccolithophorid structure. *Emiliania huxleyi* is a heterococcolith, it has a coccosphere formed from interlocking calcium carbonate plates, or liths. The particular morphological description of these plates is placoliths. They comprise a proximal and distal shield allowing them to interlock, as can be clearly seen in **Fig. 4.13**. The shield is formed of elements around a central area which is immediately bordered by a ring of 1st- cycle elements (**Fig. 4.16**) (Siesser and Winter, 1994).

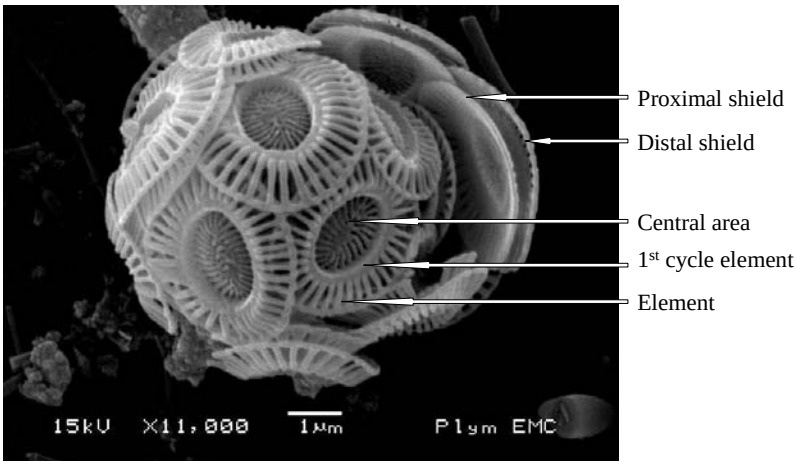

Fig. 4.13 *E. huxleyi* cell with morphological details labelled.

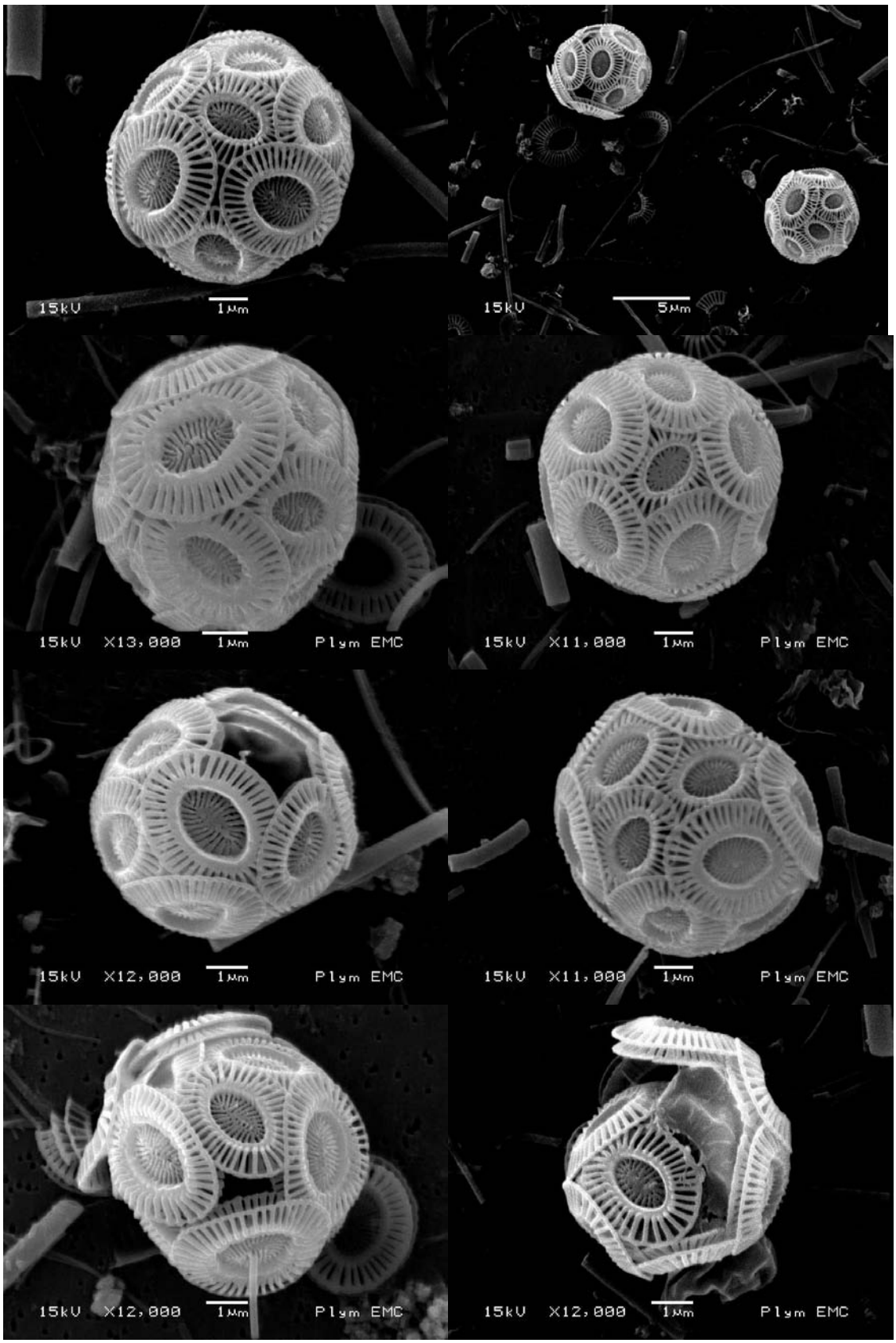

Fig. 4.14 Samples of *Emiliania huxleyi* from the high CO_2 treatment, mesocosm 1 on 8th May.

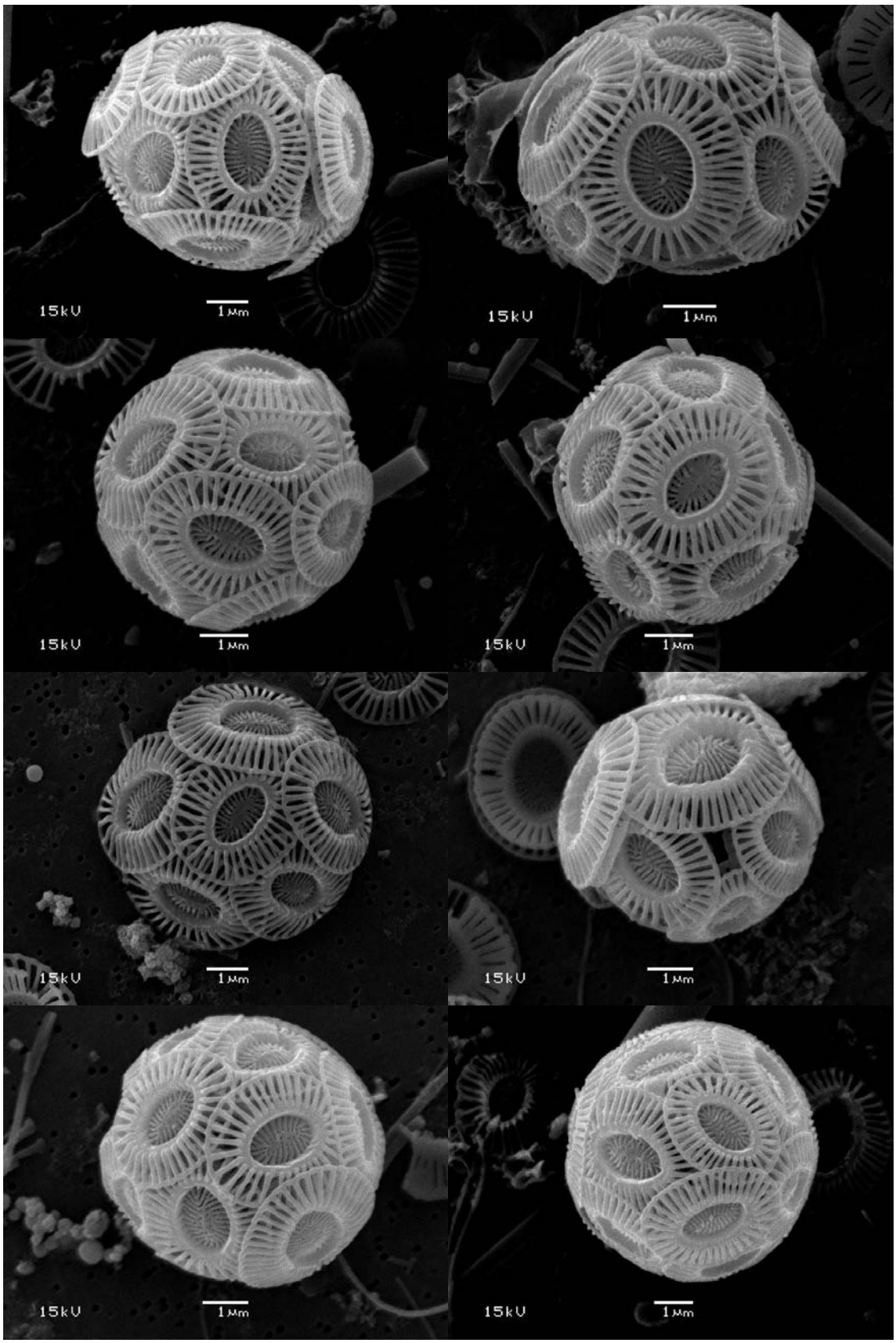

Fig. 4.15 Samples of *Emiliania huxleyi* from the present day treatment, mesocosm 6 on 8th May.

Dimensions can only be accurately measured on a lith that is parallel with the camera lens. This was ascertained from the equality in length of the elements on either side of the central area. For this reason only 9 individual cells from each treatment were analysed (**Table 4.11**). For the shield element parameters multiple measurements were taken for each cell. For all other parameters, single measurements were taken. No significant differences between the mean values of any parameter was found between treatments. However for all the ten parameters measured, mean values were greater in the present day than in the high CO_2 treatment (**Table 4.12**).

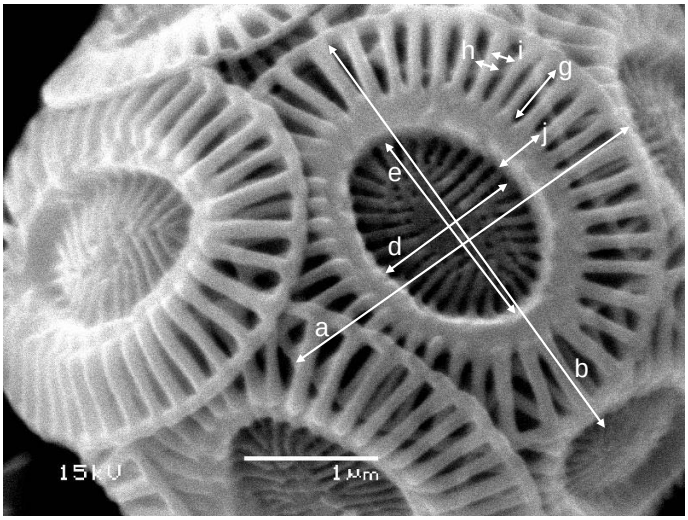

Fig. 4.16 SEM image of *Emiliania huxleyi* showing parameters of image analysis: a. distal shield width and b. length; d. central area width and e. length; g. shield element length, h. width and i. gap between shield elements; j. 1st-cycle element width.

Table 4.11 Comparison of high CO_2 and present day cell parameters examined by image analysis from scanning electron microscope images. Means and standard deviations of analyses from 9 individual cells or multiple analyses from 9 cells are shown. High CO_2 cells were taken from mesocosm 1 and present day from mesocosm 6.

	Shield width (µm)	Shield length (µm)	Shield Area (µm^2)	Central area length (µm)	Central area width (µm)	Central area Area (µm^2)	Shield element width (µm)	Shield element length (µm)	Gap between elements (µm)	1st cycle element width (µm)
High CO_2	2.85 ± 0.06	3.40 ± 0.26	7.63 ± 1.13	1.57 ± 0.12	1.04 ± 0.11	1.29 ± 0.24	0.11 ± 0.01	0.72 ± 0.06	0.12 ± 0.01	0.24 ± 0.04
Present day	3.00 ± 0.24	3.60 ± 0.17	8.35 ± 1.07	1.66 ± 0.10	1.09 ± 0.10	1.37 ± 0.20	0.11 ± 0.01	0.73 ± 0.06	0.12 ± 0.02	0.28 ± 0.03

Table 4.12 Single factor ANOVAs performed to examine differences between treatments for each parameter measured by image analysis.

	Source of Variation	*SS*	*df*	*MS*	*F*	*P-value*	*F crit*
Shield length	Between Groups	0.18	1	0.18	3.86	0.07	4.49
	Within Groups	0.76	16	0.05			
Shield area	Between Groups	2.34	1	2.34	1.92	0.18	4.49
	Within Groups	19.50	16	1.22			
Shield width	Between Groups	0.10	1	0.10	1.81	0.20	4.49
	Within Groups	0.91	16	0.06			
Shield element length	Between Groups	0.001	1	0.001	0.21	0.65	4.49
	Within Groups	0.06	16	0.01			
Shield element width	Between Groups	0.0001	1	0.0001	1.58	0.24	4.84
	Within Groups	0.001	11	0.00001			
Area of central area	Between Groups	0.03	1	0.03	0.61	0.45	4.49
	Within Groups	0.79	16	0.05			
Length of central area	Between Groups	0.03	1	0.03	2.45	0.14	4.49
	Within Groups	0.21	16	0.01			
Width of central area	Between Groups	0.01	1	0.01	1.10	0.31	4.49
	Within Groups	0.19	16	0.01			
Gap between elements	Between Groups	0.00005	1	0.00005	0.28	0.60	4.49
	Within Groups	0.003	16	0.0002			
1st-cycle element width	Between Groups	0.005	1	0.005	4.44	0.06	4.68
	Within Groups	0.02	13	0.001			

In my very small sample, the mean lith lengths were 3.60 (± 0.17) and 3.40 (± 0.26) μm in present day and high CO_2 mesocosms respectively. An ANOVA suggests that the difference between the treatments is close to the significance level despite there being only nine individual measurements for each treatment (F=3.86, p=0.07). The other measurement which is close to the significance level is 1st-cycle element width (F=4.44, p=0.06). This suggests that an increase in size of the lith may be due to an increase in the 1st –cycle element. The shield element length was very similar in the two treatments (F=0.21, p=0.65).

4.3.4e Emiliania huxleyi *morphotypes*

4.3.4e i Introduction

E. huxleyi is taxonomically a single species but a range of phenotypic and genotypic differences have been identified. Five morphotypes can be differentiated by differences in their coccolith morphology, physiological, biochemical and immunological properties (Schroeder et al. 2005). Recently it has been suggested that the variability of responses to high CO_2 in *Emiliania huxleyi* could be due to inherent differences between strains. A number of strains have been identified within the Bergen community (Martinez et al. 2007; Sorensen et al. 2009) and it is possible that different strains might be favoured by the different CO_2 treatments. DNA was extracted from samples from pre-bloom, mid-exponential and bloom peak for each of the six mesocosms. A molecular technique, denaturing gradient gel electrophoresis (DGGE) was used to determine the presence or absence of *E. huxleyi* genotypes within the communities.

Several attempts have been made to develop a molecular tool to differentiate between morphotypes (Medlin 1996; Schroeder et al. 2005; Iglesias-Rodríguez et al. 2006). Schroeder et al. (2005) developed a technique based on a protein involved in the formation of coccoliths, named GPA due to its high glutamic acid, proline and alanine content (Schroeder et al. 2005). A single base pair difference was identified, which separated the type A and B morphotypes despite having no bearing on the protein composition, as both triplets coded for the same amino acid (Schroeder et al. 2005). Further sequence differences in two untranslated regions bordering the GPA allowed identification of four genotypes (Schroeder et al. 2005).

The experimental design and methods are fully described in section 2.4.15, a brief description will follow here. DNA was extracted from samples and polymerase chain

reaction (PCR) amplified regions of DNA specific to a particular genotype. The amplified fragments were then separated by DGGE and visualized. Primers to distinguish between genetically distinct morphotypes based on variations in the GPA gene were kindly given to me by Dr. Schroeder.

4.3.4 e ii Results

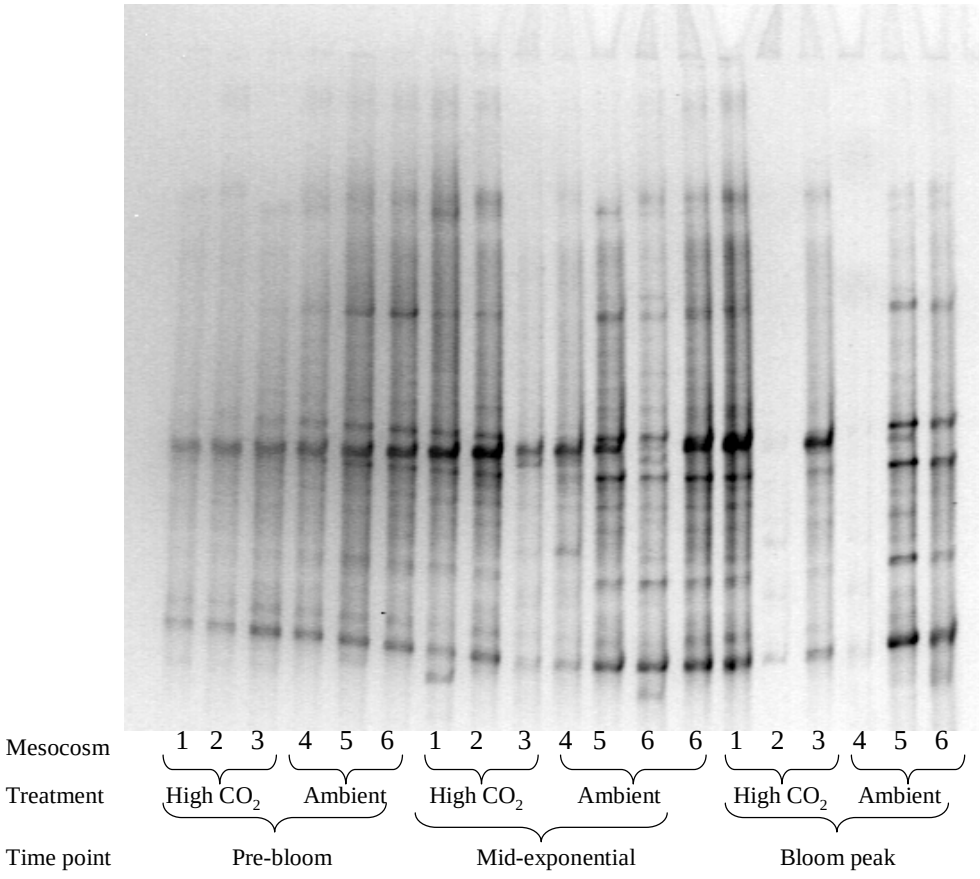

Fig. 4.17 Negative image of DGGE gel of PCR fragments amplified from samples taken from the mesocosm. DNA extracted from samples taken on 7th May (pre-bloom), 10th or 11th May (mid exponential) and 13th or 14th May (bloom peak) from mesocosms 1-6. These were amplified by nested PCR using primers for the GPA gene, run by DGGE and visualized. Bands represent *E. huxleyi* morphotypes.

4.3.4e iii Data analysis

The DGGE gel shows a series of bands of varying intensity with subtle differences in pattern (**Fig. 4.17**). Twenty two distinct bands were identified and a binary matrix of presence or absence was compiled for each band. The similarity between samples displayed as a dendrogram was produced by a CLUSTER analysis performed in PRIMER V. 6 (section 2.5) (**Fig. 4.18**). A statistical analysis (SIMPROF) was run in conjunction with the CLUSTER to determine significant differences between clusters. Where groups are separated by black lines statistically different groups exist; those with red lines cannot be significantly differentiated (**Fig. 4.18, Table 4.13**).

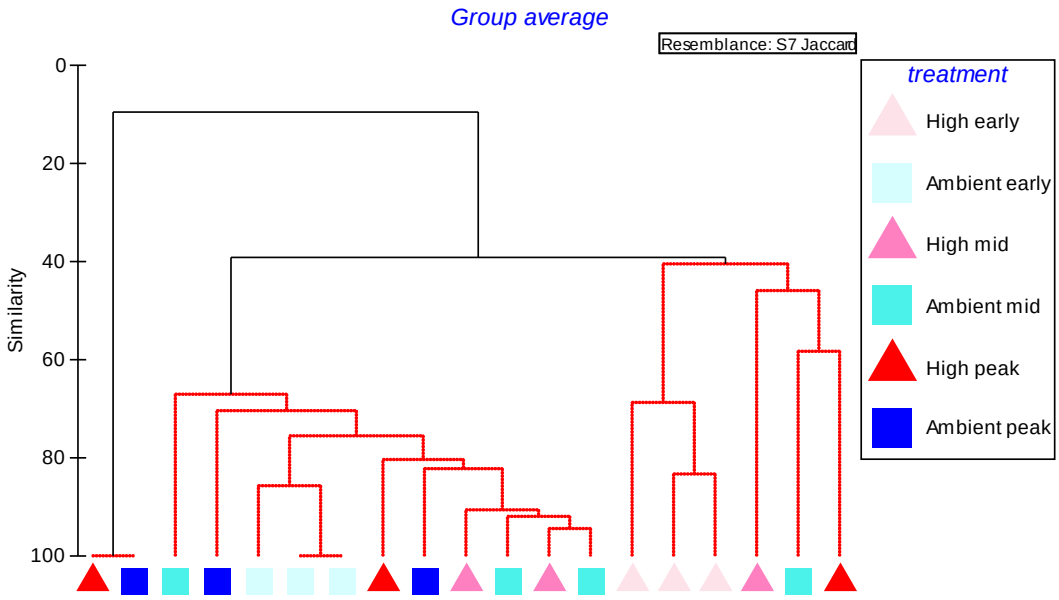

Fig. 4.18 CLUSTER dendrogram produced using PRIMER 6 data analysis software. Presence or absence data were transformed into a distance matrix using the Jaccard co-efficient calculations. Each symbol represents a separate mesocosm at one of the three time points. High CO_2 mesocosms at the early, mid-exponential and bloom peak (△△▲) and present day mesocosms (□■■). The degree of relatedness between samples is displayed on the left hand axis. Black lines indicate significant differences between groups and red lines those that cannot be significantly differentiated.

This analysis revealed clustering of the pre-bloom samples from each treatment. The early samples from the high CO_2 and present day mesocosms were significantly different from each other at 0.1% level. However these differences may be due to the clarity of the gel picture. The bands in the first three lanes were faint and more difficult to distinguish than those in lanes 4-6, the present day treatment (**Fig. 4.17**). The mid-exponential and bloom peak time points did not cluster either as treatments or time points. Two data points, mesocosms 2 and 4 at the bloom peak, were statistically differentiated from the others due to the poor quality of the banding in these samples.

Overall the presence or absence data suggested that there are no major differences in *E. huxleyi* strains (or morphotypes) between the two treatments. No attempt was made to calculate relative abundance of morphotypes from the DGGE data. There are several reasons for this. Firstly, some *E. huxleyi* strains have only one allele, and others two at this location and thus some strains may be under-represented (Schroeder et al. 2005). Secondly there may be biases in the DNA extraction and PCR steps (Martinez et al. 2007). The relative fluorescence of DGGE bands may be measured by pixel density software if the investigator is confident that the results are truly comparable (Schafer 2001).

The DGGE gel was compared with that from a previous mesocosm experiment carried out in Bergen facility (Martinez et al. 2007). The bands were very similar in position to those identified as A, B, C, E and F genotypes by Martinez et al. (2007). These bands were observed in 2000 and 2003, and identified as morphotype A, genotype CMM I. However, in the present study, I did not sequence the bands to confirm the identity of the different strains.

Table 4.13 Statistical analysis of clustering by SIMPROF in PRIMER. Two statistically significant differences were identified. At the 9.6% on the similarity scale in Fig. 4.21 two data points differ statistically. These were two samples at the final time point which had very poor banding. At 40% similarity, the remaining samples split into two groups. One contained all the pre-bloom high CO_2 and the other the pre-bloom present day data points this was significant at the 0.1% level.

Simprof Parameters
Permutations for mean profile: 1000
Simulation permutations: 999
Significance level: 5%
Resemblance:
Analyse between: Samples
Resemblance measure: S7 Jaccard
32+35 -> 36 at 39.21; Pi: 10.13 Sig (%): 0.1

4.4 EFFECTS OF PHYTOPLANKTON GROWTH ON SEAWATER CHEMISTRY

Phytoplankton growth requires carbon and nutrients which are taken from the seawater altering pCO_2, pH and nutrient regime. Precipitation of calcite decreases DIC by 1 mole and total alkalinity by 2 equivalents for each mole of calcium carbonate precipitated (Gattuso and Lavigne 2009). Nitrate assimilation also affects alkalinity, each NO_3^- taken up producing $1OH^-$. During the experiment, the physical and chemical conditions changed, these changes are the biogeochemical effects of the phytoplankton growth under the two treatments. The changes caused by the phytoplankton were often greater in magnitude than the difference between present and future scenarios. The methods for the following sections may be found in chapter 2.

4.4.1 pCO_2

The maximum pCO_2 in the high CO_2 mesocosms was 744 µatm (± 46) and 300 µatm (± 6) in the present day pCO_2 mesocosms. There was a gradual decrease in pCO_2 as the phytoplankton grew, reaching minima of 333 (± 36) and 163 (± 7) in the high CO_2 and present day mesocosms respectively on 15th May (**Fig. 4.19 A**). At this point because pCO_2 was reduced to below present day atmospheric pCO_2, mesocosms were re-bubbled to increase CO_2 to predicted future concentrations again.

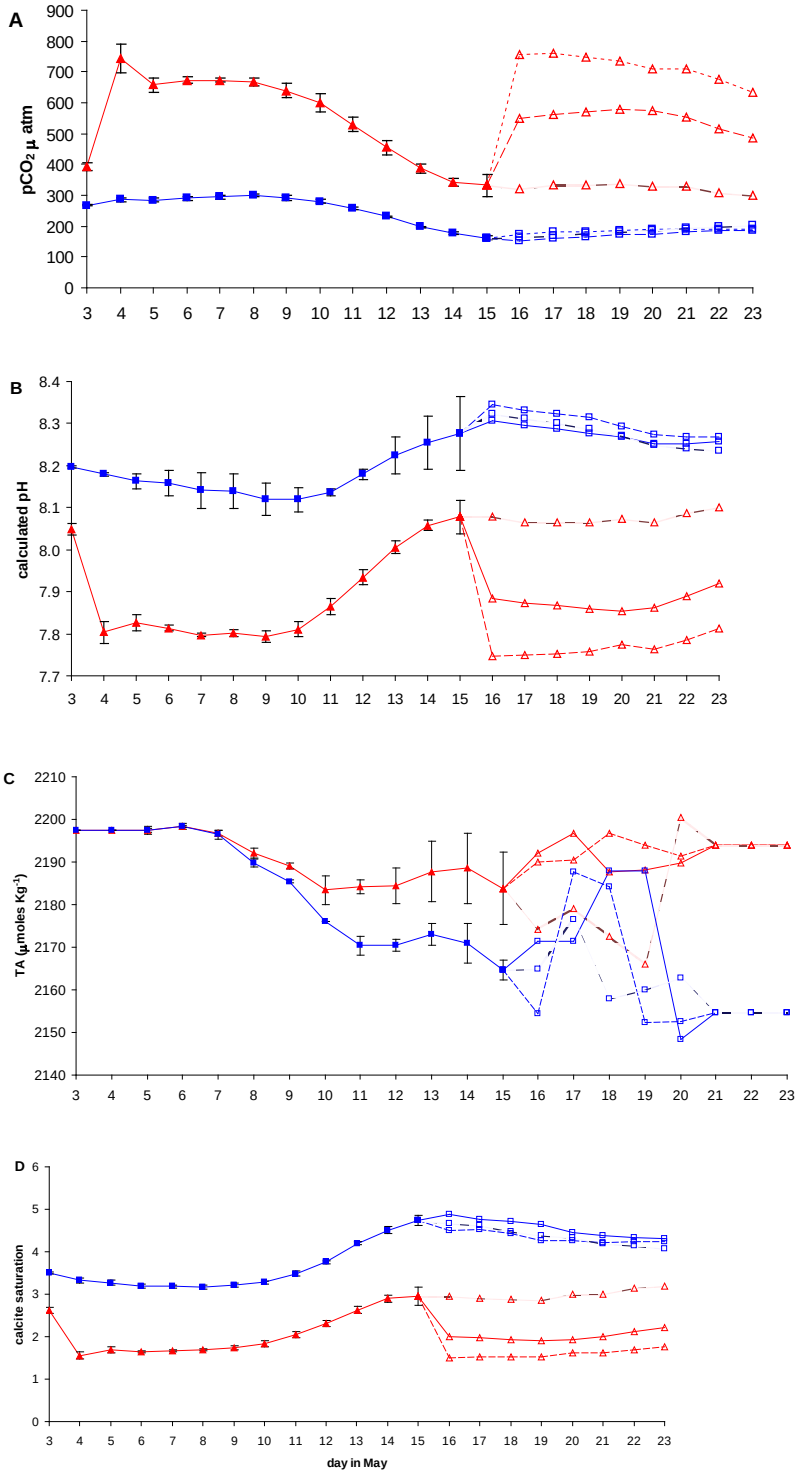

Fig. 4.19 Mean measurements from the triplicate high CO_2 mesocosms (-▲-); air mesocosms (-■-). A: pCO_2, B: Calculated pH, C: Total alkalinity and D: Calcite saturation state. Error bars show standard deviations of the triplicate mesocosms up to 15th May (closed symbols). On 15th May mesocosms 1 and 2 were re-bubbled with 760 ppm CO_2; 5 and 6 re-bubbled with air. Mesocosms 3 and 4 were not re-bubbled. Data for individual mesocosms is displayed for 15th-23rd May (open symbols).

4.4.2 Total alkalinity

Total alkalinity (TA) decreased in all mesocosms from 7th May reaching minima of 2183 (± 7) and 2164 (± 2) µmol kg^{-1} (=µEq l^{-1}) respectively in the high CO_2 and present day mesocosms, which were not re-bubbled (**Fig. 4.19 C**). Between mesocosms of the high CO_2 treatment TA was very variable, but in the present day mesocosms it was less so. By 15th May TA had fallen by mean values of 13.6 (± 7) and 32.7 (± 2) µmol kg^{-1} in the high CO_2 and present day mesocosms respectively. TA was discussed in relation to calcification and calculated carbon drawdown in section 4.3.1.e.

4.4.3 pH

As described in section 2.4.7, if two variables from the carbonate system are known then all may be calculated. pH was calculated from measurements of pCO_2 and total alkalinity. pH in the high CO_2 mesocosms remained at 7.8 or below until 10th May after which it rose sharply peaking on May 15th at maximum values of 8.08 (± 0.04) and 8.27 (± 0.09). A difference of approximately 0.2 units was maintained between the treatments for the course of the experiment (**Fig. 4.19 B**).

4.4.4 Calcite saturation state (Ω_{Cal})

The concentration of carbonate ions in seawater controls the calcite saturation state of seawater and is intimately linked to pH. Ω_{Cal} is a measure of the likelihood that calcite will dissolve due to a low concentration of carbonate ions. At saturation states below 1, calcite is likely to dissolve. Ω_{Cal} increased to maxima of 3 (± 0.2) and 4.7 (± 0.1) in the high CO_2 and present day mesocosms respectively. Prior to the re-bubbling event, there was little variability within treatments; after bubbling, the mesocosms varied greatly. At no point did Ω_{Cal} fall below 1 (**Fig. 4.19 D**).

4.4.5 Nutrient concentrations

In order to stimulate phytoplankton growth, it was necessary to add nutrients as these had been depleted in the fjord during previous phytoplankton blooms. The background silicate level was around 2 µmol l^{-1} which, due to the relative absence of diatoms in the bloom, was probably too low to sustain their growth. If nutrients are the limiting factor it is likely that they will gradually be taken up by the phytoplankton until they are exhausted. The rate of uptake should correlate with the rate of primary production in the two treatments.

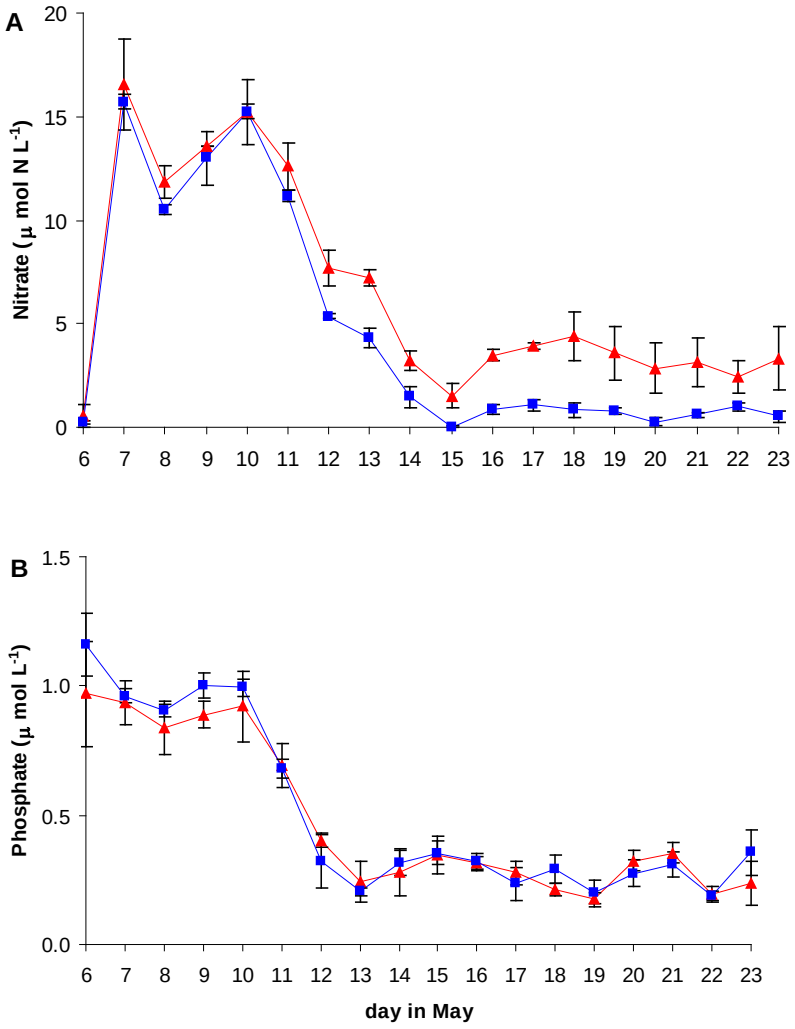

Fig. 4.20 Nitrate (A) and Phosphate (B) mean measurements of triplicate high CO_2 (-▲-) and air mesocosms (-■-). Error bars show standard deviations of the triplicate mesocosms.

Nitrate and phosphate were added to all mesocosm enclosures on 6th May at a ratio of 15:1 with final concentrations of approximately 15 and 1 µmol l^{-1}. Nitrate concentrations decreased rapidly from 10th to the 15th of May when it was almost exhausted in the present day mesocosms and an average of 0.56 µmol l^{-1} remained in the high CO_2 mesocosms. Phosphate concentration decreased to a minimum on 13th May of around 0.2 (± 0.01) and 0.24 (± 0.08) µmol l^{-1} in present day and high CO_2 treatments respectively. Phosphate then increased slightly prior to the re-bubbling which occurred on the 15th May. Nitrate concentrations rose following re-bubbling (**Fig. 4.20 A**). Phosphate was never exhausted, remaining at concentrations between 0.2 and 0.3 µmol l^{-1}. Nitrate was almost fully depleted in the present day mesocosms but remained at around 0.3-0.4 µmol l^{-1} in high CO_2 mesocosms.

4.5 DISCUSSION

This experiment yielded a strong response to increased CO_2 with significant reductions in biomass, primary production, chlorophyll, calcification (calculated) and carbon drawdown at increased CO_2. We saw a 27% reduction in primary production at increased CO_2; this is a very significant response and differs from most other CO_2 manipulation experiments (**Table 6.1**, in the general discussion section). All of the different analytical methods are consistent with this decrease in production at increased CO_2. All phytoplankton types were adversely affected, with the result that there was a reduction in carbon fixed by photosynthesis and calcification. *E. huxleyi* was expected to be out-competed or reduced in numbers at increased CO_2 due to its increased sensitivity to pH. However no phytoplankton type filled the niche it vacated. *E. huxleyi* did not dominate the mesocosms to the same extent as has been observed in previous experiments, but it was the dominant 'large' phytoplankton. Several *E. huxleyi* strains were separated by molecular analysis which persisted throughout the experiment in both

treatments. These strains were also present in mesocosm experiments performed in 2000 and 2003 (Martinez et al. 2007).

The variability between mesocosms was reasonably small despite the fact that the mesocosms are not true replicates. The volumes of water enclosed could not have contained exactly the same inocula which could lead to divergence in the measurements over the time scale of 1 month. At first glance our results appear to differ greatly from other experiments which have investigated CO_2 enrichment/ocean acidification. The majority have reported increased primary production despite decreased calcification. However, there are also many similarities with a CO_2 perturbation mesocosm experiment, and two bottle incubations, performed with the natural Bergen phytoplankton community in 2001. The apparent differences may be simply a different angle taken when reporting the results. This discussion will examine our results and compare them with previous mesocosms, further discussion in a wider context may be found in the general discussion.

4.5.1 Community production

Mesocosm experiments produce a large amount of data on many different aspects of the community response. The results require interpretation which may result in differences in reported outcomes. A close examination of the papers published from a 2001 CO_2 perturbation experiment at the Bergen facility revealed a very similar response to ours (Engel et al. 2004a; Schneider 2004; Delille et al. 2005; Engel et al. 2005).

The initial phytoplankton assemblage in May 2001 was dominated by autotrophic flagellates, predominantly *Micromonas* spp., and *Synechococcus*. *E. huxleyi* was present and rose to dominance reaching maximum cell densities of 1.5-5.6 x 10^4 cells

ml^{-1}. This was an order of magnitude higher than in our experiment with maximum densities of 0.29 x 10^4cells ml^{-1}. Large variability between replicates obscured differences between the three pCO_2 treatments: 190, 380 and 710 ppm in the 2001 mesocosm; however a systematic decrease in *E. huxleyi* growth rate was seen with increasing pCO_2, which was significant between the 190 ppm and 710 ppm treatments. Although no significant differences were reported, it appears that Chl-a in the present day pCO_2 mesocosms was significantly higher than in the high CO_2 mesocosms, ranging from approximately 9-12 and 6.5-8.5 μg l^{-1} respectively. These were very similar to our results of 9.6-11.2 and 5.7-9.2 μg l^{-1} respectively.

Also in the 2001 experiment, Schneider (2004) incubated duplicate 150 μm filtered 10 litre volumes taken from the mesocosms equilibrated to 190, 380 and 710 ppm CO_2. Nitrate, silicate and phosphate were added at molar ratio of 15:5.5:1. The most prolific growth was seen by several species of diatom, but *E. huxleyi* accounted for over 20% of the phytoplankton biomass at low CO_2 with maximum numbers of 2 x 10^3 cells ml^{-1}. At present day pCO_2, *E. huxleyi* contributed 15% and less than 4% at 710 ppm CO_2. At increased CO_2, specific growth rate was less than half that of the low CO_2 treatment. Total Chl-a was significantly higher in the low pCO_2 incubations than in the high pCO_2 although the community was slower growing. Maximum Chl-a levels of 11.7, 13.2, 16.9 μg l^{-1} were attained by the high, medium and low CO_2 treatments respectively. It was suggested, that diatoms outcompeted *E. huxleyi* due to a fertilization effect at increased pCO_2. In contrast, we saw no evidence of this as all phytoplankton groups had lower abundance in our study.

A second incubation experiment by Schneider (2004) examined the effects of light at high (150 μmol m^{-2} s^{-1}), medium (80 μmol m^{-2} s^{-1}) and low conditions (30 μmol m^{-2} s^{-1})

combined with 180, 360 and 780 ppm CO_2. Triplicate 2.4 litre incubations of 160 µm filtered water with N, Si and P added at 15:5.5:1 were performed. Chl-a concentrations declined slightly under increased CO_2. No effect of CO_2 on POC or C:N was observed. Abundances of *E. huxleyi* again decreased in response to increasing pCO_2 and also increased in response to increasing light. Maximum numbers for 180, 360 and 780 ppm CO_2 at high light were approximately 6×10^3 ($\pm 1 \times 10^3$), 4.5×10^3 ($\pm 0.5 \times 10^3$) and 2.5×10^3 ($\pm 0.5 \times 10^3$) cell ml^{-1} respectively. Results were similar at medium light intensities but *E. huxleyi* did not grow well in low light. *E. huxleyi* was the dominant species at low pCO_2 in high or medium light despite the addition of silicate to the incubations. At high pCO_2 several diatom species were more abundant. Other species that were reduced in numbers at 780 compared to 360 ppm CO_2 were *Pseudonitzschia* spp., *Ceratulina pelagica*, *Thalassiosira* spp., *Cylindrotheca closterium* and the Euglenophytes. The growth rates of *Leptocylindrus* spp. and *Skeletonema costatum* were slightly elevated however responses were different under different light regimes.

Another CO_2 manipulation mesocosm experiment had been performed in May 2005. No difference was seen between the Chl-a contributions attributed to the prymnesiophytes, identified as predominantly *E. huxleyi*, in mesocosms aerated with 350, 700 and 1,050 ppm CO_2 (Riebesell et al. 2007). Diatoms and *E. huxleyi* contributed equally to Chl-a in this bloom. Background natural $Si(OH)_4$ concentrations of 3.2 µmol l^{-1}stimulated diatom growth, and both diatom biomass and Chl-a increased at 700 and 1,050 ppm CO_2 compared to present day.

4.5.2 Calculated carbon drawdown

In our experiment, no differences in the calculated carbon loss term were detected between treatments. Increased carbon drawdown has been reported in the 2001 and

2005 mesocosms described in the previous section. The following discussion will examine the differences between the results.

A significant difference in carbon drawdown due to calcification was seen between the treatments in our mesocosms which was not reported in the 2001 and 2005 mesocosm experiments. However, on a per cell basis this was not significant. Overall, there was a much smaller reduction in total alkalinity (TA) and consequently ΔDIC_{cal} in our experiment than in the 2001 and 2005 experiments due to the lower cell numbers of coccolithophores in our study. Carbon drawdown attributed to primary production, Δ[DIC*], in the *E. huxleyi*/diatom dominated mesocosm of 2005, differed significantly between treatments with mean maximum values of 79, 100 and 110 µmol kg^{-1} in present day, 700 and 1,050 ppm CO_2 respectively. Our mean maximum Δ[DIC*] values are very similar to (Riebesell et al. 2007) but did not show a trend of increased production at higher pCO_2; present day Δ[DIC*] was 100 (± 5) and high CO_2 was 95 (± 7) µmol kg^{-1}. No difference was seen between treatments in the 2001 mesocosm. We saw no significant difference between treatments in the calculated carbon loss term, Δ[DIC*]-ΔPOC. Increased carbon loss at increased pCO_2 was reported in both the 2001 and 2005 mesocosms. We saw no significant difference between treatments in the calculated carbon drawdown per nitrate molecule term, $\Delta[DIC^*]:\Delta[NO_3^-]$. At the bloom peak, our calculated values were 8.29 (± 1.28) and 7.92 (± 0.7) mol:mol in the present day and high CO_2 mesocosms respectively. These values are very close to those reported by Engel et al (2005) of 8.11 (± 0.34) and 8.10 (± 0.17) mol:mol. A trend of increasing $\Delta[DIC^*]:\Delta[NO_3^-]$ was seen in the 2005 mesocosm with values of 6.6, 7.1 and 8 in 350, 700 and 1,050 ppm CO_2 treatments respectively. A significant increase was seen between glacial and future conditions in 2001, but there was no significant difference between present and future conditions.

These results suggest that species composition may be altered by pCO_2 with concomitant differences in carbon drawdown. Diatoms exude polysaccharides (TEP) which may increase at increased CO_2 (Engel et al. 2004b; Riebesell et al. 2007). Engel (2004) also reported a large increase in POC due to TEP production in the post-bloom period following an *E. huxleyi* bloom. This was significantly higher at increased CO_2 (Engel et al. 2004b). Overall we saw a similar pattern of response to that of the 2001 mesocosm but rather than an increase in carbon drawdown we saw a significant reduction in primary production. This was not negated by any calculated changes of carbon to nutrient ratios or carbon loss.

4.5.3 Coccolithophore morphology

Since Riebesell et al. (2000) showed highly malformed specimens of *E. huxleyi* and *Gephyrocapsa oceanica* grown at increased CO_2, there have been few further reports of this pheonomenon however see: Langer et al. (2006). I examined the *E. huxleyi* cells from our mesocosms by scanning electron microscope and saw no difference between treatments. There are several possible reasons for this. Firstly there is the choice of method of DIC manipulation around which there has recently been a well publicised debate (Iglesias-Rodriguez et al. 2008a; Riebesell et al. 2008). Riebesell et al. (2000) used acid/base addition to alter pCO_2, they report that addition of HCl to pH 7.75 decreased alkalinity by -6.4% and addition of NaOH to pH 8.2 increased it by +3.4%. A change of 9.8% equates to a decrease from 2197 µmol kg^{-1} seawater to 1990 µmol kg^{-1} seawater. As can be seen in **Fig. 4.19 C,** this is a very significant change as it is well below the alkalinity encountered at any point in our experiment. This change of 207µmol kg^{-1} is much greater than that produced by a large bloom which results in a fall of 50-60 µEq kg^{-1} (Findlay et al. 2008). A decrease in pH and total alkalinity may severely decrease the availability of carbonate ions although *E. huxleyi* has been found

to use solely bicarbonate for calcification (Buitenhuis et al. 1999). However, it has been recently suggested that carbonate ions constitute a far more efficient acceptor than bicarbonate for excess protons produced during calcification. Thus a reduction in carbonate ions may disrupt or slow the calcification process (Brownlee pers. comm.). Secondly the pCO_2 values in the Riebesell et al. (2000) study were higher at 780-850 ppm in samples with distinct malformations than in our samples bubbled with 760 ppm. The control samples were also less acidic than present day with a corresponding pCO_2 of 300 ppm. Thirdly, I studied two sets of samples in detail, although samples from across the experimental period were examined. Of these two sets, one was from 8th May, four days after aeration commenced when pH was 7.8 but there had been little time for an effect to be seen. This was far less time than the 16 days at high CO_2 that the malformed coccolithophores had experienced. The second set were from the 14th May, eight days into the experiment but the pH had been gradually increasing and had increased to above pH 8 by this time. Fourthly there is a biological explanation. In the fjord phytoplankton is exposed to constant fluctuations in alkalinity due to the salinity changes. This population may therefore have adapted to cope with pH changes possibly at a cost to their growth rate. The Riebesell samples were either from cultures or the non coastal subarctic North Pacific Ocean. Finally it is possible that the lack of significant difference is merely due to the small data set. Although I saw no significant differences between treatments during analysis of SEM images, the mean measurements for all parameters were higher in the present day treatment. An ANOVA examining lith length was significant at the 7% level, and central element width at the 6% level despite the small data set. Engel et al. (2005) examined *E. huxleyi* cells from mesocosms aerated with 180, 380 and 700 ppm CO_2 using scanning electron microscopy. They had a large number of individual size measurements, 600 for each treatment. Their results indicate that there is a significant difference between the three

treatments in terms of both coccolith and coccosphere size. The mean size of coccoliths were 3.58 (± 0.36), 3.55 (± 0.32), 3.41 (± 0.37) μm decreasing in size with increasing pCO_2. In my very small sample the mean lith lengths were 3.60 (± 0.17) and 3.40 (± 0.26) μm in present day and high CO_2 mesocosms respectively. These are very similar to those reported by Engel et al. (2005) and an ANOVA for our data suggests that the difference between the treatments was close to the significance level despite there being only nine individual measurements for each treatment ($F=3.86$, $p=0.07$). The other measurement which was close to the significance level was 1st-cycle element width ($F=4.44$, $p=0.06$) suggesting that if there was an increase in size then this was where it may lie. The shield element length was very similar in the two treatments ($F=0.21$, $p=0.65$). Clearly a larger data set would be necessary to draw firm conclusions from these data.

I also calculated calcification by the alkalinity anomaly method, which is based on the fact that the biogenic calcification causes a change in alkalinity in the seawater. I saw a difference in the change in alkalinity and, when normalized to the change in cell number during exponential growth, the difference between treatments fell just outside the $p=0.05$ significance range ($F=6.33$, $p=0.07$). In order to fully investigate the effects of high CO_2 on calcification in this study a measurement of calcite production would have been useful. The variation in the total alkalinity measurements and decrease in lith size is consistent with decreased calcification at high CO_2 but we have no precise measurements to compare with previous literature.

A second study where malformed coccospheres were observed was performed by Langer et al. (2006). They examined 500 sample coccoliths from *Coccolithus pelagicus* and *Calcidiscus leptoporus* using a qualitative scale of normal, incomplete, malformed

or malformed and incomplete. These had been subjected to either present day, 100 ppm or 920 ppm CO_2. In *C. leptoporus* most coccoliths were normal in the present day treatment whilst a 'notable' increase in malformation was seen at both higher and lower pCO_2. *C. pelagicus* showed no response. The lack of response in *C. pelagicus* suggests that the effects of increased CO_2 on calcifying phytoplankton may be species specific and may not be as sensitive as previously thought. Paleontological samples, and present-day coccolithophore species show no similar increase in malformation at periods of rapid increase in pCO_2. It is suggested that malformation may be a shock response which does not occur when there is sufficient time for phytoplankton to adjust to changes in CO_2.

The subjective nature of qualitative analyses of malformation of coccoliths, makes reproducibility difficult, but it seems that there has not been general agreement in subsequent literature that coccolithophores are always damaged by increased CO_2. As was described above very different results are found in closely related species or even strains within a species. This will be explored further in the following section.

4.5.4 E.huxleyi strains

In 1964 the cause of the naked cells appearing in laboratory cultures of *E. huxleyi* was hotly debated and several studies were performed to elucidate the mechanism, particularly focused upon nutrient regime. The outcome was a very varied response in different experiments, from which it was concluded that the response was strain specific (Paasche, 1964).

It has become increasingly obvious that many varied results have been produced during manipulative experiments involving *E. huxleyi* at different CO_2 concentrations. To

determine the degree of inter-strain variability of response, Langer et al. (2009) performed CO_2 manipulations with four *E. huxleyi* strains. Dilute batch cultures were grown at four pCO_2 values between 200 and 1200 ppm manipulated by acid/base addition. Their results were conclusive, in that no strain exhibited the same response to CO_2 manipulation. Growth rate, calcification and primary production were measured. However, only one strain increased in growth rate, a different strain increased calcification and all strains showed increased production of particulate organic carbon at 760 ppm compared to present day CO_2.

I conducted a molecular analysis to examine the *E. huxleyi* morphotypes present in the mesocosms. Comparison of my DGGE analysis with previous research suggests that six types were present, which were also present in mesocosms in Bergen in 2000 and 2003 (Martinez et al. 2007). These types were all present in the two treatments at three time points taken pre-bloom, mid-exponential and at the bloom peak. It is unfortunate that this DGGE analysis could not be quantified as subtle shifts in dominance may have occurred which would not be noted by a presence/absence analysis. With six morphotypes occurring in the community, a degree of plasticity in response to environmental changes would be expected. This may go some way to explaining the different results of different CO_2 manipulation mesocosm experiments.

4.5.5 Reduction in all phytoplankton types at increased CO_2

Interestingly there was a decrease in cell numbers of all phytoplankton groups. This would suggest that a general change in environment occurred due to increased CO_2 or decreased pH rather than a species specific response in *Emiliania huxleyi*. The sudden change of pH may cause stress to phytoplankton which may reduce growth rates either as a coping strategy or due to decreased resources available for growth. Alternatively

changes in pH may affect microzooplankton grazing. In order to understand the cause of the reduction in numbers it is probably necessary to investigate at a cellular level. Cell membrane potentials are maintained by an ion balance mechanism which could be severely affected by a sudden change in pH (Langer 2006). Although these are coastal and blooming species which can cope with pH fluctuations there may be a cost to maintenance of internal pH and the necessary membrane potentials which allow the cell to function

4.5.6 Conclusions

The explanation for these results is not simple. There is no obvious reason why many of the phytoplankton types should not thrive with increased CO_2. Fluctuations in pH are common in fjords and these species experience bloom situations several times per year. It is possible that the short time scale involved caused a shock response; however this did not occur in previous experiments. Possibly an effect of CO_2 on the grazer community may have occurred but this is not supported by microscopic analysis. It seems most probable that at a cellular level the change in pH has either directly or indirectly via nutrient speciation adversely affected cells. The results of mesocosm and monospecific laboratory manipulations differ greatly, not only in magnitude but also in direction of response. Many of the laboratory experiments reported increased primary production or POC accumulation at increased CO_2. However this response is not seen in *E. huxleyi* dominated natural communities. The mesocosms are a far better indicator of the overall response that could be expected in the natural environment in a high CO_2 world. Our results appear to suggest that there may be an overall decrease in primary production and calcification. However this was a short term experiment and the results may reflect a shock response.

The value of mesocosm experiments cannot be overestimated. Many of the shortcomings of laboratory experiments may be overcome without compromising the ability to control the necessary variables. A major criticism of laboratory experiments is that the experimental organisms have likely been in culture for many years or even decades. Having lived in a monospecific environment probably experiencing large fluctuations in pH, nutrient availability, density and available light, their use as proxies for natural communities is questionable. The use of monospecific cultures is also a poor reflection of the natural environment as all the natural interactions including those of bacterial communities and grazers are excluded. Light and nutrient regimes and cell density are artificial and usually unrealistic in laboratory cultures. Mesocosms have all the benefits of a natural community, natural light regime in a relatively dilute culture whilst variables can be constrained and are large enough samples can be taken for analysis. The drawbacks of mesocosm experiments are largely due to the cost and difficulty of running them. This necessitates a limited number of replicates which reduces the statistical power of analyses. As natural communities contain so many variables the probability that replicates will behave similarly is relatively low. In these terms our mesocosm experiment performed well with the pseudo-replicates from the two treatments agreeing surprisingly well.

Chapter 5

THE RESPONSE OF A NATURAL COMMUNITY FROM THE EASTERN ATLANTIC TO INCREASED CO_2

5.1 INTRODUCTION

In this section I will describe a deck incubation experiment that I performed to examine the effects of increased CO_2 on a natural community from the Eastern Atlantic, to the south of the Canary Islands. This region is generally described as oligotrophic, however as the experiment was performed in January, deep mixing is likely to have caused an upwelling of nutrients. As expected in this region (Bode et al. 2001) the dominant phytoplankton in the surface water, and thus the incubation, was coccoid cyanobacteria and picoeukaryotes.

The experiment was performed aboard the STS Lord Nelson, a three masted Tall Ship (**Fig. 5.1**), during the first scientific cruise organised jointly by the Jubilee Sailing Trust and the Challenger Society for Marine Science. The areas of research focused on: physical oceanography, acoustic investigation of hull hydrodynamics, phytoplankton, zooplankton, cetaceans, methanogenesis, and public understanding of science - the value of a two way process - as well as my incubation. The scientists and their areas of research are listed in **Table 5.1**, and further details may be found in the cruise report (Patching 2008). The nature of the vessel and facilities provided both opportunities and limitations for the scientists aboard. A willing team of scientists and non-scientists working together achieved twice daily sampling of phyto- and zoo plankton as well as physical oceanographic measurements. The continuous watch system, requiring teams of 10 people to sail the vessel at all times, provided ample manpower for collecting

cetacean sighting data. An investigation was carried out to investigate the benefits of conducting science aboard a sailing vessel and to observe the underwater acoustic characteristics of the ship's hull under different sail regimes. Noise, vibration and exhaust were all reduced which may benefit certain areas of study. A study to investigate methanogenesis was performed and my deck incubation examined the effects of increased CO_2 on the natural phytoplankton community.

The public outreach element of this cruise was very strong, approximately half the participants on the cruise were scientists and half were captive members of the general public. There was a necessity for team work and all participants were involved in the scientific process and in sailing the STS Lord Nelson. In order to stop the vessel for sampling it was necessary to 'heave to'. This required the main course sail to be hauled up and the fore top sail to be backed, a procedure which required at least 20 people to haul on the ropes. Some limitations were placed on the science due to the lack of facilities aboard. The 'laboratory' was housed in a shower/toilet cubicle with just enough space for microscopes. An added challenge was posed by the fact that a box of my apparatus did not clear customs in Madrid. A missing vacuum pump for the chlorophyll filtration rig was replaced with an impeller pump powered by a hand held electric drill. This improvised technique was very successful, cheap and light compared to the usual apparatus and was designed by the 1st Mate, Neil Duncan. The cruise commenced and returned to Las Palmas de Gran Canaria (Lat: 28°, 7.5' N; Long: 15°, 25.8' W) on 21st and 28th January 2008. The plan was to perform a transect to the North West of Gran Canaria into the oligotrophic ocean gyre region. However, the actual cruise track was determined by a number of factors, predominantly wind direction and strength, but also a report of pirates off the African coast (**Fig. 5.2A)**.

Fig. 5.1 The STS Lord Nelson in the Las Palmas de Gran Canaria international port.

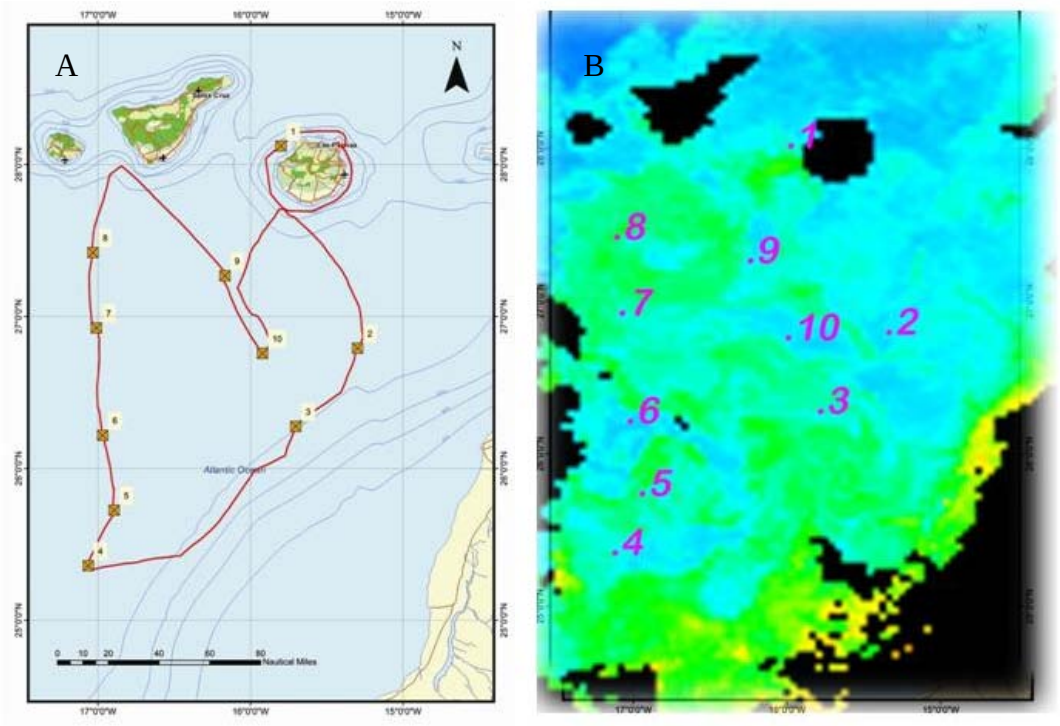

Fig. 5.2 A. Cruise track of STS Lord Nelson from 21st-28th Jan 2008. Track commences at Las Palmas de Gran Canaria passes anti-clockwise round the island, South parallel to the African coast before returning Gran Canaria via the Southern tip of Tenerife. The numbered boxes are sampling stations. B. Composite satellite image of ocean colour for the week of 17th-21st January, showing the West African coast in the lower right corner, and Gran Canaria to the right of station 1. Numbers mark the 10 stations sampled on the voyage.

My deck incubation experiment was performed with surface water collected from station 2 (Lat: 26° 47.41' N, Long: 15° 17.82' W) at 09:00 on 23rd Jan (**Fig. 5.2**). A composite satellite image for the week of 17th-21st Jan gives an indication of the surface chlorophyll present at this location (**Fig. 5.2B**). The water was found to be well mixed to ~100m with a temperature of 19°C. Four groups of phytoplankton were identified by subsequent flow cytometry. Two groups of *Synechococcus*; *Prochlorococcus* and picoeukaryotes were identified by their auto-fluorescence and scattering properties. Incubation of the community at increased CO_2 concentrations of 760 ppm did not alter either the community structure or the cell division rates compared to present day pCO_2. Flow cytometry measurements of autofluorescence give relative indications of pigments in the cells and scatter gives a relative estimate of size. No differences in fluorescence or scatter measurements were seen between the two treatments.

Few studies have specifically examined the effects of increased CO_2 on coccoid cyanobacteria (however, see Fu et al. 2007) although they have been examined as members of natural communities in mesocosms (Engel et al. 2005; this study). These small phytoplankton are numerically dominant (Falkowski et al. 2004) and may be responsible for 50% of the carbon fixed in the oceans (Fu et al. 2007). Unlike diatoms and coccolithophores they contribute little directly by the biological pump because they are too small to show significant sedimentation. However, they support higher trophic levels and therefore contribute to carbon flux in faecal pellets. A notable study by Fu et al. (2007) examined the responses of *Synechococcus* and *Prochlorococcus* to variations in pCO_2, light and temperature. At 20°C, increased CO_2 raised phycoerythrin, phycocyanin and chlorophyll in *Synechococcus* by 40%, 50% and 42% respectively, compared to present day treatments. Maximum photosynthetic rates of *Synechococcus* increased four fold in the greenhouse treatment (increased CO_2 and temperature)

compared to controls. Elevated CO_2 alone increased cellular carbon and nitrogen but not phosphorus, raising C:P and N:P ratios; C:N decreased slightly. Cellular carbon concentrations increased by 18% at 20°C in high CO_2 cultures compared to present day. Significant increases in Fv/Fm were seen with increasing temperature or CO_2. The pigments of *Prochlorococcus* showed no response to increased CO_2 but cell size was doubled at 24°C compared to 20°C (Fu et al. 2007). *Synechococcus* growth rates doubled at increased temperature and further increased slightly with a rise in CO_2, no effect was seen at 20°C with increased CO_2. *Prochlorococcus* growth rates were unaffected by temperature or CO_2 increases. *Synechococcus* native to the fjords of Western Norway have been included in several mesocosm experiments. Engel (2005) saw no change in the growth rates or maximum numbers of *Synechococcus* at increased CO_2. Conversely we saw a decrease in both in the mesocosm experiment described in this study.

Table 5.1: Scientists participating in Cruise LN684 (Patching 2008).

Name	Affiliation*	Function
Prof. John Patching	MRI	Chief Scientist
Colm Moriarty	MRI	Technical Assistance
Dr.Cilian Roden	GMIT	Phytoplankton - Genus *Histioneis*
Hazel Farrell	MRI	Phytoplankton-Dinoflagellates/Coccolithophores
Sandra Lyons	MRI	Phytoplankton-Dinoflagellates/ Coccolithophores
Evelyn Keady	NDC	Phytoplankton-Dinoflagellates/ Coccolithophores
Damien Guihen	EOS	Temperature/salinity profiles, GIS
Katharine Crawfurd	PML	On deck phytoplankton incubations
Dr Gary Caldwell	NU	Zooplankton
Susan Gebbels	DML	Community outreach. Bird/Cetacean observations
Tamsin Smith	NU	Acoustics
Eleuthera du Breuil	NU	Acoustics/Zooplankton
Dr Judy Foster-Smith	EM	Cetacean observations
Dr Arlene Rowan	SAMS	Methanogenisis in the pelagos

*Abbreviations: MRI – Martin Ryan Institute, National University of Ireland, Galway, Ireland; GMIT – Galway Mayo Institute of Technology, Galway. Ireland; NDC – National Diagnostics Centre, National University of Ireland. Galway. Ireland; IOS – Earth and Ocean Sciences, National University of Ireland, Galway. Ireland; PML – Plymouth Marine Laboratory, UK; DML - Dove Marine Laboratory, Newcastle University, Cullercoats, Tyne and Wear, NE30 4PZ, UK; NU – School of Marine Science and Technology, Newcastle University, UK; EM - Envision Mapping Ltd., Horsley, Northumberland, UK; SAMS – Scottish Association for Marine Science, Dunstaffnage, Scotland.

5.2 PHYSICAL OCEANOGRAPHY AND NATURAL PHYTOPLANKTON ASSEMBLAGE OF THE CANARIES REGION

5.2.1 Background

The Canary Islands lie in the tropical Eastern Atlantic, close to the West African coast. The islands are volcanic and shelve steeply with depths of several kilometres common close to the shore. Despite their proximity to the upwelling region along the West African coast, a strong current brings nutrient poor water from the North Atlantic gyre through the region and sweeps down the coast taking nutrient rich water south. The area is described as oligotrophic, as stratification usually separates the nutrient rich deeper waters from the nutrient poor surface layer except during the period of winter mixing (Bode et al. 2001). Eddies are created as the water passes between the islands and turbulent mixing of the cooler, nutrient rich, up-welled water with the relatively warm Atlantic water means that eddies may be viewed by thermal satellite imagery. These eddies are stable dynamic features which are periodically shed by the islands and can be followed as they move in a South Westerly direction into the Atlantic (Sangrà et al. 2009). The nutrient regime of the area is therefore highly variable as can be seen in satellite images of the ocean colour, pertaining to chlorophyll distribution (**Fig. 5.2B**). Episodic dust inputs from the Sahara deposit trace metals, particularly iron into the waters (Bode et al. 2001).

The dominant phytoplankton in this region is coccoid cyanobacteria which reach abundances of 10^4 cells ml^{-1} in the sub-surface maxima (Bode et al. 2001). Phytoplankton biomass is generally low apart from a short bloom following winter mixing. Zooplankton and heterotrophic bacteria generally utilise all the primary production in this area; indeed in summer heterotrophic bacterial biomass greatly outweighs phytoplankton biomass (Bode et al. 2001).

5.2.2 Oceanographic measurements

Temperature, conductivity and pressure were sampled at each of the 10 stations, from the surface to approximately 130 m depth (**Fig. 5.3**). This showed the surface layer to be well mixed to 100 meters at most stations. Mean SST of all stations was 19.7°C, with station 2, where the deck incubation water was taken from, being slightly cooler than the others with a mean of 19°C.

5.2.3 Phytoplankton sampling

Phytoplankton net hauls at 50 and 200 m were performed at each station. The results reflected the patchiness observed in the satellite image of the area. At three stations, diatoms were very numerous and at others, including station 2 very little biomass was recovered. However, the hauls at station 2 were still diatom dominated with a similar assemblage at both depths sampled. The water obtained for the deck incubation experiment was collected from the surface due to the logistics of sampling. Flow cytometry analysis showed no larger phytoplankton in the incubation, which may have been a true reflection or they may not have been well preserved. Three groups of cyanobacteria and one of pico-eukaryotes were identified by flow cytometry.

5.2.4 Zooplankton sampling

It was hoped that zooplankton had been excluded from the incubation experiment. However the phytoplankton community in bottle 1 was not as abundant as in the other bottles which may have been due to the presence of grazers. Zooplankton net hauls were carried out at each station and a variety of species were collected. These were typically dominated by calanoid copepods and larval stages of marine metazoans.

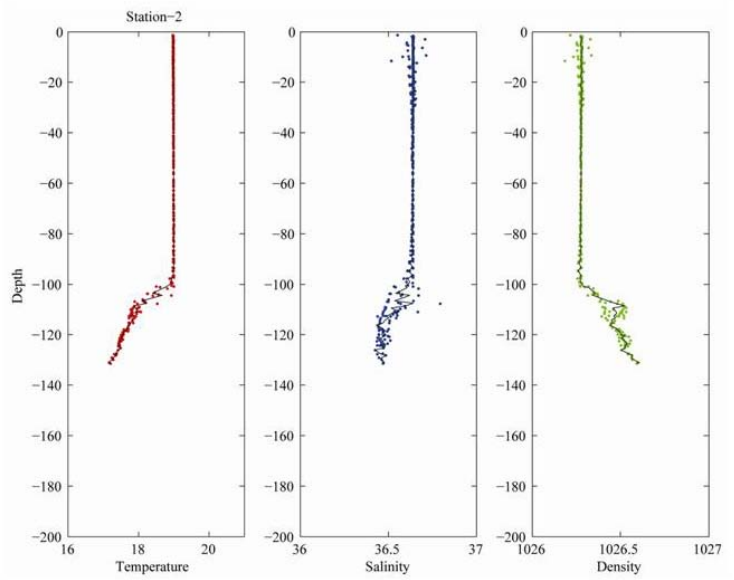

Fig. 5.3 Temperature and salinity profiles for station 2, where water was collected for the incubation experiment. Individual data points are marked with a dot while the mean for each metre of depth is shown with a black line. Courtesy of Damien Guihen, National University of Ireland, Galway.

5.3 DECK INCUBATION ON THE STS LORD NELSON

5.3.1 Methods

Water was taken from the surface layer at station 2: 26^{o} 47.40' N 15^{o} 17.82' W at 09:00-10:00 on 23rd Jan 2008. The bottles were filled using an acid washed bucket and funnel with a 50 µm gauze secured around the end of a piece of wide bore plastic tubing attached to the funnel. This apparatus aimed to remove large grazers and lower the phytoplankton gently to the bottom of the bottles. The deck incubator was filled with seawater and the temperature monitored. If the temperature rose above the sea temperature it was refreshed with seawater. Occasionally the apparatus was covered with a thin white sheet if it was in full sun. All bottles were aerated using glass diffusers attached to the air or gas supply: bottles 1, 2 and 3 with air at 760 ppm CO_2; 4, 5 and 6 with air via a small air pump (**Fig. 5.4**). The bottles were incubated on the aft deck for the 5 day voyage. Nutrients were not added.

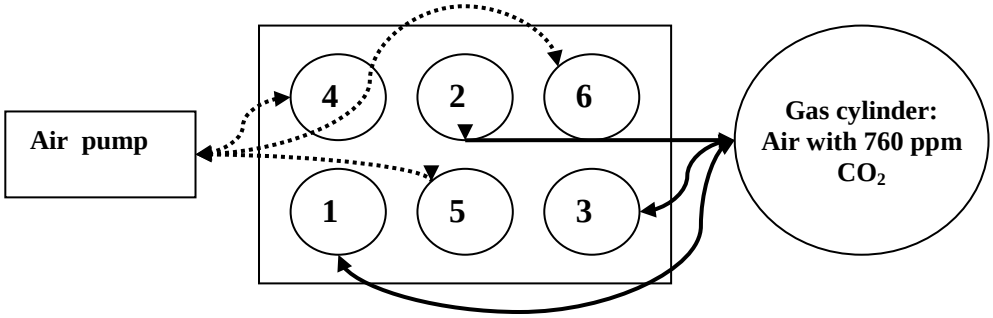

Fig. 5.4 Deck incubation apparatus. 1-6 represent 20 litre Nalgene bottles containing seawater, 1-3 aerated with an air mix with CO_2 at 760 ppm, 4-6 aerated with air.

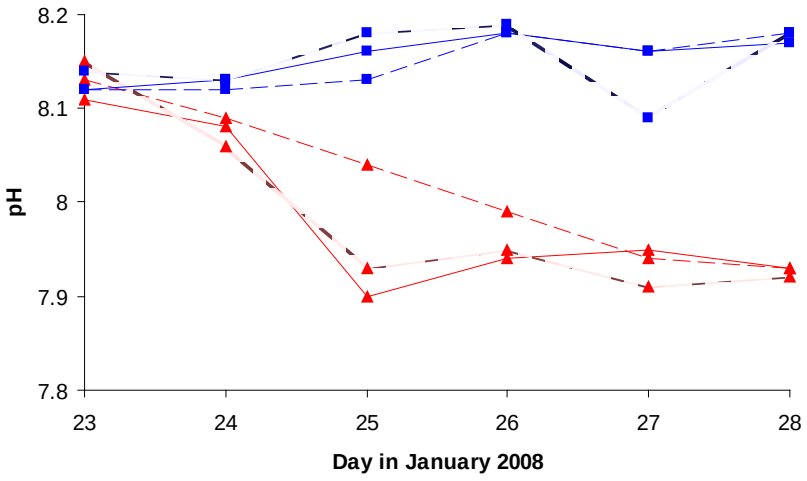

Fig. 5.5 pH of each of six 20 litre incubations aerated with air enhanced with 760 ppm CO_2 1:(-▲-) , 2 :(---▲---), 3: (····▲····), present day: 4: (-■-), 5: (---■---) and 6: (···■····).

Each day at 10:00 (GMT), approximately two hours after sunrise, the pH and temperature of each bottle was measured. Duplicate 2 ml samples were taken using a syringe and were preserved with 1% formalin, final concentration, in cryovials.

5.3.2 Results

5.3.2.a pH

The pH in the deck incubation water rapidly decreased when aerated with 760 ppm CO_2 in air (**Fig. 5.5**). Aeration continued throughout the experimental period and pH did not increase significantly in response to phytoplankton growth.

5.3.2.b Temperature

Temperature in the incubation bottles did not rise above 20°C which was lower than the sea surface temperature at some stations. The wind probably cooled the water in the incubator allowing the temperature to remain reasonably low (**Fig. 5.6**).

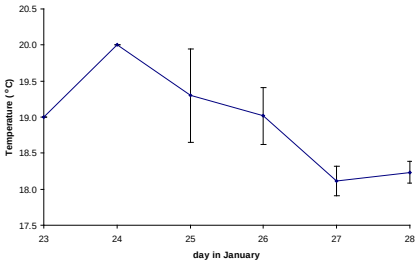

Fig. 5.6 Mean temperature of all 6 bottles with error bars showing one standard deviation.

5.3.2.c Phytoplankton counts

Duplicate 2ml samples were taken daily and fixed with 1% formalin. These were analysed by flow cytometer in Plymouth. Four groups were distinguished by their auto-fluorescence and light scattering properties (section 2.4.2). Two groups had high orange fluorescence signals from phycoerythrin typical of *Synechococcus*. A large group with greater orange fluorescence (10^1-10^3 flow cytometer units) increased in

numbers over the course of the experiment was distinguishable from a smaller group with dimmer orange fluorescence ($10^{0.5}$-10^{1} flow cytometry units). Two further groups were identified as *Prochlorococcus* and pico-eukaryotes.

Over the course of the experiment these four groups of phytoplankton grew exponentially until they reached stationary phase. As nutrients were not added to the incubations this growth was sustained by natural nutrient concentrations. These were not analysed but may have been reasonably high due to the well mixed seawater. Growth of the phytoplankton may have been stimulated by the slight temperature rise on 24th Jan and there may also have been more constant light than experienced in the surface ocean which was rather turbulent. On 24th Jan all groups grew exponentially with mean doubling times of 13-24 hours for all groups although variability within treatments was quite high. Minimum doubling times of 6-8 hours for pico-eukayotes and 8-9 hours for *Synechococcus* bright, show the rapidity at which the cells multiplied. The community within bottle 1 did not grow as well as the other replicates but there was still an increase in the number of cells of all types. An ANOSIM performed in primer 6 (methods 2.5) revealed no significant differences between cell abundances of the four groups during the experiment (R=0, p=0.6, **Table. 5.2**). An examination of the data revealed no obvious differences between either the pattern or the magnitude of the differences between the groups (**Fig. 5.7**). The percentage abundances of each phytoplankton type are displayed in **Fig. 5.8**.

Table 5.2 ANOSIM to examine differences between the abundances of the four identified phytoplankton types in the two treatments.

Global Test of differences in abundance of phytoplankton between treatments
Sample statistic (Global R): 0
Significance level of sample statistic: 60%
Number of permutations: 10 (All possible permutations)
Number of permuted statistics greater than or equal to Global R: 6

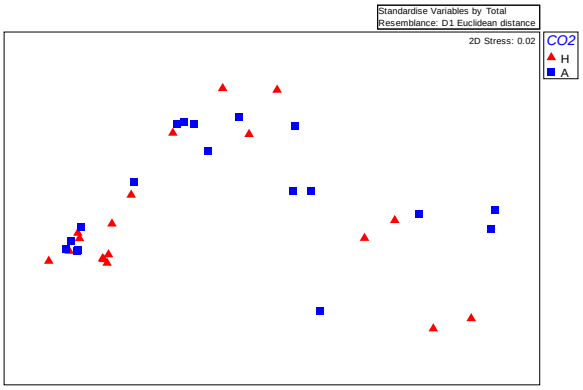

Fig. 5.7 Scaling plot representing cell numbers of phytoplankton groups as estimated by flow cytometry. High CO_2 bottles, ▲; present day bottles: ■. Data were standardized to totals, and a distance matrix created using Euclidean distances.

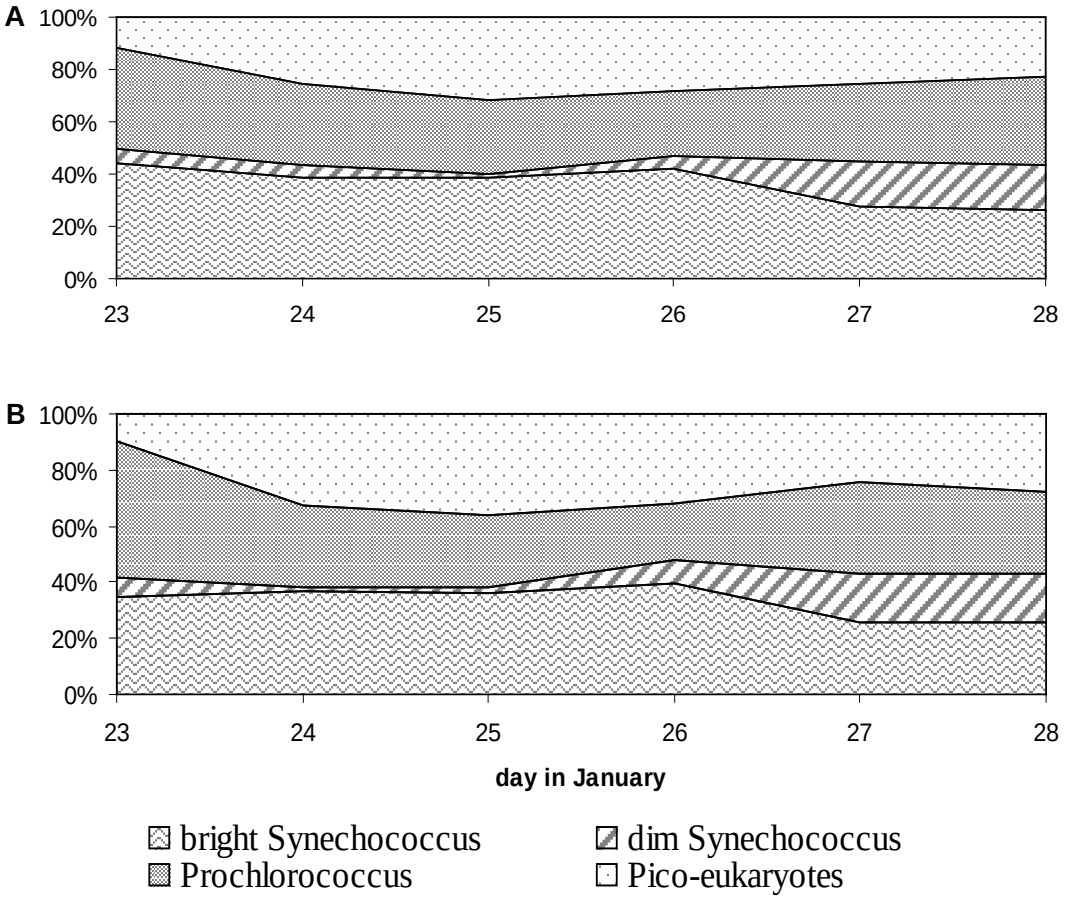

Fig. 5.8 A: high CO_2 bottle 2; B: present day bottle 6. Percentage abundance of the 4 different groups identified during the experiment, as quantified by flow cytometry.

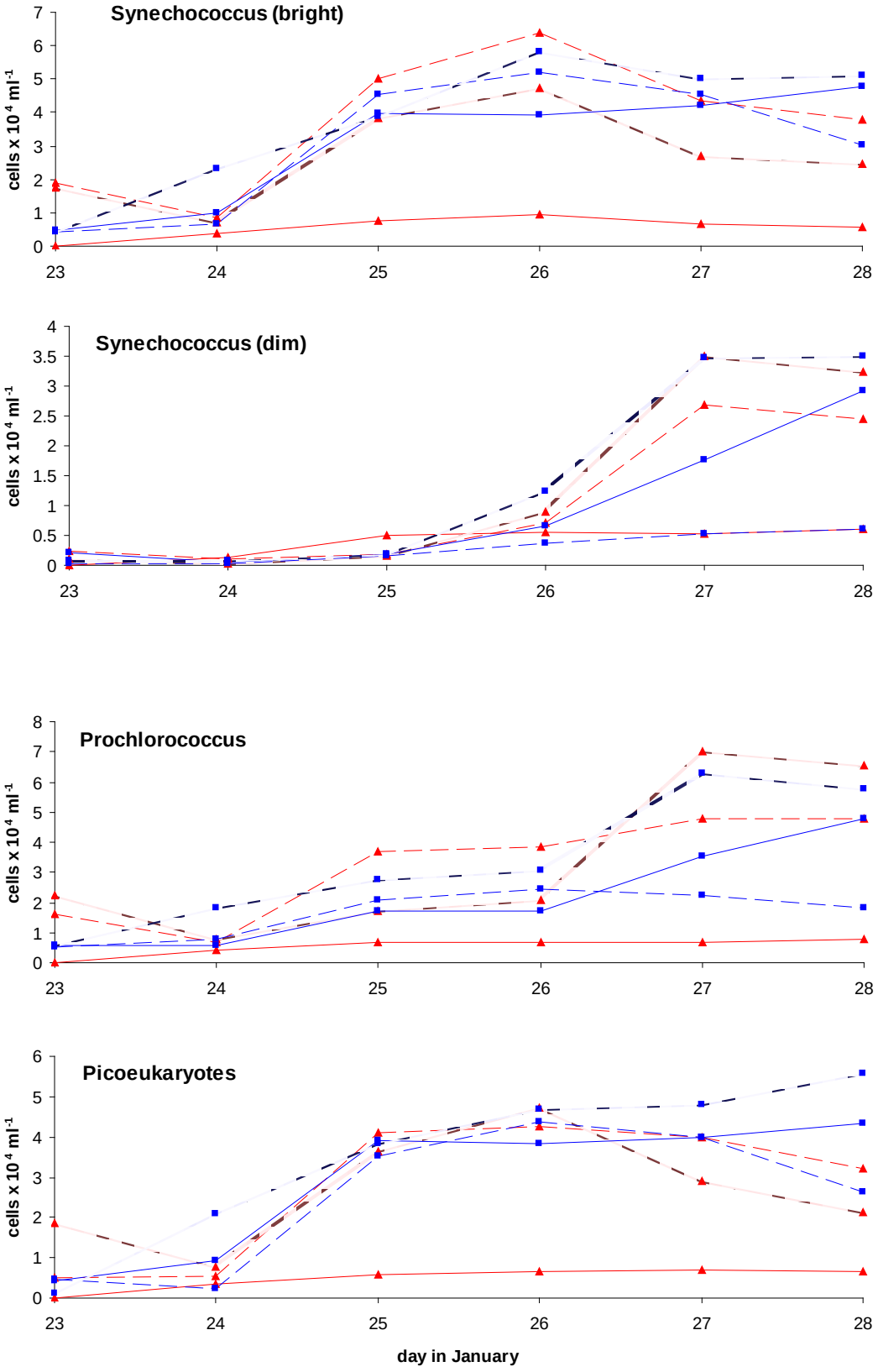

Fig. 5.9 Cell abundance of the 4 groups of phytoplankton as quantified by flow cytometry.

5.3.2.d Scatter and auto-fluorescence

Side scatter; orange and red fluorescence per cell were analysed by the flow cytometer. As mentioned previously, *Synechococcus* has high levels of phycoerythrin which gives high levels of orange fluorescence when analysed in the flow cytometer. All groups have chlorophyll which is detected as red fluorescence. The scatter caused by the cells passing through the laser beam relates to their size. There is evidence that pigment levels in *Synechococcus* may respond to increased CO_2 and that cell size of *Prochlorococcus* responds to increased temperature (Fu et al. 2007). Neither red fluorescence (R=-0.148, p=0.9) nor side scatter (R=0.037, p=0.5) differed between treatments (**Table 5.3**). As observed in the laboratory study, these appeared to be related to growth phase.

Table. 5.3 ANOSIM to examine differences in side scatter and red fluorescence measurements of individual cells (section 2.5)

Global Test side scatter
Sample statistic (Global R): 0.037
Significance level of sample statistic: 50%
Number of permutations: 10 (All possible permutations)
Number of permuted statistics greater than or equal to Global R: 5

Global Test red fluorescence
Sample statistic (Global R): -0.148
Significance level of sample statistic: 90%
Number of permutations: 10 (All possible permutations)
Number of permuted statistics greater than or equal to Global R: 9

5.4 DISCUSSION

Cyanobacteria dominate vast oligotrophic regions of the oceans and are the most numerically abundant group of phytoplankton (Falkowski et al. 2004). Despite, potentially, contributing 50% of the carbon fixed in marine systems, their response to increased CO_2 has hardly been studied. A single study of the response of *Synechococcus* and *Prochlorococcus*, two common species, has been performed (Fu et

al. 2007). *Synechococcus* has also been included in several mesocosm experiments as part of the natural population (Engel et al. 2005; and this study).

My experiment examined the response of a natural community, with 4 identifiable groups of pico-phytoplankton, to CO_2 concentrations expected at the end of this century. This allowed not only an examination of the response of the separate groups, but also any shifts in dominance between these groups could be observed. In the North Atlantic *Synechococcus* and *Prochlorococcus* commonly occur together, with *Synechococcus* blooms succeeded by increased abundances of *Prochlorococcus* (Fu et al. 2007). *Prochlorococcus* has a deeper distribution than *Synechococcus* possibly due to the increased use of chlorophyll, which is more efficient at light harvesting than are phycobilins (Raven et al. 2000). At the depths of below 100m, where *Prochlorococcus* dominates, the pH is usually ~8.0, whilst at the surface it is 8.12 (Fu et al. 2007). Although the deck incubation water was collected from the surface, there may be genetic differences between the species favouring *Prochlorococcus* at lower pH. The types 1A and 1B RuBisCOs of the cyanobacteria have a lower specificity for CO_2, compared to O_2 than the eukaryotic RuBisCOs (see section 1.4.4). In order to maintain efficient photosynthesis cyanobacteria may be more reliant on CCMs than eukaryotes. If CCMs are suppressed with more available CO_2, then the energy required for this process may be available for growth or other processes (Beardall and Raven 2004; Tcherkez et al. 2006). In this experiment I saw no evidence to support this hypothesis. The cyanobacteria did not benefit from increased CO_2 more than the pico-eukaryotes, and no shifts in community structure were seen. In fact, none of the groups of phytoplankton appeared to benefit from increased CO_2, in terms of increased growth rates, competitive ability, pigment concentrations or size.

Although initially appearing to contrast with the findings of Fu et al. (2007) my experiment supports their findings. Uni-algal cultures of *Synechococcus* strain CCMP1334 and *Prochlorococcus* strain CCMP1986 did not show significantly increased cell division rates with increased CO_2. They did, however, find that *Synechococcus* µ increased with increased temperature, and this was further increased in their greenhouse treatment. The temperature control in the deck incubator, was sufficiently good that this did not compare to the 4°C rise in temperature in the greenhouse treatment of Fu et al. (2007). Although I did not examine the physiology in as much depth as Fu et al. (2007) any changes in fitness which resulted in a shift in dominance would have been seen.

Like the Bergen mesocosm assemblage, this community inhabits a region of variable temperature, nutrient regime and pH due to blooms supported by the upwelling of nutrients and the mixing of different bodies of water. They are therefore probably able to adapt to changing conditions. There was no evidence of a shock response to the added CO_2, neither did cells appear to suffer from the physical effects of bubbling. The lack of increased cell division at high CO_2 suggests that no group in this community is carbon limited. There was no evidence that any group benefited from suppression of a CCM, as hypothesised for the cyanobacteria.

Cyanobacteria are widespread and thus must be either very adaptable or exist as many strains within the species. The different responses seen in these few experiments are probably due to different strains, location and history. The species used by Fu et al. (2007) had been cultured for 15 and 25 years. The Bergen and Canary Islands assemblages inhabit very different regions. It is possible that further studies may, as with *E. huxleyi*, uncover more strain specific responses from which general conclusions

are difficult to draw. I feel that the incubation of natural assemblages is a more constructive method of examining responses to future conditions. Increased fitness in itself does not necessarily equate to dominance. Theoretical advantages due to RuBisCO kinetics create hypotheses to test but may have little bearing on actual responses, or competitiveness of species.

Chapter 6.

GENERAL DISCUSSION

The work presented here addresses several gaps in our current knowledge of the effects of increased CO_2 on the marine phytoplankton. Firstly, although there have been a great number of studies over the past decade, few have examined the growth of phytoplankton in steady state, balanced growth with increased CO_2 provided by gas equilibration. Many studies, due to the difficulty of maintaining high CO_2 concentrations in actively growing cultures, have either used acid/base techniques to maintain pCO_2, or have examined short term batch cultures. Secondly, this is, to my knowledge, the first experiment which has tested the effects of exposure to increased CO_2 for >100 generations of marine phytoplankton. This is again due to the difficulty of running experiments and this project had aimed to examine much longer term effects. Thirdly, we currently lack a thorough understanding of the mechanisms underlying observed effects of increased CO_2 on the phytoplankton. This study examined the effects of increased CO_2 on the transcription of genes crucial to carbon acquisition and fixation.

The marine phytoplankton is a large and diverse assemblage, whose response to rising CO_2 is unclear. Predictive models are increasingly attempting to incorporate biological responses. This is a necessary step towards a holistic understanding of the Earth System, however it is surprisingly difficult to extract any definitive responses of any group of phytoplankton. Even calcification, which appeared to simply decrease at lower pH, has been found to increase in certain strains whilst decreasing in others within a species (Langer et al. 2006; Ridgwell et al. 2009). Thus the task of supplying general

rules which can be used in predictive models is proving more difficult than anticipated. In this chapter I will discuss my results in the context of the literature. The discussion of my laboratory experiments will focus on: growth rates and their significance to biogeochemical cycling; acclimation and adaptation of phytoplankton in a high CO_2 world, and the impact on phytoplankton fitness. This section will include RuBisCO and carbonic anhydrase gene transcription in phytoplankton acclimated to increased CO_2. A discussion of the Bergen mesocosm experiment will follow, with reference to community productivity and structure. The conclusion to this section will refer back to the questions, posed in the Thesis Aims section of the introduction. Finally I will suggest the direction that further research on this topic could take.

6.1 STEADY STATE GROWTH

6.1.1 CO_2 manipulation methods

In several recent reviews of the effects of ocean acidification on the phytoplankton, the method of CO_2 manipulation has been implicated as the cause of apparent contradictions between experimental results (Rost et al. 2008). The topic most hotly disputed has been the effects of acid/base manipulation compared to gas bubbling (Iglesias-Rodriguez et al. 2008a; Iglesias-Rodriguez et al. 2008b; Riebesell et al. 2008). The difference in chemistry associated with CO_2 manipulation at relevant levels, by these two methods has been well described (Ridgwell et al. 2009). The relevance of these chemical changes on phytoplankton physiology has also been discussed. During this project I experimented with gas bubbling, buffers and dilution from a pre-equilibrated reservoir of media as methods of creating future CO_2 conditions. I will briefly discuss my observations.

Batch culture has been widely used in CO_2 manipulation experiments, particularly in mesocosms, where it may be the only feasible approach. The drawback of this technique is that CO_2 is depleted at a high rate, often in excess of any additional CO_2 supplied during the experiment. Even in the relatively dilute mesocosm experiments, pCO_2 was rapidly reduced to present day concentrations. These experiments simulate bloom conditions in a future world.

Organic buffers are not recommended in future ocean simulations, because they cause large deviations from the natural system, and complicate calculation of the carbonate system parameters from total alkalinity (Rost et al. 2008). I, and others, have found that buffers can severely affect phytoplankton growth (Blanchemain et al. 1994).

Although I did not use acid/base manipulation in this project, a brief discussion of the effect of this method compared to gas bubbling is necessary in order to evaluate the literature. The addition of HCl and NaOH is an easy way to manipulate the carbonate system but does not reflect the natural seawater chemistry as accurately as gas bubbling (Rost et al. 2008). However, it is argued that the differences in the carbonate parameters between acid/base and bubbling are not critical (Hurd et al. 2009; Ridgwell et al. 2009). Using gas bubbling compared to acid/base manipulation, results in ~17% higher CO_2 at pH 7.75. Theoretically this could affect phytoplankton relying on diffusive CO_2 uptake or result in down-regulation of CCMs (Hurd et al. 2009). HCO_3^- is ~20% higher when bubbling rather than acid/base is used at pH 7.5 (Hurd et al. 2009). This will make little difference to phytoplankton using HCO_3^- for photosynthesis, because HCO_3^- is already saturating (Hurd et al. 2009). The saturation state of calcite, Ω_{cal} is similar for both methods of manipulation but the increase in HCO_3^- may have some effect on calcification. There is no evidence in the literature of a

correlation between the type of manipulation used and the direction of the calcification response (Hurd et al. 2009; Ridgwell et al. 2009). The addition of $NaHCO_3$ and HCl has been proposed as an alternative method of increasing pCO_2 (Rost et al. 2008; Hurd et al. 2009). This would supply extra HCO_3^- ions, and exactly neutralise the alkalinity decrease caused by the HCl. The method has not been widely adopted to date.

Gas bubbling has been found to adversely affect the calcifying strain of *E.huxleyi* PLY M219 (Shi et al. 2009). In experiments where acid/base was used to manipulate pCO_2 to 760 ppm, these investigators found that there was a slight increase in growth rate, whereas when cultures were gently bubbled with 760 ppm CO_2 in air, there was no difference in growth rate. The control cultures showed no difference in growth rate whether bubbled with air or not. One observation on the use of gas bubbling to maintain pCO_2 is that this must be accurately and continuously monitored. It cannot be assumed that pCO_2 will be maintained because the rate of CO_2 removal by phytoplankton can be greater than the dissolution of CO_2. Over the course of a 5 day experiment (Shi et al. 2009), DIC, Ω, pH and alkalinity all decreased in both bubbled cultures and acid/base cultures. The carbonate chemistry was not identical in the two treatments. Therefore it is not possible to discern whether the physical effects of bubbling or differences in chemistry caused the observed differences in growth rate. Different phytoplankton species have been found to be differentially sensitive to bubbling (Thomas and Gibson 1990 in Hurd et al. 2009). Green algae were less sensitive than cyanobacteria, then diatoms, and dinoflagellates were most sensitive. However, I saw no evidence of this in my experiments with natural communities. I found that *T. pseudonana* and *E. huxleyi* grew well despite being gently bubbled with gas. Diffusers were used to create small bubbles and a slow bubbling rate was used, this method was employed in all my experiments regardless of other manipulations.

Dilution from reservoirs of pre-equilibrated media in both semi continuous and continuous cultures was a successful method of controlling the pH rise, and thus pCO_2. I found that the use of dilute cultures was necessary to prevent pH from rising; this has also been recommended by others (Rost et al. 2008).

For future experiments it may be possible to maintain pCO_2 with an overlying headspace and gentle mixing rather than bubbling, combined with dilution with pre-equilibrated media, especially if using slower growing species. This system could be used with natural communities on a larger scale and species dominance could be more accurately evaluated. It would also be preferable to gradually increase pCO_2 over a period of time in order to more accurately simulate the future rise in pCO_2 and control for any shock response. An increase of pCO_2 in the headspace, and dilution with pre-equilibrated media so that a rise from present day pCO_2 to 760 ppm would occur over the course of weeks to months rather than days. There is a balance to be struck between ideal conditions and maintaining pH with a growing phytoplankton community.

6.1.2 Growth (μ), blooms and competitive fitness

"growth rate is a primary determinant of community trophic dynamics and ecosystem productivity"

Flynn 2009

In my laboratory experiments I generally found that an increase in pCO_2 from present day concentrations to 760 ppm did not affect cell division rate of *T. pseudonana* CCMP1335 or *E. huxleyi* strains CCMP1516 and CCMP371. However, in my early experiments using batch culture I did find a significant enhancement of μ in *T. pseudonana*. This was accompanied by a slight (but un-quantified) difference in phytoplankton colour between the treatments. This would suggest that in batch cultures

of this diatom, with changes in seawater chemistry being more similar to those that occur in a bloom than steady state conditions, μ may be increased with pCO_2. Blooms are of major importance for carbon drawdown (Westbroek et al. 1993) although, as they depend upon up-welled nutrients, where the warming of the water tends to cause CO_2 release this may offset any added carbon drawn down by actively growing phytoplankton. In batch cultures and blooms diatoms may become carbon limited (Riebesell et al. 1993), however, it is probable that many diatoms are capable of active HCO_3^- uptake (Giordano et al. 2005). An increase in available CO_2 under these circumstances, may reduce the amount of active transport necessary, to provide adequate CO_2 to RuBisCO. This energy saving may result in increased growth rates (Raven et al. 2000).

Cell division rate has been seen to increase in response to increased pCO_2 in the diatoms *Skeletonema costatum* (Kim et al. 2006) and *Chaetoceros muelleri* (Beardall and Raven 2004; Tortell et al. 2008a). However no differences were seen in *Thalassiosira pseudonana* (Pruder and Bolton 1979) or *T. weissflogii* (Shi et al. 2009). The reason for this difference may be that *S. costatum* and *C. muelleri* are chain forming diatoms, and both were in direct competition with smaller single celled diatoms of *Nitzschia spp.* (Kim et al. 2006) and *Pseudonitzschia subcurvata* (Tortell et al. 2008a). In a natural situation where resources are limiting, a species with the ability to increase cell division rate will have a competitive advantage over other species. Species shifts between genera have also been reported, and Tortell et al. (2002) found a shift from *Phaeocystis* to diatoms at increased CO_2. This may impact on higher trophic levels and affect biogeochemical cycles through the biological pump. *Phaeocystis* species are less easily ingested than diatoms, due to their mucus layer and aggregation into large colonies (Beardall and Raven 2004). However *Phaeocystis* species are reported to be more

efficiently recycled than diatoms resulting in less carbon drawdown (Smetacek 1999). Diatom species also differ in their contribution to the biological pump (Smetacek 1999).

What does give one species an advantage over another? It is observed that larger species tend to benefit from increased CO_2, which may be due to their reduced surface area to volume quotient, which would give an advantage to smaller cells at lower pCO_2 (Tortell et al. 2008b). Hypothetically those species with the ability of suppress CCMs or those relying on diffusive entry of CO_2 may benefit from increased CO_2. Species with less specific RuBisCO with higher maximum rates of carboxylation should benefit most and those with more specific RuBisCO with lower maximum carboxylation rates should benefit least (see introduction section 1.4.4). However, in natural assemblages diatoms appear to be most able to benefit from increased pCO_2. They have suppressible CCMs (Fielding et al. 1998) but highly selective RuBisCO (Raven et al. 2000) and should not stand to benefit more than most other groups of phytoplankton, according to this hypothesis. These strands of evidence suggest that size may be more influential than RuBisCO kinetics.

It has been reported in a number of recent studies that phytoplankton may release greater concentrations of dissolved organic carbon (DOC) at higher pCO_2 (Engel et al. 2004a; Riebesell 2007). An estimate pertaining to this DOC can be calculated by subtracting measured particulate organic carbon from carbon drawdown attributed to primary production. DOC may be of great significance in carbon drawdown, particularly during diatom blooms (Passow et al. 1994). The formation of large aggregates, of which diatom cells make up <13% of the total carbon, the rest being DOC, results in export of large quantities of carbon during blooms (Passow et al. 1994). The reasons for DOC production are unclear but healthy phytoplankton and bacterial cells produce large quantities. It is suggested that it may aid aggregation of cells,

bacterial, or coccolith attachment or simply be an overflow mechanism (Passow et al. 1994; Engel et al. 2004a). *E. huxleyi* has been found to release DOC (Nanninga et al.; Engel et al. 2004a). In the 2005 mesocosms (Engel et al. 2004a), a 37% increase in calculated DOC release was seen in mesocosms at 760 ppm CO_2 compared to present day treatments. In our mesocosms a more modest 15% increase was found. Although the mean calculated DOC was higher in our high CO_2 mesocosms there was variability between mesocosms. Calculated DOC loss did not correlate with increased cell number, as would be expected if *E. huxleyi* cells were releasing excess carbon as DOC. It also did not correlate with reduced cell numbers which would suggest viral lysis was responsible for increased DOC.

Blooms are generally terminated by nitrate exhaustion followed by mass aggregation and sinking out (Smetacek 1999) or viral lysis (Bratbak et al. 1993). If there are no shifts in species dominance or changes in exuded DOC then can increases in growth rate affect carbon drawdown? It has been suggested that they can (Riebesell et al. 1993). As the rate of build-up of algal biomass per unit area is a function of both algal growth rate and loss, predominantly due to grazing, the biomass build-up during the bloom is directly proportional to the growth rate (Riebesell et al. 1993). Because the rate of particle sinking is a function of biomass, increased growth rates may affect vertical fluxes and increase remineralisation depth (Riebesell et al. 1993). Thus a greater proportion of the available nutrients will sink out of the surface waters. Ultimately this may have no effect on carbon drawdown because the nutrients will then be less available for those phytoplankton species that usually follow the bloom.

E. huxleyi has probably been the most well studied species in its response to increased CO_2. Unfortunately the results are bewilderingly diverse. One suggested cause for this

is that differences may be strain specific (Langer et al. 2006; Ridgwell et al. 2009). In my laboratory experiments I examined the effects of increased CO_2 on *E. huxleyi* strain CCMP371. A very similar experiment using this strain was performed by Feng et al. (2008). Both studies manipulated pCO_2 by gas bubbling of semi-continuous cultures with either present day or 750-760 ppm CO_2. Feng et al. (2008) used two light conditions, low, 50 and high, 400 µmol photons m^{-2} s^{-1}; and two temperatures, 20°C and 24°C. The light conditions in my experiment were 25 µmol m^{-2} s^{-1}, and temperature 24°C. Therefore a direct comparison between the low light, high temperature results for both CO_2 treatments may be made. Feng et al. (2008) saw a significant increase in µ from ~0.6 to ~0.7 (d^{-1}) with increased CO_2 under low light, high temperature conditions. The specific growth rates in my study were much higher, 0.96 ± 0.11 (d^{-1}) in the high CO_2 treatments, and 0.97 ± 0.04 (d^{-1}) in the present day CO_2 controls and not significantly different (F=0.05, p=0.82). One reason for this may be that my cultures had been grown at 24°C for at least a month. The experimental cultures of Feng et al. (2008) were analysed after 7 generations at higher temperature, the result could reflect short term increases in metabolic rate, which may decrease with time. Feng et al. (2008) saw increased Fv/Fm at increased temperature under low light conditions, and this was further increased in the greenhouse treatment to 0.66. Conversely, I found slightly higher Fv/Fm values in the present day cultures, 0.7 ± 0.008, and 0.69 ± 0.007 in the high CO_2 treatment, this was significant at the <10% level (F=3.25, p=0.08). The reasons for these differences cannot be due to strain or differences in carbonate system manipulation but may be due to differences in other experimental conditions. The very low light regime in my experiment may have had some effect, although the high growth rates suggest that light was not limiting. Theoretically low light would be limiting. If light was limiting, this would reduce the energy available for carbon uptake and fixation. Thus increased CO_2 would be more likely to have a beneficial effect as cells

could theoretically reduce CCM capacity and depend more upon diffusive CO_2 uptake. This theory is supported by the fact that the low light treatments showed much larger effects of increased CO_2 and/or temperature on photosynthetic parameters (Feng et al. 2008). The chl-a normalised rate of carbon fixation (P^B_{max}) at low light and high temperature was increased from ~2.5 to ~3.5 mg C (mg chl-a)$^{-1}$ h^{-1} by increased pCO_2 (Feng et al. 2008). The results of my laboratory experiments are in accordance with other previous research suggesting that growth is not carbon limited in *E. huxleyi* (Paasche 1996; Buitenhuis et al. 1999; Clark and Flynn 2000; Riebesell et al. 2000a; Feng et al. 2008). The responses of species, and even strains, to increased CO_2 appear to be individual and it may be difficult to predict or generalise responses based on their taxonomy or properties such as RuBisCO kinetics. This reduces the ability to accurately model future phytoplankton community dynamics.

6.2 ACCLIMATION AND ADAPTATION

6.2.1 Growth and physiological measurements

The aim of this project was to examine the long term effects of increased CO_2 on the marine phytoplankton; however, this was not an easy task. The final experiment ran for 3 months and probably ~100 generations. Collins and Bell (2004) suggest that genetic changes may occur within several hundred generations, however it is likely that any differences seen within 100 generations would be due to acclimation rather than adaptation. In *Chlamydomonas reinhardtii* grown at increased CO_2 for 1,000 generations Collins and Bell (2004) found no evidence of adaptation to increased CO_2 but neutral mutations may have caused the observed reduction in the capacity of cells grown at high CO_2 to function at present day pCO_2 (Collins and Bell 2004).

In my experiment there was little significant effect of long term increases in CO_2 on *T. pseudonana*. Cultures did not grow faster neither did the C:N ratio, red fluorescence

cell^{-1}, size or Fv/Fm alter. On returning to ambient CO_2 after this treatment cultures did not fare worse than if they remained at high CO_2 or were never grown at high CO_2. Therefore no acclimation response was seen. If cells had adapted this would have been seen as an advantage at high CO_2, to cells grown at high CO_2 for many generations, this was not seen. To determine whether the dominance of *T. pseudonana* would be affected it is necessary to determine the responses of many other species.

Others have found responses in various measurements such as pigment content (Collins and Bell 2004; Fu et al. 2007), C:N (Feng et al. 2008), Fv/Fm (Fu et al. 2007), size (Collins and Bell 2004; Fu et al. 2007; Iglesias-Rodriguez et al. 2008b) which have related to increased growth at high CO_2. The overall picture seems to hint that certain species, eg. *Synechococcus* and *Chlamydomonas reinhardtii* are capable of increasing their pigment concentrations. This may lead to more available energy for carbon fixation, if light levels are low, or may divert resources away from machinery more relevant to growth, eg. RuBisCO and ribosomes, if light is saturating. The trend towards increased size appears to occur when cell division remains constant or is reduced and may be due to additional carbon fixed. The only obvious differences in my experiments were that all the above measurements varied greatly over a cell cycle and were affected by growth rate.

6.2.2 Gene expression

The analysis of gene transcription to examine microbial physiology is a relatively new field. As gene transcription does not necessarily equate to increases in proteins one must be cautious when drawing conclusions from the analyses but molecular techniques have provided opportunities for greater understanding of microbial physiology. In higher C_3 plants, it is currently believed that, in response to a build up of leaf

carbohydrate at increased CO_2, the RuBisCO small sub unit gene (*rbcs*) is downregulated resulting in less RuBisCO protein causing a reduction in photosynthetic capacity (Moore et al. 1999). I found no consistent effect of increased CO_2 on *rbcs* transcription in *T. pseudonana*. This is consistent with other recent work (Roberts et al. 2007; Granum et al. 2009) which found no effect of decreased CO_2 of 100 ppm on the RuBisCO large subunit (*rbcL*) compared to present day concentrations. Carbonic anhydrases are a family of enzymes with many cellular functions. In phytoplankton they often play a key role in carbon acquisition, within the carbon concentrating mechanisms (CCMs). Reduced carbonic anhydrase production has been suggested as a method by which phytoplankton may save energy and cellular resources with increased CO_2 availability (Raven and Johnston 1991). In my experiments I found no evidence of consistent downregulation of any of the 4 carbonic anhydrases examined at CO_2 concentrations of 760 ppm compared to present day concentrations. This agrees with the results of McGinn and Morel (2007) who found that gene transcripts and proteins were not up-regulated until pH reached 8.8. This suggests that *T. pseudonana* relies on CCM activity at the very low pCO_2 present in blooms and not during steady state growth. This is consistent with the fact that the RuBisCO found in diatoms is more specific for CO_2 compared to O_2 than that of most other phytoplankton groups examined, thus there is less need for them to concentrate CO_2 at the RuBisCO active site. If this is the case, then *T. pseudonana*, and other diatoms using CCMs only during blooms, will not benefit greatly from increased CO_2 at the concentrations expected during this century. In my batch cultures of *T. pseudonana* no increase in cell number was seen once cultures had reached pH 8.8 which coincided with the beginning of the stationary phase.

My laboratory experiments proved that there was little effect of increased CO_2 on *T. pseudonana*, when in mono-culture. This is valuable information, but the effort and cost of examining its genetic apparatus for effects on gene transcription may have been better targeted at understanding an observed difference in response. The use of mono-culture experiments is most profitable when a difference between treatments has already been established. Experiments may then be designed which examine the physiological mechanisms and test specific hypotheses without the complications of extraneous variables.

6.3 MESOCOSM COMMUNITY PRODUCTIVITY AND STRUCTURE

In our mesocosm experiment we saw a 27% reduction in marine primary production at increased pCO_2. In an examination of the literature, this result appears to be quite unique. Of twelve experiments examining *E. huxleyi* mono-cultures or mesocosms dominated by *E. huxleyi*, POC production increased in nine, remained unchanged in three and decreased only in a nitrate limited study (Sciandra et al. 2003) (**Table 6.1**). No major shifts in species dominance were seen in our mesocosms. However phytoplankton groups were differentially sensitive to increased CO_2, which resulted in a change in community structure. Large picoeukaryotes and *Synechococcus* were most reduced with mean abundances in the high CO_2 treatment being 36% and 26% of abundance in the present day treatment, respectively. Coccolithophore abundance in the high CO_2 mesocosms was 55% that of the present day mesocosms. Cryptophytes were also reduced by approximately half but the response was more variable. Nanoflagellates and small picoeukaryotes were also reduced but less dramatically than the other groups. There was an extended growing period in the present day mesocosms, with maximum abundances of most phytoplankton types a day later than in the high CO_2 mesocosms.

	Species and strain	manipulation	pCO_2 (ppm)	Response at increased CO_2 compared to ambient					
				μ	POC	PIC	PIC:POC	C:N	Cell Vol.
1	*E. huxleyi* non-calcifying PML 92A	Nutrient limited chemostats	360, 2000	↑	High light N limited 46% ↑			High Light ↑	
2	*E. huxleyi*	mesocosms	190, 410, 710	↓	↔ but, 24% ↓ Δ[POC]:Δ[DIC]*	40% ↓ NCC	Slight ↑	↑exuded	↓
3	*E. huxleyi* CAWP06	batch	280, 300, 490, 750	↓	100% ↑	100% ↑	↔	8.3 (750 ppm) 6.8 (280 ppm)	↑
4	*E. huxleyi* PLY M219	Gas bubbled Acid/base	380, 750	↑	↑	↑			
5	*E. huxleyi* Ch 24-90	Acid/base		↔	↑	↔	↓	↔	
6	*E. huxleyi* CCMP371	Semi-cont	375, 750	↔	↔	High light 40-50%↓		C:P,C:N high light ↑	
7	*E. huxleyi* PML B92/11	Acid/base	180-750	↔	10% ↑	10% ↓		C:N ↑	
7	N Pacific *E. huxleyi*	Acid/base	250-800		↔	36-83% ↓			
8	*E. huxleyi* PML B92/11	Acid/base	280-800	↔	20% ↑	25% ↓			
9	*Gephyrocapsa oceanica*	Acid/base			18.6% ↑	44.7% ↓	52.5% ↓		
10	*E. huxleyi* PML B92/11	Acid/base	150-850	↔	Up to 50% ↑	↔			
11	*E. huxleyi* TW1	N limited	400,700	↔	15% ↓	10-25% ↓			↓

Table 6.1 Summary of effects of increased CO_2 on *E. huxleyi*. Where an increase or decrease is found between treatments this is reported as ↑ or ↓ and relates to an increase or decrease at high CO_2 compared to present day. If there is no difference they are reported as ↔. References in column 1: 1 (Leonardos and Geider 2005), 2 (Engel et al. 2005) (Delille et al. 2005), 3(Iglesias-Rodriguez et al. 2008b), 4 (Iglesias-Rodriguez et al. 2008b; Shi et al. 2009), 5 (Buitenhuis et al. 1999), 6 (Feng et al. 2008), 7 (Riebesell et al. 2000a), 8 (Zondervan et al. 2001), 9 (Schneider 2004; Hurd et al. 2009) 10 (Zondervan et al. 2002) 11 (Sciandra et al. 2003)

There is no previous evidence for a reduction in *Synechococcus* at increased CO_2. In the Northeastern Atlantic community deck incubation, aboard the STS Lord Nelson in this study no changes were seen in response to increased CO_2. Engel (2005) saw no change in the growth rates or maximum numbers of *Synechococcus* at increased CO_2. There are many differences between the deck incubation and Bergen communities; nutrient supply, competition and strain differences are likely as two distinct groups were found in the deck incubation. It is more difficult to explain the differences between our results and those seen in the previous mesocosm (Engel et al. 2005). It is possible that, as described earlier, smaller cells have the advantage at lower CO_2 due to their greater surface area to volume quotient.

A molecular analysis of the community was performed to examine the strains of *E. huxleyi* present and to determine whether any shifts in dominance of strains had occurred. No major differences were found and the strains present appeared to be those found in previous mesocosms in 2000, and 2003 at this location (Martinez et al. 2007).

Calcification was not directly assessed during this study, but calcification may be calculated as half the change in alkalinity plus the change in nitrate concentration (section 4.3.1e). Despite the fact that the mean change in total alkalinity in the high CO_2 mesocosms was only a third that of the present day, when normalised to cell number, no significant difference was found. *E. huxleyi* cells were examined for malformation and changes in size. The results showed no significant differences in these parameters. The wide range of effects of pCO_2 on *E. huxleyi* has already been described and is shown in **Table 6.1**.

This distinction between mesocosm and mono-culture responses to increased pCO_2 was also noted by Ridgwell et al. (2009). They observe that general increases in carbon fixation by photosynthesis occur in mono-cultures whilst decreases are found in mesocosms and ship-board incubations. This suggests that in a future world there may be a reduction in phytoplankton numbers leading to reduced primary production. However, there are several reasons why this response may have been seen. Firstly, there may have been a shock response or some exacerbation of the mechanical effects of bubbling by the reduced pH. In the long term it is unlikely that there would be a reduction in phytoplankton numbers of all types. We expected to see a shift in dominance between phytoplankton types or *E. huxleyi* morphotypes but this did not occur. Refering back to the questions I posed in the introduction, my research provides strong evidence to support or reject these hypotheses, which I will discuss here.

6.4 DISCUSSION OF HYPOTHESES

6.4.i.Does specific growth rate increase if more carbon is available?

I found no evidence of increased or decreased growth rates of *T. pseudonana* or *E. huxleyi* when grown in steady state continuous, or semi-continuous, cultures bubbled with air enhanced with 760 ppm CO_2. This agrees with recent research indicating a decrease in μ of *E. huxleyi* only at a pCO_2 concentration of <1000 μatm (Müller et al. 2010). When in batch culture, where nutrient, including carbon, limitation may be experienced there was some evidence of increased growth rates of *T. pseudonana* but not of *E. huxleyi* at 760 ppm CO_2. In the mesocosm experiment reduced growth rates of most phytoplankton types were seen in reponse to increased CO_2 whilst in the deck incubation experiment there were no significant effects on growth rate of cyanobacteria or pico-eukaryotes. There is no evidence to accept the hypothesis, for phytoplankton growing in steady state, or in natural communities.

6.4.ii.Does the C:N ratio increase with more CO_2 available?

In laboratory cultures C:N was significantly lower in the future CO_2 cultures than in the present day treatment. This result does not support the recent suggestion (Riebesell, 2007) that increased CO_2 may increase productivity in the absence of increased nutrients. However, most of the evidence supporting this theory is based on mesocosms, reaching nutrient limited conditions, and nutrient limited cultures. My results therefore show that in steady state there is no increase in the C:N ratio however in blooms there may be an increase in the C:N ratio when cells become nutrient limited. In the mesocosm experiment in Bergen in 2006, included in this thesis, there was no significant change in C:N during exponential growth, however the post bloom period was not analysed.

6.4.iii.Does RuBisCO or carbonic anhydrase expression decrease with more CO_2?

There appears to be some effect of increased CO_2 on transcription of both the RuBisCO small subunit (*rbcs*) and three of the four carbonic anhydrases, with CA4 being most sensitive. In the long term continuous cultures CA4 was up-regulated with enhanced pCO_2 and no other genes were affected. In the second phase of the experiment pH was not controlled and the results are less easy to interpret as pCO_2 altered over the course of the experiment. CA2 and CA4 were less variable in their expression than CA1 and CA3. CA3 was more highly expressed than the other carbonic anhydrases which showed similar expression levels. There is no reason to believe that these results are not accurate as rigorous optimization was performed, therefore it is likely that CA4 is up-regulated by increased pCO_2. A possible explanation for this could be that it converts CO_2 to bicarbonate within the cytoplasm thus preventing leakage of CO_2 from the cell. Diatoms are thought to be capable of active uptake of both bicarbonate and CO_2 (Tortell et al. 1997) and could favour CO_2 if more is available (Laws et al. 1998), thus requiring

enhanced expression of this gene. If may be possible to localize the enzyme by an examination of the genetic sequence for signal peptides allowing access to cellular compartments. The hypothesis behind this question was that both carbonic anhydrase and *rbcs* may be down regulated with more CO_2 available, potentially saving resources, I found no evidence to accept this hypothesis.

6.4.iv.Do phytoplankton adapt to increased pCO_2?

By returning cells which had been grown at increased pCO_2 for 3 months to lower (present day) pCO_2 conditions it can be seen whether any genetic adaptation to the higher CO_2 conditions has occurred (Collins, 2010). The hypothesis is that mutations may have occurred during the 100 generations at increased pCO_2 which have not been selected against. When these cells are then returned to lower pCO_2 conditions the genetic changes may prove to be disadvantageous and these cells may have reduced competitive ability. I saw no significant reduction in growth rate or other evidence of reduced fitness in these cells. CA4 was increased in these cultures over those cells maintained in high CO_2 conditions, this is consistent with the results from the continuous cultures as described above. Although it is likely that phytoplankton will adapt to increasing pCO_2 over longer time periods I saw no evidence of this during my experiment.

6.4.v.Does primary production increase with increased pCO_2?

Rather than an increase in primary production as anticipated, a large decrease was seen in the Bergen mesocosm experiment. This suggests that the community response may be far more important than the response of individual phytoplankton species. This will be discussed in the section on further research. I saw no evidence to support this hypothesis.

6.4.vi.Is calcification reduced at lower pH?

Coccolithophore abundance was reduced at increased pCO_2 and the decrease in total alkalinity caused by calcification was also reduced, this suggests that total calcification was reduced at increased CO_2. I saw no evidence of deformed cells or reduced calcification of individual coccolithophores, however I did not directly measure PIC or calcite per cell so my results are not directly comparable with others. The evidence above suggests that total calcification may be reduced at increased pCO_2. There is much support for this hypothesis in the literature (eg. Engel et al. 2005; Feng et al. 2008; Zondervan et al. 2002), however there are grounds for debate (Iglesias-Rodriguez et al., 2008b; Shi et al. 2009).

6.4.vii.Is the community structure altered by increased CO_2?

In the Bergen mesocosms we saw altered community structure with elevated pCO_2. The major effect was a reduction in all phytoplankton types, however small picoeukaryotes appeared less sensitive than many other phytoplankton groups and peaked in abundance earlier. Diatoms did not rise to dominance as may have been expected. The shift in community structure has several implications; firstly, picoeukaryotes are likely to be recycled in the surface waters rather than contribute to the biological pump whilst reduced numbers of coccolithophores, which are heavier and sink more easily, would reduce the efficiency of the biological pump. Secondly, CO_2 is produced during calcification and reduced coccolithophore abundance would reduce net CO_2 production from calcification. Thirdly higher trophic levels are impacted by changes in community structure at the phytoplankton level (Rose et al. 2009). I found evidence supporting this hypothesis, in accordance with previous research (Tortell et al. 2002, 2008b) but contrasting with previous mesocosm experiments in Bergen (Schneider 2004, Riebesell et al. 2007). Shifts in community structure may be of great

importance and have been highlighted as an area for increased research effort by several international programmes (BIOACID, UK OA, EPOCA).

6.4.viii. Do the RuBisCO selectivity and CCMs have any bearing on the dominance of different groups of phytoplankton?

The hypothesis is that diatoms with more selective RuBisCO are less reliant on CCMs than those phytoplankton with less specific RuBisCO, such as cyanobacteria. As the abundance of CO_2 increases, groups more reliant on CCMs may benefit more due to reduced resource allocation to CCMs. There was no evidence in the Bergen mesocosm or N.E Atlantic deck incubation assemblages to support this hypothesis. Carbonic anhydrase is often involved in CCMs and theoretically down –regulation of CCMs and CAs may occur simultaneously. The lack of reduced CA transcription in the laboratory cultures is consistent with the lack of evidence for this hypothesis, although this is not direct evidence as *T. pseudonana* was not identified within the mesocosms.

6.5 FUTURE WORK

6.5.1 Modelling

Modelling is necessary to quantitatively predict changes which may occur in the future (Rost et al. 2008; Joint et al. 2010). Modellers are keen to have data on biological processes to incorporate into models, and several models are running with biological parameters (Ridgwell et al. 2009). These are based on sparse data from a few papers and they generate predictions on a grand scale. Key processes or phytoplankton types may be missed from these data and it is difficult to fill the gaps with any degree of certainty due to the vastness of the marine microbial population. How can we most effectively provide the necessary information? This question has been discussed by the leading scientists in the field of ocean acidification, forming the objectives of a number of

national and internationally funded programmes: The European programmes, MEECE and EPOCA; the German BIOACID, the UK OA programme, and the international SOLAS/IMBER project. First, it is necessary that we understand the processes underlying the changes seen in natural, and mesocosm community experiments. Changes in community structure, energy transfer to higher trophic levels and interactions within the microbial community are key processes that we strive to model (BIOACID theme 4, UKOA, EPOCA). Mono-cultures may be necessary for process understanding but phytoplankton that has been in culture for many decades may have adapted to the unnatural conditions. Molecular tools may allow us to identify changes within mesocosms and natural communities which underlie the observed species shifts. Secondly, although cost and difficulty may make this impossible, greater numbers of replicates should be included in mesocosm, and laboratory studies (Havenhand et al. 2010). This would greatly increase our ability to determine whether effects are consistent. In our mesocosm experiment, coccolithophores were as abundant in one high CO_2 mesocosm, as in the present day mesocosms. Although mean numbers were decreased and statistically a change was found, a greater number of replicates would increase our confidence in the results. From a practical point of view, these replicates could be smaller in volume, than those currently used. Thirdly, although mesocosms appear to give the most realistic approach, they are batch cultures, and as such simulate bloom conditions. It would be preferable to allow greater periods of time for equilibration to increased CO_2 but this increases the cost and difficulty of such an experiment (Riebesell et al. 2010). There are a few alternatives. Firstly, more, smaller, semi-continuous cultures with natural assemblages, diluted with pre-equilibrated filtered natural seawater, could be examined, such as thoe described by Feng et al. (2009). Secondly, natural variations in pCO_2 and their associated phytoplankton may be examined, this approach has been highly recommended by a team of experts (Joint et al.

2010; Barry et al. 2010b). However, the lack of control of variables may make this difficult to interpret.

Adaptation of phytoplankton is addressed by the international programmes for ocean acidification research, BIOACID theme 1, the UK OA programme and described in Joint et al. 2010, as it is a concept which is integral to modelling the responses of future microbial communities. Despite the difficulties involved in maintaining long term continuous cultures they are recommended in the majority of international projects on ocean acidification (Riebesell et al. 2010; BIOACID theme 1; EPOCA).

6.5.2 Temperature and light in a future world

The additive effects of increased temperature and changes in light climate have not been addressed by this study, however an increase in pCO_2 in the atmosphere will almost certainly lead to increased temperatures (IPCC, 2007). Studies of the combined effects of temperature and pCO_2 are highly recommended within the national and international OA programmes (BIOACID theme 1, MEECE, EPOCA). Over the coming century the ocean surface temperature is predicted to rise by 1.4-5.8°C depending on the regime and model used (IPCC 2007). This is expected to be most extreme in the highly productive polar regions. Temperature increases will increase metabolism (Finkel et al. 2010), decrease solubility of CO_2 in seawater (Beardall and Raven 2004) and increase ocean stratification, which will reduce nutrient supply to much of the ocean (Sarmiento et al. 2004). This has been seen in the northwestern Mediterranean Sea, where an 80% reduction in phytoplankton biomass over the past decades has been related to reduced vertical mixing and nutrient limitation (Goffart et al. 2002). At high latitudes a reduction in vertical mixing may increase the light available to phytoplankton which

currently spend much time entrained in water at depths where light is limiting to photosynthesis (Sarmiento et al. 2004).

Some excellent laboratory studies have been carried out using a factorial design with pCO_2, temperature and light (Fu et al. 2007; Feng et al. 2008). It appears that increased pCO_2 may cause additional carbon fixation above that seen when temperature is increased, although a longer study would be useful to determine whether acclimation to temperature reduces this effect. This group also performed a ship-board incubation with the natural late spring bloom, coccolithophore dominated, assemblage from the North Atlantic (Feng et al. 2009). Here they found that a rise in temperature from 12°C to 16°C increased community production and a rise in pCO_2 from 390-690 ppm did not have a significant additive effect on the POC production of this community. The community structure was altered by pCO_2 and temperature alone, and in concert (greenhouse treatment). Coccolithophores were favoured in the greenhouse treatment, diatoms by high pCO_2 alone and chrysophytes by high temperature alone. Despite a significant increase in abundance of coccolithophores there was a large decrease in PIC production and consequently the PIC:POC ratio. The shifts in the phytoplankton assemblage were identified as the likely cause of the observed shifts in the microzooplankton community, with size of phytoplankton and potential unpalatability of coccolithophores identified as drivers of change (Rose et al. 2009). Increasing temperature will increase the substrate-saturated reaction rate of RuBisCO and thus the growth rates of phytoplankton if growth is not limited by any other substrate (Beardall and Raven 2004). A rise in temperature is likely to increase metabolic activity in some species whilst pushing others beyond their temperature optima, thus affecting species composition (Beardall and Raven 2004). UV radiation has inhibiting and damaging effects on phytoplankton (Beardall and Raven 2004; Gao et al. 2009). Depletion of the

stratospheric ozone layer may increase UV radiation, as some phytoplankton possess UV screening compounds they may be relatively benefited by increased UV. One species which has high UV screening compounds in *Phaeocystis* (Beardall and Raven 2004) so future changes in UV, temperature and pCO_2 should ideally be examined before predictions of species dominance are made. The combined effects of UV and pCO_2 on *E. huxleyi* were investigated by Gao et al. (2009). They found that thinning of the coccolith layer associated with increased pCO_2 increased the inhibitory effects of UV on calcification and photosynthesis. Coccolithophores dominate in high light regions, probably due to the reflective nature of their liths (Zondervan et al. 2002), thus thinning may have severe consequences for these species. Light regime is also important because it provides the energy for carbon fixation and active carbon acquisition. If light energy is limiting very different responses may be seen (Hurd et al. 2009).

Nutrient concentrations may be altered by future climate change due to changes in wind deposition of dust into the ocean (Duce and Tindale 1991; Sunda 2010), upwelling events (Hughen et al. 1996) and ocean acidification which may affect nutrient speciation and bioavailability of nutrients (Shi et al. 2010). The chemical speciation of iron is sensitive to changes in pH and its bioavailability to coccolithophores and diatoms has been found to decline as pH decreases (Shi et al. 2010). Iron limitation may reduce total primary production and possible alter community structre, favouring smaller species with larger surface area to volume ratios. Although it may not be possible to examine the complete picture, an understanding of the effects of multiple variables will aid our ability to predict future changes.

There have been few studies of the effects of grazing at increased CO_2, however see Suffrian et al. (2008) and Rose et al. (2009) and there are some observations that this

may be of great importance. In Narragansett Bay a 4-5 fold decrease in chlorophyll has been seen in recent years, due to increased grazing pressure in response to increased temperatures. Similar observations have been recorded in Massachusetts Bay (Keller et al. 1999; Keller et al. 2001). The effects of grazing may far outweigh any benefit gained from increases in $CO_{2,}$ although additional growth of phytoplankton would provide more food for higher trophic levels and carbon would still be drawn down. Alterations in species composition of the phytoplankton could severely affect higher trophic levels, as has been seen in a ship-board incubation study (Rose et al. 2009). Reduced standing stocks of biomass would decrease the effectiveness of the biological pump. A further factor influencing the biological pump is the activity of heterotrophic bacteria which are responsible for the remineralisation of 75-95% of the organic matter produced by photosynthesis (Piontek et al. 2010). It has been found that bacterial degradation of polysaccharides increases as pH falls (Piontek et al. 2010) as does protein degradation, whilst protease (Grossart et al. 2006) and glucosidase activities rise (Grossart et al. 2006; Piontek et al. 2010). These enzymes are extracellular and in direct contact with the seawater, rather than in a pH controlled internal compartment. Changes in ionization states may affect physical structures of the substrates and this appears to increase the rate of reaction which would reduce the effectiveness of the biological pump.

In order to be able to compare results from different studies it is important that all variables are reported. For example, light climate may have great effects on the response of phytoplankton to increased CO_2 (Hurd et al. 2009). The recent publication, The Guide for best practices for ocean acidification research (Riebesell et al. 2010) thoroughly examines the experimental research to date and sets out guidelines for future research. This includes set, target pCO_2 concentrations, to allow experiments to be

easily compared, the reporting of all relevant variables, such as light, temperature, day length, strain and nutrient regime (Engel et al. 2010). At least two components of the carbonate system should be measured and reported to allow a full description of the carbonate system (Dickson 2010, LaRoche et al. 2010) and total alkalinity should not be used if nutrient levels are high (Engel et al. 2010). It is acknowledged in the guide that these measurements are not simple to perform and most require specialist equipment and trained personnel. It is suggested that samples may be better sent for analysis to specialist laboratories for quality assurance (Dickson 2010). Alternatively researchers should use certified standard materials and regularly test blind samples (Dickson 2010). Sufficient replication within experiments is necessary and researchers should beware of pseudo-replication, for example with mesocosms. The recommendations are that cultures should be run in triplicates and the entire experiment repeated with different batches of media (LaRoche et al. 2010). A further recommendation is that a wider range of pCO_2 is examined even at the expense of reduced replication, in order to characterise the functional relationship between carbonate system parameters and organism or ecosystem performance (Barry et al. 2010a). Within the experimental systems it is recommended that cultures are kept very dilute to avoid depletion of DIC, self shading and nutrient limitation, DIC uptake should be below 5% of the total DIC (LaRoche et al. 2010). Cultures should be acclimated to the experimental conditions for a minimum of 5 generations prior to the investigation (LaRoche et al. 2010). In chemostats cell density and effluent volume should be recorded daily (LaRoche et al. 2010).

The guidelines for mesocosm experiments are described by Riebesell et al. (2010b). They include that the enclosures should be filled simultaneously from a single reservoir, although this may be logistically very difficult, this would ensure similarity of starting

populations. The starting populations must be well described prior to experimental manipulation and spatial distribution of organisms and organic matter should be examined, and appropriate sampling strategies employed. Enclosures should be impermeable with a headspace at the appropriate pCO_2 and lid allowing penetration of the full spectrum of sunlight. The method and effectiveness of mixing must be described and should simulate natural conditions. Further recommendations are that as broad a range of measurements as possible is described during a mesocosm experiment and that appropriate laboratory experiments should be performed to complement and further our understanding of the underlying mechanisms in order to extrapolate from mesocosm studies.

Some notes for bottle experiments including deck incubations are that full acclimation is unlikely to occur in the short time scale of these experiments, and time for acclimation may also increase the confounding effects of containment (Engel et al. 2010). During containment grazing and growth of heterotrophic bacteria may affect results and these should be controlled for, for example a grazer-free control should be run (LaRoche et al. 2010).

6.6 CONCLUSIONS

The results of my experiments showed that increased CO_2 had little effect on the growth rates of the diatom, *Thalassiosira pseudonana* CCMP1335 or the coccolithophore *Emiliania huxleyi* strains 1516 and 371. Additionally *T. pseudonana* did not show any acclimation or adaptation to growth for ~100 generations at 760 ppm CO_2 in pH controlled continuous cultures. The technique of pCO_2 manipulation, gas bubbling and dilution from a reservoir of pre-equilibrated media was successful in controlling pH rise. In the mesocosm experiment we saw a large reduction in community productivity

and an associated change in community structure at 760 ppm CO_2. The dominant phytoplankton, *E. huxleyi* was reduced in number but cells were not malformed neither were there any major shifts in strain within the assemblage. In the Northeastern Atlantic assemblage I found no effect of increased CO_2 on the cyanobacteria and pico-eukaryotes. The investigations of the effects of increased CO_2 on the phytoplankton to date have yielded a very incoherent set of results. The reason for this may be differences between strains. If strains and even genetic lines (Collins and Bell 2004) have been found to differ in their response to increased CO_2 then our ability to predict responses may be very limited. Marine phytoplankton will doubtless adapt, if necessary, and thrive in a world with increased CO_2, however further research will be required before we can predict their response.

REFERENCES

Anderson, M., J & Robinson, J. 2001. Permutation tests for linear models. *Australia and New Zealand Journal of Statistics* 43:75-88.

Anderson, M. J. 2001. Permutation tests for univariate or multivariate analysis of variance and regression. *Canadian Journal of Fisheries and Aquatic Science* 58:626-39.

Anderson, M. J., Gorley, R.N., Clarke, K.R. 2008 Permanova + for primer: Guide to software and statistical methods. Primer-e, Plymouth, UK.

Antia, N. J., McAllistel, C. D., Parsons, T. R., Stephens, K. & Strickland, J. D. H. 1963. Further measurements of primary production using a large volume plastic sphere. *Limnology and Oceanography* 8:166-83.

Armbrust, E. V., Berges, J. A., Bowler, C., Green, B. R., Martinez, D., Putnam, N. H., Zhou, S., Allen, A. E., Apt, K. E., Bechner, M., Brzezinski, M. A., Chaal, B. K., Chiovitti, A., Davis, A. K., Demarest, M. S., Detter, J. C., Glavina, T., Goodstein, D., Hadi, M. Z., Hellsten, U., Hildebrand, M., Jenkins, B. D., Jurka, J., Kapitonov, V. V., Kroger, N., Lau, W. W. Y., Lane, T. W., Larimer, F. W., Lippmeier, J. C., Lucas, S., Medina, M., Montsant, A., Obornik, M., Parker, M. S., Palenik, B., Pazour, G. J., Richardson, P. M., Rynearson, T. A., Saito, M. A., Schwartz, D. C., Thamatrakoln, K., Valentin, K., Vardi, A., Wilkerson, F. P. & Rokhsar, D. S. 2004. The genome of the diatom *Thalassiosira pseudonana*: Ecology, evolution, and metabolism. *Science* 306:79-86.

Badger, M. R., John Andrews, T., Whitney, S. M., Ludwig, M., Yellowlees, D. C., Leggat, W. & Dean Price, G. 1998. The diversity and coevolution of RuBisCO, plastids, pyrenoids, and chloroplast-based CO_2-concentrating mechanisms in algae *Canadian Journal of Botany* 76:1052-71.

Badger, M. R., Price, G. D. 2003. CO_2 concentrating mechanisms in cyanobacteria: Molecular components, their diversity and evolution. *Journal of Experimental Botany* 54:609-22.

Barry, J.P., Tyrrell, T., Hansson, L., Plattner, G.K., and Gattuso, J.P. 2010a Atmospheric CO_2 targets for ocean acidification perturbation experiments *In* Riebesell U., Fabry V. J., Hansson L. & Gattuso J.-P. (Eds.), 2010. Guide to best practices for ocean acidification research and data reporting, 260 p. Luxembourg: Publications Office of the European Union. Chapter 3.

Barry, J. P., Hall-Spencer, J. M., and Tyrrell, T. 2010b *In situ* perturbation experiments: natural venting sites, spatial/temporal gradients in ocean pH, manipulative *in situ* p(CO_2) perturbations *In* Riebesell U., Fabry V. J., Hansson L. & Gattuso J.-P. (Eds.), 2010. Guide to best practices for ocean acidification research and data reporting, 260 p. Luxembourg: Publications Office of the European Union. Chapter 8.

Beardall, J. & Raven, J. A. 2004. The potential effects of global climate change on microalgal photosynthesis, growth and ecology *Phycologia* 43:26-40.

Benthien, A., Zondervan, I., Engel, A., Hefter, J., Terbrüggen, A. & Riebesell, U. 2007. Carbon isotopic fractionation during a mesocosm bloom experiment dominated by *Emiliania huxleyi*: Effects of CO_2 concentration and primary production. *Geochimica et Cosmochimica Acta* 71:1528-41.

Berges, J. A., Varela, D. E. & Harrison, P. J. 2002. Effects of temperature on growth rate, cell composition and nitrogen metabolism in the marine diatom *Thalassiosira pseudonana* (bacillariophyceae). *Marine Ecology Progress Series* 225:139-46.

Blanchemain, A., Grizeau, D. & Guary, J.-C. 1994. Effect of different organic buffers on the growth of *Skeletonema costatum* cultures; further evidence for an autoinhibitory effect *Journal of Plankton Research* 16:1433-40.

Bode, A., Barquero, S., Varela, M., Braun, J. G. & de Armas, D. 2001 Pelagic bacteria and phytoplankton in oceanic waters near the Canary Islands in summer. *Marine Ecology Progress Series* 209:1-17.

Bratbak, G., Egge, J. K. & Heldal, M. 1993. Viral mortality of the marine alga *Emiliania huxleyi* (haptophyceae) and termination of algal blooms *Marine Ecology Progress Series* 93:39-48

Brewer, P. G. & Riley, J. P. 1965. The automatic determination of nitrate in seawater. *Deep-Sea Research* 12:765-72.

Buitenhuis, E. T., de Baar, H. J. W. & Veldhuis, M. J. W. 1999. Photosynthesis and calcification by *Emiliania huxleyi* (prymnesiophyceae) as a function of inorganic carbon species. *Journal of Phycology* 35:949-59.

Burkhardt, S., Amoroso, G., Riebesell, U. & Sultemeyer, D. 2001. CO_2 and HCO_3^- uptake in marine diatoms acclimated to different CO_2 concentrations. *Limnology and Oceanography* 46:1378-91.

Burkhardt, S., Riebesell, U. & Zondervan, I. 1999a. Effects of growth rate, CO_2 concentration, and cell size on the stable carbon isotope fractionation in marine phytoplankton. *Geochimica et Cosmochimica Acta* 63:3729-41.

Burkhardt, S., Zondervan, I. & Riebesell, U. 1999b. Effect of CO_2 concentration on C:N:P ratio in marine phytoplankton: A species comparison. *Limnology and Oceanography* 44:683-90.

Burns, B. D. & Beardall, J. 1987. Utilisation of inorganic carbon by marine algae. *Journal of Experimental Marine Biology and Ecology* 107:65-86.

Castberg, T., Larsen, A., Sandaa, R. A., Brussaard, C. P. D., Egge, J. K., Heldal, M., Thyrhaug, R., van Hannen, E. J. & Bratbak, G. 2001. Microbial population dynamics and diversity during a bloom of the marine coccolithophorid *Emiliania huxleyi* (haptophyta). *Marine Ecology Progress Series* 221 39-46.

Chen, C. Y. & Durbin, E. G. 1994. Effects of pH on the growth and carbon uptake of marine phytoplankton. *Marine Ecology Progress Series* 109:83-94.

Chisholm, J. R. M. & Gattuso, J.-P. 1991. Validation of the alkalinity anomaly technique for investigating calcification and photosynthesis in coral reef communities. *Limnology and Oceanography* 36:1232-9.

Clark, D. R. & Flynn, K. J. 2000. The relationship between the dissolved inorganic carbon concentration and growth rate in marine phytoplankton. *Proceedings of the Royal Society of London B.* 267:953-9.

Clarke, K. R. & Gorley, R. N. 2001. Primer v5: User manual/tutorial. *PRIMER-E, Plymouth.*

Collins, S. & Bell, G. 2004. Phenotypic consequences of 1,000 generations of selection at elevated CO_2 in a green alga. *Nature* 431:566-9.

Collins, S. 2010 Comment on “Effects of long-term high CO_2 exposure on two species of coccolithophores” by Müller et al. 2010. *Biogeosciences Discuss.*, 7, 2673–2679

Crawford, D. W. & Purdie, D. A. 1997. Increase of pCO_2 during blooms of *Emiliania huxleyi*: Theoretical considerations on the asymmetry between acquisition of HCO_3^- and respiration of free CO_2. *Limnology and Oceanography* 42:365-72.

Delille, B., Harlay, J., Zondervan, I., Jacquet, S., Chou, L., Wollast, R., Bellerby, R. G. J., Frankignoulle, M., Borges, A. V., Riebesell, U. & Gattuso, J.-P. 2005. Response of primary production and calcification to changes of pCO_2 during

experimental blooms of the coccolithophorid *Emiliania huxleyi*. *Global Biogeochemical Cycles* 19:GB2023, doi:10.1029/2004GB002318.

Dickson, A. G. 2010 The carbon dioxide system in seawater: equilibrium chemistry and measurements *In* Riebesell U., Fabry V. J., Hansson L. & Gattuso J.-P. (Eds.), 2010. Guide to best practices for ocean acidification research and data reporting, 260 p. Luxembourg: Publications Office of the European Union. Chapter 1.

Doney, S. C., Fabry, V. J., Feely, R. A. & Kleypas, J. A. 2009. Ocean acidification the other CO_2 problem. *Annual Review of Marine Science* 1:169-92.

Duce, R. A. & Tindale, N. W. 1991. Atmospheric transport of iron and its deposition in the ocean *Limnology and Oceanography* 36:1715-26.

Egge, J. K. & Aksnes, D. L. 1992 Silicate as regulating nutrient in phytoplankton competition. *Marine Ecology Progress Series* 83:281-9.

Engel, A., Delille, B., Jacquet, S., Riebesell, U., Rochelle-Newall, E., Terbrüggen, A. & Zondervan, I. 2004a. Transparent exopolymer particles and dissolved organic carbon production by *Emiliania huxleyi* exposed to different CO_2 concentrations: A mesocosm experiment. *Aquatic microbial ecology* 34:93-104.

Engel, A., Goldthwait, S., Passow, U. & Alldredge, A. 2002 Temporal decoupling of carbon and nitrogen dynamics in a mesocosm diatom bloom. *Limnology and Oceanography* 47:753-61.

Engel, A., Thoms, S., Riebesell, U., Rochelle-Newall, E. & Zondervan, I. 2004b. Polysaccharide aggregation as a potential sink of marine dissolved organic carbon. *Nature* 428:929-32.

Engel, A., Zondervan, I., Aerts, K., Beaufort, L., Benthien, A., Chou, L., Delille, B., Gattuso, J.-P., Harlay, J., Heemann, C., Hoffmann, L., Jacquet, S., Nejstgaard, J., Pizay, M.-D., Rochelle-Newall, E., Schneider, U., Terbrueggen, A. &

Riebesell, U. 2005. Testing the direct effect of CO_2 concentration on a bloom of the coccolithophorid *Emiliania huxleyi* in mesocosm experiments. *Limnology and Oceanography* 50:493-507.

Engel, A., Barcelos e Ramos, J., Geider, R., Hutchins, D. A., Lee, C., Rost, B., Röttgers, R., and Thingstad, F. 2010 Production and export of organic matter *In* Riebesell U., Fabry V. J., Hansson L. & Gattuso J.-P. (Eds.), 2010. Guide to best practices for ocean acidification research and data reporting, 260 p. Luxembourg: Publications Office of the European Union. Chapter 11.

Falkowski, P. G., Katz, M. E., Knoll, A. H., Quigg, A., Raven, J. A., Schofielf, O. & Taylor, F. J. R. 2004. The evolution of modern eukaryotic phytoplankton. *Science* 305:354-60.

Falkowski, P. G. & Raven, J. A. 1997. *Aquatic photosynthesis*. Blackwell science, Malden, MA, USA.

Feng, Y., Warner, M. E., Zhang, Y., Sun, J., Fu, F.-X., Rose, J. M. & Hutchins, D. A. 2008. Interactive effects of increased pCO_2, temperature and irradiance on the marine coccolithophore *Emiliania huxleyi* (prymnesiophyceae). *European Journal of Phycology* 43:87 - 98.

Feng, Y. Y., Hare, C. E., Leblanc, K., Rose, J.M., Zhang, Y., DiTullio, G.R., Lee, P.A., Wilhelm, S.W., Rowe, J.M., Sun, J., Nemcek, N., Gueguen, C., Passow, U., Benner, I., Brown, C., Hutchins, D.A. 2009. Effects of increased pCO_2 and temperature on the North Atlantic spring bloom. I. The phytoplankton community and biogeochemical response. *Marine Ecology Progress Series* 388: 13-25.

Fernandéz, E., Marãnon, E., Harbour, D. S., Kristiansen, S. & Heimdal, B. R. 1996. Patterns of carbon and nitrogen uptake during blooms of *Emiliania huxleyi* in two Norwegian fjords. *Journal of plankton research* 18:2349-66.

Ferrari, V. C. & Hollibaugh, J. T. 1999. Distribution of microbial assemblages in the central Arctic Ocean basin studied by PCR/DGGE: Analysis of a large data set. *Hydrobiologia* 401:55-68.

Field, C. B., Behrenfeld, M. J., Randerson, J. T. & Falkowski, P. 1998. Primary production of the biosphere: Integrating terrestrial and oceanic components. *Science* 281:237-40.

Fielding, A. S., Turpin, D. H., Guy, R. D., Calvert, S. E., Crawford, D. W. & Harrison, P. J. 1998. Influence of the carbon concentrating mechanism on carbon stable isotope discrimination by the marine diatom *Thalassiosira pseudonana*. *Canadian Journal of Botany* 76:1098-103.

Findlay, H. S., Tyrrell, T. Bellerby R. G. J., Merico, A., and Skjelvan, I. 2008. Carbon and nutrient mixed layer dynamics in the Norwegian Sea *Biogeosciences* 5:1395-410.

Finkel, Z. V., Beardall, J., Flynn, K. J., Quigg, A., Rees, T. A. V., Raven, J. A. (2010). Phytoplankton in a changing world: cell size and elemental stoichiometry. *Journal of Plankton Research* 32: 119-137.

Flynn, K. J., Raven, J. A., Rees, T. A. V., Finkel, Z., Quigg, A. & Beardall, J. 2009. Is the growth rate hypothesis applicable to microalgae? *Journal of Phycology* 45:1-12.

Frankignoulle, M., Canon, C. & Gattuso, J. P. 1994 Marine calcification as a source of carbon dioxide: Positive feedback of increasing atmospheric CO_2. *Limnology and Oceanography* 39:458-62.

Fu, F.-X., Warner, M. E., Zhang, Y., Feng, Y. & Hutchins, D. A. 2007. Effects of increased temperature and CO_2 on photosynthesis, growth, and elemental ratios in marine *Synechococcus* and *Prochlorococcus* cyanobacteria. *Journal of Phycology* 43:485-96.

Gao, K. S., Z. X. Ruan, Villafañe, V. E., Gattuso, J.-P. and Helbing, E. W. 2009. Ocean acidification exacerbates the effect of UV radiation on the calcifying phytoplankter *Emiliania huxleyi*. *Limnology and Oceanography* 54(6): 1855-1862.

Gattuso, J.-P. & Lavigne, H. 2009. Technical note: Approaches and software tools to investigate the impact of ocean acidification. *Biogeosciences* 6: 2121-33.

Gattuso, J.-P., Pichon, M. & Frankingnoulle, M. 1995. Biological control of air-sea CO_2 fluxes: Effect of photosynthetic and calcifying marine organisms and ecosystems. *Marine Ecology Progress Series* 129:307-12.

Geider, R. J. & La Roche, J. 2002. Redfield revisited: Variability of C:N:P in marine microalgae and its biochemical basis. *European Journal of Phycology* 37:1

Gervais, F. & Riebesell, U. 2001. Effect of phosphorus limitation on elemental composition and stable carbon isotope fractionation in a marine diatom growing under different CO_2 concentrations. *Limnology and Oceanography* 46:497-501.

Giordano, M., Beardall, J. & Raven, J. A. 2005. CO_2 concentrating mechanisms in algae: Mechanisms, environmental modulation, and evolution. *Annual Review of Plant Biology* 56:99-131.

Goffart, A., Hecq, J.-H. & Legendre, L. 2002. Changes in the development of the winter-spring phytoplankton bloom in the Bay of Calvi (NW Mediterranean) over the last two decades: A response to changing climate? *Marine Ecology Progress Series* 236:45-60.

Granum, E., Roberts, K., Raven, J. A. & Leegood, R. C. 2009. Primary carbon and nitrogen metabolic gene expression in the diatom *Thalassiosira pseudonana* (bacillariophyceae): Diel periodicity and effects of inorganic carbon and nitrogen. *Journal of Phycology* 45:1083-92.

Grossart, H. P., Allgaier, M., Passow, U. and Riebesell, U. 2006. Testing the effect of CO_2 concentration on the dynamics of marine heterotrophic bacterioplankton. *Limnology and Oceanography* 51(1): 1-11.

Havenhand, J., Dupont, S., and Quinn, G. P. 2010 Designing ocean acidification experiments to maximise inference *In* Riebesell U., Fabry V. J., Hansson L. & Gattuso J.-P. (Eds.), 2010. Guide to best practices for ocean acidification research and data reporting, 260 p. Luxembourg: Publications Office of the European Union. Chapter 4.

Holm-Hansen, O., Lorenzen, C. J., Holmes, R. W. & Strickland, J. D. H. 1965. Fluorometric determination of chlorophyll. *Journal du Conseil Permanent International pour l'Exploration de la Mer* 30:3-15.

Hughen, K. A., Overpeck, J. T., Peterson, L. C. & Trumbore, S. 1996. Rapid climate changes in the tropical Atlantic region during the last deglaciation. *Nature* 380:51-4.

Hurd, C. L., Hepburn, C. D., Currie, K. I., Raven, J. A. & Hunter, K. A. 2009. Testing the effects of ocean acidification on algal metabolism: Considerations for experimental designs. *Journal of Phycology* 45:1236-51.

Iglesias-Rodriguez, M. D., Buitenhuis, E. T., Raven, J. A., Schofield, O., Poulton, A. J., Gibbs, S., Halloran, P. R. & de Baar, H. J. W. 2008a. Response to comment on "phytoplankton calcification in a high-CO_2world" *Science* 322:1466c.

Iglesias-Rodriguez, M. D., Halloran, P. R., Rickaby, R. E. M., Hall, I. R., Colmenero-Hidalgo, E., Gittins, J. R., Green, D. R. H., Tyrrell, T., Gibbs, S. J., von Dassow, P., Rehm, E., Armbrust, E. V. & Boessenkool, K. P. 2008b. Phytoplankton calcification in a high-CO_2 world. *Science* 320:336-40.

Iglesias-Rodríguez, M. D., Oscar, M. S., Batley, J., Medlin, L. K. & Hayes, P. K. 2006. Intraspecific genetic diversity in the marine coccolithophore *Emiliania huxleyi* (prymnesiophyceae): The use of microsatellite analysis in marine phytoplankton population studies. *Journal of Phycology* 42:526-36.

IPCC. 2007. Climate change 2007: The physical science basis. Contribution of working group 4 to the fourth assessment report of the intergovernmental panel on climate change. In Solomon, S., Qin, D., Manning, M., Chen, Z., Marquis, M., Averyt, K. B., Tignor, M., and & Miller, H. L. [Eds.]. Cambridge University Press, Cambridge, UK.

Jacquet, S., Heldal, M., Iglesias-Rodriguez, D., Larsen, A., Wilson, W. & Bratbak, G. 2002. Flow cytometric analysis of an *Emiliana huxleyi* bloom terminated by viral infection. *Aquatic Microbial Ecology* 27:111-24.

Jeffrey, S. W., Mantoura, R. F. C. & Wright, S. W. 1997. Phytoplankton pigments in oceanography. *UNESCO*.

Joint, I. R. & Pomroy, A. J. 1983. Production of picoplankton and small nanoplankton in the Celtic Sea. *Marine Biology* 77:19-27.

Joint I., Karl, D. M., Doney, S. C., Armbrust, E. V., Balch, W., Beman, M., Bowler, C., Church, M., Dickson, A., Heidelberg, J., Iglesias-Rodriguez, D., Kirchman, D., Kolber, Z., Letelier, R., Lupp, C., Maberly, S., Park, S., Raven, J.A., Repeta, D.J., Riebesell, U., Steward, G., Tortell, P., Zeebe, R. E., Zehr, J.P. 2009 Consequences of high CO_2 and ocean acidification for microbes in the global ocean

Keller, A. A., Oviatt, C. A., Walker, H. A. & Hawk, J. D. 1999. Predicted impacts of elevated temperature on the magnitude of the winter-spring phytoplankton bloom in temperate coastal waters: A mesocosm study. *Limnology and Oceanography* 44:244-356.

Keller, A. A., Taylor, C., Oviatt, C., Dorrington, T., Holcombe, G. & L., R. 2001. Phytoplankton production patterns in Massachusetts Bay and the absence of the 1998 winter-spring bloom *Marine Biology* 138:1051-62.

Khatiwala, S., Primeau, F. & Hall, T. 2009. Reconstruction of the history of anthropogenic CO_2 concentrations in the ocean. *Nature* 462:346-9.

Kim, J.-M., Lee, K., Shin, K., Kang, J.-H., Lee, H.-W., Kim, M., Jang, P.-G. & Jang, M.-C. 2006. The effect of seawater CO_2 concentration on growth of a natural phytoplankton assemblage in a controlled mesocosm experiment. *Limnology and Oceanography* 51:1629-36.

Kirkwood, D. S. 1989. Simultaneous determination of selected nutrients in seawater. *ICES CM:C:* 29.

Körtzinger, A., Koeve, W., Kähler, P. & Mintrop, L. 2001. C : N ratios in the mixed layer during the productive season in the northeast Atlantic Ocean. *Deep Sea Research Part I: Oceanographic Research Papers* 48:661-88.

Kruskopf, M. & Flynn, K. J. 2006. Chlorophyll content and fluorescence responses cannot be used to gauge reliably phytoplankton biomass, nutrient status or growth rate. *New Phytologist* 169:525-36.

Langer, G., Geisen, M., Baumann, K.-H., Klas, J., Riebesell, U., Thoms, S. & Young, J. R. 2006. Species-specific responses of calcifying algae to changing seawater carbonate chemistry. *Geochemistry, Geophysics, Geosystems* 7:1525-2027.

Langer, G., Nehrke, G., Probert, I., Ly, J. & Ziveri, P. 2009. Strain specific responses of *Emiliania huxleyi* to changing seawater carbonate chemistry. *Biogeosciences* 6:4361–83.

Larsen, A., Fonnes Flaten, G. A., Sandaa, R.-A., Castberg, T., Thyrhaug, R., Erga, S. R., Jacquet, S. p. & Bratbak, G. 2004. Spring phytoplankton bloom dynamics in

Norwegian coastal waters: Microbial community succession and diversity. *Limnology and Oceanography* 49:180-90.

LaRoche, J., Rost, B., and Engel, A. 2010 Bioassays, batch culture and chemostat experimentation *In* Riebesell U., Fabry V. J., Hansson L. & Gattuso J.-P. (Eds.), 2010. Guide to best practices for ocean acidification research and data reporting, 260 p. Luxembourg: Publications Office of the European Union. Chapter 5.

Laws, E. A., Thompson, P. A., Popp, B. N. & Bidigare. R. A. 1998. Sources of inorganic carbon for marine microalgal photosynthesis: A reassessment of $\delta^{13}C$ data from batch culture studies of *Thalassiosira pseudonana* and *Emiliania huxleyi*. *Limnology and Oceanography* 43:136-142

Le Quéré, C., Raupach, M. R., Canadell, J. G., Marland, G. & et al. 2009. Trends in the sources and sinks of carbon dioxide. *Nature Geoscience* 2:831-6.

Leonardos, N., Read, B., Thake, B., & Young, J.R. 2009. No mechanistic dependence of photosynthesis on calcification in the coccolithophorid *Emiliania huxleyi* (haptophyta). *Journal of Phycology* 45:1046-51.

Leonardos, N. & Geider, R. J. 2005. Elevated atmospheric carbon dioxide increases organic carbon fixation by *Emiliania huxleyi* (haptophyta), under nutrient-limited high-light conditions. *Journal of Phycology* 41:1196-203.

Levitan, O., Rosenberg, G., Setlik, I., Setlikova, E., Grigel, J., Klepetar, J., Prasil, O. & Berman-Frank, I. 2007. Elevated CO_2 enhances nitrogen fixation and growth in the marine cyanobacterium *Trichodesmium*. *Global Change Biology* 13:531-8.

Long, S. P., Ainsworth, E., A.,, Rogers, A. & Ort, D. R. 2004. Rising atmospheric carbon dioxide: Plants face the future. *Annual Review of Plant Biology* 55:591-628.

Marie, D., Simon, N. & Vaulot, D. 2005. Phytoplankton cell counting by flow cytometry. *In Algal Culturing Techniques*. Academic press.

Martinez, J. M., Schroeder, D. C., Larsen, A., Bratbak, G. & Wilson, W. H. 2007. Molecular dynamics of *Emiliania huxleyi* and cooccurring viruses during two separate mesocosm studies. *Applied and Environmental Microbiology* 73:554-62.

McGinn, P. J. & Morel, F. M. M. 2007. Expression and regulation of carbonic anhydrases in the marine diatom *Thalassiosira pseudonana* and in natural phytoplankton assemblages from Great Bay, New Jersey. *Physiologia Plantarum*:1-14.

McMinn, A. & Hegseth, E. N. 2004. Quantum yield and photosynthetic parameters of marine microalgae from the Southern Arctic Ocean, Svalbard. *Journal of the Marine Biological Society of the UK* 84:865-71.

Medlin. L. K., Barker, G. L. A., Campbell, L.J., Green, C., Hayes, P. K., Marie, D., Wrieden, S. and Vaulot, D. 1996. Genetic characterisation of *Emiliania huxleyi* (haptophyta). *Journal of Marine Systems* 9:13-31.

Menden-Deuer, S. & Lessard, E. J. 2000. Carbon to volume relationships for dinoflagellates, diatoms, and other protist plankton. *Limnology and Oceanography* 45:569-79.

Moore, B. D., Cheng, S.-H., Sims, D. & Seemann, J. R. 1999. The biochemical and molecular basis for photosynthetic acclimation to elevated atmospheric CO_2. *Plant, Cell and Environment* 22:567-82.

Müller, M. N., Schulz, K. G. and Riebesell, U. 2010. Effects of long-term high CO_2 exposure on two species of coccolithophores. *Biogeosciences* 7: 1109–1116.

Nanninga, H. J., Ringenaldus, P. & Westbroek, P. Immunological quantitation of a polysaccharide formed by *Emiliania huxleyi*. *Journal of Marine Systems* 9: 67-74.

Nejstgaard, J. C., Gismervik, I. & Solberg, P. T. 1997. Feeding and reproduction by *Calanus finmarchicus* and microzooplankton grazing during mesocosm blooms of diatoms and the coccolithophore *Emiliania huxleyi*. *Marine Ecology Progress Series* 147:197-217.

Nicot, N., Hausman, J.-F., Hoffmann, L. & Evers, D. 2005. Housekeeping gene selection for real-time RT-PCR normalization in potato during biotic and abiotic stress. *Journal of Experimental Botany,* 56:2907–2914

Nielsen, M., V. . 1995. Photosynthetic characteristics of the coccolithophorid *Emiliania huxleyi* (prymnesiophyceae) exposed to elevated concentrations of dissolved inorganic carbon. *Journal of Phycology* 31:715-9.

Orr, J. C., Fabry, V. J., Aumont, O., Bopp, L., Doney, S. C., Feely, R. A., Gnanadesikan, A., Gruber, N., Ishida, A., Joos, F., Key, R. M., Lindsay, K., Maier-Reimer, E., Matear, R., Monfray, P., Mouchet, A., Najjar, R. G., Plattner, G.-K., Rodgers, K. B., Sabine, C. L., Sarmiento, J. L., Schlitzer, R., Slater, R. D., Totterdell, I. J., Weirig, M.-F., Yamanaka, Y. & Yool, A. 2005. Anthropogenic ocean acidification over the twenty-first century and its impact on calcifying organisms. *Nature* 437:681-6.

Paasche, E., Brubak, S., Skattebol, S., Young J. R., Green, J. C. 1996. Growth of the coccolithophorid *Emiliania huxleyi* (Haptophyceae) at low salinity. *Phycologia* 35:394-403

Paasche. 2002. A review of the coccolithophorid *Emiliania huxleyi* (prymnesiophyceae), with particular reference to growth, coccolith formation, and calcification-photosynthesis interactions. *Phycologia* 40:503-29.

Parker, M. S., Armbrust, E. V., Provia-Scott, J. Keil, R. G. 2004. Induction of photorespiration by light in the centric diatom *Thalassiosira weissflogii* (bacillariophyceae): Molecular characterization and physiological consequences. *Journal of Phycology* 40:557-67.

Passow, U., Alldredge, A. L. & Logan, B. E. 1994. The role of particulate carbohydrate exudates in the flocculation of diatom blooms. *Deep Sea Research(Part I)* 41:335-57.

Patching, J. 2008. STS Lord Nelson cruise report LN684.

Pierce, R.H., Henry, M.S., Blum, P.C., Hamel, S.L., Kirkpatrick, B., Cheng, Y.S., Zhou, Y., Irvin, C.M., Naar, J., Weidner, A., Fleming, L.E., Backer, C., and Baden, D.G. 2005. Brevetoxin composition in water and marine aerosol along a Florida beach: Assessing potential human exposure to marine biotoxins *Harmful Algae* 4 (6): 965-972

Pierrot, Lewis, D. E. & Wallace, D. W. R. 2006. Co2sys_calc_xls. *In MS Excel Program Developed for CO_2 System Calculations.*

Piontek, J., Lunau, M., Händel1, N. Borchard, C. Wurst, M. and Engel, A. 2010. Acidification increases microbial polysaccharide degradation in the ocean. *Biogeosciences* 7: 1615-1624.

Pruder, G. D. & Bolton, E. T. 1979. The role of CO_2 enrichment of aerating gas in the growth of an estuarine diatom *Aquaculture* 17:1-15.

Raven, J., Caldeira, K., Elderfield, H., Hoeg-Guldberg, O. & others, a. 2005. Ocean acidification due to increasing atmospheric carbon dioxide. The Royal Society, London.

Raven, J. A. 1991. Physiology of inorganic C acquisition and implications for resource use efficiency by marine phytoplankton: Relation to increased CO_2 and temperature. *Plant, Cell and Environment* 14:779-94.

Raven, J. A. 2009. Contributions of anoxygenic and oxygenic phototrophy and chemolithotrophy to carbon and oxygen fluxes in aquatic environments. *Aquatic Microbial Ecology* 56:177-92.

Raven, J. A. & Falkowski, P. G. 1999. Oceanic sinks for atmospheric CO_2. *Plant Cell and Environment* 22:741-755

Raven, J. A. & Johnston, A. M. 1991. Mechanisms of inorganic carbon acquisition in marine phytoplankton and their implications for the use of other resources. *Limnology and Oceanography* 36:1701-14.

Raven, J. A., Kubler, J. E. & Beardall, J. 2000. Put out the light, and then put out the light. *Journal of the Marine Biological Society of the UK* 80:1-25.

Raven, J. A. G., R. D. 2003. Adaptation, acclimation and regulation of photosynthesis in algae. *In* Larkum, A. W. D., Douglas, S. E. & Raven, J. A. [Ed.] *Photosynthesis in algae*. Kluwer Academic Publishers, Dordrecht, the Netherlands, pp. 385-412.

Redfield, A. C. 1934. On the proportions of organic derivatives in sea water and their relation to the composition of plankton. *In* Daniel, R. J. [Ed.] *James Johnstone memorial volume*, University of Liverpool, pp. 176-92.

Ridgwell, A., Schmidt, D. N., Turley, C., Brownlee, C., Maldonado, M. T., Tortell, P. A. & Young, J. R. 2009. From laboratory manipulations to earth system models: Scaling calcification impacts of ocean acidification. *Biogeosciences* 6:2611-23.

Riebesell, U., Bellerby, R. G. J., Engel, A., Fabry, V. J., Hutchins, D. A., Reusch, T. B. H., Schulz, K. G. & Morel, F. M. M. 2008. Comment on "phytoplankton calcification in a high-CO_2 world". *Science* 322:1466b.

Riebesell, U., Revill, A. T., Holdsworth, D. G. & Volkman, J. K. 2000a. The effects of varying CO_2 concentration on lipid composition and carbon isotope fractionation in *Emiliania huxleyi*. *Geochimica et Cosmochimica Acta* 64:4179-92.

Riebesell, U., Schulz, K. G., Bellerby, R. G. J., Botros, M., Fritsche, P., Meyerhofer, M., Neill, C., Nondal, G., Oschlies, A., Wohlers, J., and Zollner, E. 2007. Enhanced biological carbon consumption in a high CO_2 ocean. *Nature* 450:545-8.

Riebesell, U., Wolf-Gladrow, D. A. & Smetacek, V. 1993. Carbon dioxide limitation of marine phytoplankton growth rates. *Nature* 361:249-51.

Riebesell, U., Zondervan, I., Rost, B., Tortell, P. D., Zeebe, R. E. & Morel, F. M. M. 2000b. Reduced calcification of marine plankton in response to increased atmospheric CO_2. *Nature* 407:364-7.

Riebesell U., Fabry V. J., Hansson L. & Gattuso J.-P. (Eds.), 2010a. Guide to best practices for ocean acidification research and data reporting, 260 p. Luxembourg: Publications Office of the European Union.

Riebesell, U., Lee, K., and Nejstgaard, J.C. 2010b. Pelagic mesocosms *In* Riebesell U., Fabry V. J., Hansson L. & Gattuso J.-P. (Eds.), 2010. Guide to best practices for ocean acidification research and data reporting, 260 p. Luxembourg: Publications Office of the European Union. Chapter 6.

Roberts, K., Granum, E., Leegood, R. C. & Raven, J. A. 2007. C3 and C4 pathways of photosynthetic carbon assimilation in marine diatoms are under genetic, not environmental, control *Plant Physiology* 145:230–5.

Rocap, G., Larimer, F. W., Lamerdin, J., Malfatti, S., Chain, P., Ahlgren, N. A., Arellano, A., Coleman, M., Hauser, L., Hess, W. R., Johnson, Z. I., Land, M., Lindell, D., Post, A. F., Regala, W., Shah, M., Shaw, S. L., Steglich, C., Sullivan, M. B., Ting, C. S., Tolonen, A., Webb, E. A., Zinser, E. R. & Chisholm, S. W. 2003. Genome divergence in two *Prochlorococcus* ecotypes reflects oceanic niche differentiation. *Nature* 424:1042-7.

Rose, J. M., Y. Y. Feng, Gobler, C.J., Gutierrez, R., Hare, C. E., Leblanc, K., Hutchins, D.A. 2009. Effects of increased pCO_2 and temperature on the North Atlantic spring bloom. II. Microzooplankton abundance and grazing. *Marine Ecology Progress Series* 388: 27-40.

Rost, B., Zondervan, I. & Riebesell, U. 2002. Light-dependent carbon isotope fractionation in the coccolithophorid *Emiliania huxleyi*. *Limnology and Oceanography* 47:120-8.

Rost, B., Zondervan, I. & Wolf-Gladrow, D. 2008. Sensitivity of phytoplankton to future changes in ocean carbonate chemistry: Current knowledge, contradictions and research directions. *Marine Ecology Progress Series* 373:227-37.

Sambrotto, R. N., Savidge, G., Robinson, C., Boyd, P., Takahashi, T., Karl, D. M., Langdon, C., Chipman, D., Marra, J. & Codispoti, L. 1993. Elevated consumption of carbon relative to nitrogen in the surface ocean. *Nature* 363:248-50.

Sangrà, P., A. Pascual, Á. Rodríguez-Santana, F. Machín, E. Mason, J.C. McWilliams, J.L. Pelegrí,, C. Dong, A. R., J. Arístegui, Á. Marrero-Díaz, A. Hernández-Guerra, A. Martínez-Marrero, M. & Auladell. 2009. The Canary eddy corridor: A major pathway for long-lived eddies in the subtropical North Atlantic. submitted to *Deep Sea Research II*.

Sarmiento, J. L., Slater, R., Barber, R., Bopp, L., Doney, S. C., Hirst, A. C., Kleypas, J., Matear, R., Mikolajewicz, U., Monfray, P., Soldatov, V., Spall, S. A. & Stouffer, R. 2004. Response of ocean ecosystems to climate warming. *Global Biogeochemical Cycles* 18:GB3003.

Satlantic. *Operation manual for: Fire fluorometer system document number: Sat-dn-00265*. Richmond Terminal, Halifax, Nova Scotia

Schafer, H. 2001. Dynamics of the genetic diversity of marine bacterial assemblages. PhD thesis, Department of *Biologie/Chemie*. Universitat Bremen, Bremen.

Schneider. 2004. Influence of carbonate chemistry and light intensity on natural phytoplankton assemblages with emphasis on species composition. PhD thesis, Department of *Biologie/Chemie*. Universitat Bremen, Bremen.

Schroeder, D. C., Biggi, G. F., Hall, M., Davy, J., Martınez Martınez, J., Richardson, A. J., Malin, G. & Wilson, W. H. 2005. A genetic marker to separate *Emiliania huxleyi* (prymnesiophyceae) morphotypes. *Journal of Phycology* 41:874-9.

Schroeder, D. C., Oke, J., Hall, M., Malin, G. & Wilson, W. H. 2003. Virus succession observed during an *Emiliania huxleyi* bloom. *Applied and Environmental Microbiology* 69:2484-90.

Schulz, K. G., Barcelos, J., Ramos, E., Zeebe, R. E. & Riebesell, U. 2009. CO_2 perturbation experiments: Similarities and differences between dissolved inorganic carbon and total alkalinity manipulations. *Biogeosciences* 6:2145-53.

Sciandra, A., Harlay, J. R., Lefèvre, D., Lemée, R., Rimmelin, P., Denis, M. & Gattuso, J.-P. 2003. Response of coccolithophorid *Emiliania huxleyi* to elevated partial pressure of CO_2 under nitrogen limitation. *Marine Ecology Progress Series* 261:111-22.

Sellner, K.G., Doucette, G.J., Kirkpatrick, G.J., 2003 Harmful algal blooms: causes, impacts and detection *Journal of Industrial Microbiology and Biotechnology* 30(7):383-406.

Shi, D., Xu, Y. & Morel, F. M. M. 2009. Effects of the pH/pCO_2 control method on medium chemistry and phytoplankton growth. *Biogeosciences* 6:1199-207.

Shi, D. Xu, Y., Hopkinson, B. M., Morel, F.M.M. 2010 . Effect of Ocean Acidification on Iron Availability to Marine Phytoplankton._www.sciencexpress.org_/: 1 / 10.1126/science.118351

Smetacek, V. 1999. Diatoms and the ocean carbon cycle. *Protist* 150:25-32.

Søndergaard, M., Williams, P. J le B., Cauwet, G., Riemann, B., Robinson, C., Terzic, S., Woodward, E.M.S., Worm, J. 2000. Net accumulation and flux of dissolved organic carbon and dissolved organic nitrogen in marine plankton communities. *Limnology and Oceanography* 45(5): 1097–1111

Sorensen, G., Baker, A. C., Hall, M. J., Munn, C. B. & Schroeder, D. C. 2009. Novel virus dynamics in an *Emiliania huxleyi* bloom. *Journal of Plankton Research* 31:787-91.

Strickland, J. D. H. & Parsons, T. R. 1968. *A practical handbook of seawater analysis*. Fisheries research board of Canada, Ottawa.

Suffrian, K., Simonelli, P., Nejstgaard, J. C., Putzeys, S., Carotenuto, Y. & Antia, A. N. 2008. Microzooplankton grazing and phytoplankton growth in marine mesocosms with increased CO_2 levels. *Biogeosciences* 5:1145-56.

Sunda, W. G. (2010). Iron and the Carbon Pump. *Science* 327(5966): 654-655.

Tcherkez, G. G. B., Farquhar, G. D. & Andrews, T. J. 2006. Despite slow catalysis and confused substrate specificity, all ribulose bisphosphate carboxylases may be nearly perfectly optimized. *Proceedings of the National Academy of Science* 103:7246-51.

Thellin, O., Zorzi, W., Lakaye, B., De Borman, B., Coumans, B., Hennen, G., Grisar, T., Igout, A. & Heinen, E. 1999. Housekeeping genes as internal standards: Use and limits. *Journal of Biotechnology* 75:291-5.

Thompson, P. A. and Calvert, S.E. 1994. Carbon-isotope fractionation by a marine diatom: The influence of irradiance, daylength, pH, and nitrogen source *Limnology and Oceanography* 39:1835-1844.

Toggweiler. J. R. 1993. Carbon overconsumption. *Nature*. 363:210-211

Tortell, P. D. 2000. Evolutionary and ecological perspectives on inorganic carbon acquisition in phytoplankton. *Limnology and Oceanography* 45:744-50.

Tortell, P. D., DiTullio, G. R., Sigman, D. M. & Morel, F. M. M. 2002. CO_2 effects on taxonomic composition and nutrient utilization in an equatorial Pacific phytoplankton assemblage. *Marine Ecology Progress Series* 236:37-43.

Tortell, P. D., Payne, C., Gueguen, C., Strzepek, R. F., Boyd, P. W. & Rost, B. 2008a. Inorganic carbon uptake by Southern ocean phytoplankton. *Limnology and Oceanography* 53:1266-78.

Tortell, P. D., Payne, C. D., Li, Y., Trimborn, S., Rost, B., Smith, W. O., Riesselman, C., Dunbar, R. B., Sedwick, P. & DiTullio, G. R. 2008b. CO_2 sensitivity of Southern Ocean phytoplankton. *Geophysical Research Letters* 35.

Tortell, P. D., Rau, G. H. & Morel, F. M. M. 2000. Inorganic carbon acquisition in coastal Pacific phytoplankton communities. *Limnology and Oceanography* 45:1485-500.

Tortell, P. D., Reinfelder, J. R. & Morel, F. M. M. 1997. Active uptake of bicarbonate by diatoms. *Nature* 390 243-4.

Westbroek, P., Brown, C. W., Bleijswijk, J. V., Brownlee, C., Brummer, G. J., Conte, M., Egge, J. K., Fernández, E., Jordan, R., Knappertsbusch, M., Stefels, J., Veldhuis, M., van der Wal, P. & Young, J. 1993. A model system approach to biological climate forcing. The example of *Emiliania huxleyi*. *Global and Planetary Change* 8:27-46.

Wolf-Gladrow, D., Riebesell, U., Burkhardt, S. & Bijma, J. 1999. Direct effects of CO_2 concentration on growth and isotopic composition of marine plankton. *Tellus* 51B:461-76.

Wurts, W. A. Durborow, R. M.1992. Interactions of pH, carbon dioxide, alkalinity and hardness in fish ponds. *Southern Regional Aquaculture Center Publication No. 464*.

Yang, Y. & Gao, K. 2003. Effects of CO_2 concentrations on the freshwater microalgae, *Chlamydomonas reinhardtii*, *Chlorella pyrenoidosa* and *Scenedesmus obliquus* (chlorophyta). *Journal of Applied Phycology* 00:1-11.

Zeebe, R. E. & Wolf-Gladrow, D. 2001. *CO_2 in seawater: Equilibrium, kinetics, isotopes*, *Elsevier Oceanography Series*, 65, (Elsevier, Amsterdam, 2001).

Zondervan, I., Rost, B. & Riebesell, U. 2002. Effect of CO_2 concentration on the PIC/POC ratio in the coccolithophore *Emiliania huxleyi* grown under light-limiting conditions and different daylengths. *Journal of Experimental Marine Biology and Ecology* 272:55-70.

Zondervan, I., Zeebe, R. E., Rost, B. & Riebesell, U. 2001. Decreasing marine biogenic calcification: A negative feedback on rising atmospheric pCO_2. *Global Biogeochemical Cycles* 15:507-16.